



# Ligand Self Assembly to Enhance the Strength and Selectivity of Metal Extraction

**Clare Squires**

**PhD Thesis  
The University of Edinburgh  
2001**



## **Dedication**

This work is dedicated to my family for encouraging me all the way.

## Abstract

This thesis investigates the role of hydrogen-bonding in sulfonamido ligands to assess the importance of ligand association prior to or accompanying complexation to Co(II), Ni(II), Cu(II) and Zn(II), making comparisons with commercial phenolic oxime copper extractants in which the strength and selectivity are thought to be due to the formation of a hydrogen-bonded *pseudo*-macrocycle formed around the metal ion.

A series of relatively simple bidentate monosulfonamidodiamine ligands of the formula  $R^2NHRNHSO_2R^1$  has been prepared from the parent diamines. R is a bridging group of two or three methylene units,  $R^1$  is a tolyl group or a *p*-<sup>t</sup>Bu-phenyl group, and  $R^2$  is a hydrogen atom or a benzyl, an *n*-butyl or a 2-ethylhexyl group. The solid state structures of these ligands are difficult to predict and indicate that a surfeit of hydrogen-bond donors and acceptors incorporated into a relatively flexible ligand leads to a variety of hydrogen-bond interactions in the solid-state and hence a range of complicated secondary structures including two and three dimensional arrays. The ethane-bridged ligands form *pseudo*-macrocycles around copper(II) and nickel(II) centres in the complexes  $[Cu(L-H)_2]$  and  $[Ni(L-H)_2]$ , but not in the analogous zinc complex  $[Zn(L-H)_2]$ . The ligands are quite weak extractants,  $pH_{1/2}$  4-6, when used in a pH-swing process. Increasing the size of the chelate ring from five to six leads to a weaker extractant.

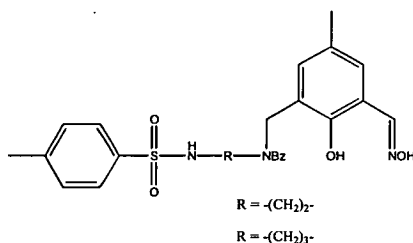
A series of sulfonamido-oxime ligands  $1-\{2-[N-(4-R-benzenesulfonamido)]-R^1$  which have an  $N_2^-$  chelating unit analogous to the  $NO^-$  unit in the commercial *ortho*-phenolic oximes has been synthesised and characterised. R is a methyl, propyl, <sup>t</sup>butyl or pentyl group and  $R^1$  is an ethan-1-one oxime, ethan-1-one O-methyloxime, or a (phenyl)methanone oxime. The majority of solid-state structures contain hydrogen-bonded dimers and appear to be independent of small substituent changes in the ligand. However the *E*, *Z* isomerism of the oxime is important. The *Z* isomer only forms polymeric species. Complex formation by the sulfonamido-oxime ligands is less predictable than with the monosulfonamidodiamines and both 2:1 and

1:1, ligand to metal complexes are observed for 1-{2-[N-(4-methylbenzene sulfonamido)]-phenyl}ethan-1-one oxime forming the complexes  $[\text{Cu}(\text{L-H})_2]$ ,  $[\text{Ni}(\text{L-H})_2]$ ,  $[\text{Cu}_4(\text{L-H})_2(\text{L-2H})_2(\text{MeOH})_2(\text{MeO})_2]$ ,  $[\text{Ni}_2\text{Na}_2(\text{L-H})_2(\text{L-2H})_2(\text{MeOH})_4]$  and  $[\text{Ni}_4(\text{OH})_2(\text{L-H})_2(\text{L-2H})_2(\text{MeOH})_5]$  from methanol solution. In addition to the expected bonding of the sulfonamido and oximic nitrogen atoms, the bonding of the sulfonamido oxygen atoms and the deprotonated oximic oxygen atom to metal ions is also observed.

ESI-MS shows evidence for dimer formation for both the monosulfonamidodiamine ligands and the sulfonamido-oxime free ligand systems. VPO and IR analyses of monosulfonamidodiamines show that self-association occurs in solution and is concentration and solvent dependent. VPO shows that this is also the case for sulfonamido-oximes and  $^1\text{H}$  nmr was used to determine the equilibrium constant  $K$  and  $\Delta G$ ,  $\Delta H$  and  $\Delta S$  for a monomer-dimer equilibrium of 1-{2-[N-(4-methylbenzenesulfonamido)]-phenyl}ethan-1-one oxime in chloroform- $d_1$  and 1-{2-[N-(4-pentylbenzenesulfonamido)]-phenyl}ethan-1-one oxime in chloroform- $d_1$  and toluene- $d_8$ . The development of monosulfonamidodiamine and sulfonamido-oxime ligands with high solubility in solvents of low polarity such as toluene is described. The possibility of replacing the sulfonamido group with a sulfinamido group was considered and the synthesis of sulfinyl chlorides and prototype sulfinamido ligands is described; the latter are shown to have insufficient stability to be useful ligands under conditions required for extraction from aqueous media.

The attempted development of *pseudo*-macrocyclic and *pseudo*-cage structures using ternary metal/sulfonamide/amine systems is described. Bidentate sulfnamido ligands are of the type  $\text{R}\{\text{NHSO}_2(4\text{-CH}_3\text{C}_6\text{H}_5)\}_2$  where R is a 1,2-ethane, a 1,2-*trans*-cyclohexane or an *o*-phenylene group. Tridentate sulfonamido ligands studied of the type  $\text{R}\{\text{NHSO}_2(4\text{-CH}_3\text{C}_6\text{H}_5)\}_3$  where R is a  $\text{N}(\text{CH}_2\text{CH}_2)_3$ , a *cis,cis*-1,3,5-cyclohexane- or a  $\text{CH}_3(\text{CH}_2)_3$  unit. *Bis*- and *tris*-sulfonamido ligands have been synthesised and their solid state structures found to contain complicated arrays of hydrogen-bonds. The formation of metal complexes of these ligands proved difficult and no ternary complexes were isolated.

Ligands combining the monosulfonamidodiamine and phenylketoxime units were synthesised in an attempt to develop potentially dinucleating ligands which offer the possibility of more efficient metal transport based on higher metal:ligand (2:2) mass ratios. 6-Hydroxy-3-methyl-5{2,6-diaza-2-benzyl-6[N-(4-methylbenzenesulfonyl)]hex-1-yl}benzaldehyde oxime and its ethane-bridged analogue readily form copper complexes. A mononuclear complex  $[Cu(L-H)_2]$  of the propane-bridged ligand has been shown by X-ray crystallography to have a pseudo-macrocyclic structure very similar to that in the copper complexes of the commercial phenolic oxime extractants; the phenolate oxygen atom and the oximic nitrogen atom are coordinated to the metal centre and the oximic hydrogens are hydrogen-bonded to phenolate oxygen atoms.



## **Preface and Declaration**

Since graduating from the University of Sheffield in 1998 with a MChem degree in Chemistry with European Study, the author has been engaged in a programme of full time research under the supervision of Professor P. A. Tasker at the University of Edinburgh and Mr. J. Campbell at Avecia (Blackley, Manchester).

No part of the work referred to in this thesis has been submitted in support of an application for another degree or qualification from this or any other university or other institute of learning.

Clare Squires

December 2001

## **List of conferences attended**

Scottish Dalton Meeting, University of St Andrews,

Coordination Chemistry Discussion Group, University of Bristol, July 1999.

USIC meeting, University of Strathclyde, September 1999.

International Coordination Chemistry conference, University of Edinburgh, July 2000.

Crystal Engineering Discussion Group, University of Bologna, September 2000.

## Acknowledgements

I would like to thank my supervisor, Prof. Peter Tasker, for all his help, support and many interesting discussions throughout my Ph.D. In addition, I would like to thank Dr. Domenico Cupertino, Mr. Ron Swart, Mr. John Campbell, Mrs. Sue Owens and Dr. Aid Bisson at Avecia. I also wish to thank the EPSRC and Avecia for funding this project.

I would like to say a big thankyou to Dr. Hamish McNab who saved the day with so many organic chemistry problems. I thank Dr. David White, Dr. Timothy Higgs, Dr. Hamish Millar, Dr. Andrew Smith, Dr. Lucy Emeleus, Dr. David Nation, Dr. Lee West and Dr. Paul Plieger for their help and guidance and all those many questions which they answered, and also all the past and present Tasker group members for an enjoyable three years.

I thank Mr. John Millar and Mr. Wesley Kerr for their NMR work and Dr. David Reed for his help with the 360 machine. I am grateful to Mr. Alan Taylor and Mr. Harry Mackenzie for all the mass spectrometry they have done for me, and to Dr. Lorna Eades and Mr. Tim Calder for C/H/N analyses. I would like to thank Dr. Lesley Yellowlees and Mr. Ken McNamara for all their help with the electrochemistry and epr work. In addition I would like to thank Professor Christopher Hunter for the loan of the VPO machine. I am very grateful to Dr. Simon Parsons and especially to Mr. Andrew Parkin (for his patience) for X-ray structural analysis of my compounds. I am also grateful for the work which Christopher Baxter did on monosulfonamidodiamines.

Finally I would like to thank all the good friends I have made in Edinburgh. A special thanks goes to Caroline, Jenny and Karen for the heaps of support and the many laughs and to Kostas and Anna for their home comforts. Last but definitely not least, many thanks go to my Mum, Dad and Helen and of course Georgios.



# Table of contents

Dedication .....	ii
Abstract .....	iii
Preface and Declaration .....	vi
List of conferences attended.....	vii
Acknowledgements .....	viii
Table of Contents .....	ix
Abbreviations .....	xv
Thesis format.....	xviii
Index of compounds.....	xviii
<b>Chapter 1: General Introduction.....</b>	<b>1</b>
1.1 Aims .....	3
1.2 The science of metal recovery .....	3
1.2.1 Pyrometallurgy .....	3
1.2.2 Hydrometallurgy .....	5
1.3 The hydrometallurgical procedure of copper .....	8
1.3.1 Leaching .....	9
1.3.2 Extraction .....	9
1.3.3 Stripping.....	10
1.3.4 Electrowinning .....	10
1.4 P50: Avecia's reagent for copper recovery .....	12
1.5 The design of an extractant.....	13
1.5.1 The thermodynamic stability of complexes .....	14
1.5.2 The chelate effect .....	16
1.5.3 Metal geometry and ligand flexibility .....	18
1.5.3.1 The coordination chemistry of cobalt .....	18
1.5.3.2 The coordination chemistry of nickel .....	19
1.5.3.3 The coordination chemistry of copper .....	20
1.5.3.4 The coordination chemistry of zinc .....	20
1.6 Objectives .....	21
1.7 Supramolecular chemistry.....	21
1.7.1 Crystal engineering.....	22
1.7.2 The hydrogen-bond .....	23
1.7.3 The design of a supramolecular synthon.....	24
1.7.4 The sulfonamide group as a supramolecular synthon .....	26
1.8 Sulfonamides .....	27
1.8.1 Synthesis of sulfonamides .....	28
1.8.2 Sulfonamides as ligands .....	30
1.8.3 Sulfonamide complexes as metal extractants.....	40
1.9 References .....	46
<b>Chapter 2: Monosulfonamidodiamine ligands .....</b>	<b>52</b>
2.1 Introduction .....	55
2.2 Synthesis of simple monosulfonamidodiamines and their metal complexes ....	56
2.2.1 Free ligands .....	57

2.2.2 Metal complexes .....	58
2.3 Characterisation of simple monosulfonamidodiamines .....	59
2.3.1 Infrared Spectroscopy.....	59
2.3.2 NMR Spectroscopy .....	59
2.3.3 Mass Spectrometry.....	60
2.3.4 X-ray crystallography.....	60
2.4 Solid State structures of ligands and complexes .....	61
2.4.1 Free Ligands.....	61
2.4.1.1 N-(3-aminopropyl)-4-methylbenzenesulfonamide ( <b>5</b> ).....	63
2.4.1.2 N-(N-butyl-2-aminopropyl)-4-methylbenzenesulfonamide ( <b>9</b> )..	65
2.4.1.3 N-(2-aminoethyl)-4-methylbenzenesulfonamide ( <b>1</b> ).....	67
2.4.1.4 N-(N-benzyl-2-aminopropyl)-4-methylbenzenesulfonamide ( <b>7</b> )	69
2.4.1.5 N-(2-amino-phenyl)-4-methylbenzenesulfonamide ( <b>10</b> ).....	70
2.4.2 Hydrogen-bonding in monosulfonamidodiamine ligands.....	71
2.4.3 Monosulfonamidodiamine complexes .....	73
2.4.3.1 Bis[N-(2-aminoethyl)-4-methylbenzenesulfonamidato].....	
zinc(II) ( <b>12</b> ).....	73
2.4.3.2 Bis[N-(2-aminoethyl)-4-methylbenzenesulfonamidato].....	
nickel(II) ( <b>13</b> ).....	76
2.4.3.3 Bis[N-(2-aminoethyl)-4- <i>t</i> -butylbenzenesulfonamidato].....	
copper(II) ( <b>16</b> ).....	78
2.4.4 Hydrogen-bonding in sulfonamidodiamine complexes .....	80
2.4.5 Hole sizes, bite angles and torsion angles. ....	82
2.4.6 Geometry of amido and sulfonamido nitrogens .....	87
2.4.7 Geometry of the sulfonamido nitrogen in monosulfonamidodiamine ....	
ligands.....	88
2.4.8 Geometry of amides of carboxylic and sulfonic acids in the .....	
Cambridge Structural Database (CSD).....	92
2.5 Equilibrium constants of monosulfonamidodiamines.....	94
2.5.1 Speciation of monosulfonamidodiamines .....	95
2.5.2 Prediction of the selectivity of monosulfonamidodiamines.....	96
2.6 Solvent extraction.....	97
2.6.1 'S'-Curve determination.....	97
2.6.2 Selectivity of monosulfonamidodiamine ligands .....	98
2.7 An electrochemical study of monosulfonamidodiamine complexes.....	100
2.7.1 The stabilisation of metal(III) centres by deprotonated amide groups....	100
2.7.2 Cu(III) and Ni(III) peptide complexes .....	101
2.7.3 Electrochemical studies of monosulfonamidodiamine complexes .....	103
2.8 Conclusions .....	105
2.9 Experimental .....	106
2.9.1 Instrumentation.....	106
2.9.2 Solvent and reagent pretreatment.....	107
2.9.3 Ligands and their precursor .....	107
2.9.4 Monosulfonamidodiamine complex synthesis .....	114
2.9.5 Solvent extraction experiments from sulfate media .....	118
2.9.6 X-ray crystallography.....	119
2.10 References .....	122

<b>Chapter 3: Sulfonamido oxime ligands .....</b>	<b>124</b>
3.1 Introduction .....	127
3.2 Synthesis of simple monosulfonamido oxime ligands and their metal complexes.....	128
3.2.1 Free Ligands.....	128
3.2.2 Metal complexes .....	129
3.3 Characterisation of sulfonamido oxime ligands .....	130
3.3.1 Nuclear magnetic resonance (NMR) spectroscopy.....	130
3.3.2 Mass spectrometry and IR spectroscopy.....	131
3.3.3 X-ray crystallography.....	132
3.4 Solid state structures of sulfonamido oxime ligands and their complexes.....	132
3.4.1 Free ligands .....	133
3.4.1.1 1-{2-[N-(4-methylbenzenesulfonamido)]phenyl} ethan-1-one oxime ( <b>28</b> ).....	133
3.4.1.2 1-{2-[N-(4-t-butylbenzenesulfonamido)]phenyl} ethan-1-one oxime ( <b>29</b> ).....	134
3.4.1.3 1-{2-[N-(4-methylbenzenesulfonamido)]phenyl} ethan-1-one O-methyloxime ( <b>32</b> ).....	136
3.4.1.4 1-{2-[N-(4-methylbenzenesulfonamido)]-phenyl}(phenyl) methanone oxime ( <b>33</b> ) .....	137
3.4.2 Oxime stereochemistry.....	140
3.4.3 Hydrogen-bonding in sulfonamido oxime ligands.....	141
3.4.4 Sulfonamido oxime [ML <sub>2</sub> ] complexes .....	143
3.4.4.1 Bis[1-{2-[N-(4-methylbenzenesulfonamidato)]phenyl} ethan-1-one oxime] copper(II) ( <b>34</b> ) .....	144
3.4.4.2 Bis[1-{2-[N-(4-methylbenzenesulfonamidato)]phenyl} ethan-1-one oxime] nickel(II) ( <b>36</b> ).....	145
3.4.5 Sulfonamido oxime cluster complexes .....	147
3.4.5.1 [Cu <sub>4</sub> ( <b>28</b> -H) <sub>2</sub> ( <b>28</b> -2H) <sub>2</sub> (CH <sub>3</sub> OH) <sub>2</sub> (CH <sub>3</sub> O) <sub>2</sub> ] ( <b>35</b> ) .....	147
3.4.5.2 [Ni <sub>2</sub> Na <sub>2</sub> ( <b>28</b> -H) <sub>2</sub> ( <b>28</b> -2H) <sub>2</sub> (CH <sub>3</sub> OH) <sub>4</sub> ] ( <b>38</b> ).....	150
3.4.5.3 [Ni <sub>4</sub> ( <b>28</b> -H) <sub>2</sub> ( <b>28</b> -2H) <sub>2</sub> (OH) <sub>2</sub> (MeO) <sub>5</sub> ] ( <b>39</b> ) .....	153
3.4.6 Coordination sites of sulfonamido oxime ligands.....	156
3.4.7 Hydrogen-bonding in sulfonamido oxime complexes .....	158
3.4.8 Hole size, bite distances and torsion angles .....	159
3.4.9 Geometry of the sulfonamido nitrogen .....	163
3.5 A study of the solution properties of <b>34</b> and <b>35</b> .....	166
3.6 Equilibrium constants.....	167
3.7 Conclusion.....	168
3.8 Experimental .....	169
3.8.1 Instrumentation.....	169
3.8.2 Solvent and reagent Pretreatment.....	170
3.8.3 Synthesis of sulfonamido intermediates.....	170
3.8.4 Synthesis of sulfonamide oximes.....	173
3.8.5 Synthesis of sulfonamido oxime complexes .....	177
3.8.6 X-ray crystallography.....	180
3.9 References .....	184

<b>Chapter 4: Solution studies on monosulfonamidodiamine and sulfonamido-oxime ligands .....</b>	<b>185</b>
4.1 Introduction .....	188
4.2 Improving ligand solubility .....	188
4.2.1 Reducing the number of hydrogen-bond donors and acceptors .....	189
4.2.1.1 An introduction to sulfinamides .....	189
4.2.1.2 Sulfinamide target molecules.....	192
4.2.2 Ligand solubilisation by the introduction of a lipophilic group .....	197
4.2.2.1 The introduction of a lipophilic group into .....	
monosulfonamidodiamine ligands .....	197
4.2.2.2 The introduction of a lipophilic group into .....	
sulfonamido oxime ligands .....	199
4.2.3 Synthesis of sulfonyl chlorides.....	199
4.2.3.1 2-Ethylhexylsulfonyl chloride .....	202
4.2.3.2 Synthesis of aryl sulfonyl chlorides.....	204
4.3 Investigation of ligand association in solution.....	206
4.3.1 Electrospray ionisation mass spectrometry .....	206
4.3.2 Vapour pressure osmometry.....	207
4.3.3 NMR spectroscopy.....	207
4.3.4 Infrared spectroscopy.....	208
4.4 Solution studies of monosulfonamidodiamine ligands .....	208
4.4.1 ESI spectra of monosulfonamidodiamines.....	208
4.4.2 VPO of monosulfonamidodiamine ligands .....	211
4.4.3 Proton nmr of monosulfonamidodiamine ligands .....	213
4.4.4 IR of monosulfonamidodiamine ligands .....	214
4.5 Solution studies of sulfonamido oxime ligands .....	214
4.5.1 ESI spectra of sulfonamido oxime ligands.....	214
4.5.2 VPO of sulfonamido oxime ligands .....	216
4.5.3 Proton nmr of sulfonamido oxime ligands .....	217
4.5.3.1 Preliminary studies.....	217
4.5.3.2 Determination of equilibrium constants for the association .....	
of sulfonamido oxime ligands.....	219
4.5.3.3 Thermodynamic data for the association of sulfonamido .....	
oxime ligands .....	223
4.5.4.4 Speciation of sulfonamido oxime ligands.....	223
4.6 Conclusions .....	225
4.7 Experimental .....	226
4.7.1 Instrumentation.....	226
4.7.2 Solvent and reagent pretreatment.....	227
4.7.3 Synthesis of sulfinyl chlorides .....	227
4.7.4 Synthesis of sulfinamides and protected amines.....	228
4.7.5 Introduction of a lipophilic group into monosulfonamidodiamines.....	230
4.7.6 Synthesis of alkyl sulfonyl chlorides.....	231
4.7.7 Synthesis of alkyl-substituted arylsulfonyl chlorides.....	232
4.8 References .....	236

<b>Chapter 5: Ternary sulfonamido ligand complexes .....</b>	<b>241</b>
5.1 Introduction .....	244
5.2 Bidentate bis-sulfonamidodiamine ligand systems .....	245
5.2.1 Synthesis of bis-sulfonamidodiamine ligands .....	245
5.2.2 Characterisation of bis-sulfonamidodiamine ligands .....	245
5.2.2.1 NMR spectroscopy.....	245
5.2.2.2 Mass spectrometry, IR spectroscopy and micro-analysis .....	246
5.2.2.3 X-ray crystallography .....	247
5.2.3 Solid state structures of bis-sulfonamidodiamine ligands .....	247
5.2.3.1 1, 2-Di(4-methylbenzenesulfonamido)ethane ( <b>57</b> ) .....	247
5.2.3.2 1, 2-Di(4-methylbenzenesulfonamido)cyclohexane ( <b>58</b> ) .....	249
5.2.3.3 1,2-Di(4-methylbenzenesulfonamido)benzene ( <b>59</b> ) .....	250
5.2.4 Hydrogen-bonding in bis-sulfonamidodiamine ligands .....	252
5.2.5 Attempted formation of transition metal complexes of .....	
bis-sulfonamidodiamine ligands .....	252
5.3 Tridentate tris-sulfonamidotriamino ligand systems .....	253
5.3.1 Synthesis of tridentate tris-sulfonamidotriamine ligands .....	253
5.3.2 Characterisation of tris-sulfonamidotriamine ligands .....	256
5.3.2.1 NMR spectroscopy.....	256
5.3.2.2 Mass spectrometry, IR spectroscopy, X-ray crystallography .....	
and micro-analysis .....	257
5.3.3 Solid state structures of tris-sulfonamidotriamine ligands .....	258
5.3.3.1 Tris-(2-(4-methylbenzenesulfonamido)ethyl)amine ( <b>60</b> ) .....	258
5.3.3.2 Cis-cis-1,3,5, tris-(4-methylbenzenesulfonamido)- .....	
cyclohexane ( <b>61</b> ) .....	260
5.3.3.3 N,N',N''-tris-(4-methylbenzenesulfonyl)-2-aminomethyl- .....	
2- methylpropane-1, 3-diamine ( <b>62</b> ) .....	263
5.3.4 Hydrogen-bonding in tris-sulfonamidotriamine ligands .....	264
5.3.5 Coordination chemistry of tris-sulfonamidotriamine ligands .....	265
5.3.5.1 Attempted formation of transition metal complexes of .....	
tris-sulfonamidotriamine ligands .....	265
5.3.5.2 N,N',N'',N'''[Tris-(2-(4-methylbenzenesulfonylamino)ethyl) ..	
aminato] copper(II) potassium(I) ( <b>70</b> ) .....	266
5.3.6 Attempted methylation of tris-[2-(4-methylbenzenesulfonylamino).....	
ethyl]amine ( <b>60</b> ).....	267
5.3.7 Nitrogen geometry of bis- and tris-sulfonamide ligands.....	268
5.4 Conclusion .....	271
5.5 Experimental .....	272
5.5.1 Instrumentation.....	272
5.5.2 Solvent and reagent pretreatment .....	272
5.5.3 Synthesis of bis-sulfonamidodiamine ligands .....	273
5.5.4 Synthesis of tris-sulfonamidotriamine ligands .....	275
5.5.5 Complexes of tris-sulfonamidotriamine ligands .....	282
5.5.6 X-ray crystallography .....	282
5.6 References .....	286

<b>Chapter 6: Dinucleating sulfonamido-oxime ligands.....</b>	<b>287</b>
6.1 Introduction .....	289
6.2 Synthesis of dinucleating sulfonamido oxime ligands .....	289
6.3 Characterisation of dinucleating sulfonamido oxime ligands .....	291
6.3.1 NMR spectroscopy.....	291
6.3.2 IR spectroscopy and mass spectrometry .....	293
6.4 Complexation study of ligands <b>72</b> and <b>73</b> .....	294
6.4.1 Complexation of <b>72</b> .....	294
6.4.2 Complexation of <b>73</b> .....	294
6.5 Solid state structures of dinucleating sulfonamido oxime ligands .....	295
6.5.1 6-Hydroxy-3-methyl-5{2, 6-diaza-2-benzyl-6[N-(4-methylbenzene.....	
sulfonyl)]hex-1-yl} benzaldehyde ( <b>76</b> ).....	295
6.5.2 Bis(6-hydroxy-3-methyl-5{2, 6-diaza-2-benzyl-6[N-(4-methylbenzene	
sulfonyl)]hex-1-yl}benzaldehyde oximato)copper(II) ( <b>78</b> ).....	296
6.6 Conclusion .....	298
6.7 Experimental .....	299
6.7.1 Instrumentation.....	299
6.7.2 Solvent and reagent pretreatment .....	299
6.7.3 Ligand syntheses .....	300
6.7.4 Metal complexes .....	305
6.7.5 X-Ray Crystallography.....	306
6.8 References .....	308
 <b>Chapter 7: Conclusions.....</b>	 <b>309</b>
 <b>Appendix I.....</b>	 <b>313</b>
 <b>Appendix II.....</b>	 <b>319</b>

## Abbreviations

$\theta$	$\theta$ circle diffraction angle (X-ray)
$\mu$	absorption coefficient (X-ray)
%	percentage
°	degree
\$	dollar
°C	degree Centigrade
Å	Angstrom
AAS	atomic Absorption Spectrometer
acetonitrile- <i>d</i> <sub>3</sub>	deuterated acetonitrile
Ar	aryl
$\beta$	complex formation constant
bz	benzyl
br	broad
bp	boiling point
calc.	Calculated
CDCl <sub>3</sub>	deuterated chloroform
<i>cf.</i>	compared with
CFSE	crystal field stabilisation energy
ch.	chapter
<i>cis</i>	<i>cisoid</i>
cm <sup>-1</sup>	wave number (IR)
cm <sup>3</sup>	centimetre cubed
Cov.	covariance
CSD	Cambridge Structural Database
d	doublet
$\delta$	chemical shift
$\delta_C$	chemical shifts for carbon nmr
$\delta_H$	chemical shifts for proton nmr
$\Delta$	delta
$\Delta\rho$	residue electron density in difference electron density map
$\Delta H$	heat of formation
$\Delta H^\circ$	standard heat of formation
$\Delta G^\circ$	Gibbs free energy
$\Delta S^\circ$	standard entropy
$\Delta_o$	octahedral crystal field splitting parameter
$D_c$	crystal density
DMSO	dimethylsulfoxide
DMSO- <i>d</i> <sub>6</sub>	deuterated dimethylsulfoxide
dd	doublet of doublets
decomp.	Decomposed
DEPT	Distortionless Enhancement through Polarization Transfer
dm <sup>3</sup>	decimetre cubed
DMF	dimethylformamide
d.p.	decimal places

<i>E</i>	entgegen (isomerism)
ee	enantiomeric excess
$E^{\circ}$	standard electrode potential
$E_p$	electrode potential
ed.	editor
edn.	edition
EI	electron impact (MS)
ESI	electrospray ionisation (MS)
Et	ethyl
<i>et al</i>	et alli (and others)
e.u.	entropy units ( $\text{JK}^{-1}\text{mol}^{-1}$ )
FAB	fast atom bombardment (MS)
g	gram
$\text{gl}^{-1}$	grams per litre
hr.	hour
Hz	Hertz
HR	high resonance
ICP-AES	inductively coupled plasma optical emission spectrometry
IR	infra-red
$\text{JK}^{-1}\text{mol}^{-1}$	Joules per Kelvin per mole
$K_a$	acid dissociation constant
K	equilibrium constant
kg	kilogram
$\text{kJmol}^{-1}$	kilo Joules per mole
m	medium (IR)
m	multiplet (NMR)
mm	millimetre
<i>m</i>	meta
mol	moles
mmol	milli moles
<i>m/z</i>	mass per unit charge
M	molar
Me	methyl
MHz	mega Hertz
min	minute
mp	melting point
NMR	nuclear magnetic resonance
no.	number
n	normal (alkyl chain)
MS	mass spectrometry
<i>o</i>	ortho
<i>p</i>	para
pH	negative logarithm (base ten) of the hydrogen ion concentration
$\text{pH}_{1/2}$	pH at which half the metal is extracted into the organic phase
$\text{pK}_a$	negative logarithm (base ten) of the acid dissociation constant
pp.	pages
ppm	parts per million



q	quartet
R	residual factor (X-ray)
$R_{\text{int}}$	independent reflections
s	strong (IR)
s	singlet (NMR)
t	triplet (NMR)
t	tertiary
T	temperature
THF	tetrahydrofuran
<i>trans</i>	<i>transoid</i>
U	crystal volume
UV	ultra violet
V	volts
vol.	Volume
vpo	vapour pressure osmometry
$\nu$	wavenumber (IR)
w	weak
$wR(F^2)$	weighted residual factor
Z	number of asymmetric units per unit cell
Z	Zusammen (isomerism)

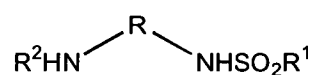
## Thesis Format

Each chapter in this thesis is written as a separate entity, such that, figures, tables and references are individual to each chapter. However, the numbering of compounds runs through the thesis. All X-ray data may be found on the compact disk at the back of the thesis. It must be noted that estimated standard deviation values for all hydrogen bond lengths are not quoted as it was not possible to determine the exact position of some hydrogen atoms. The compound numbering for chapters 2-6 is summarised in the following section

## Index of compounds

### Chapter 2:

#### Monosulfonamidodiamine ligands



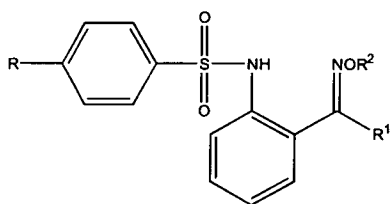
	R	R <sup>1</sup>	R <sup>2</sup>
1	-(CH <sub>2</sub> ) <sub>2</sub> -	tolyl	H
2	-(CH <sub>2</sub> ) <sub>2</sub> -	<sup>t</sup> BuPh	H
3	-(CH <sub>2</sub> ) <sub>2</sub> -	tolyl	benzyl
4	-(CH <sub>2</sub> ) <sub>2</sub> -	tolyl	2-ethylhexyl
5	-(CH <sub>2</sub> ) <sub>3</sub> -	tolyl	H
6	-(CH <sub>2</sub> ) <sub>3</sub> -	<sup>t</sup> BuPh	H
7	-(CH <sub>2</sub> ) <sub>3</sub> -	tolyl	benzyl
8	-(CH <sub>2</sub> ) <sub>3</sub> -	tolyl	2-ethylhexyl
9	-(CH <sub>2</sub> ) <sub>3</sub> -	tolyl	butyl
10	<i>o</i> -phenylene	tolyl	H
11	<i>o</i> -phenylene	<sup>t</sup> BuPh	H

## Monosulfonamidodiamine complexes

12	[Zn(1-H) <sub>2</sub> ]
13	[Ni(1-H) <sub>2</sub> ]
14	[Co(1-H) <sub>2</sub> ]
15	[Cu(1-H) <sub>2</sub> ]
16	[Cu(2-H) <sub>2</sub> ]
17	[Ni(4-H) <sub>2</sub> ]
18	[Co(4-H) <sub>2</sub> ]
19	[Cu(4-H) <sub>2</sub> ]
20	[Co(5-H) <sub>2</sub> ]
21	[Cu(5-H) <sub>2</sub> ]
22	[Cu(5-H) <sub>2</sub> ]
23	[Zn(5-H) <sub>2</sub> ]
24	[Cu(8-H) <sub>2</sub> ]
25	[Ni(10-H) <sub>2</sub> ]
26	[Cu(10-H) <sub>2</sub> ]
27	[Zn(10-H) <sub>2</sub> ]

## Chapter 3:

### Sulfonamido oxime ligands



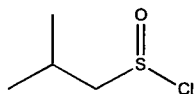
	R	R <sup>1</sup>	R <sup>2</sup>
28	methyl	methyl	H
29	<sup>t</sup> butyl	methyl	H
30	propyl	methyl	H
31	pentyl	methyl	H
32	methyl	methyl	methyl
33	methyl	phenyl	H

## Sulfonamido oxime complexes

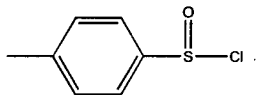
- 34 [Cu(28-H)<sub>2</sub>]  
35 [Cu<sub>4</sub>(28-H)<sub>2</sub>(28-2H)<sub>2</sub>(MeOH)<sub>2</sub>(MeO)<sub>2</sub>]  
36 [Ni(28-H)<sub>2</sub>]  
37 [Ni(28-H)<sub>2</sub>]  
38 [Ni<sub>2</sub>Na<sub>2</sub>(28-H)<sub>2</sub>(28-2H)<sub>2</sub>(MeOH)<sub>4</sub>]  
39 [Ni<sub>4</sub>(OH)<sub>2</sub>(28-H)<sub>2</sub>(28-2H)<sub>2</sub>(OCH<sub>3</sub>)<sub>4</sub>]  
40 [Ni(30-H)<sub>2</sub>]  
41 [Cu(33-H)<sub>2</sub>]

## Chapter 4:

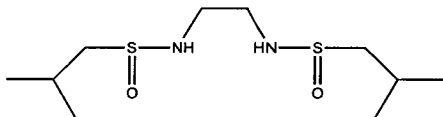
42



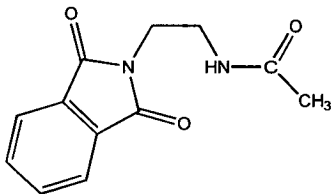
43



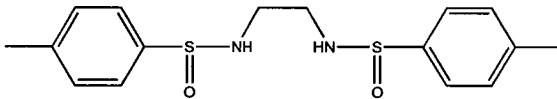
44



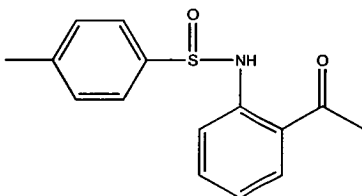
45



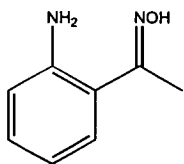
46



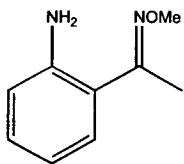
47



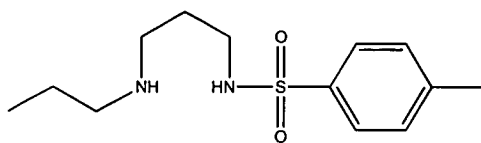
48



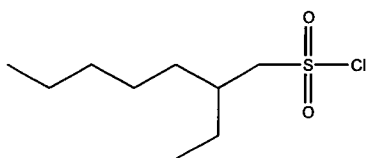
49



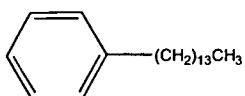
50



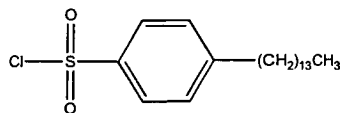
51



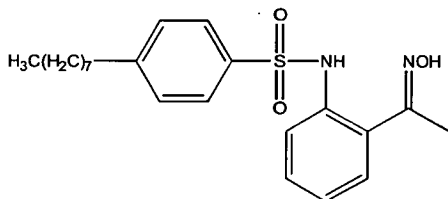
52



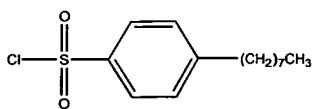
53



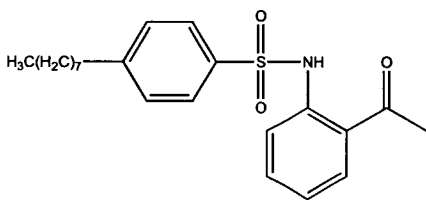
54



55

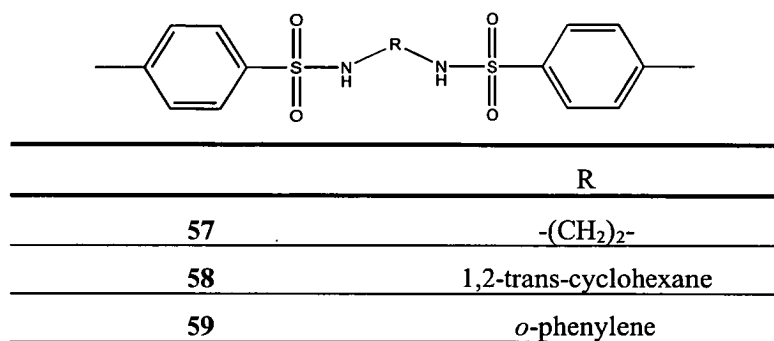


56



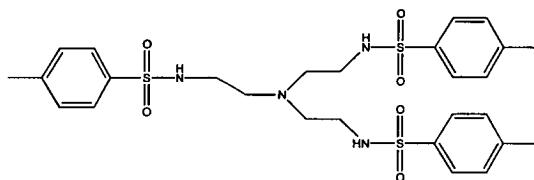
## Chapter 5:

### Bis-sulfonamidodiamine ligands

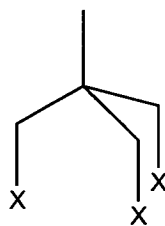


### Tris-sulfonamidotriamine ligands

60

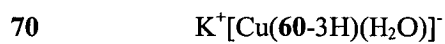


X	
61	-NHTs
63	-CONHOCH <sub>2</sub> C <sub>6</sub> H <sub>6</sub>
64	-NH <sub>3</sub> <sup>+</sup> Br <sup>-</sup>

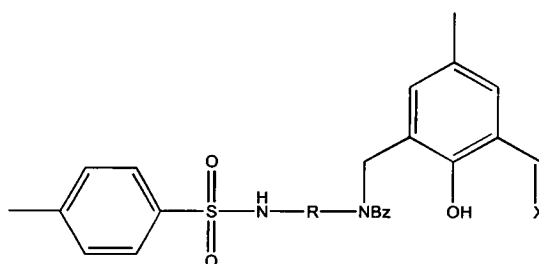


	X
62	-NHTs
65	-OTs
66	-N <sub>3</sub>
67	-NH <sub>2</sub>
68	-OSO <sub>2</sub> CH <sub>3</sub>
69	-Br

### Tris-sulfonamidotriamine complexes

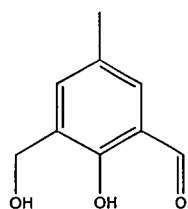


### Chapter 6:

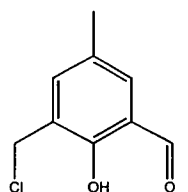


	R	X
73	-(CH <sub>2</sub> ) <sub>2</sub> -	NOH
77	-(CH <sub>2</sub> ) <sub>2</sub> -	O
72	-(CH <sub>2</sub> ) <sub>3</sub> -	NOH
76	-(CH <sub>2</sub> ) <sub>3</sub> -	O

74



75



### Complexes

- |    |   |
|----|---|
| 78 | [Cu(72-H) <sub>2</sub> ]                |
| 79 | [Ni(72-H) <sub>2</sub> ]                |
| 80 | [Cu(73-H) <sub>2</sub> ]                |
| 81 | [Cu <sub>2</sub> (73-2H) <sub>2</sub> ] |
| 82 | [Ni(73-H) <sub>2</sub> ]                |
| 83 | [Co(73-H) <sub>2</sub> ]                |



**Chapter 1 :**  
**Introduction**

<b>Contents</b>	<b>Page</b>
1.1 Aims .....	3
1.2 The science of metal recovery .....	3
1.2.1 Pyrometallurgy .....	3
1.2.2 Hydrometallurgy .....	5
1.3 The hydrometallurgical procedure of copper .....	8
1.3.1 Leaching .....	9
1.3.2 Extraction .....	9
1.3.3 Stripping .....	10
1.3.4 Electrowinning .....	10
1.4 P50: Avecia's reagent for copper recovery .....	12
1.5 The design of an extractant.....	13
1.5.1 The thermodynamic stability of complexes .....	14
1.5.2 The chelate effect .....	16
1.5.3 Metal geometry and ligand flexibility .....	18
1.5.3.1 The coordination chemistry of cobalt .....	18
1.5.3.2 The coordination chemistry of nickel .....	19
1.5.3.3 The coordination chemistry of copper .....	20
1.5.3.4 The coordination chemistry of zinc .....	20
1.6 Objectives .....	21
1.7 Supramolecular chemistry .....	21
1.7.1 Crystal engineering.....	22
1.7.2 The hydrogen-bond .....	23
1.7.3 The design of a supramolecular synthon .....	24
1.7.4 The sulfonamide group as a supramolecular synthon .....	26
1.8 Sulfonamides .....	27
1.8.1 Synthesis of sulfonamides .....	28
1.8.2 Sulfonamides as ligands .....	30
1.8.3 Sulfonamide complexes as metal extractants .....	40
1.9 References .....	46

## 1.1 Aims

The aim of the thesis was to establish whether secondary bonding, *e.g.* hydrogen-bond formation can be exploited in the design of ligands to be used in metal extraction processes. Principles of supramolecular chemistry and crystal engineering will be employed in the design of such ligands. It is of particular interest to establish whether such secondary bonding can be used to enhance the strength and selectivity of metal extractants. If observed this could potentially lead to the development of relatively simple, and thus inexpensive, tailor-made extractants. The solid state structure of the designed ligands and their complexes will be investigated and the colligative properties of the ligands in solution will be studied along with the solvent extraction properties of the systems. The class of ligands chosen to begin this investigation is based upon a bidentate amine-sulfonamide framework.

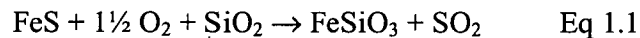
## 1.2 The science of metal recovery

Currently there are two main methodologies for the recovery of metals from their ores, pyrometallurgy, an ancient practice of removing metal from rock by smelting, and hydrometallurgy which involves the recovery of metals *via* their dissolution as ions in water.

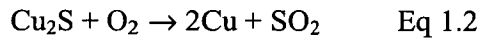
### 1.2.1 Pyrometallurgy

Pyrometallurgy is an excellent method of producing metal from ores, which are rich in the required metal. Until the 1970s this was the only technology used to produce base metals. An example is the production of copper by smelting.<sup>1</sup> The sulfide ore is concentrated using froth flotation methods<sup>1</sup> where the ore is first crushed to produce a slurry which is passed into a flotation tank where it is aerated. An oil reagent, to assist frothing, and a surfactant salt which makes the copper sulfide ore

particles hydrophobic are added. Air bubbles stick to the copper mineral particles causing them to float to the surface and form a froth “concentrate” which is then roasted in a flash furnace with lime, CaO, and a converter slag at approximately 1300°C. This produces two immiscible layers, a slag of molten oxides of iron, silicon and other impurities and a second “matte” layer containing Cu<sub>2</sub>S and some FeS. Air is then blown through the matte layer in a converter and sand added producing a silicate slag from the FeS (Equation 1.1).



The Cu<sub>2</sub>S is then reduced to copper above 1250°C (Equation 1.2).



Copper of 98% purity is produced and this can be purified further electrolytically.

To generate the high temperatures needed to produce molten ores the plant often requires a lot of energy. This leads to difficult and hazardous working conditions. Pyrometallurgical processing of sulfidic ores creates the potential problem of sulfur dioxide being discharged into the atmosphere. If the level of production is high enough it can be used to produce acids however when production is low this method of disposal is not available and alternative, more expensive, methods must be found such as the scrubbing of the gases with water which then must be disposed of.<sup>2</sup> Some residues of pyrometallurgical processes such as slags in the silicate phase do not chemically pollute the environment<sup>2</sup> but the sheer quantity of material to be disposed of and landfill shortages make its disposal a sensitive public relations issue.

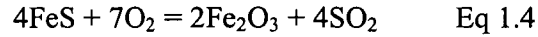
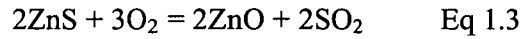
### 1.2.2 Hydrometallurgy

Modern hydrometallurgy began at the end of the 19<sup>th</sup> century with the discovery of two major processes, the cyanidation process and the Bayer process.<sup>2</sup> It has developed significantly since then and has now replaced pyrometallurgical methods in some areas. One of the main reasons why the replacement of pyrometallurgical methods with hydrometallurgical ones is so attractive is that sulfide ores can potentially be treated without the generation of SO<sub>2</sub>.<sup>2</sup>

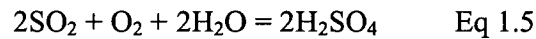
Hydrometallurgy requires lower operating temperatures than pyrometallurgy. Working temperatures are usually less than 100°C compared with approximately 1200°C used to smelt the ores.<sup>2</sup> This means that less fuel, and less heat management technology are needed and in addition that less harmful dust is created.

There are disadvantages linked specifically with hydrometallurgy. Water pollution can be a problem due to sludging after leaching and the draining of liquid waste streams. The finely divided waste residues of hydrometallurgy can be difficult to dispose of, when exposed to the atmosphere they can create dust problems in dry conditions and in wet conditions release metal ions leading to contamination of the surrounding area. Also when solvent extraction forms part of the process the toxicity and flammability of the hydrocarbon solvents used are of concern.<sup>3</sup>

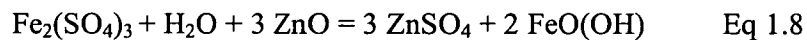
Metal recovery from primary sources involves four “unit operations”; concentration, separation, reduction and refining. Concentration describes the whole process from start to finish, an ore of low metal content is converted to pure metal. Separation involves the removal of all other materials from the metal, the last stage of which is the “reduction” of metal compounds to the metal. The refining of the metal takes place when very pure metal is required. The separation and reduction steps can be achieved either pyrometallurgically or hydrometallurgically. An example of a hydrometallurgical process is the roast/neutral-leach/electrowinning method used to produce zinc. The concentration of the sulfidic ore is achieved by froth flotation and the concentrate is then roasted to produce zinc oxide<sup>4</sup> (Equations 1.3 and 1.4).



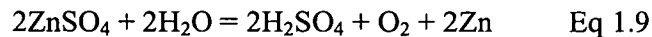
Sulfuric acid is produced from the sulfur dioxide emitted which is then used to yield metal sulfates (Equations 1.5, 1.6 and 1.7).



There are significant amounts of impurities in the ore such as iron, manganese, lead and copper which must be removed<sup>5</sup> from the impure solution of metal ions before the zinc is electrowon. This involves the selective leaching or precipitation of the impurities. Iron is removed by neutral leaching which precipitates the iron in the form of natural iron(III) oxides, hydroxides, and oxyhydroxides. (Equation 1.8).



The zinc is then electrowon using aluminium cathodes (Equation 1.9).



The most difficult aspect of zinc recovery is the elimination of all other metal salts and impurities from the zinc sulfate solution. Solvent extraction “is a separation process that depends on the transfer of the component to be separated from one liquid phase to a second liquid phase that is immiscible with the first”.<sup>6</sup> This technique can be used to produce a pure solution of metal ions from an impure leach

solution, hence if it were to be applied to zinc production it would enormously simplify the separation step by selectively extracting zinc leaving all other metals in the raffinate, the depleted solvent. Stripping the loaded organic solution could then be used to generate a pure electrolyte for “electrowinning”. Concentration would also be unnecessary as a strong and highly selective reagent removes the need for a concentrated leach solution. Concentration is achieved by the extraction and stripping processes.

Solvent extraction was first used in hydrometallurgy by the Manhattan Project<sup>7</sup> in the USA to produce high purity uranyl nitrate solution.  $\text{HNO}_3$  was used to dissolve uranium concentrate, the uranium was then selectively extracted by diethylether and this solution was stripped with water to give a pure uranyl nitrate solution. Other pure expensive metals were then produced in this way. In the 1960s this method was first applied to the extraction of copper, a relatively cheap metal.

To explain why hydrometallurgy is replacing pyrometallurgy in the production of some metals the economics of the two technologies must be compared. Pyrometallurgy can be a very economical method to treat metal rich ores. However, for poorer low grade ores this treatment is not as cost effective. The use of selective extractants in hydrometallurgy mean that the metal may be recovered in a more efficient way. The potential range of extractants makes this process viable for low grade ores and more specialised small scale productions.

In copper production a sulfide ore is required and in most cases deposits are found under a layer of oxidic copper ore,  $\text{CuO}$ . Therefore to recover the sulfidic ore the oxidic ore has also to be removed which until the development of the solvent extraction process had no known use and was left in heaps as waste. This has meant that a ready supply of this ore is available at a lower cost than sulfide ore which is becoming less readily available.

### 1.3 The hydrometallurgical procedure of copper

The hydrometallurgically based process for copper production involves four steps, leaching, extraction, stripping and electrowinning (Figure 1.1). The heap leach pad (1) consisting of the oxide ore is sprayed with sulfuric acid, thus leaching metal ions into what is known as the “pregnant leach solution”. This is stored in a pond (2) before it is mixed with the immiscible extractant for approximately two minutes. The mixture passes over a weir to a settling tank (3). Upon separation the aqueous raffinate is returned to the heap leach pad and the organic phase containing pure copper is transferred to a second mixer where it is contacted with a second acidic stripping solution of low pH. The mixture then passes over a second weir to settling tank (4). The separated regenerated organic extractant is recycled and the concentrated copper aqueous solution, the “advanced electrolyte”, passes into the electrowinning tankhouse (5).

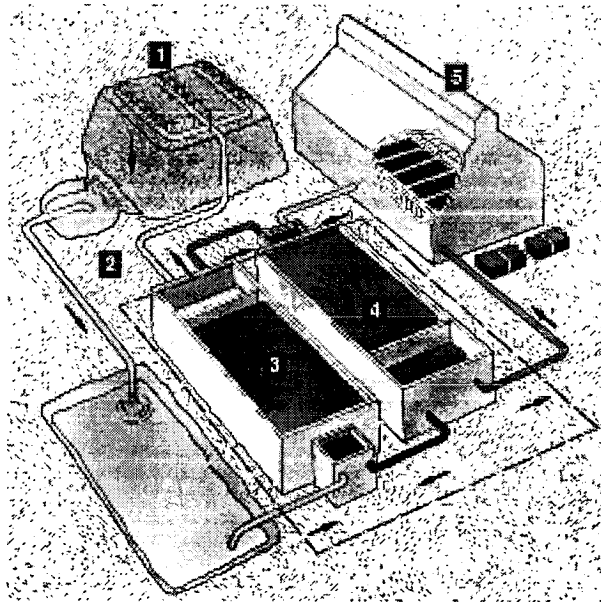
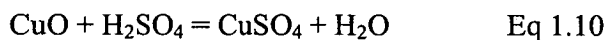


Figure 1.1: Solvent extraction plant for copper recovery.<sup>8</sup>



### 1.3.1 Leaching

In most of the current operations the copper is leached from oxidic ores using sulfuric acid (Equation 1.10).



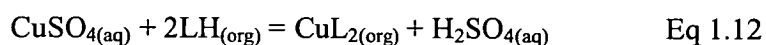
Heap leaching was first practiced in the Harz mountains area of Germany and in the Rio Tinto mines in Spain in the sixteenth century<sup>9</sup> where copper sulfate was leached from pyrite containing copper sulfide by an oxidative process involving rainwater and air (Equation 1.11).



Modern plants use aqueous  $\text{H}_2\text{SO}_4$  at pH 2 to leach metals from crushed oxidic or “transition ores” (partially oxidised sulfides). The metal oxides react with the sulfuric acid according to Equation 1.10. This is not a selective process and many metals are dissolved leading to a dilute and impure solution which is referred to as the pregnant leach solution. The solvent extraction step must concentrate and purify the solution to provide a copper sulfate solution suitable for use in the electrolysis tankhouse.

### 1.3.2 Extraction

The extraction stage is used to selectively transport copper from the aqueous phase into the immiscible organic phase (Equation 1.12).

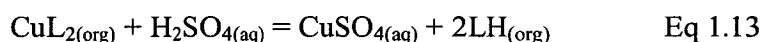


This is accomplished by the hydrocarbon-soluble acidic ligand, LH, which forms a neutral copper complex with a metal to ligand ratio of 1:2 in hydrocarbon solvents. This complex must have a very low solubility in the aqueous raffinate. This

produces a “loaded-organic” phase containing only copper and regenerates sulfuric acid for leaching.

### 1.3.3 Stripping

The third step involves stripping the copper out of the complex into a second aqueous phase, the “advanced electrolyte”, reversing the complex formation by using stronger sulfuric acid with  $\text{pH} \approx 0$ , (Equation 1.13).



The sulfuric acid provides protons to regenerate the extractant which is recycled back to the extraction step, and produces a pure and concentrated aqueous solution of copper sulfate.

### 1.3.4 Electrowinning

This strip solution, advanced electrolyte, is sent to the tankhouse where the copper is electrowon to produce copper of at least 99.99% purity (Equation 1.14).<sup>10</sup>



Figure 1.2 shows schematically how the reagents used are recycled to make solvent extraction an economically favourable process.

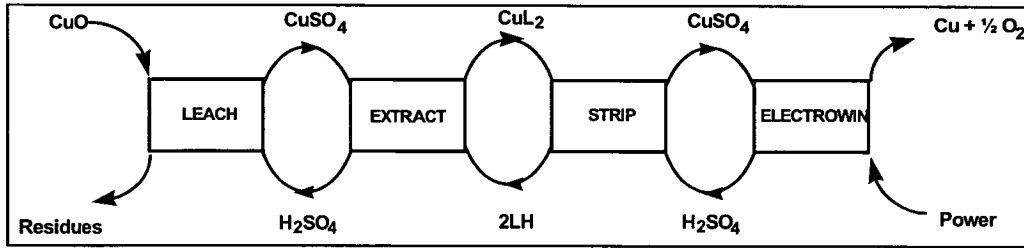
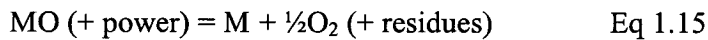
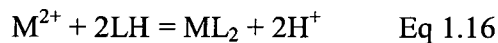


Figure 1.2: The four stages of the solvent extraction process.

The sulfuric acid used to leach the copper is regenerated in the extraction step, the ligand used to extract the metal into the hydrocarbon phase is regenerated when the copper is stripped back and finally the sulfuric acid used to strip the metal into the advanced electrolyte is regenerated when the copper is electrowon. This leads overall to Equation 1.15.



The mechanism behind the solvent extraction process is pH swing based. Equation 1.16 is the important equilibrium to consider.



This equation leads to the following equilibrium constant describing the transportation of copper between phases (Equation 1.17).

$$K_{eq} = \frac{[ML_2][H^+]^2}{[M^{2+}][LH]^2} \quad \text{Eq 1.17}$$

Whether the metal is transferred to the organic phase or back into an aqueous phase depends on the pH of the system. As the concentration of hydrogen ions varies with pH the equilibrium is moved to the left or the right to maintain  $K_{eq}$ . The concentration of hydrogen ions in the pregnant leach solution is low and so more

hydrocarbon soluble metal complex is produced. The reverse occurs during the stripping stage when the  $[H^+]$  is high.

#### 1.4 P50: Avecia's reagent for copper recovery

The most important class of copper extractants is based on phenolic oximes. These are currently marketed by Avecia and Henkel. The structure of such extractants is below in Figure 1.3. Avecia supplies 5-nonylsalicylaldoxime as P50 where R is H and  $R^1$  is a branched nonyl chain. Henkel's extractants are ketoximes where R is a methyl and  $R^1$  a solubilising branched alkyl group. Both companies supply the ligands as a mixture of isomeric forms of the solubilising group  $R^1$  to inhibit crystallisation.

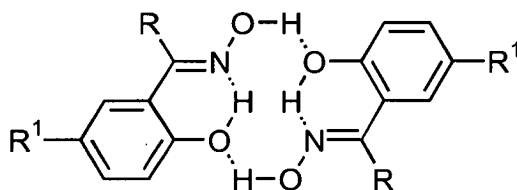


**Figure 1.3:** A hydrogen-bonded P50 dimer.

Various factors contribute to why P50 is a very effective copper extractant. The Irving-Williams series predicts that the most stable complexes of divalent first transition series metals will be formed with copper ions. Secondly, the nitrogen and oxygen combination of donor atoms is favoured by copper and finally it benefits from the chelate effect. However many bidentate ligand systems with identical donor atoms are much weaker extractants than P50 therefore these observations do not fully account for the exceptional properties of P50.

One difference between P50 and other extractants which may account for its superiority is the ability of P50 ligand to preorganise itself into dimers (Figure 1.3) and also to form *intra*-molecular hydrogen-bonds in the copper complex creating a *pseudo*-macrocycle around the copper(II) ion (Figure 1.4).<sup>11</sup>

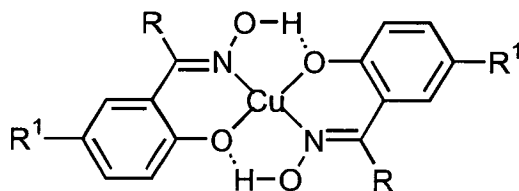


**Figure 1.4:** A 1:2 copper, P50 complex.

Important features of the phenolic oxime extractants are their very high selectivity for copper over iron and a “ $\text{pH}_{1/2}$ ” value of less than two. The pH at which an extractant is loaded to half its maximum capacity is called its  $\text{pH}_{1/2}$ . A low value of  $\text{pH}_{1/2}$  is desirable so that the pH of the pregnant leach solution does not have to exceed two, which would create conditions for the unfavourable precipitation of iron.

The use of P50 in the extraction step of the process has led to the price of copper dropping significantly. The price per kilogram<sup>10</sup> of copper obtained by pyrometallurgical processing is \$2.20 in comparison with 90 cents per kilogram when a hydrometallurgical solvent extraction process has been used.

## 1.5 The design of an extractant

When designing a new extractant many things must be considered. First of all cheap and accessible precursors of the ligand must be available, the ligands must be able to form stable complexes and have the ability to preorganise. Selectivity for one metal is very important and this can often be optimised at designated pH ranges. The ligands as well as the resulting complexes must have high solubility in hydrocarbon solvents. The kinetics of extraction must be fast in order to avoid having to use large

holding tanks or reaction vessels. The metal complexation should also be reversible so that the metal can be stripped from the organic phase. The reagent should be relatively stable so that it can be recycled repeatedly, it should be water insoluble to prevent significant loss into the aqueous phase, further the reagent should not cause or stabilize emulsions. The reagent should not react with or load significant quantities of acid. The structure of the ligands can be modified to try and improve these properties. Theories, which help us, make preliminary assumptions about ligand behaviour are explained in the following sections.

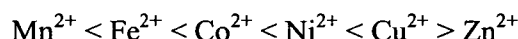
### 1.5.1 The thermodynamic stability of complexes

The principle factors affecting thermodynamic stability are the nature of the ligand and the nature of the metal. Ligand donor atoms are Lewis bases and cationic metal centres are Lewis acids, they can be classified as either hard or soft depending on the stability of the complex they form with certain acids or bases respectively. Pearson first introduced such classification.<sup>12,13</sup> For a soft base the donor atom may be easily polarised, has low electronegativity and is easily oxidised. They are also associated with empty, low-lying orbitals, examples are  $I^-$ ,  $CN^-$  and  $H^-$ . A hard base is of low polarisability and high electronegativity, they are difficult to oxidise and are associated with empty orbitals of high energy and are hence inaccessible, for example  $F^-$ ,  $NH_3$  and  $OH^-$ . Soft acids have an acceptor atom of low positive charge and large size and several easily excited outer electrons, *e.g.*  $Cu^+$ ,  $Au^+$  and  $Cd^{2+}$ . Hard acids have an acceptor atom of high positive charge and small size and do not have easily excited outer electrons. Examples are  $H^+$ ,  $Na^+$  and  $Al^{3+}$ . Pearson stated that “hard acids prefer to coordinate to hard bases and soft acids to soft bases”.<sup>12</sup> Therefore in the ligand design to selectively coordinate one metal of a specific oxidation state, the choice of donor atoms is very important. Some Lewis acids and bases do not fall easily into either the hard or the soft category and are called borderline. The following table gives examples of Lewis acids and bases.

**Table 1.1:** The classification of Lewis acids and bases.<sup>13</sup>

	Hard	Borderline	Soft
Acids	H <sup>+</sup> , Li <sup>+</sup> , Na <sup>+</sup> , K <sup>+</sup> , Be <sup>2+</sup> , Mg <sup>2+</sup> , Ca <sup>2+</sup> , Cr <sup>2+</sup> , Cr <sup>3+</sup> , Al <sup>3+</sup> , SO <sub>3</sub> , BF <sub>3</sub>	Fe <sup>2+</sup> , Co <sup>2+</sup> , Ni <sup>2+</sup> Cu <sup>2+</sup> , Zn <sup>2+</sup> , Pb <sup>2+</sup> , SO <sub>2</sub> , BBr <sub>3</sub>	Cu <sup>+</sup> , Ag <sup>+</sup> , Au <sup>+</sup> , Tl <sup>+</sup> , Hg <sup>+</sup> , Pd <sup>2+</sup> , Cd <sup>2+</sup> , Pt <sup>2+</sup> , Hg <sup>2+</sup> , BH <sub>3</sub>
Bases	F <sup>-</sup> , OH <sup>-</sup> , H <sub>2</sub> O, NH <sub>3</sub> , CO <sub>3</sub> <sup>2-</sup> , NO <sub>3</sub> <sup>-</sup> , O <sub>2</sub> <sup>-</sup> , SO <sub>4</sub> <sup>2-</sup> , PO <sub>4</sub> <sup>3-</sup> , ClO <sub>4</sub> <sup>-</sup>	NO <sub>2</sub> <sup>-</sup> , SO <sub>3</sub> <sup>2-</sup> , Br <sup>-</sup> , N <sub>3</sub> <sup>-</sup> , N <sub>2</sub> , C <sub>6</sub> H <sub>5</sub> N, SCN <sup>-</sup>	H <sup>-</sup> , R <sup>-</sup> , CN <sup>-</sup> , CO, I <sup>-</sup> , SCN <sup>-</sup> , R <sub>3</sub> P, C <sub>6</sub> H <sub>6</sub> , R <sub>2</sub> S

For metal ions which are neither particularly hard or soft a series called the ‘Irving-Williams’ series<sup>14</sup> has been established to predict the stability of complexes formed with a given ligand (Figure 1.5).

**Figure 1.5:** The Irving Williams series.

The series may be explained in terms of two physical properties of the M<sup>2+</sup>.<sup>15</sup> The greater the power of M<sup>2+</sup> to accept electrons the higher the stability constant of complex formation, *i.e.* if the second ionisation potential of M is high it can be said that the metal can accept electrons easily. The series can also be explained by the ionic potential of the ion or  $z/r$ , where  $z$  is the ionic charge and  $r$  the ionic radius, which indicates the hardness of the acid.

$\Delta G$  is determined by  $\Delta S$  and  $\Delta H$  according to Equation 1.18 and shows how stable a complex is.

$$\Delta G = \Delta H - T\Delta S \quad \text{Eq 1.18}$$

The Gibbs free energy must be negative for a complex to form spontaneously.<sup>16</sup> Many things can affect the entropy and enthalpy of a complex and these are summarised in Table 1.2.

**Table 1.2:** Factors influencing solution stability of complexes.<sup>17</sup>

Enthalpy effects	Entropy effects
<ul style="list-style-type: none"> <li>• Variation of bond strength with electronegativities of metal ions and ligand donor atoms.</li> <li>• Ligand field effects.</li> <li>• Steric and electrostatic repulsion between ligands in complex.</li> <li>• Enthalpy effects related to conformation of uncoordinated ligand.</li> <li>• Other coulombic forces involving chelate ring formation.</li> <li>• Enthalpy of solution of ligands and that of complexes.</li> <li>• Changes in bond strength when ligand is charged (same donor and acceptor atom).</li> </ul>	<ul style="list-style-type: none"> <li>• Number of chelate rings.</li> <li>• Size of chelate rings.</li> <li>• Changes of solvation of ligands and metal ion on complex formation.</li> <li>• Arrangement of chelate rings.</li> <li>• Entropy variations in uncoordinated ligands.</li> <li>• Effects resulting from differences in configurational entropies of the ligand in complex compound.</li> <li>• Entropy of solution of ligands.</li> <li>• Entropy of solution of coordinated metal ions.</li> </ul>

### 1.5.2 The chelate effect

The chelate effect<sup>14</sup> refers to the observation that a complex, which contains chelated rings, is usually more stable than the most similar complex containing only monodentate ligands. An example of this can be seen in Figure 1.6.

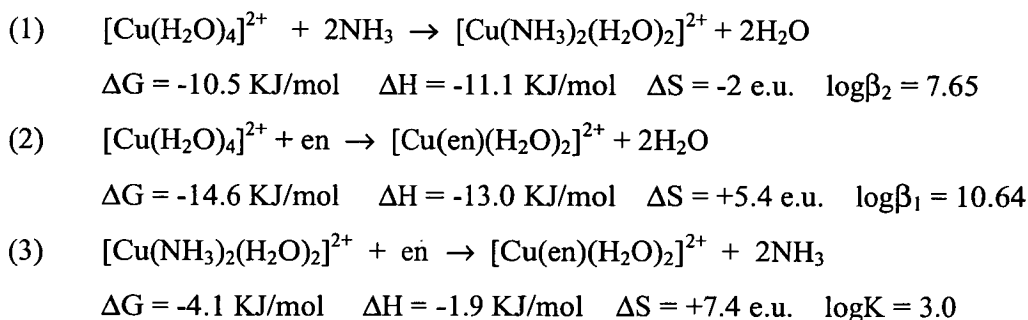


**Figure 1.6:** An illustration of the chelate effect.



The more negative value of  $\Delta G$  of (2) than (1) tells us that replacement of two coordinated water molecules by the chelating 1,2 diaminoethane (en) ligand is more thermodynamically favourable than replacement by two ammonia ligands. As a consequence the displacement of two ammonia ligands by 1,2-diaminoethane is thermodynamically favourable (3).

The enthalpy change incurred by the substitution of monodentate by bidentate ligands into a complex can become positive if significant steric strain is associated with forming the chelate ring. Strain depends on the size of the rings involved, five membered rings are the most stable followed by six and seven membered rings. In these cases  $\Delta G$  is only negative when a large positive entropy change occurs. When most simple metal salts are dissolved in water the metal ion is in the form of an aqua complex and so the formation of a complex involves the displacement of water molecules by ligands.

Complex stability usually increases as the number of rings formed in the complex increases and a macrocyclic ligand forms a more stable complex than the similar open chain ligand.<sup>18</sup> Figure 1.7 shows an example of this effect. The entropy change involved in this reaction will be positive as two rigid starting materials produce one rigid product and the flexible long chain ligand. The complexation of the macrocycle and the displacement of the more flexible ligand is enthalpically favourable as enthalpic repulsions between nitrogen lone pairs are greater for the macrocyclic ligand as it is unable to move to create the maximum distance between the nitrogens unlike the long chain ligand. Other factors to consider are the probable proximity of remaining binding sites of a macrocycle when one atom is bound in contrast with those of an open chain polydentate ligand or simple monodentate ligands. The effects of cooperative binding will however be reduced for open chain polydentate ligands with longer backbones as here remaining binding sites will have a higher probability of being close to other metal centres forming a bridging ligand.

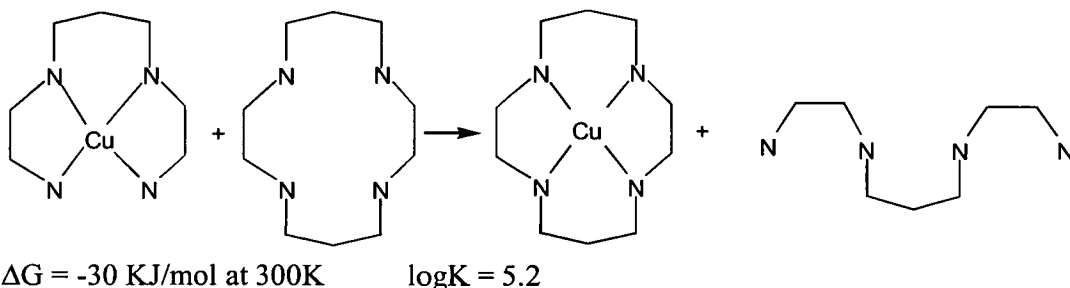


**Figure 1.7:** Preferential binding of a tetradentate macrocycle over a similar open chain ligand.

Macrocyclic ligands are known for their selectivity and ability to form very stable complexes and consequently could be useful in metal recovery processes. The drawback is that they are very expensive to synthesise and the kinetics of metal complexation/decomplexation are often poor. By using simpler ligands which are easy to synthesise, but which have the possibility to organise themselves into *pseudo*-macrocycles it should be possible to develop much cheaper “strong” and selective ligands which show good kinetics of metal transport.

### 1.5.3 Metal geometry and ligand flexibility

It is well known that the preferred geometry of complexes vary from metal to metal. This is an important factor when we consider which metal complexes would benefit from the complexation of a ligand which has been designed to form a planar tetradentate *pseudo*-macrocyclic structure to enhance complex stability. The coordination chemistry of four metals, cobalt, nickel, copper and zinc, which are commonly found in the leach stream are mentioned briefly below.

#### 1.5.3.1 The coordination chemistry of cobalt

Complexes of cobalt in oxidation states I, II, III and IV are known, however cobalt tends to be stable in the lower oxidation states and Co(II) complexes are the most common. Co(II) forms numerous complexes, most of which are octahedral or tetrahedral however five coordinate species are also formed. A tetrahedral geometry

is common for Co(II) as a  $d^7$  electron configuration disfavours a tetrahedral geometry relative to an octahedral one to a smaller extent by ligand field stabilisation energies.<sup>19</sup> Very few low spin Co(II) complexes are encountered, and very strong field ligands are necessary to achieve the required ligand field splitting parameter.<sup>20</sup> A Jahn-Teller distortion is observed for such low spin octahedral compounds.

In the presence of oxygen and stabilising ligands with strong ligand field contributions, in particular those incorporating N donors, the Co(II) ion is quite readily oxidised to Co(III).<sup>19</sup> Almost all of these compounds are octahedral, however tetrahedral, planar and anti prismatic complexes are known.

### 1.5.3.2 The coordination chemistry of nickel

Complexes of nickel in oxidation state I to IV are known however Ni(II) complexes are by far the most common.<sup>21</sup> Unlike cobalt, nickel commonly shows only the +2 oxidation state in aqueous solution.<sup>22</sup> Most Ni(II) complexes have coordination numbers of four, five and six. Complexes with coordination numbers of three, seven and eight are still quite rare. The vast majority of four coordinate Ni(II) complexes are planar due to the  $d^8$  configuration. The eight electrons occupy four d orbitals but leave the strongly anti-bonding  $dx^2-dy^2$  orbital vacant. Therefore only ligands with steric bulk are able to force the complexes from planarity. Trigonal bipyramidal and square pyramidal five coordinate geometries occur with nickel and the complexes are usually low spin. For almost all Ni(II) six coordinate complexes the metal has a *pseudo*-octahedral stereochemistry.<sup>23</sup> Ni(III) complexes are formed with macrocyclic or peptide type ligands.

### 1.5.3.3 The coordination chemistry of copper

Coordination numbers of up to eight with copper oxidation states of I to IV are known, with Cu(I) and Cu(II) oxidation states as the most abundant.<sup>24</sup> Cu(I) is readily oxidised to Cu(II) and the stability of Cu(I) complexes depends upon the nature of the anions or the ligands present, however further oxidation to Cu(III) is more difficult. Cu(I) is a soft acid and prefers sulfur and phosphorus based ligands whereas Cu(II) is a borderline hard acid and prefers oxygen and nitrogen based ligands.<sup>25</sup> The solid state stereochemistry of Cu(I) is dominated by four coordination, which are generally tetrahedral. A significant number of two, three and five coordinate complexes are known however six coordination is unknown.

For Cu(II) the best donor is oxygen followed by nitrogen and chloride ions.<sup>25</sup> The majority of six coordinate Cu(II) complexes involve a Jahn-Teller distorted octahedral structure. Five coordinate Cu(II) may have regular square pyramidal or trigonal pyramidal stereochemistry but generally involve distortion. A regular square planar geometry may be achieved however it may involve a slight tetrahedral distortion. A regular tetrahedral geometry is not possible and a significant compression along the  $S_4$  symmetry axis is always involved.

Cu(III) complexes almost all have square or five-coordination geometry, until quite recently only few Cu(III) compounds were known however it has since been established that Cu(III) has an important biological role and a number of model complexes have been made.<sup>24</sup>

### 1.5.3.4 The coordination chemistry of zinc

Zinc is regarded<sup>26</sup> as a non-transition element as it does not form any compounds where the d shell is other than full as only the two 4s electrons are readily lost. However Zn(II) has some resemblance to d-group elements in its ability to form

complexes, particularly with ammonia, amines, halide ions and cyanide. A large number of Zn(II) complexes are known with oxygen, nitrogen, sulfur and to a lesser extent phosphorus ligands.<sup>27</sup> Coordination numbers of four, five and six are commonly known with five being the most common. Because for Zn(II) complexes there is no ligand field stabilization energy (LFSE) their stereochemistry is determined solely by considerations of size, electrostatic forces and covalent bonding forces.

## 1.6 Objectives

The objective of this thesis was to identify new classes of compounds which have hydrogen-bond donor and acceptor sites which can form strong *inter*-ligand hydrogen-bonds in metal complexes, generating *pseudo*-macrocyclic structures and thus beneficially influencing the properties of the extractants. The structures produced by secondary bonding were studied both for the free ligand and the metal complexed species.

Assembled systems have been characterised using both solid state and solution techniques. The effects of such self-assembly will be evaluated with respect to ligand strength and selectivity. This will determine how important preorganisation and other design criteria are in the design of new metal extractants.

## 1.7 Supramolecular chemistry

The self assembly of complementary components into designed architectures has become an important theme in recent supramolecular chemistry. Many studies have been undertaken to try to establish how by careful molecular design the substructural units in a supermolecule can be identified and hence the structure of a material can be predicted. To quote Jean-Marie Lehn 'supermolecules are to molecules and the *inter*-molecular bond what molecules are to atoms and the covalent bond.'<sup>28</sup> Thus in supermolecular design *inter*-molecular bonds have a very important role to play and

the tertiary structure within crystals is determined solely by the strength and directionality of *inter*-molecular or *inter*-ionic interactions.<sup>29</sup> Hydrogen-bonds are often used as the *inter*-molecular link as they are directional enough that the orientation of molecules can be predicted with a reasonable degree of accuracy. However, there is no absolute correlation between lone-pair regions and acceptor angles.<sup>30</sup> By the designed placement of hydrogen-bond donor and acceptor functional groups into a molecule a supramolecular synthon can be generated. The term supramolecular synthon is used to describe a structural unit within a supermolecule which is assembled involving intermolecular interactions.<sup>31</sup>

### 1.7.1 Crystal engineering

‘Crystal engineering seeks to understand intermolecular interactions and recognition phenomena in the context of crystal packing.’<sup>31</sup> One type of directional *inter*-molecular interaction that has been widely studied in this context is the hydrogen-bond. Many recent studies into crystal engineering are centred around conventional hydrogen-bonding of the OH---O or the NH---O type.<sup>32,33</sup> However studies using weaker and possibly less directional interactions have proved successful, for example CH---O, I---I, N---Br interactions.<sup>34,35,36,37,38</sup> Methods of predicting packing arrangements based on the principle that the strongest hydrogen-bond acceptor should be paired up with the strongest hydrogen-bond donor have been proposed.<sup>39</sup> Studies into the effects of superfluous hydrogen-bond donor or acceptors in molecules on the resulting *inter*-molecular interactions have also been conducted.<sup>40,41,42</sup> It is more common that the hydrogen-bond acceptor moieties should be in excess and when this is the case the acceptors find the next most acidic hydrogens, for example, the weaker C-H---X hydrogen-bonds (X = O, N) may be formed. When there is an excess of hydrogen-bond donors, weak X-H--- $\pi$  hydrogen-bonds may be observed. A second method by which the deficiency in H-bond acceptors is accommodated is through a change in the hybridisation of the molecule.<sup>42</sup> When two NH<sub>2</sub> groups are present an NH<sub>2</sub> group can become sp<sup>3</sup> hybridised and hydrogen-bonds between the sp<sup>2</sup> hydrogens of a second NH<sub>2</sub> group

and the  $sp^3$  lone pair are seen. Despite the extensive study of hydrogen-bonding and the ability to predict the most likely and thermodynamically stable hydrogen-bonded motif for a molecule the precise solid state tertiary structure remains quite unpredictable.<sup>29</sup> This is because the effect of other non-covalent interactions or crystal packing is not yet predictable with any certainty. The role of solvent molecules may also have an important role due to their ability to act as competitive hydrogen-bond donor and acceptors or be enclathrated as guest molecules.<sup>29</sup>

### 1.7.2 The hydrogen-bond

Although many definitions of the hydrogen-bond have been published it is extremely difficult to state in a concise manner what it is. In 1989 Atkins stated that “A hydrogen-bond is a link formed by a hydrogen atom lying between two strongly electronegative atoms”.<sup>43</sup> However, in the last decade researchers have progressed from the X-H---X conventional hydrogen-bond, where X is an electronegative element, to explore the chemistry of weaker types of interaction such as the C-H---O bond which is now universally accepted as a hydrogen-bond. This bond along with many other weaker interactions falls a long way outside the description of Atkins. As the net effect of a hydrogen-bond is to weaken the X-H bond they can be detected and their energies determined by a wide range of spectroscopic, structural and thermodynamic techniques. A hydrogen-bonding interaction between neutral molecules may have a strength in the range of 10-65  $\text{kJmol}^{-1}$ , however when one component is ionic the bond strength rises to between 40 and 190  $\text{kJmol}^{-1}$ .<sup>30</sup> Hence, a strong hydrogen-bond, for example HCOOH---F- has a similar energy to the covalent F-F bond.

Interest in the role of *inter*-molecular hydrogen-bonding is wide ranging from the modelling of the self assembly properties of nucleotide bases to the use of hydrogen-bonds to control molecular aggregation.<sup>44,45,46,47</sup> An important aim of this thesis was to look at the effects which secondary bonding can have on the strength and selectivity of metal extractants. Hydrogen-bond donors and acceptors were

incorporated into the ligand design and it was therefore very important to be able to study the predicted recognition processes of the free ligand and the effect of any *intra-complex* hydrogen-bonding. X-ray crystallography was an extremely useful tool to probe the structure of molecules in the solid state however the behaviour of the ligand in solution also had to be studied. Recent studies in aprotic solvents have shown that hydrogen-bonds can form in solution, but their stabilities are highly solvent dependent.<sup>48,49,50,51</sup> There are several ways in which the solution behaviour of molecules can be studied including variable concentration <sup>1</sup>H nmr, IR, X-ray crystallography, vapour pressure osmometry, cryoscopy and ESI-MS.

### 1.7.3 The design of a supramolecular synthon

To study the effect which secondary bonding can have on the strength and selectivity of metal extractants careful ligand design is required. Primarily the size of the chelate ring and the number of donor atoms must afford a favourable metal complex geometry and the number of sites for possible deprotonation must result in a neutral complex. Hydrogen-bond donor and acceptor atoms must then be introduced so that a 'head-to-tail hydrogen-bonded macrocycle may be possible.

To begin with the most simple system a similar template to P50 was followed of two bidentate monoanionic ligands coordinating first row transition metals of oxidation state two (Figure 1.8). Each ligand requires two coordinating atoms (**X**) and one site for deprotonation (**XH**) to produce a monoanionic ligand which is essential to generate a neutral complex with solubility in non-polar hydrocarbon solvents. To enable a 'head-to-tail' hydrogen-bonded arrangement one hydrogen-bond acceptor site (**A**) and one hydrogen-bond donor site (**D**) per ligand are also required. R is a bridging group.



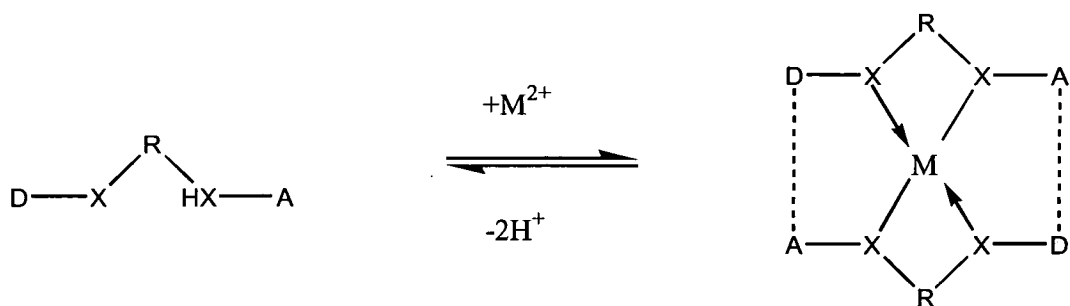


**Figure 1.8:** P50 type template for the complexation of divalent metal ions.

Structural studies of such systems showed that they were able to form *pseudo*-macrocycles. The idea of introducing *inter*-ligand hydrogen-bonding into metal complexes by design was then extended to look at similar AB type systems where ligand A incorporates two hydrogen-bond donor functions and ligand B two hydrogen-bond acceptor functions, see Figure 1.9.

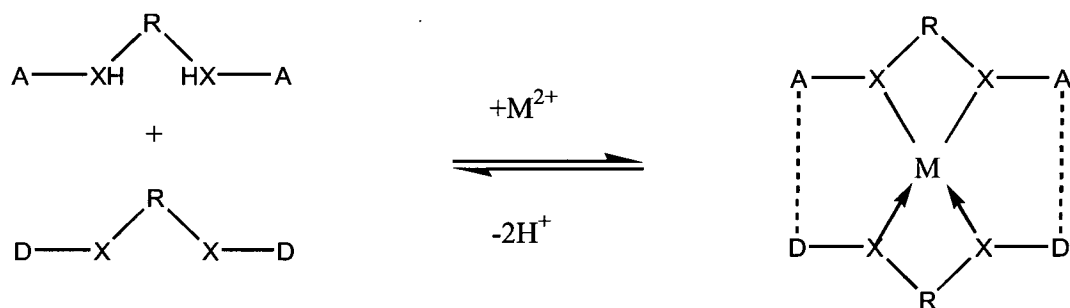


**Figure 1.9:** Bidentate AB type metal chelate systems for *pseudo*-macrocycle formation.

It was proposed that such AB type systems could lead to the greater versatility of the ligands as solvent extractants if different A type ligands (incorporating hydrogen-bond acceptor groups) and B type ligands (incorporating hydrogen-bond donor groups) may be interchanged. This may permit the fine-tuning of a system for one metal, and could also be applied to octahedral systems, Figure 1.10.

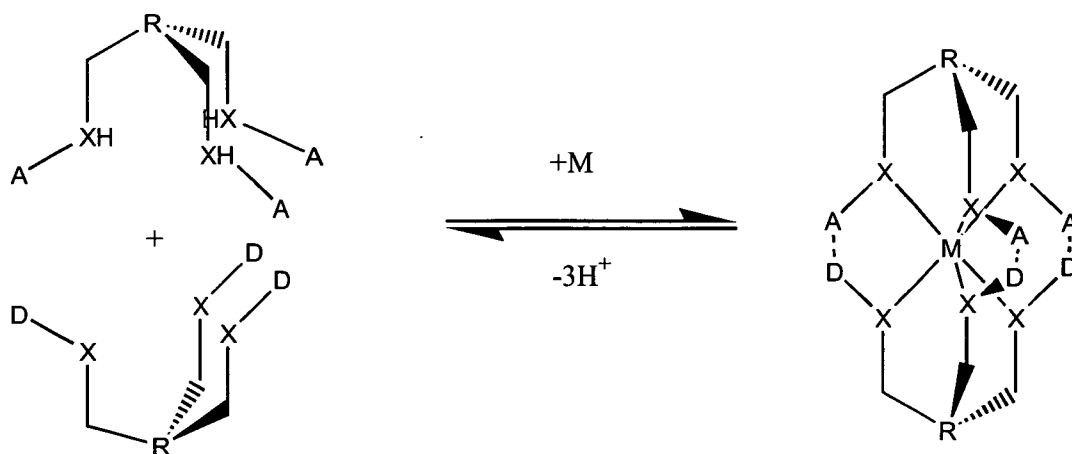


**Figure 1.10:** Tridentate AB type metal chelate systems to accommodate an octahedral metal geometry.

A final area proposed for investigation in this thesis was the possibility of increasing the ligand:metal ratio of a complex from 2:1 to 2:2. Ligand design included a similar ligand template to P50 of one hydrogen-bond donor and acceptor function per ligand but with an increased number of donor atoms (**X**) to coordinate to two metal centres. Such a system could increase the efficiency of a ligand as a metal extractant by 100%.

#### 1.7.4 The sulfonamide group as a supramolecular synthon

A sulfonamido moiety was introduced into ligand systems for several reasons. The acidic sulfonamido proton is easily lost and deprotonation of the sulfonamido nitrogen enhances its nucleophilicity. Finally the sulfonamido oxygens provide a total of four hydrogen-bond acceptor sites.

Reprotonation of sulfonamido ligands should allow the metal to be stripped back into aqueous solution at low pH providing that the complex formed is labile. Sulfonamides are also able to stabilise highly oxidizing metal centres due to the strong  $\sigma$  donating deprotonated sulphonamide groups.<sup>52</sup>

To complete the system a second donor atom and a hydrogen-bond acceptor site was introduced. One of two functional groups were used, an amino group or an oxime group. Both are able to bind to a metal centre *via* the nitrogen atom and have hydrogen atoms suitable for strong hydrogen-bond formation.

## 1.8 Sulfonamides

Sulfonamides have been widely used for treatment of bacterial or viral infections and are also found in drugs such as diuretics, hypoglycemic, antimalarial agents and many others.<sup>53</sup> Until relatively recently there had not been a large amount of work published on metal complexes of sulfonamides. The nitrogen atom in the neutral sulfonamide has always been considered as poorly coordinating due to the electron withdrawing ability of the sulfonyl group. The canonical form resulting is shown in Figure 1.11.

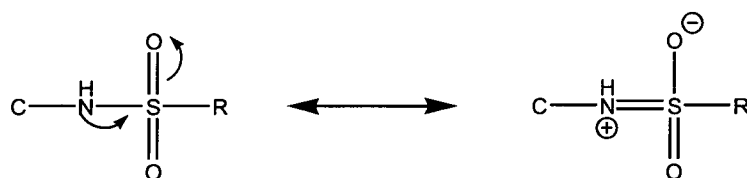


**Figure 1.11:** The electron withdrawing effect of the SO<sub>2</sub> group in sulfonamides.

This, however, can be used as an attractive feature in molecular design. Primarily due to the acidic nature of the sulfonamido proton the group can be readily deprotonated to produce an anionic ligand species. Of interest in the design of metal extractants is that the low basicity of the nitrogen which will prevent double protonation on stripping. Finally, due to the highly electron withdrawing nature of the sulfonyl group the sulfonamido nitrogen is a poor electron donor and the resulting complexes are Lewis acids. This has led to sulfonamido ligands being used to prepare complexes, which are efficient catalysts.

### 1.8.1 Synthesis of sulfonamides

Sulfonamides are usually prepared by treating ammonia, a primary amine, or a secondary amine with a sulfonyl chloride in the presence of some base, Figure 1.12.<sup>54</sup>

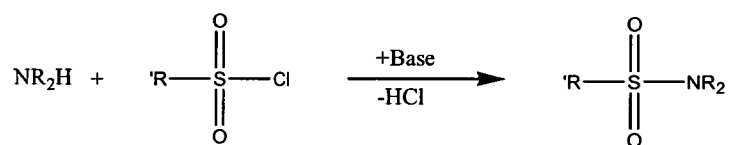


**Figure 1.12:** The common preparation of sulfonamides.

It is thought that this reaction proceeds by a simple nucleophilic substitution mechanism and mechanistic studies have shown it to be solvent dependent.<sup>54</sup>

Sulfonamides can also be made several other ways, for example from aryl sulfonates; here the amine nucleophile substitutes on the sulfur and not on the aromatic carbon. Aryl sulfinates may also be used as a precursor to sulfonamides, they are prepared by the reaction of aryllithiums with sulfur dioxide, and the subsequent treatment of the arylsulfinates produced with chloramine,  $\text{C}_6\text{H}_4\text{SO}_2\text{N}(\text{Cl})\text{Na}$  or hydroxylamine-O-sulfonic acid, Figure 1.13.

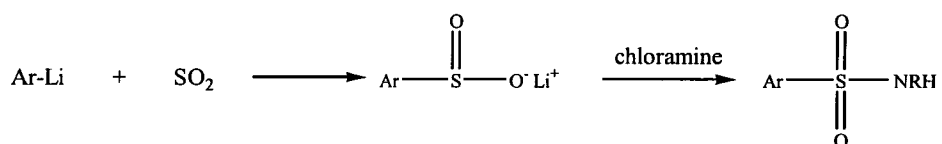


**Figure 1.13:** Conversion of methylsulfoxes to sulfonamides.

However the second step is often incompatible with other existing functional groups and so Huang *et al* developed a novel convenient one-pot synthesis of sulfonamides from methyl sulfones under very mild reaction conditions with base and trialkylboranes to give sulfinic acid salts which are then converted to sulfonamides during an oxidative-amination workup, Figure 1.14.<sup>55</sup>

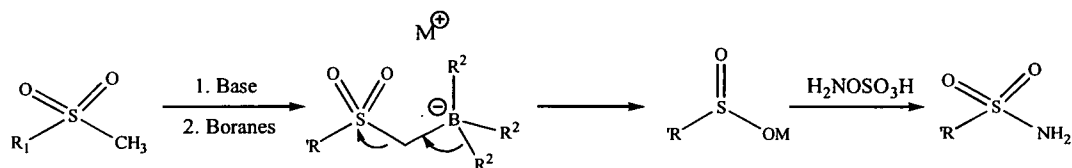


**Figure 1.14:** A one-pot synthesis of sulfonamides from methyl sulfones.

Developments in the preparation of N-alkylaryl sulfonamides have also been made. Initial preparations had such drawbacks as the requirement of harsh conditions, only *para*-substituted product formation and several reaction steps were also required for the preparation of sulfonamides to build up the functionality. Neumann *et al* developed a new route to N-alkylaryl sulfonamides using a trialkylstannyl leaving group in ipso electrophilic aromatic substitutions, Figure 1.15.<sup>56</sup>

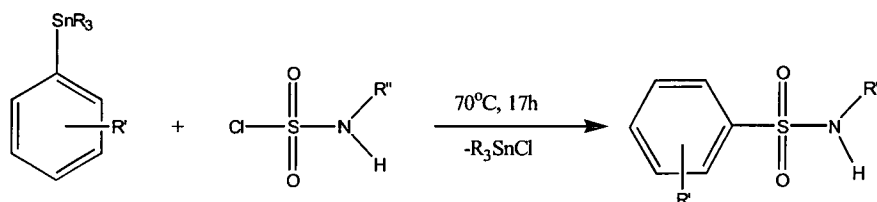


**Figure 1.15:** A route to N-alkylaryl sulfonamides.

Unsubstituted sulfonamides may be prepared by the hydrolysis of sulfonyl isocyanates, the reduction of sulfonyl azides or the treatment of sulfinyl chlorides with hydroxylamine. Sulfonamide synthesis has also been achieved by solid phase synthesis.<sup>57</sup>

### 1.8.2 Sulfonamides as ligands

The coordination chemistry of sulfonamides has been widely explored over the last 10 years. Work initially done by Peng aimed to discover if a ligand incorporating a sulfonamido group would exhibit as interesting a coordination chemistry as similar amide ligands.<sup>58,59,60</sup> He chose to work with the simple ligand systems in Figure 1.16.

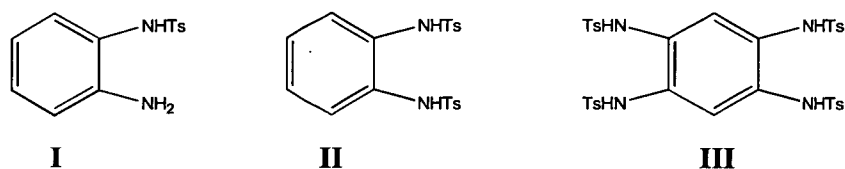
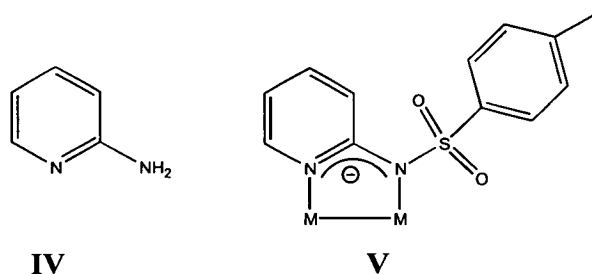


Figure 1.16: Simple *o*-phenylenediamine sulfonamide ligands.

Peng postulated that due to the strong  $\sigma$  donating deprotonated sulfonyl amido groups the complexes would stabilise highly oxidising metal centres.<sup>59</sup> Complexes of **I** with Co(II), Ni(II) and Cu(II) were prepared in dimethylformamide and the complex  $[\text{CuL}_2(\text{dmf})](\text{dmf})_2$  was characterised by X-ray crystallography.<sup>58</sup> Osmium(VI) produced dinuclear species with **II** and complexation work was also done with Co(II), Ni(II) and Cu(II) in pyridine.<sup>59</sup> Complexation of **III** with Cu(II) and Ni(II) produced dinuclear species where **III** acts as a bridging ligand.<sup>60</sup> This work will be described in more detail in chapter two where **I** is included in the initial ligand systems that were prepared.

The sulfonamido group is often introduced into ligands in view of its ability to deprotonate producing an anionic species. An example is seen in other work of Peng.<sup>61</sup> 2-aminopyridine, **IV**, is a poor coordination site due the delocalisation of the lone pair electrons of the nitrogen atom to the pyridine ring and there are no reports of it acting as a bridging ligand. However after sulfonylation and deprotonation to yield **V** the amino pyridine molecule becomes a good anionic ligand capable of forming bridged dinuclear species (Figure 1.17).



**Figure 1.17:** 2-Aminopyridine (IV) and 4-methyl-N pyridin-2-yl-benzenesulfonamide (V).

Sulfonamido complexes have several applications. Studies on  $d^{10}$  metal ions and transition metal complexes of sulfonamide drugs was initiated by Kessissoglou *et al* following the discovery that sulfonyl urea compounds are able to reduce blood sugar levels without affecting glucose tolerance and the discovery that Zn(II) had been implicated in the release mechanism of insulin.<sup>62</sup> The sulfonamide dansylamide (Figure 1.18) has found use in the development of zinc fluorophores, an indicator which uses fluorescence, following the discovery that sulfonamides inhibit zinc containing carbonic anhydrase.<sup>63</sup>

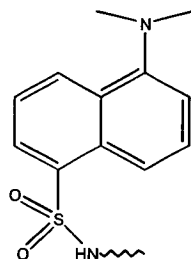


**Figure 1.18:** Dansylamide.

Carbonic anhydrase is a zinc enzyme. It catalyses the reversible hydration of carbon dioxide in red blood cells to form the bicarbonate anion and a proton *via* a tandem chemical process (Figure 1.19).<sup>64</sup>

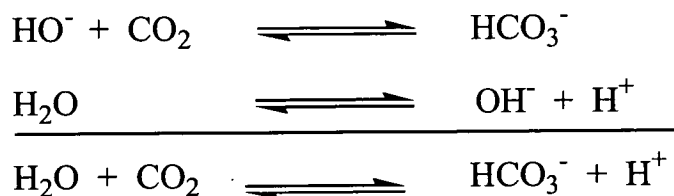


**Figure 1.19:** Catalysed reactions of carbonic anhydrase.

A shift in the dansyl emission peak is observed when zinc is bound to carbonic anhydrase, therefore by the incorporation of a dansylamide group into a macrocyclic or chelating ligand for zinc leads to a very useful sensor for Zn(II) or carbonic anhydrase.

An area where sulfonamido ligands and in particular disulfonamido ligands have found important application is in catalysis. Chiral bis(sulfonamide) ligands are known to stereospecifically catalyse Diels-Alder, Claisen, [2+2] cycloaddition, and enolisation-amination reactions. Elements used at the core of these catalysts are titanium, aluminium, ruthenium, boron, copper, zinc, magnesium and lanthanide metals. Titanium bis(sulfonamide) complexes of the type shown in Figure 1.20 are known to catalyse the enantioselective formation of C-C bonds through the addition of alkyl groups to aldehydes with dialkylzinc reagents.<sup>65,66,67,68</sup>

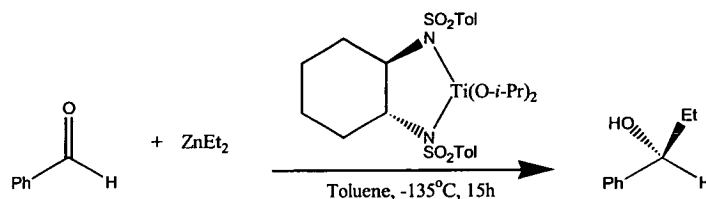


**Figure 1.20:** Enantioselective formation of a C-C bond through the addition of an ethyl group to benzaldehyde.<sup>66</sup>

The titanium catalyst is prepared *in situ* from  $\text{Ti}(\text{O-}i\text{-Pr})_4$  and the disulfonamido ligand. The mechanism for the catalysis of this reaction has not been adequately explored however it is proposed that the asymmetric reaction involves the initial formation of the chiral titanium complex.<sup>69</sup> An interesting feature of disulfonamide-titanium chemistry is that it is not uncommon that coordination of the sulfonamide oxygens to the metal centre should be observed this has also been noted in



disulfonamide-lanthanide chemistry, which will be mentioned later. It is thought that the coordination of the oxygen atoms may be due to the Lewis acid metal centre, however it is also proposed that coordination may be the result of crystal packing forces. Corey *et al* have reported the catalysis of Diels-Alder reactions with similar ligands (Figure 1.21) using an aluminium core.<sup>70,71,72,73</sup>

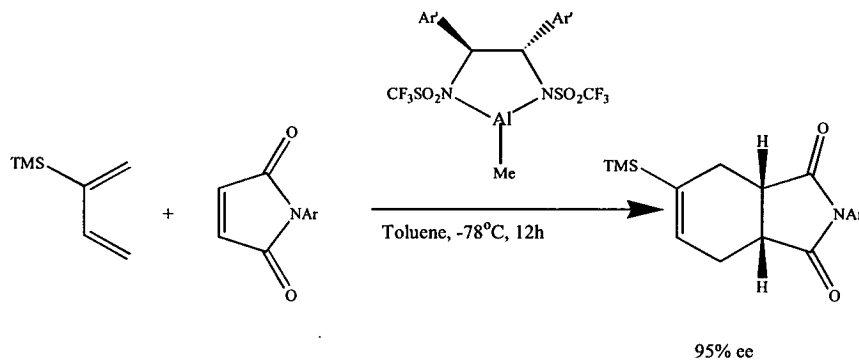


**Figure 1.21:** The reaction of 2-((trimethylsilyl)methyl)-butadiene with N-(2-*t*-butylphenyl) maleimide.<sup>70</sup>

Aluminium complexes with related bis(sulfonamide) ligands (Figure 1.22) are also known to catalyse [2+2] cycloadditions.<sup>74</sup>

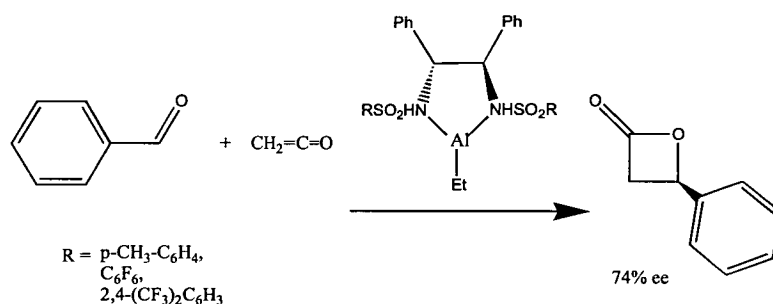


**Figure 1.22:** Asymmetric [2+2] cycloaddition of ketene with benzaldehyde.

To a stirred solution of the enantiopure bis(sulfonamide) complex in dry toluene an aldehyde was added under  $N_2$  at  $-78^\circ C$  and after ten minutes ketene was bubbled into the mixture for several minutes.<sup>74</sup> The following steric model (Figure 1.23) was postulated to explain the observed enantioselectivity. The aldehyde appears to coordinate to the catalyst by the lone pair electrons of the carbonyl oxygen in a manner *anti* to the alkyl substituent.

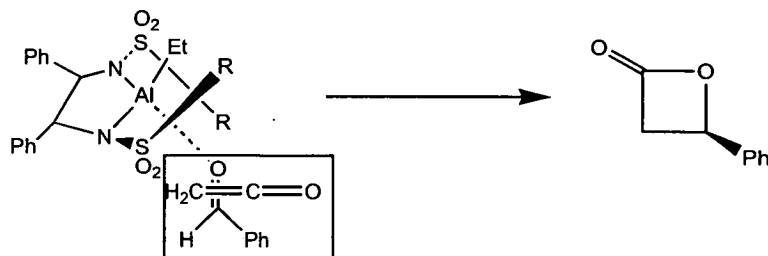


**Figure 1.23:** A steric model to explain the resulting enantioselectivity of a [2+2] cycloaddition.<sup>74</sup>

Monosulfonamido ligands can be complexed to ruthenium(II) centres *in situ* to generate catalysts for the asymmetric hydrogen transfer to ketones or imines from stable organic hydrogen donors such as 2-propanol and formic acid (Figure 1.24).<sup>75,76,77</sup>

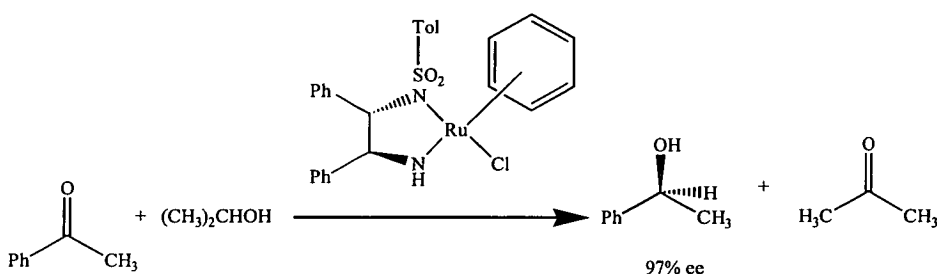


**Figure 1.24:** Asymmetric hydrogenation of 1-phenyl-ethanone.<sup>77</sup>

The catalyst is generated *in situ* from  $[\text{RuCl}_2(\eta^6\text{-benzene})]_2$  and free ligand.<sup>77</sup> The real nature of the catalyst remains unknown and the ruthenium complex in Figure 1.24 is thought to be the catalyst precursor.

Bis(sulfonamide) complexes of boron have found a wide range of applications. The complex in Figure 1.25 is known to catalyze aldol reactions.<sup>73</sup>

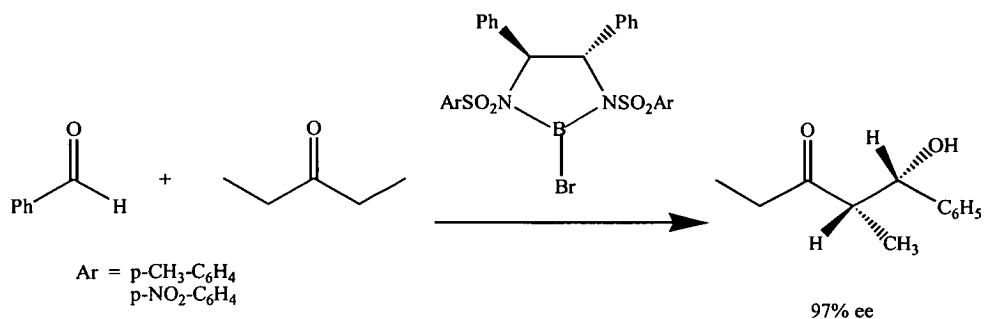


**Figure 1.25:** The aldol condensation of benzaldehyde and pentan-3-one.

Identical complexes where an allylic group replaces the bromide are used to catalyse the enantioselective addition of allyl groups to the carbonyl function of aldehydes to form chiral secondary homoallylic alcohols (Figure 1.26).<sup>78</sup>

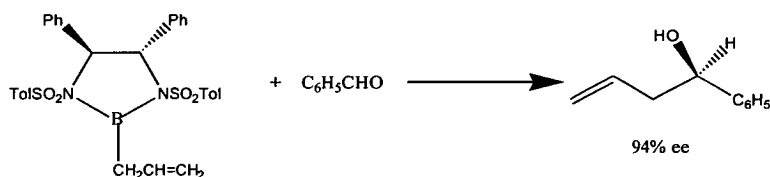


**Figure 1.26:** Enantioselective addition of propene to benzaldehyde.

Enantioselectivity is explained by a predicted chair-like transition state with optimum stereoelectronics and minimum steric repulsion between appendages on the five-membered ring, the optimum arrangement being depicted in Figure 1.27.<sup>78</sup>

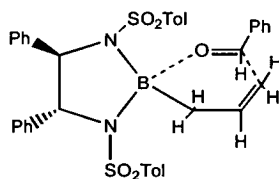


**Figure 1.27:** Postulated transition state for the enantioselective addition of propene to benzaldehyde.

Similar boron complexes also catalyse the Claisen rearrangement as illustrated in Figure 1.28.<sup>79</sup>

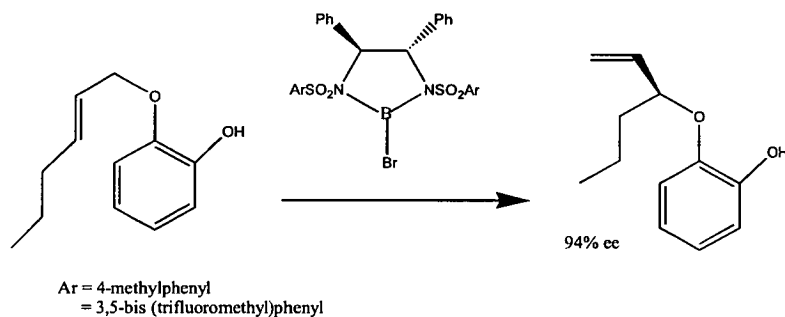


**Figure 1.28:** The Claisen rearrangement of 2-((E)-Hex-2-enyloxy)-phenol.

The mechanism of enantioselectivity can be explained as follows.<sup>79</sup> The phenoxy group binds to the chiral boron reagent followed by coordination of the allylic oxygen to the boron atom forming a rigid five-membered cyclic intermediate. The *re*-site of the benzene ring of the substrate may be shielded by one tolyl group of the sulfonamide ligand. Therefore, the approach of the allylic moiety should occur on the *si*-face (Figure 1.29).

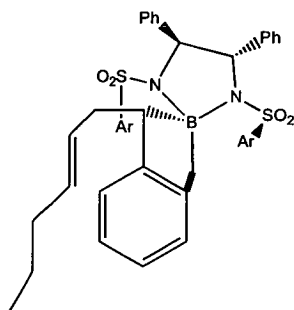


**Figure 1.29:** The intermediate formed in the Claisen rearrangement.

Cu(II) complexes with ligands of the type (number) are employed in the asymmetric cyclopropanation of olefins with diazoacetate, Figure 1.30.<sup>80</sup>

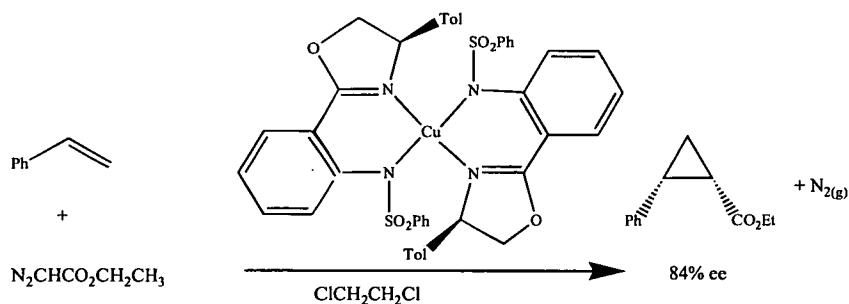


**Figure 1.30:** Asymmetric cyclopropanation of vinyl-benzene by a copper-chiral 2-(2-arylsulfonylamino)phenyl-1,3-oxazoline.

The copper complex in Figure 1.30 is considered to be the pre-catalyst. Upon activation with diazoacetate it is proposed that one chiral ligand is lost to form copper(I):chiral ligand = 1:1 complexes. The styrene can approach the copper centre from above and below and selectivity is thought to be dependent on the bulkiness of the ester part.

Zinc(II) complexes of chiral bis(sulfonamide) ligands are effective catalysts for the enantioselective cyclopropanation of allylic alcohols (Figure 1.31).<sup>81</sup>

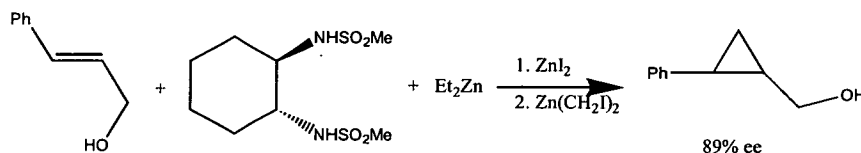


**Figure 1.31:** Enantioselective cyclopropanation of (*E*)-3-Phenyl-prop-2-en-1-ol.

The catalyst is generated in situ by the reaction of the disulfonamide ligand with diethylzinc to yield a 1:1 complex (Figure 1.32).

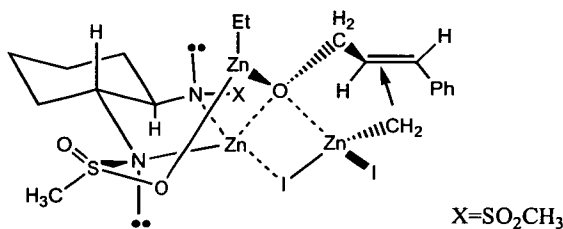


**Figure 1.32:** Transition state rationale for sulfonamide-promoted cyclopropanation.<sup>82</sup>

Zinc iodide and bis(iodomethyl)zinc react to form (iodomethyl) zinc iodide. The simultaneous coordination of the two reactive species, namely the substrate ethylzincalkoxide and the reagent iodomethylzinc iodide, by the zinc atom in the catalyst implies that it acts as an organisational centre. At the same time the reactivity of the methylene group of (iodomethyl) zinc iodide is enhanced by virtue of the electron-deficient and geometrically distorted zinc atom.

Chiral magnesium bis(sulfonamide) complexes can mediate the enolisation and enantioselective electrophilic amination of aryl-substituted carboximides (Figure 1.33), [boc =  $-\text{CO}_2\text{C}(\text{CH}_3)_3$ ].<sup>83</sup>

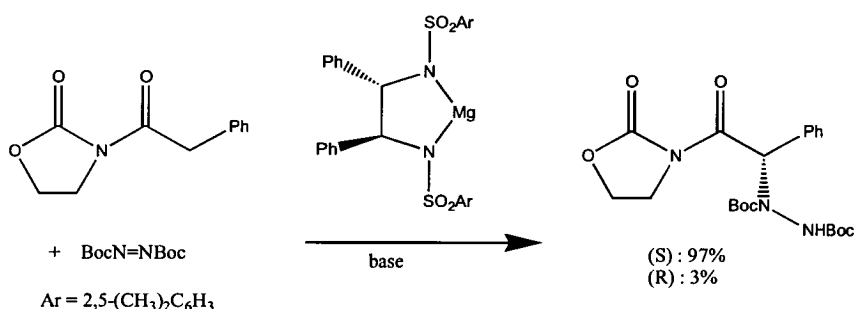


**Figure 1.33:** The asymmetric amination of 3-(2-phenyl-ethanoyl)-oxazolidin-2-one.

The role of N-methyl-p-toluenesulfonamide in this catalytic process is not yet completely elucidated however it has been concluded that the catalyst turnover is the rate determining step.

Lanthanide complexes with chiral bis(sulfonamide)ligands were also developed with a view to their being used as catalysts, (Figure 1.34),<sup>84</sup> however to date their application in this field has not been published.

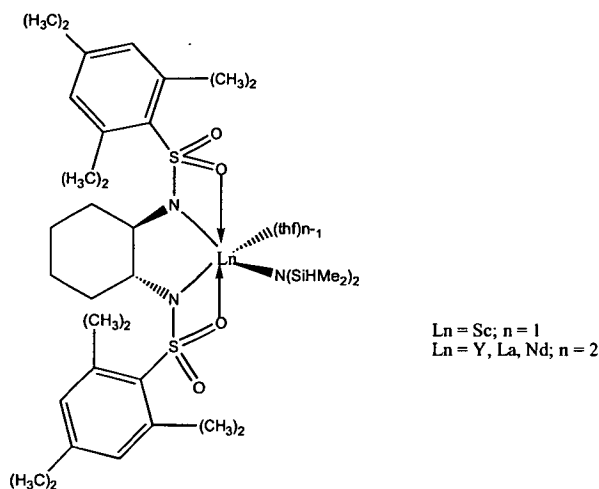


**Figure 1.34:** Lanthanide complexes of trans-1,2-bis(2,4,6-triisopropylbenzene sulfonamido) cyclohexane

$\text{M(IV)Cp}^*\text{Me}_3$  complexes are known to complex a variety of  $\text{N}_2\text{H}_x$  or  $\text{NH}_y$  ligands which can be cleaved in  $\eta^2$ -hydrazine to give ammonia in the presence of protons and a reducing agent.<sup>85</sup>  $\text{M(IV)Cp}^*\text{Me}_3$  complexes are not stable in protic solvents and related systems were required which did not contain metal-carbon bonds.<sup>85</sup> The complex  $\text{W(NAr)[N(NTs)}_2\text{]Cl}_2$ , ( $\text{N(NTs)}_2 = 2,6\text{-NC}_5\text{H}_3\text{-(CH}_2\text{Ntosyl)}_2$ ,  $\text{Ar} = 2,6\text{-C}_6\text{H}_3\text{-}i\text{Pr}_2$ ) is isolobal, to  $\text{MCp}^*\text{Me}_3$ . Fragments are isolobal if their uppermost orbitals have the same symmetry, similar energies, and the same electron occupation. It was found that upon substitution of the Cl on (VI) with triflate to give VII and subsequent reaction with hydrazine gave  $\text{W(NAr)[N(NTs)}_2\text{]}(\eta^2\text{-NHNH}_2)\text{Cl}$  (VIII). This complex can be reduced by zinc amalgam and subsequent addition of concentrated HCl to the reaction mixture generates 1.19 equivalents of  $\text{NH}_3$  to produce ammonia.<sup>85</sup>

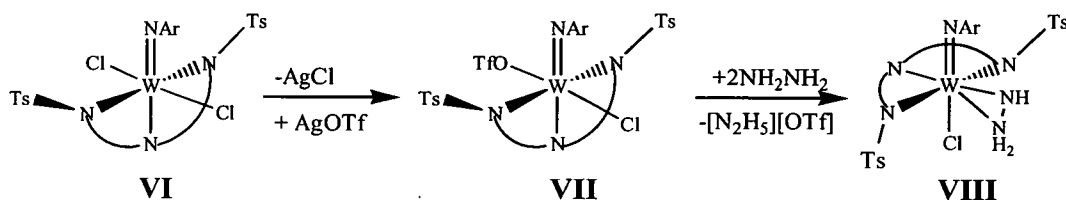


**Figure 1.35:** Route to a tungsten complex which upon reduction produces ammonia.

### 1.8.3 Sulfonamide complexes as metal extractants

Takagi *et al*<sup>86</sup> published a study of several sulfonamide ligands including the bis(sulfonamide)phenylenediamine ligand shown in Figure 1.36.

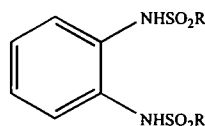
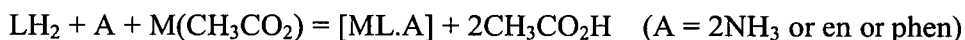


**Figure 1.36:** Bis(sulfonamide)phenylenediamine [R = Me (**IX**), R = *n*-C<sub>8</sub>H<sub>17</sub> (**X**)]

Neutral complexes of divalent metals (Co, Ni, Cu, Zn) can be formed from the disulfonamide ligand (**IX**, LH<sub>2</sub>) in the presence of neutral monodentate or bidentate ligands as Equation 1.19 illustrates.<sup>86</sup>



Eq 1.19

The lipophilic ligand (**X**, with R=*n*-C<sub>8</sub>H<sub>17</sub>) extracts copper and zinc into toluene in the presence of 4-benzylpyridine or 1,2-bis(hexylthio)ethane.

The coordinative behaviour of pyridyl substituted benzene sulfonamide ligands (**XI**, **XII** and **XIII**, LH) towards cobalt(II) and iron(III) were studied by Döring *et al*<sup>87</sup> as models for the LIX34 (**XIV**) extractant (Figures 1.37 and 1.38).

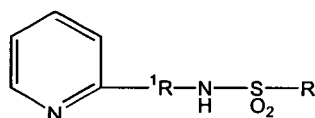


**Figure 1.37:** Sulfonamide model, [R<sup>1</sup> = CH<sub>2</sub> and R = C<sub>6</sub>H<sub>5</sub> or *p*-CH<sub>3</sub>C<sub>6</sub>H<sub>4</sub>, **XI**. R<sup>1</sup> = (CH<sub>2</sub>)<sub>2</sub> and R = C<sub>6</sub>H<sub>5</sub> **XII** or *p*-CH<sub>3</sub>C<sub>6</sub>H<sub>4</sub>, **XIII**].

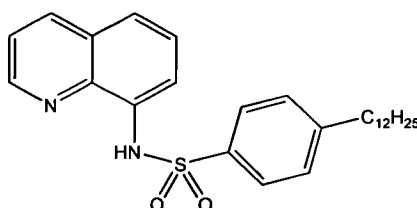


**Figure 1.38:** LIX34 (**XIV**).



The complex formed by **XIII** with cobalt  $\text{Co}(\text{L})_2$  has distorted tetrahedral geometry and a sulfonamide bridged tetramer with pentacoordinate cobalt(II) is formed with **XI**. Iron(III) forms complex salts with **XII**,  $[\text{Fe}(\text{LH})_2(\text{L})](\text{NO}_3)_2 \cdot x\text{H}_2\text{O}$ , and **XIII**,  $[\text{Fe}(\text{LH})_2(\text{L})](\text{NO}_3)_2 \cdot x\text{H}_2\text{O}$ , which are insoluble in organic solvents.

Subsequent to the identification of sulfonamide oxime ligands as target molecules an exhaustive literature search uncovered a further paper by Döring *et al*<sup>88</sup>. This paper covers a wide range of ligands but of particular interest are results reported on the two ligands **XV** and **XVI** (Figure 1.39).

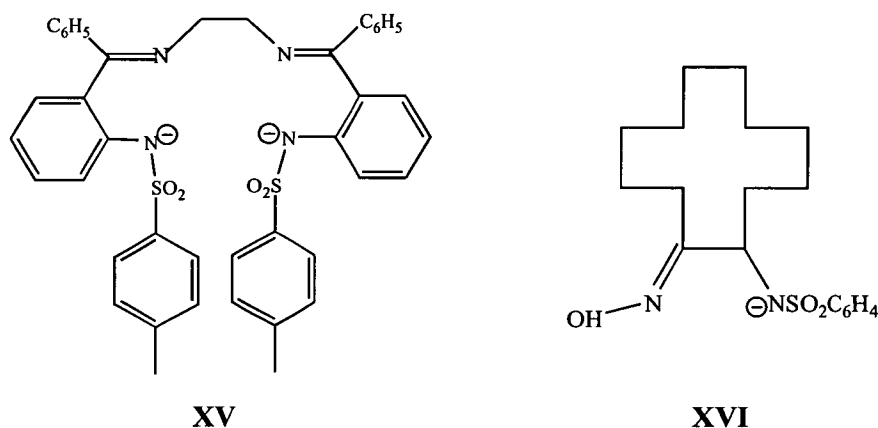


**Figure 1.39:** Bis [*o*-(*p*-toluene sulfonamido)benzophenone]-ethylene diamine (**XV**) and N-(2-hydroxyimino-cyclododecyl)-4-methyl-benzenesulfonamide (**XVI**).

Magnetic studies, electronic and IR spectra suggest a distorted tetrahedral structure for cobalt(II), copper(II) and nickel(II) complexes of **XV**.<sup>88</sup> A distorted tetrahedral geometry is also proposed for the copper complex of **XVI**.

The solvent extraction properties of two industrial extractants, P50 and SME529 are compared with those of **XV** and **XVI**. The  $\text{pH}_{1/2}$  values of **XV** and **XVI** are claimed to be higher than those of the commercial extractants. By using EPR to study the copper complexes of these ligands it was concluded that P50 and SME529 are better extractants than the sulfonamides due to the planarity of the copper(II) complexes and the hydrogen-bonding between ligands in the complex.<sup>88</sup> This type of hydrogen-bonding is not observed in complexes with **XV** and **XVI** due to their distorted tetrahedral geometry which causes them to be weaker extractants. Another molecule

of interest to us (XVII) is also mentioned in the paper and the coordination chemistry is briefly described however, no solvent extraction studies were done.

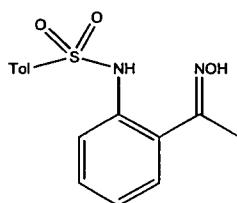


**Figure 1.40:** 1-{2-[N-(4-methylbenzenesulfonamido)]phenyl}ethan-1-one oxime (XVII).

A final paper considers the use of macrocyclic ligands containing proton-ionizable sulfonamide groups in the transport of alkali metal cations (Figure 1.41).<sup>89</sup> The function of the sulfonamido groups is that they can easily be deprotonated and upon the incorporation of a divalent metal cation into the macrocyclic cavity a neutral coordination compound is produced.

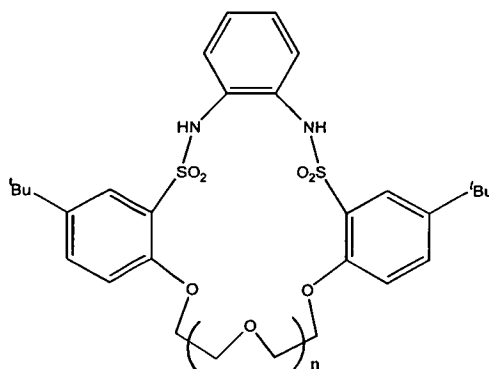


**Figure 1.41:** A sulfonamide extractant for alkali metals.

Seven patents which cover a wide range of sulfonamido ligands as solvent extractants were published by the Henkel Corporation between 1979 and 1981. The patents include the detailed molecular structure of the extractants and their solvent extraction properties. Their contents, including figures of their basic molecular structure are described briefly below. Metal extraction from aqueous solution by all of the sulfonamido ligands was found to be dependent upon a number of factors. These included, the concentration of the metal ion, the particular anions present, the pH of and/or ammonia concentration in the aqueous solutions, as well as the particular ligand and its concentration in the organic phase. The first patent published covered sulfonamide oxime ligands<sup>90</sup> (Figure 1.42).

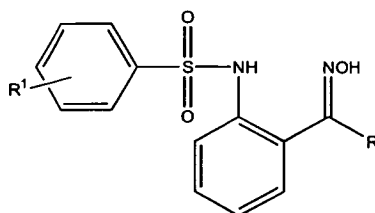


**Figure 1.42:** Sulfonamide oxime extractants.

These ligands were found to be useful for the recovery of Cu(II), Ni(II), Zn(II), Co(II) and Co(III) and to a lesser extent to Ag(I), Hg(II), Cd(II) and Pb(II). Copper may be extracted from all values of acidic pH, however nickel and cobalt may only be extracted at pH values above six. Extraction levels greater than 50% were achieved for Cu(II), Co(II), Ni(II) and Zn(II).

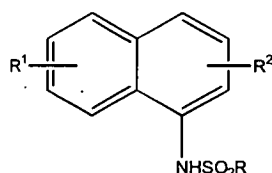


**Figure 1.43:** Sulfonamido quinoline extractants.

Sulfonamido quinoline extractants<sup>91</sup> (Figure 1.43) were found to be useful in the extraction of Cu(II), Ni(II), Zn(II), Co(II), Cd(II), Hg(II), Ag(I) and Pb(II). The ligands have good copper/iron selectivity ratios, and most can be recovered from ammoniacal solution.

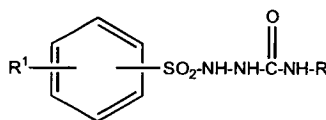


**Figure 1.44:** Sulfonylthiosemicarbazides ligands.

Sulfonylthiosemicarbazides<sup>92</sup> (Figure 1.44) were found to be useful reagents for Cu(II), Ni(II), Zn(II), Co(II) and Co(III) and may also be applied to a lesser extent to Cd(II), Hg(II), Ag(I) and Pb(II) recovery from ammoniacal solution.

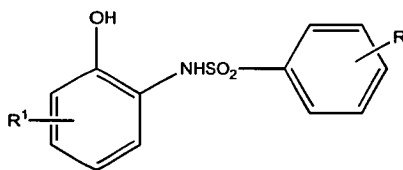


**Figure 1.45:** Sulfonamidophenol extractants.

Sulfonamido phenol extractants<sup>93</sup> (Figure 1.45) may be applied to the recovery of Cu(II), Ni(II) and Zn(II). The ligands are also weaker extractants for Cd(II), Hg(II), Ag(I), Pb(II) and Co(II) recovery. Sulfonamido phenols readily extract copper(II) at acid pH values and copper is also readily extracted from ammoniacal solutions. Good zinc(II) and nickel(II) extraction is also effected from such ammoniacal solutions.

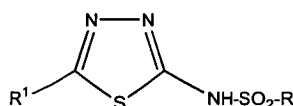


**Figure 1.46:** Sulfonamidothiadiazole.

Sulfonamidothiadiazole extractants<sup>94</sup> (Figure 1.46) may be used to extract Cu(II), Ni(II), Zn(II), Co(II) and Co(III) and are weaker extractants for Cd(II), Hg(II), Ag(I) and Pb(II). Copper(II) may be extracted from acidic aqueous solution at all pH values however, Ni(II), Zn(II) and Co(II) require a pH above five. All the previously mentioned metals may be extracted from ammoniacal solutions.

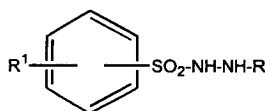


**Figure 1.47:** Sulfonylhydrazine extractants.

Sulfonyl hydrazines<sup>95</sup> (Figure 1.47) may be used to extract Cu(II), Ni(II), Zn(II), Co(II) and Co(III) and are weaker extractants for Cd(II), Hg(II), Ag(I) and Pb(II). The extractants have also been found to be mildly effective in extracting uranium, molybdenum, vanadium and iron.

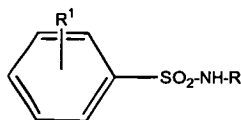


**Figure 1.48:** Sulfonamido pyrimidine extractants.

Sulfonamido pyrimidines<sup>96</sup> (Figure 1.48) are useful for the recovery of Cu(II), Ni(II), Zn(II), Co(II) and Co(III) and can also be applied to Cd(II), Hg(II), Ag(I) and Pb(II).

Although the patents have explored the solvent extraction properties of the ligands in detail little time was spent investigating complex stoichiometry. Studies of the solid state structures of the ligands and their complexes and their behaviour in solution were not undertaken.

## 1.9 References

- <sup>1</sup> T. W. Swaddle, in *Inorganic Chemistry an Industrial and Environmental Perspective*, Academic Press Ltd, London, 1997, ch. 17, pp. 357-386.
- <sup>2</sup> F. Habashi, *A Textbook of Hydrometallurgy*, Imprimerie d'Edition Marquis Limité, Quebec, 1993, ch. 2, pp. 13-26.
- <sup>3</sup> J. Szymanowski, *Hydroxyoximes and Copper Hydrometallurgy*, CRC Press, London, 1993, ch. 1, p. 6.
- <sup>4</sup> H. Fabian, H. W. Richardson, F. Habashi, *Handbook of Extractive Metallurgy*, Wiley – VCH, Weinheim, 1997, vol. 2, ch. 8, p. 491.
- <sup>5</sup> F. Habashi, *A Textbook of Hydrometallurgy*, Imprimerie d'Edition Marquis Limité, Quebec, 1993, ch. 10, p. 249.
- <sup>6</sup> T. C. Lo, *Encyclopedia of Chemical Technology*, John Wiley and sons, New York, 3<sup>rd</sup> edn., 1980, vol. 9, p.672.
- <sup>7</sup> F. Habashi, *A Textbook of Hydrometallurgy*, Imprimerie d'Edition Marquis Limité, Quebec, 1993, p. 409 .
- <sup>8</sup> M. C. Sneed, R.C. Brasted, *Comprehensive Inorganic Chemistry*, D.Van Nostrand Company Inc., 1955, Vol. 4, pp.9-33.
- <sup>9</sup> F. Habashi, *A Textbook of Hydrometallurgy*, Imprimerie d'Edition Marquis Limité, Quebec, 1993, ch. 1, p. 4.
- <sup>10</sup> J. Campbell, Avecia, private communication.
- <sup>11</sup> D. A. Fletcher, R. F. Meeking and D. J. Parkin, *J. Chem. Inf. Comput. Sci.*, 1996, 36, 746-749. Version 5.18 of the CCDC.
- <sup>12</sup> R. G. Person, *J. Am. Chem. Soc.*, 1963, **85**, 3533.
- <sup>13</sup> D. F. Shriver, P. W. Atkins and C. H. Langford, in *Inorganic Chemistry*, Oxford University Press, Oxford, 2<sup>nd</sup> edn, 1994, ch. 5, pp. 212-215.
- <sup>14</sup> F. Keith and J. C. K. Purcell, *Inorganic Chemistry*, Holt-Saunders International Editions, Japan, 1985, ch. 13, pp. 694-755.

- <sup>15</sup> J. J. R. Frausto da Silva and R. J. P. Williams, *The Inorganic Chemistry of life*, Clarendon Press, Oxford, 1991, ch. 2, pp. 28-57.
- <sup>16</sup> D. F. Shriver, P. W. Atkins and C. H. Langford, in *Inorganic Chemistry*, Oxford University Press, Oxford, 2<sup>nd</sup> edn, 1994, ch. 7, p. 276.
- <sup>17</sup> R. T. Meyers, *Inorganic Chemistry*, 1978, 17, 952.
- <sup>18</sup> F. A. Cotton, G. Wilkinson, in *Advanced Inorganic Chemistry*, John Wiley and Sons Inc., New York, 5<sup>th</sup> edn., 1988, part 1, ch. 1, p. 45.
- <sup>19</sup> N. N. Greenwood and E. A. Earnshaw, *Chemistry of the Elements*, Permangon Press, Oxford, 1984, ch. 26, p. 1290.
- <sup>20</sup> D. Nicholls, in *Comprehensive Inorganic Chemistry*, ed. J. C. Bailar, H. J. Emeléus, Sir R. Nyholm and A. F. Trotman-Dickenson, Permangon Press, Oxford, 1973, vol. 3, ch. 41, p1053.
- <sup>21</sup> N. N. Greenwood and E. A. Earnshaw, *Chemistry of the Elements*, Permangon Press, Oxford, 1984, ch.27, p. 1328.
- <sup>22</sup> D. Nicholls, in *Comprehensive Inorganic Chemistry*, ed. J. C. Bailar, H. J. Emeléus, Sir R. Nyholm and A. F. Trotman-Dickenson, Permangon Press, Oxford, 1973, vol. 3, ch. 42, p 1109.
- <sup>23</sup> L. Sacconi, F. Mani and A. Bencini, in *Comprehensive Coordination Chemistry, Late Transition Elements*, ed. Sir G. Wilkinson, R. D. Gillard and J. A. McCleverty, Permangon Press, Oxford, 1987, vol. 4, ch. 50, p. 1.
- <sup>24</sup> N. N. Greenwood and E. A. Earnshaw, *Chemistry of the Elements*, Permangon Press, Oxford, 1984, ch. 28, p. 1364.
- <sup>25</sup> B. J. Hathaway, in *Comprehensive Coordination Chemistry, Late Transition Elements*, ed. Sir G. Wilkinson, R. D. Gillard and J. A. McCleverty, Permangon Press, Oxford, 1987, vol. 5, ch. 53, p 533.
- <sup>26</sup> N. N. Greenwood and E. A. Earnshaw, *Chemistry of the Elements*, Permangon Press, Oxford, 1984, ch. 29, p. 1395.
- <sup>27</sup> R. H. Prince, in *Comprehensive Coordination Chemistry, Late Transition Elements*, ed. Sir G. Wilkinson, R. D. Gillard and J. A. McCleverty, Permangon Press, Oxford, 1987, vol. 5, ch. 56, p 925.

- 28 J.-M. Lehn, *Angew. Chem. Int. Ed. Engl.*, 1988, **100**, 91.
- 29 S. Subramanian and M. J. Zaworotko, *Coord. Chem. Rev.*, 1994, **137**, 357.
- 30 C. B. Aakeröy and K. R. Seddon, *Chem. Soc. Rev.*, 1993, 399.
- 31 G. R. Desiraju, *Angew. Chem. Int. Ed. Engl.*, 1995, **34**, 2311-2327
- 32 S. Rau, M. Ruben, T. Buttner, C. Temme, S. Dautz, H. Gorgs, M. Rudolph, D. Walther, A. Brodkorb, M. Duati, C. O'Connor and J. G. Vos, *J. Chem. Soc. Dalton Trans.*, 2000, **20**, 3649-3657.
- 33 C. J. Burchell, G. Ferguson, A. J. Lough, C. Glidewell, *Acta Crystallogr. C*, 2001, **57**, 88.
- 34 C. E. Marjo, R. Bishop, D. C. Craig and M. L. Scudder, *Eur. J. Org. Chem.*, 2001, **5**, 863.
- 35 K. Biradha, C. V. K. Shama, K. Panneerselvam, L. Shimoni, H. L. Carrell, D.E. Zacharias, G.R. Desiraju, *J. Chem. Soc. Chem. Commun.*, 1993, 1473.
- 36 M. Bremer, P. S. Gregory, P. von R. Schleyer, *J. Org. Chem.* 1989, **54**, 3796.
- 37 V. R. Pedireddi, D. S. Reddy, B. S. Gour, D. C. Craig, A. D. Rae, G. R. Desiraju, *J. Chem. Soc. Perkin Trans.*, 1994, **2**, 2353.
- 38 D. S. Reddy, D. C. Craig, A. D. Rae, G. R. Desiraju, *J. Chem. Soc. Chem. Commun.*, 1993, **23**, 1737.
- 39 J.-M. Lehn, *Supramolecular Chemistry*, VCH, Weinheim, 1995.
- 40 R. Taylor and O. Kernard, *J. Am. Chem. Soc.*, 1982, **104**, 5063.
- 41 C. A. Hunter, *J. Chem. Soc., Chem Commun.*, 1991, 749.
- 42 P. Seiler and J. D. Dunitz, *Helv. Chim. Acta*, 1985, **68**, 2093.
- 43 P. W. Atkins, *General Chemistry*, Scientific American books, New York, 1989.
- 44 O. F. Schall and G. W. Gokel, *J. Am. Chem. Soc.*, 1994, **116**, 6089.
- 45 O. F. Schall and G. W. Gokel, *J. Org. Chem.* 1996, **61**, 1449.
- 46 M. Simard, D. Su, and J. D. Wuest, *J. Am. Chem. Soc.* 1991, **113**, 4696.
- 47 K. C. Russell, E. Leize, A. Van Dorsselaer, and J.-Marie Lehn, *Angew. Chem. Int. Ed. Engl.*, 1995, **34**, 209.
- 48 S. Shan, D. J. Herschlag, *J. Am. Chem. Soc.*, 1996, **118**, 5515.
- 49 C. L. Perrin, J. B. Nielson, *J. Am. Chem. Soc.*, 1997, **119**, 12734.



- 50 Y. Kato, L. M. Toledo, J. Rebek, *J. Am. Chem. Soc.*, 1996, **118**, 8575.
- 51 G. A. Kumar and M. A. McAllister, *J. Org. Chem.*, 1998, **63**, 6968.
- 52 W.-H. Leung, S.-M. Peng, *Polyhedron*, 1993, **12**, 13.
- 53 H.-C. Huang, and D. B. Reitz, *Tetrahedron Letters*, 1994, **35**, 7201.
- 54 D. N. Jones, *Comprehensive Organic Chemistry*, Pergamon Press, Oxford, 1979, Vol. 3, p 346.
- 55 H.-C. Huang, E. J. Reinhard and D. B. Reitz, *Tetrahedron Letters*, 1994, **35**, 7201.
- 56 P. Neumann and Christian Wicenc, *Chem. Ber.*, 1993, **126**, 763.
- 57 B. Raju and T. P. Kogan, *Tetrahedron Letters*, 1997, **38**, 3373.
- 58 H.-Y. Cheng, P.-H. Cheng, C.-F. Lee and S.-M. Peng, *Inorganica Chimica Acta*, 1991, **181**, 145.
- 59 P.-H. Cheng, H.-Y. Cheng, C.-C. Lin and S.-M. Peng, *Inorganica Chimica Acta*, 1990, **169**, 19.
- 60 H.-Y. Cheng, G.-H. Lee and S.-M. Peng, *Inorganica Chimica Acta*, 1992, **191**, 25.
- 61 W.-H. Leung, E. K.-F. Chow and S.-M. Peng, *Polyhedron*, 1993, **12**, 1635.
- 62 D. P. Kessissoglou, G. E. Manoussakis, A.G. Hatzidimitiou and M.G. Kanatzidis, *Inorganic Chemistry*, 1987, **26**, 1395.
- 63 E. Kimura and T. Koike, *Chemical Society Reviews*, 1998, **27**, 179.
- 64 D. E. Fenton, in *Biocoordination chemistry*, ed by J. Evans, Oxford University Press, Oxford, 1995, 1<sup>st</sup> edn, ch. 6, p. 61.
- 65 S. Pritchett, P. Gantzel, and P. J. Walsh, *Organometallics*, 1997, **16**, 5130-5132
- 66 L. T. Armistead, P. S. White, and Michel R. Gagné, *Organometallics*, 1998, **17**, 216-220
- 67 S. Pritchett, D. H. Woodmansee, P. Gantzel, and P. J. Walsh, *J. Am. Chem. Soc.*, 1998, **120**, 6423.
- 68 L. T. Armistead, P. S. White, and M. R. Gagné, *Organometallics*, **18**, **17**, 4232.
- 69 C. Guo, J. Qiu and X. Zhang, D. Verdugo, M. L. Larter, R. Christie, P. Kenney and P. J. Walsh, *Tetrahedron*, 1997, **53**, 4145.

- 70 E. J. Corey and Michael A. Letavic, *J. Am. Chem. Soc.*, 1995, **117**, 9616.
- 71 E. J. Corey, S. Sarshar, and D.-H. Lee, *J. Am. Chem. Soc.*, 1994, **116**, 12089.
- 72 E. J. Corey and S. Sarshar, J. Bordner, *J. Am. Chem. Soc.*, 1992, **114**, 7938.
- 73 E. J. Corey, R. Imwinkelried, S. Pikul, and Y. B. Xiang, *J. Am. Chem. Soc.*, 1989, **111**, 5493.
- 74 Y. Tamai, H. Yoshiwara, M. Someya, J. Fukumoto and S. Miyano, *J. Chem. Soc., Chem. Commun.*, 1994, 2281.
- 75 S. Hashiguchi, A. Fujii, J. Takehara, T. Ikariya, and R. Noyori, *J. Am. Chem. Soc.*, 1995, **117**, 7562.
- 76 K.-J. Haack, S. Hashiguchi, A. Fujii, T. Ikariya, and R. Noyori, *Angew. Chem. Int. Ed. Engl.*, 1997, **36**, 285.
- 77 A. Fujii, S. Hashiguchi, N. Uematsu, T. Ikariya, and R. Noyori, *J. Am. Chem. Soc.*, 1996, **118**, 2521.
- 78 E. J. Corey, C.-M. Yu, and S. Soo Kim, *J. Am. Chem. Soc.*, 1989, **111**, 5495.
- 79 H. Ito, A. Sato, and T. Taguchi, *Tetrahedron Letters*, 1997, **38**, 4815.
- 80 T. Ichiyangi, M. Shimizu, T. Fujisawa, *Tetrahedron*, 1997, **53**, 9599.
- 81 S. E. Denmark, S. P. O'Connor, and S. R. Wilson, *Angew. Chem. Int. Ed.* 1998, **37**, 1149
- 82 S. E. Denmark and S. P. O'Connor, *J. Org. Chem.*, 1997, **62**, 584.
- 83 D. A. Evans and S. G. Nelson, *J. Am. Chem. Soc.*, 1997, **119**, 6452.
- 84 H. W. Görlitzer, M. Spiegler, and R. Anwander, *Eur. J. Inorg. Chem.*, 1998, 1009.
- 85 S. Cal and R. R. Schrock, *Inorg. Chem.*, 1991, **30**, 4105.
- 86 M. Takagi, S. Matsuo, S. Matsuo, K. Ueno, S. Ide, *Chemistry Letters*, 1980, 387.
- 87 V. E. Uhlig, M. Döring, *Z. Anorg. Allg. Chem.*, 1982, **492**, 52.
- 88 M. R. Döring and E. Uhlig, *Z. anorg. allg. Chem.*, 1987, **554**, 217.
- 89 M. Bochenska, J. F. Biernat, M. Topolski, J. S. Bradshaw, R. L. Bruening, R. M. Izatt and N. K. Dalley, *Journal of Inclusion Phenomena and Molecular Recognition in Chemistry*, 1989, **7**, 599.

- 90 *US Pat.*, 4,160,807, 1979.
- 91 *US Pat.*, 4,209,419, 1980.
- 92 *US Pat.*, 4,237,062, 1980.
- 93 *US Pat.*, 4,239,699, 1980.
- 94 *US Pat.*, 4,251,664, 1981.
- 95 *US Pat.*, 4,252,959, 1981.
- 96 *US Pat.*, 4,294,965, 1981.



**Chapter 2:**  
**Monosulfonamidodiamine ligands**

<b>Contents</b>	<b>Page</b>
2.1 Introduction .....	55
2.2 Synthesis of simple monosulfonamidodiamines and their metal complexes .....	56
2.2.1 Free ligands .....	57
2.2.2 Metal complexes .....	58
2.3 Characterisation of simple monosulfonamidodiamines .....	59
2.3.1 Infrared Spectroscopy.....	59
2.3.2 NMR Spectroscopy .....	59
2.3.3 Mass Spectrometry .....	60
2.3.4 X-ray crystallography.....	60
2.4 Solid State structures of ligands and complexes .....	61
2.4.1 Free Ligands .....	61
2.4.1.1 N-(3-aminopropyl)-4-methylbenzenesulfonamide ( <b>5</b> ).....	63
2.4.1.2 N-(N-butyl-2-aminopropyl)-4-methylbenzenesulfonamide ( <b>9</b> )....	65
2.4.1.3 N-(2-aminoethyl)-4-methylbenzenesulfonamide ( <b>1</b> ).....	67
2.4.1.4 N-(N-benzyl-2-aminopropyl)-4-methylbenzenesulfonamide ( <b>7</b> ) .	69
2.4.1.5 N-(2-amino-phenyl)-4-methylbenzenesulfonamide ( <b>10</b> ).....	70
2.4.2 Hydrogen-bonding in monosulfonamidodiamine ligands.....	71
2.4.3 Monosulfonamidodiamine complexes .....	73
2.4.3.1 Bis[N-(2-aminoethyl)-4-methylbenzenesulfonamidato].....	
zinc(II) ( <b>12</b> ) .....	73
2.4.3.2 Bis[N-(2-aminoethyl)-4-methylbenzenesulfonamidato].....	
nickel(II) ( <b>13</b> ).....	76
2.4.3.3 Bis[N-(2-aminoethyl)-4- <i>t</i> -butylbenzenesulfonamidato] .....	
copper(II) ( <b>16</b> ).....	78
2.4.4 Hydrogen-bonding in sulfonamidodiamine complexes .....	80
2.4.5 Hole sizes, bite angles and torsion angles. ....	82
2.4.6 Geometry of amido and sulfonamido nitrogens .....	87
2.4.7 Geometry of the sulfonamido nitrogen in monosulfonamidodiamine .....	
ligands .....	88

2.4.8 Geometry of amides of carboxylic and sulfonic acids in the Cambridge Structural Database (CSD).....	92
2.5 Equilibrium constants of monosulfonamidodiamines .....	94
2.5.1 Speciation of monosulfonamidodiamines .....	95
2.5.2 Prediction of the selectivity of monosulfonamidodiamines .....	96
2.6 Solvent extraction.....	97
2.6.1 'S'-Curve determination.....	97
2.6.2 Selectivity of monosulfonamidodiamine ligands .....	98
2.7 An electrochemical study of monosulfonamidodiamine complexes.....	100
2.7.1 The stabilisation of metal(III) centres by deprotonated amide groups.....	100
2.7.2 Cu(III) and Ni(III) peptide complexes .....	101
2.7.3 Electrochemical studies of monosulfonamidodiamine complexes .....	103
2.8 Conclusions .....	105
2.9 Experimental .....	106
2.9.1 Instrumentation.....	106
2.9.2 Solvent and reagent pretreatment.....	107
2.9.3 Ligands and their precursor .....	107
2.9.4 Monosulfonamidodiamine complex synthesis .....	114
2.9.5 Solvent extraction experiments from sulfate media.....	118
2.9.6 X-ray crystallography.....	119
2.10 References .....	122

## 2.1 Introduction

Bidentate diamino-monosulfonamides have two nitrogen donors for coordination to a metal. The acidic sulfonamido hydrogen ( $pK_a \sim 9$ ) can be lost to produce a monoanionic ligand which upon coordination to a metal (II) ion, in a ratio of 2 ligands to 1 metal, will produce a neutral four coordinate complex. The organisation of two ligands through “head to tail” interactions is possible, *via* hydrogen-bonding between the amino group hydrogen donor(s) and the sulfonamido oxygen acceptor sites, to form a dimeric centrosymmetric *pseudo*-macrocycle in an analogous way to P50 (Figure 2.1).

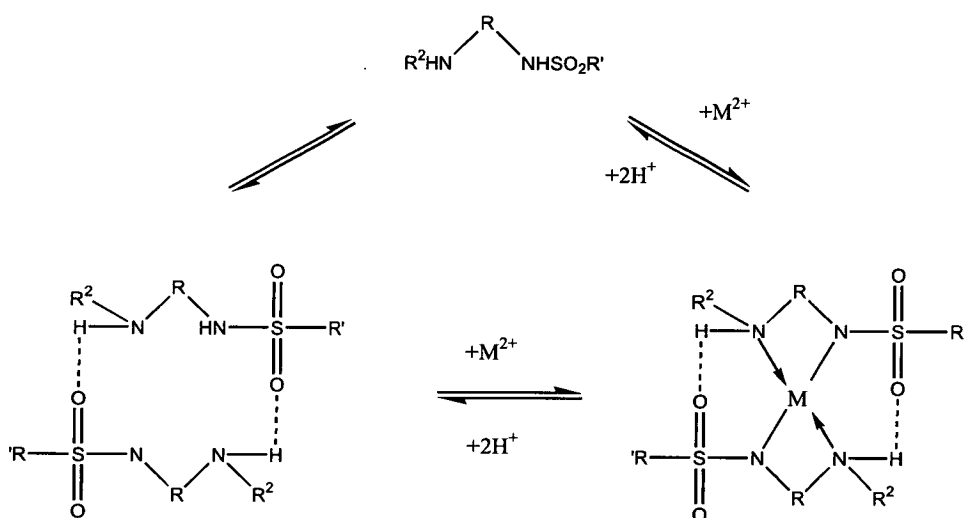


**Figure 2.1:** Schematic representation of ligand assembly involving monosulfonamidodiamines.

## 2.2 Synthesis of simple monosulfonamidodiamines and their metal complexes

The simple monosulfonamidodiamine ligands prepared in this project are summarised in Figure 2.2.

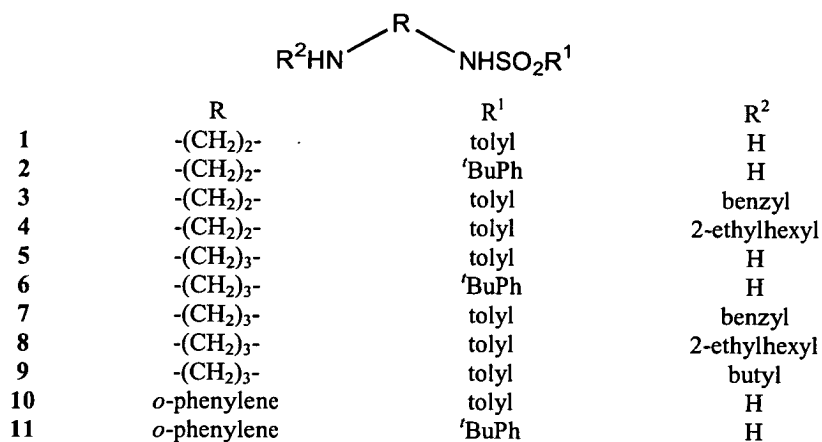


Figure 2.2: Generic form of the monosulfonamidodiamine ligand.

The complexes which were isolated upon complexation of these ligands are listed in Table 2.1.

Table 2.1: Complexes of simple monosulfonamidodiamine ligands.

Abbreviation	12	13	14	15	16
Complex	[Zn(1-H) <sub>2</sub> <sup>b</sup> ]	[Ni(1-H) <sub>2</sub> <sup>b</sup> ]	[Co(1-H) <sub>2</sub> <sup>a</sup> ]	[Cu(1-H) <sub>2</sub> <sup>a</sup> ]	[Cu(2-H) <sub>2</sub> <sup>b</sup> ]
17	18	19	20	21 <sup>1</sup>	22
[Ni(4-H) <sub>2</sub> <sup>a</sup> ]	[Co(4-H) <sub>2</sub> <sup>a</sup> ]	[Cu(4-H) <sub>2</sub> <sup>a</sup> ]	[Co(5-H) <sub>2</sub> <sup>a</sup> ]	[Cu(5-H) <sub>2</sub> <sup>bc</sup> ]	[Cu(5-H) <sub>2</sub> <sup>bc</sup> ]
23	24	25	26	27	
[Zn(5-H) <sub>2</sub> <sup>a</sup> ]	[Cu(8-H) <sub>2</sub> <sup>a</sup> ]	[Ni(10-H) <sub>2</sub> <sup>a</sup> ]	[Cu(10-H) <sub>2</sub> <sup>a</sup> ]	[Zn(10-H) <sub>2</sub> <sup>a</sup> ]	

<sup>a</sup> Formula consistent with C/H/N analytical data. <sup>b</sup> Formula confirmed by X-ray crystallography. <sup>c</sup> This complex exists in blue and green polymorphs.



## 2.2.1 Free ligands

Ligands **1**, **5** and **10** (Figure 2.3) were prepared in the early stages of the project.

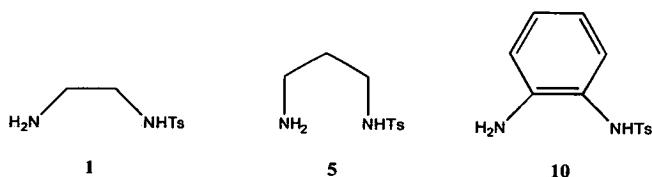
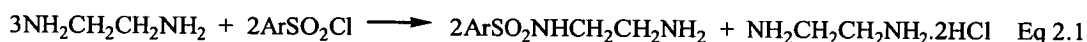


**Figure 2.3:** The three principle monosulfonamido ligands investigated.

Literature preparations<sup>2,3</sup> were followed. Conversion of 1,2-diaminoethane and 1,3-diaminopropane into the monotosyl derivatives **1** and **5** was crucially dependent on reaction conditions. Kirsanov<sup>2</sup> established that the addition of the diamine to the 4-methylbenzenesulfonyl chloride (TsCl) leads only to the formation of a disubstituted species and that by the addition of the 4-methylbenzenesulfonyl chloride to the diamine a monosubstituted species can be obtained. Different ratios of reagents were tested and the best yields were found at the diamine to sulfonyl chloride ratio of three to one instead of the expected three to two, (Equation 2.1).



Following this optimisation of reaction conditions, one equivalent of 4-methylbenzenesulfonyl chloride in toluene was added dropwise to three equivalents of diamine in toluene at room temperature to prepare both **1** and **5** (Figure 2.4).

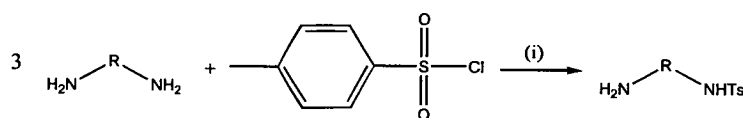


**Figure 2.4:** The synthesis of **1** and **5**. R =  $-(\text{CH}_2)_2-$  (**1**) or  $-(\text{CH}_2)_3-$  (**5**). (i) Toluene, 25°C.

The preparation of **10** was reported<sup>3</sup> by Cheng in 1991. The ligand was prepared from the reaction of *o*-phenylene diamine and 4-methylbenzenesulfonyl chloride in a ratio of 1:1 in a solution of pyridine which was quenched with HCl (Figure 2.5).

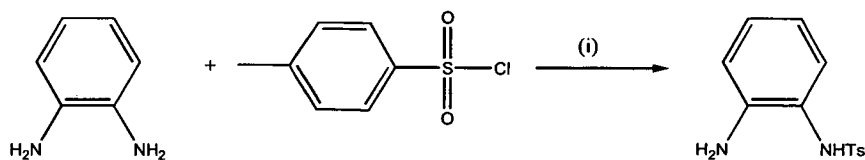


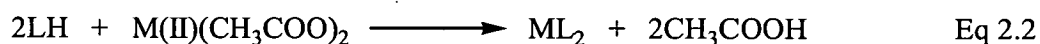
**Figure 2.5:** The synthesis of **10**. (i) Pyridine, 25°C.

Molecules **1**, **5** and **10** have sufficient solubility for analytical purposes and for studies of their complexational behaviour. However, to study their colligative properties and to undertake electrochemical and solvent-extraction studies their solubility had to be improved. This is discussed further in chapter 4.

The high number of hydrogen-bond donor and acceptor sites present in these ligands means that there are large numbers of possible *intra*- and *inter*-molecular interactions. In order to investigate these in the solid state, X-ray crystal structures have been determined for the ligands where possible.

### 2.2.2 Metal complexes

Metal complexes of simple monosulfonamidodiamines were synthesised by the standard method of reaction of two equivalents of the appropriate ligand with one equivalent of the appropriate divalent metal acetate,<sup>4</sup> (Equation 2.2). The acetate counterions effectively buffer the reaction mixture, promoting the formation of the monoanionic ligand.



## 2.3 Characterisation of simple monosulfonamidodiamines

### 2.3.1 Infrared Spectroscopy

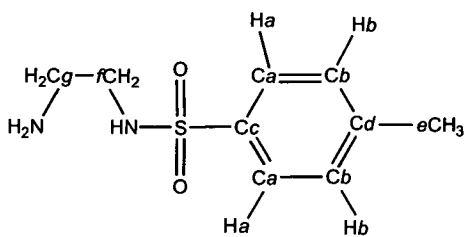
Infrared (IR) spectroscopy can be used to confirm the presence of the sulfonamide group in the products. One strong band is expected in the 1370-1330  $\text{cm}^{-1}$  region and another in the 1180-1160  $\text{cm}^{-1}$  region for the  $-\text{SO}_2\text{-N}$  group.

### 2.3.2 NMR Spectroscopy

$^1\text{H}$  NMR spectroscopy is particularly useful since the *p*-alkylarylsulfonamides show characteristic resonances in the aromatic region of the spectrum. The four aromatic protons fall into two magnetically equivalent sets in *a* and *b* (Figure 2.6) which have sufficiently different chemical shifts to give rise to two doublets, observed around 7.8 and 7.3 ppm depending on the exact structure, and with a coupling constant  $^3J_{\text{HH}}$  of typically 6 Hz. The *a* protons were shifted to lower field with respect to the *b* protons due to the deshielding effect of the sulfonyl group. For the *p*-methylaryl sulfonamides a further characteristic singlet was seen around 2.5 ppm for the methyl group, whereas for the *p*-*t*butyl group a resonance assigned to nine methyl hydrogens was observed around 1.3 ppm.

As an example, N-(2-aminoethyl)-4-methylbenzenesulfonamide (**1**), shows further triplet resonances at 2.8 and 3.0 ppm assigned to the methylene hydrogens of the ethane linkage group (Figure 2.6). The resonance at 3.0 ppm was due to the methylene hydrogens (*H<sub>f</sub>*) adjacent to the sulfonamide group as these were more deshielded due to the electron withdrawing effect of the sulfonamide group.

$^{13}\text{C}$  NMR is also useful in confirming the structures. Assignments for N-(2-aminoethyl)-4-methylbenzenesulfonamide (**1**) are given in Figure 2.6. Spectra are easily assigned using DEPT techniques.<sup>5</sup> The methyl signal is usually found at 20 ppm with the two methylene signals further downfield. The remaining signals are easily identified in the aromatic region.



Label	$^{13}\text{C}$ NMR (ppm)	$^1\text{H}$ NMR (ppm)
<i>a</i>	130	7.8
<i>b</i>	127	7.3
<i>c</i>	136	—
<i>d</i>	143	—
<i>e</i>	21	2.4
<i>f</i>	45	3.0
<i>g</i>	41	2.8

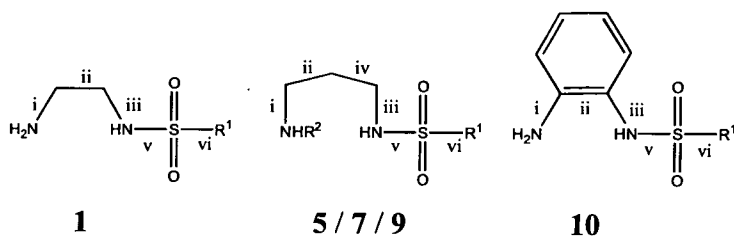
**Figure 2.6:** NMR assignments for N-(2-aminoethyl)-4-methylbenzenesulfonamide (**1**).

### 2.3.3 Mass Spectrometry

Mass spectrometry was also routinely used for characterisation. Of the techniques available (EI, FAB and ESI) electron impact has been used primarily. In addition, preliminary work has been performed using the gentler ESI technique to probe the solution structure of these compounds, this is discussed in chapter 4.

### 2.3.4 X-ray crystallography

Ligands **1**, **5**, **7**, **9** and **10** were also characterised by X-ray crystallography. Bond lengths in the central components of the ligands are listed in Figure 2.7.



Bond	1 <sup>a</sup>	5	7	9	10 <sup>a</sup>
i	1.464(5) 1.465(5)	1.4665(19)	1.469(7)	1.466(4)	1.367(4) 1.374(4)
ii	1.512(6) 1.503(6)	1.522(2)	1.522(7)	1.511(4)	1.399(4) 1.399(4)
iii	1.478(5) 1.486(5)	1.4740(18)	1.475(7)	1.471(4)	1.437(4) 1.446(4)
iv		1.515(2)	1.502(7)	1.506(4)	
v	1.614(4) 1.593(4)	1.6081(12)	1.607(5)	1.610(3)	1.612(3) 1.627(3)
vi	1.763(4) 1.779(5)	1.7670(14)	1.759(5)	1.773(3)	1.755(3) 1.766(3)

<sup>a</sup> In **1** and **10** two independent molecules exist per asymmetric unit.

**Figure 2.7:** Bond lengths (Å) for the central components of sulfonamido diamine ligands **1** ( $R^1 = \text{Tol}$ ), **5** ( $R^1 = \text{Tol}$ ,  $R^2 = \text{H}$ ), **7** ( $R^1 = \text{Tol}$ ,  $R^2 = \text{benzyl}$ ), **9** ( $R^1 = \text{Tol}$ ,  $R^2 = \text{butyl}$ ) and **10** ( $R^1 = \text{Tol}$ ).

Ligands **1**, **5**, **7** and **9** have comparable bond lengths. **10** has shorter i, ii and iii bond lengths due to the aromatic nature of the ligand backbone. Delocalisation of the aromatic  $\pi$  electrons of the phenyl ring over bonds i and iii leads to stronger and thus shorter bonds.

## 2.4 Solid State structures of ligands and complexes

### 2.4.1 Free Ligands

Although the crystalline structures of ligands **1**, **5**, **7**, **9** and **10** may bear little relation to their behaviour in solution, some information on the propensity of these ligands to form the desired *pseudo*-macrocyclic motif (see chapter 1) can be achieved. We proposed that this could give rise to increased stability of the metal complexes, as seen for phenolic oximes.

The principles of crystal engineering have shown that the number of hydrogen-bond acceptor and donor sites in the molecule is very important in determining the observed structure. Empirical rules of hydrogen-bonding in crystals suggest<sup>6</sup> that the structure will be dominated by the strongest hydrogen-bond donor interacting with the strongest hydrogen-bond acceptor. Any further acceptors or donors in the system will give rise to additional interactions and may lead to unusual crystal architectures.

Simple monosulfonamidodiamines have several hydrogen-bond donor and acceptor functions (Figure 2.8).

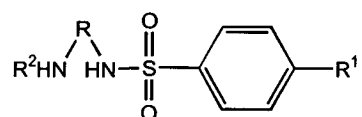


**Figure 2.8:** The hydrogen-bond donor (blue) and acceptor atoms (red) in simple monosulfonamidodiamines.

The number of hydrogen-bond donor and acceptor atoms are tabulated in Table 2.2 below. Each oxygen atom has two hydrogen-bond acceptor sites as they have two lone pairs of electrons. It is easy to see from Table 2.2 that a wide range of hydrogen-bonded structures are likely to be observed for the free ligands. These are described in detail in this section.

**Table 2.2:** The numbers of hydrogen-bond donor and acceptor sites in simple monosulfonamidodiamine free ligand molecules.

	R <sup>2</sup> = alkyl / aryl	R <sup>2</sup> = H
Number of hydrogen-bond acceptor sites	6	6
Number of hydrogen-bond donor atoms	2	3

### 2.4.1.1 N-(3-aminopropyl)-4-methylbenzenesulfonamide (5)

Of the five determined ligand X-ray structures only two, **5** and **9**, exhibit head-to-tail hydrogen-bonding to create a *pseudo*-macrocycle in the solid state. Figure 2.9 shows the hydrogen-bonded dimeric unit of **5**.

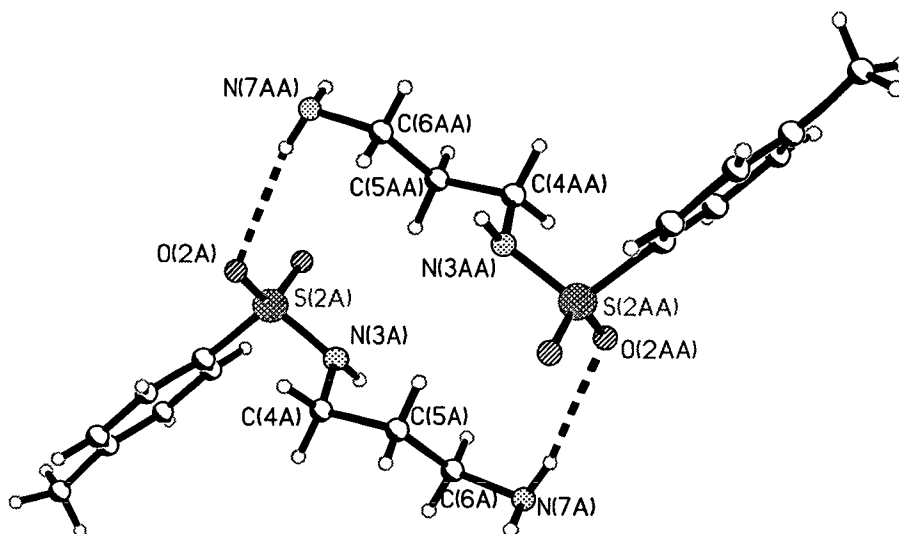


**Figure 2.9:** The hydrogen-bonded dimer of N-(3-amino-propyl)-4-methylbenzenesulfonamide (**5**), showing the atom labelling scheme.

Two hydrogen-bonds between sulfonamido oxygen and amino nitrogen atoms [N(7A)-H---O(2A), 3.2610(17) Å; N-H-O, 165°] form a *pseudo*-macrocycle. These dimeric units are linked by hydrogen-bonds between an amino hydrogen atom, N(7A)-H, and a sulfonamido oxygen atom, O(1A), to form a chain parallel to the *b* axis as depicted in Figure 2.10.

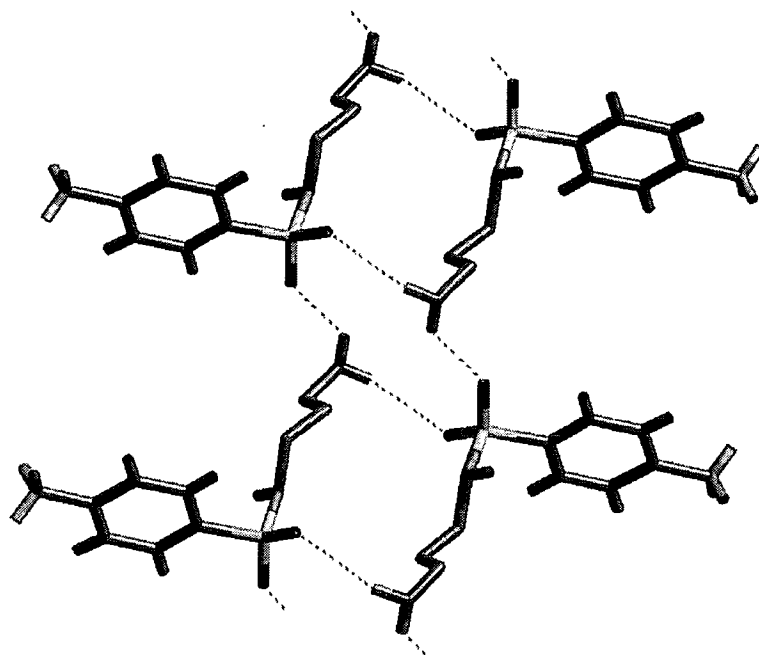


**Figure 2.10:** The hydrogen-bonded chain of dimeric units along the  $b$  axis.

Adjacent strands of dimer units run in opposite directions parallel to the  $b$  axis and are linked by four hydrogen-bonds from each dimer between the amino nitrogen atoms N(7A) and the sulfonamido hydrogen atom H(3A) to create a hydrogen-bonded sheet along the  $bc$  plane (Figure 2.11).

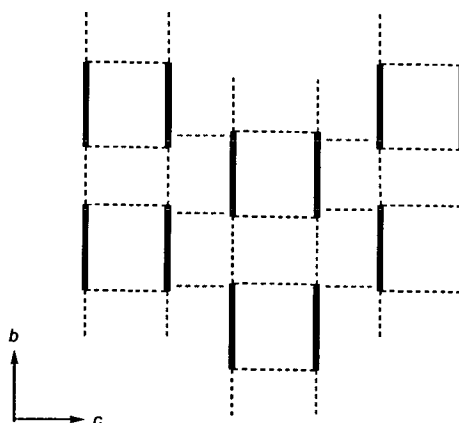


**Figure 2.11:** A schematic diagram to represent the two dimensional hydrogen-bonded sheet of molecules of **5**. The dimer units are represented by the squares in black with hydrogen-bonds indicated by a dashed line and the ligand backbone by a solid line. The N(7A)-H...O(1A) hydrogen-bonds linking the units along the  $b$  axis are in blue and the N(3A)-H...N(7A) hydrogen-bonds linking the chains along the  $c$  axis are marked in red.



### 2.4.1.2 N-(N-butyl-2-aminopropyl)-4-methylbenzenesulfonamide (9)

The other structure to exhibit a hydrogen-bonded dimeric motif was N-(2-butylaminopropyl)-4-methylbenzenesulfonamide (9) (Figure 2.12).

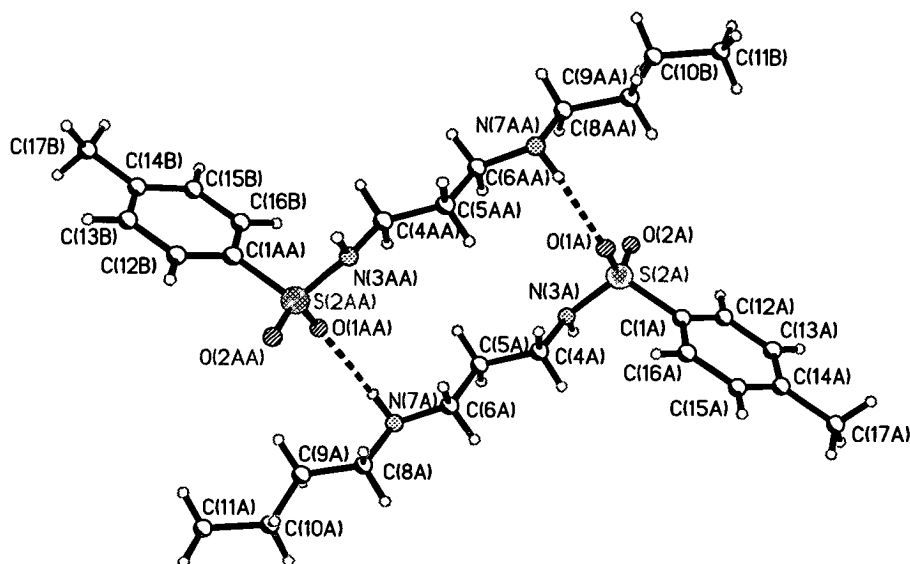


Figure 2.12: The hydrogen-bonded dimer of N-(2-butylaminopropyl)-4-methylbenzenesulfonamide (9).

Each molecule is involved in two types of hydrogen-bonding. Hydrogen-bonds between sulfonamido oxygen atoms and amino hydrogen atoms, [N(7A)-H---O(1A/1AA), 3.125(4) Å; N-H-O, 144(3)°] link two molecules of 9 to create a *pseudo*-macrocycle. A second type of hydrogen-bond between an amino nitrogen atom acceptor site, N(7A), and a sulfonamido hydrogen donor atom, N(3A)-H link each of these ligands to two other molecules [N(3A)-H---N(7A), 2.96 Å, N-H-N, 167°] (Figure 2.13). This leads to a two dimensional hydrogen-bonded sheet of molecules along the *bc* plane.

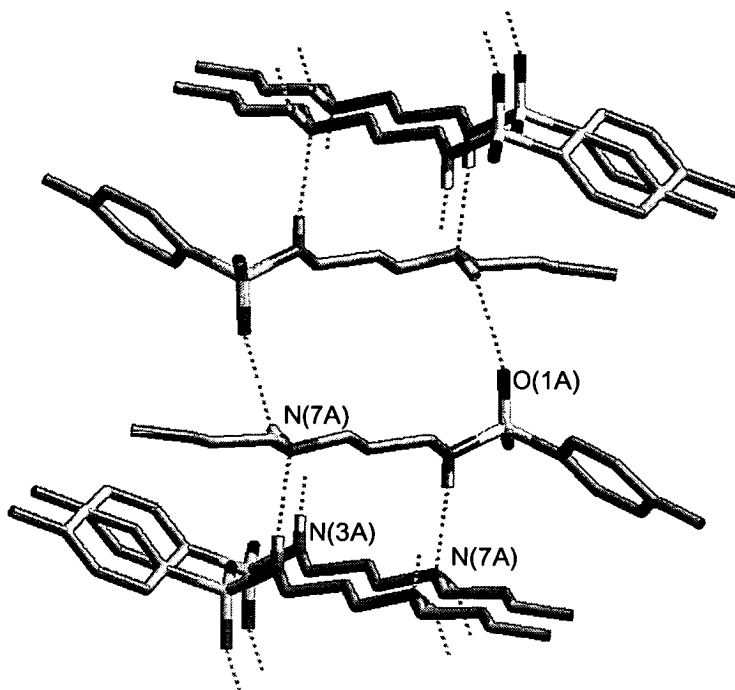
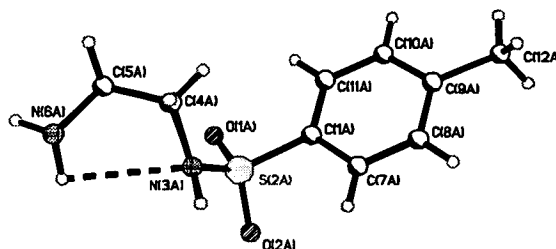


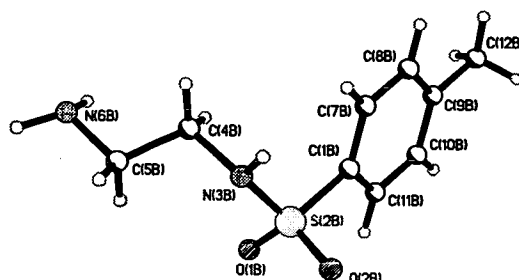
Figure 2.13: The hydrogen-bonded network of 9 cross-linking dimers along the *c* axis.

### 2.4.1.3 N-(2-aminoethyl)-4-methylbenzenesulfonamide (1)

There are two crystallographically independent molecules of **1**, type A and type B, in the unit cell (Figure 2.14). Type A molecules, unlike type B, are folded due to an *intra*-molecular hydrogen-bond between the sulfonamido nitrogen atom and the amino hydrogen atom [N(6A)-H---N(3A), 2.88 Å; N-H-N, 95°].



A



B

**Figure 2.14:** The two crystallographically independent molecules (Type A and Type B) of N-(2-aminoethyl)-4-methylbenzenesulfonamide **1**, showing the atom labelling scheme.

Molecule **1** has an extensive *inter*-molecular hydrogen-bonded structure. Type A molecules are linked together *via* type B molecules with hydrogen-bonds between the sulfonamido hydrogen atoms, H(3A) and H(3B) and amino nitrogen atoms N(6B) and N(6A) respectively to create a “parallel-stacked” AB chain orientated along the *a* axis (Figure 2.15).

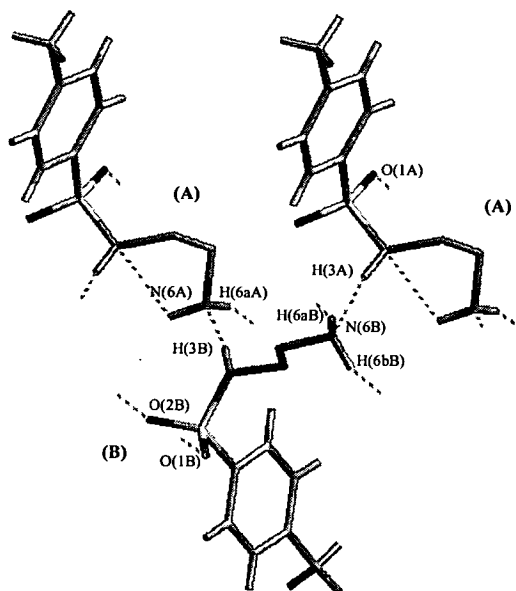


**Figure 2.15:** The hydrogen-bonded chain of type A and type B molecules of **1** along the *a* axis.

Type B molecules are also hydrogen-bonded to two other type A molecules *via* two sulfonamido oxygen atoms, O(1A) and O(1B), and two amino hydrogen atoms, H(6aB) and H(6aA), along the *b* axis to create a hydrogen-bonded sheet along the *ab* plane. Finally, type B molecules are also linked to each other in a hydrogen-bonded chain along the *b* axis *via* N(6B)-H(6bB)---O(2B) hydrogen-bonds. This two dimensional hydrogen-bonded array is shown schematically in Figure 2.16.

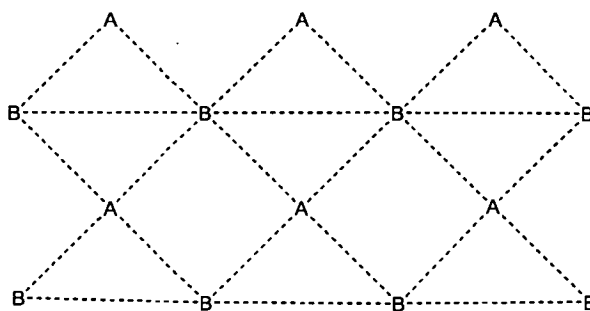


**Figure 2.16:** The two dimensional hydrogen-bonded sheet of **1**. The dashed lines represent hydrogen-bonds.

## 2.4.1.4 N-(N-benzyl-2-aminopropyl)-4-methylbenzenesulfonamide (7)

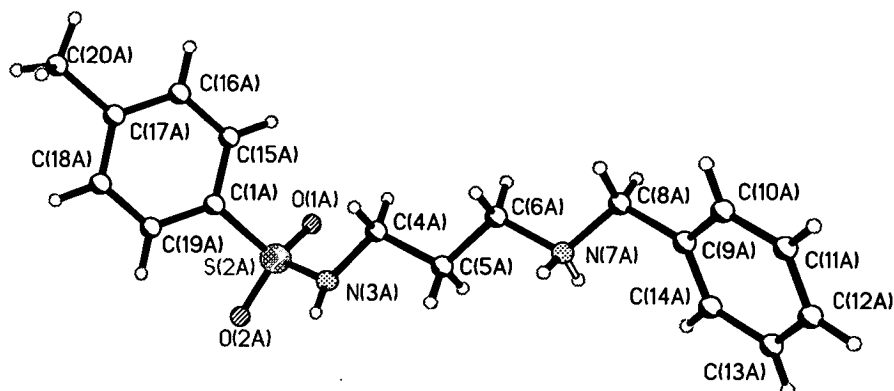


Figure 2.18: The X-ray structure of N-(N-benzyl-2-aminopropyl)-4-methylbenzenesulfonamide (7).

Each molecule of **7** is linked to two other molecules with four hydrogen-bonds along the *c* axis to form a chain. Molecules are linked by hydrogen-bonds between the sulfonamido nitrogen atom N(3A) and the amino hydrogen atom N(7A)-H, [N(7A)-H...N(3A), 2.997(7) Å; N-H-N, 158(11)°], and between the sulfonamido hydrogen atom N(3A)-H and the amino nitrogen atom N(7A), [N(3A)-H...N(7A), 3.00 Å; N-H-N, 170°] as shown in Figure 2.18 below.

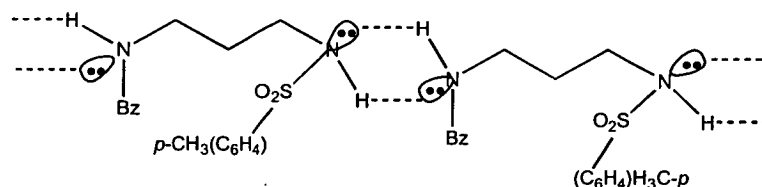
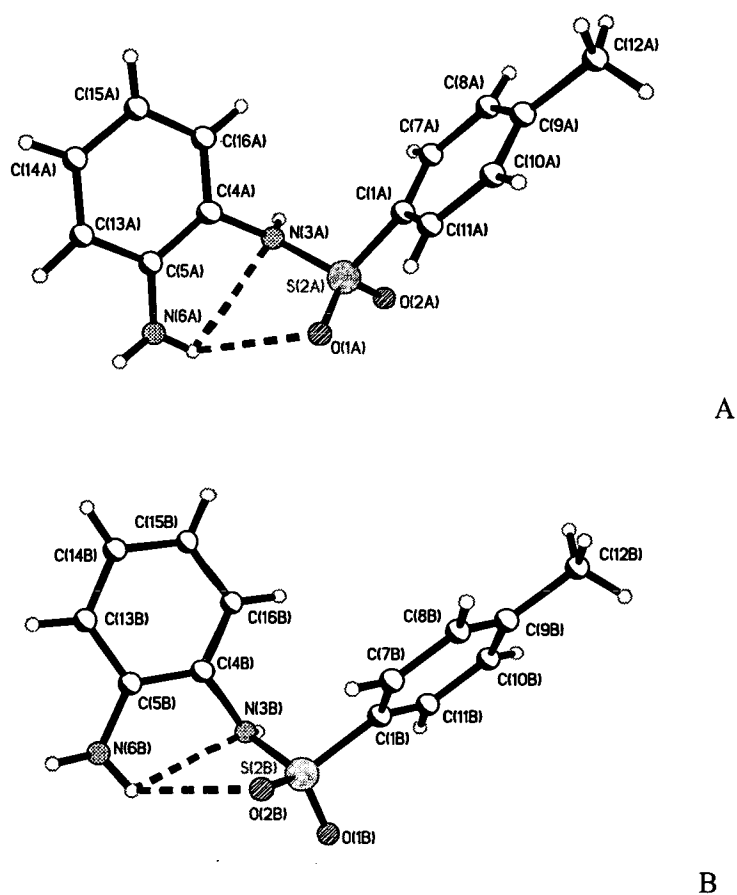


Figure 2.17: The 4-membered hydrogen-bonded ring linking molecules of **7** along the *c* axis.

A feature of the secondary hydrogen-bonded structure of **7** is that the sulfonamido oxygens are not involved in any hydrogen-bonding. According to the rules of crystal engineering<sup>6</sup> the strongest hydrogen-bonds form first. This suggests that for **7** the combination of the amino hydrogen atom to sulfonamido nitrogen atom and the amino nitrogen atom to sulfonamido hydrogen atom bonds is stronger than any interaction involving the sulfonamido oxygen atoms.

### 2.4.1.5 N-(2-amino-phenyl)-4-methylbenzenesulfonamide (10)

There are two molecules of **10** in the asymmetric unit, designated as A and B. Both have very similar *intra*-molecularly hydrogen-bonded structures and are shown in Figure 2.19. Both have two *intra*-molecular hydrogen-bonds, between a sulfonamido oxygen atom and an amino hydrogen atom [N(6)-H---O(1), 3.117(5) Å and 3.179(4) Å; N-H-O, 126(3)° and 125(5)° in molecules A and B respectively]. The amino hydrogen atom N(6)-H acts as a bifurcated hydrogen-bond donor also bonding to the sulfonamido nitrogen atom [N(6)-H---N(3), 2.797(5) Å and 2.808(5) Å; N-H-N, 100(3)° and 102° in molecules A and B respectively].



**Figure 2.19:** The structure of A and B molecules of [N-(2-aminophenyl)-4-methylbenzenesulfonamide] (**10**), showing atom labelling schemes.

Type A molecules and type B molecules form individual hydrogen-bonded chains along the *b* axis. Linear chains of type A molecules are formed *via* two hydrogen-bonds to two other molecules through the sulfonamido oxygen atom not involved in *intra*-molecular hydrogen-bonding, O(2A), and the sulfonamido hydrogen atom, H(3A). Type B molecules form more complicated chains involving four *inter*-molecular hydrogen-bonds to two molecules (Figure 2.20). The sulfonamido oxygen atom not involved in *intra*-molecular hydrogen-bonding, O(2A), is bifurcated and hydrogen-bonds to the amino hydrogen atom of one molecule, H(B6A), and the sulfonamido hydrogen atom, H(3A), of a second molecule thus forming a chain.

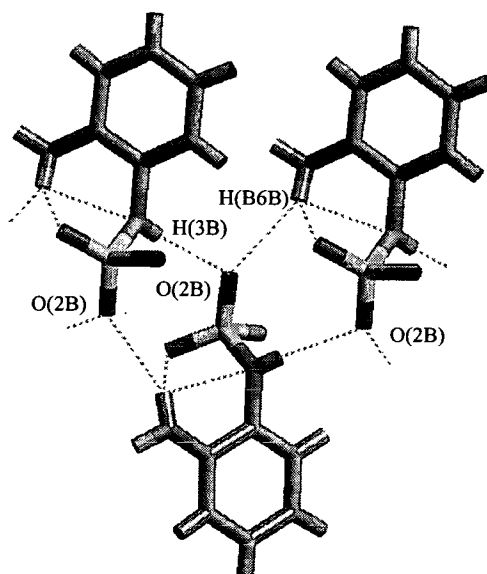


**Figure 2.20:** Hydrogen-bonded chain of type B molecules along the *b* axis in the structure of **10**. The tolyl groups have been removed for clarity.

#### 2.4.2 Hydrogen-bonding in monosulfonamidodiamine ligands

The length D...A (Å), where D is the oxygen or nitrogen atom of the hydrogen-bond donors and A the acceptor, and the angles D-H...D (°) for all the hydrogen-bonding interactions in ligands **1**, **5**, **7**, **9** and **10** are tabulated in Tables 2.3, 2.4 and 2.5.

**Table 2.3:** *Intra*-molecular hydrogen-bond lengths (Å) and angles (°) of ligands **1** and **10**.

Ligand	Interaction	Hydrogen-bond length / Å	Hydrogen-bond angle / °
<b>1A<sup>a</sup></b>	N( <i>A</i> )-H---O( <i>S</i> )	2.88	95
<b>10A<sup>a</sup></b>	N( <i>A</i> )-H---O( <i>S</i> )	3.117(5)	126(3)
	N( <i>A</i> )-H---N( <i>S</i> )	2.797(5)	100(3)
<b>10B<sup>a</sup></b>	N( <i>A</i> )-H---O( <i>S</i> )	3.179(4)	125(3)
	N( <i>A</i> )-H---N( <i>S</i> )	2.808(5)	102(3)

<sup>a</sup> Ligands **1** and **10** have two crystallographically independent molecules, A and B, per asymmetric unit. Atoms labelled *A* are contained in an amino group. Atoms labelled *S* are contained in a sulfonamido group.

**Table 2.4:** Hydrogen-bond lengths (Å) and angles (°) in ligands **5** and **9** which form *pseudo*-macrocylic structures in the solid state.

Ligand	Interaction	Number of interactions	Hydrogen-bond length / Å	Hydrogen-bond angle / °
<b>5</b>	N( <i>A</i> )-H---O( <i>S</i> )	2	3.2610(17)	164.7(14)
<b>9</b>	N( <i>A</i> )-H---O( <i>S</i> )	2	3.125(4)	143(3)

Atoms labelled *A* are contained in an amino group. Atoms labelled *S* are contained in a sulfonamido group.

**Table 2.5:** *Inter*-molecular hydrogen-bond lengths (Å) and angles (°) of ligands **1**, **5**, **7**, **9** and **10**.

Ligand	Interaction	Number of interactions	Hydrogen-bond length / Å	Hydrogen-bond angle / °	
<b>1<sup>a</sup></b>	molecule A	N( <i>A</i> )---H-N( <i>S</i> )	1	2.83	172
		N( <i>S</i> )-H---N( <i>A</i> )	1	2.852(6)	170(3)
		O( <i>S</i> )---H-N( <i>A</i> )	1	3.11	155
	molecule B	N( <i>A</i> )-H---O( <i>S</i> )	1	3.070(5)	151(3)
		N( <i>S</i> )-H---N( <i>A</i> )	1	2.83	172
		N( <i>A</i> )---H-N( <i>S</i> )	1	2.85	170
		N( <i>A</i> )-H---O( <i>S</i> )	1	3.111(5)	155(4)
		O( <i>S</i> )---H-N( <i>A</i> )	1	3.07	152
		N( <i>A</i> )-H---O( <i>S</i> )	2	3.169(4)	156(5)
<b>5</b>	N( <i>S</i> )-H---N( <i>A</i> )	2	2.91	174	
	N( <i>A</i> )-H---O( <i>S</i> )	2	3.1751(18)	134.9(14)	
<b>7</b>	N( <i>S</i> )-H---N( <i>A</i> )	2	2.997(7)	158(11)	
	N( <i>A</i> )-H---N( <i>S</i> )	2	3.00	170	
<b>9</b>	N( <i>S</i> )-H---N( <i>A</i> )	2	2.96	167	
<b>10<sup>a</sup></b>	molecule A	N( <i>A</i> )-H---O( <i>S</i> )	1	2.817(4)	172(4)
		O( <i>S</i> )---H-N( <i>A</i> )	1	2.81	172
	molecule B	N( <i>A</i> )-H---O( <i>S</i> )	2	3.197(4)	144(5)
		N( <i>S</i> )-H---O( <i>S</i> )	2	2.945(4)	174(3)

<sup>a</sup> These ligands have two crystallographically independent molecules A and B, per asymmetric unit. Atoms labelled *A* are contained in an amino group. Atoms labelled *S* are contained in a sulfonamido group.

Each ligand is involved in between 4 and 6 hydrogen-bonding interactions. The bond length and angles of *inter*-molecular hydrogen-bonding N(*A*)-H---O(*S*) interactions are



independent of whether or not the bond is involved in *pseudo*-macrocyclic ligand formation (mean values are 3.12 *c.f.* 3.05 Å and 154 *c.f.* 145°). The lengths of the *intra*-molecular N(*A*)-H---O(*S*) bonds (mean 3.06 Å) are very similar however the bond angles are smaller (mean 115°) which is usually associated with a weaker bond due to the non-linear nature of the interaction.

For N(*A*)-H---N(*S*) interactions a significantly smaller bond angle is also observed for *intra*-molecular interactions (mean 101°), than for *inter*-molecular interactions (mean 168°). However, the lengths are very similar, 2.81 and 2.93 Å respectively.

### 2.4.3 Monosulfonamidodiamine complexes

#### 2.4.3.1 Bis[N-(2-aminoethyl)-4-methylbenzenesulfonamidato]zinc(II) (12)

The asymmetric unit of **12** contains two zinc complexes [Zn(1-H)<sub>2</sub>] and two methanol molecules. The two complexes, referred to as complexes (1) and (2) below in the asymmetric unit have very similar geometries. The structure of the Zn(1) complex is shown in Figure 2.21.

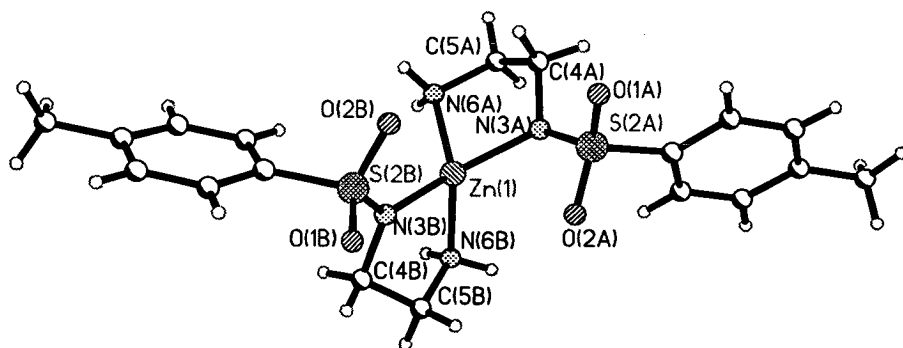


**Figure 2.21:** The X-ray structure of one of the two [Zn(1-H)<sub>2</sub>] complexes (complex 1 containing Zn(1)) in the asymmetric unit of bis[N-(2-aminoethyl)-4-methylbenzenesulfonamidato]zinc(II) (**12**).

In [Zn(1-H)<sub>2</sub>] the zinc atom is distorted from tetrahedral coordination geometry. The N(3)-Zn(1)-N(6) and N(3)-Zn(2)-N(6) chelate angles are significantly smaller, 84.6(3)°, 84.9(3)° and, 84.7(3)°, 85.3(3)° respectively, than 109.5° which is expected for a perfect tetrahedral complex. This can be attributed to the five-membered chelate ring which restricts the size of the bite distances, the distance between the two nitrogen atoms, which range from 2.69 to 2.72 Å. The dihedral angle between the Zn, N(3A) and N(6A) planes and the Zn, N(3B) and N(6B) planes are 90.2 and 88.3° for the Zn(1) and Zn(2) complexes respectively. These values are close to 90° which would be observed for a perfectly tetrahedral system. The Zn-N<sub>(sulfonamido)</sub> bond lengths range from 1.949(8) to 1.975(8) Å and are significantly shorter than the Zn-N<sub>(amino)</sub> bonds which range from 2.035(7) to 2.059(7) Å, suggesting that the anionic sulfonamidato nitrogen bonds more strongly than the amino nitrogen.

No hydrogen-bonding is observed between the two chelated N-(2-aminoethyl)-4-methylbenzenesulfonamidato ligands. The hydrogen-bond donors and acceptors of the ligands have been twisted out of any interaction range by the *pseudo*-tetrahedral geometry of the metal which forces the chelate units to be almost perpendicular to each other. There is, however, extensive hydrogen-bonding present within the lattice. The Zn(1) and Zn(2) complexes each form individual polymeric hydrogen-bonded chain along the *a* axis *via* three strong *inter*-molecular N-H---O interactions between sulfonamidato oxygen atoms, O(1A), O(2A) and O(1B), and amino hydrogen atoms, H(6aA), H(6aB) and H(6bB) in adjacent complexes. This is illustrated for the Zn(1) complexes in Figure 2.22.

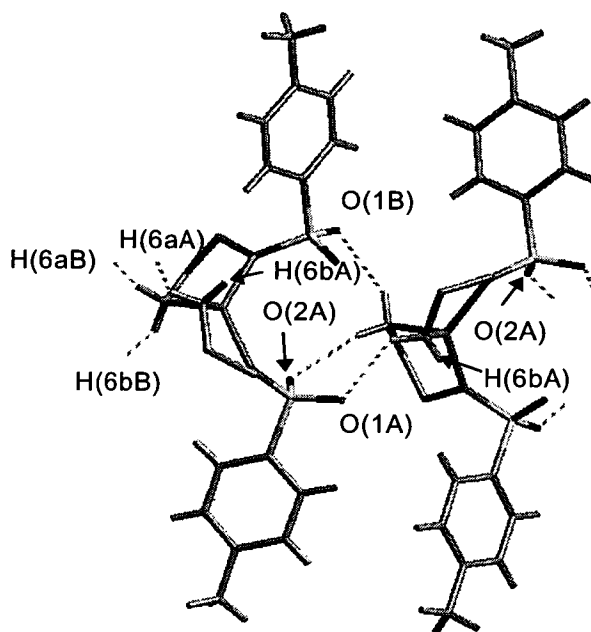


**Figure 2.22:** The hydrogen-bonded secondary structure of the Zn(1) complex along the  $a$  axis in the X-ray structure of  $[\text{Zn}(\text{1-H})_2]$ .

The number and nature of the *inter*-molecular hydrogen-bonds linking the Zn(2) complexes are the same as those linking the Zn(1) complexes and only their lengths and angles differ, presumably due to the different orientations of the complexes. The chains of Zn(1) and Zn(2) complexes alternate along the  $c$  axis and are bonded together by two similar hydrogen-bonded bridges *via* a methanol molecule between the bifurcated sulfonamidate oxygen atoms [O(2A) and O(2C)] and the amino hydrogen atoms [H(6bA) and H(6aC)] of Zn(1) and Zn(2) units respectively creating a two dimensional sheet. The atoms of Zn(1) complexes involved in forming these bridges are marked by arrows in Figure 2.22. The schematic diagram in Figure 2.23 illustrates how the two chains of zinc complexes are linked together.

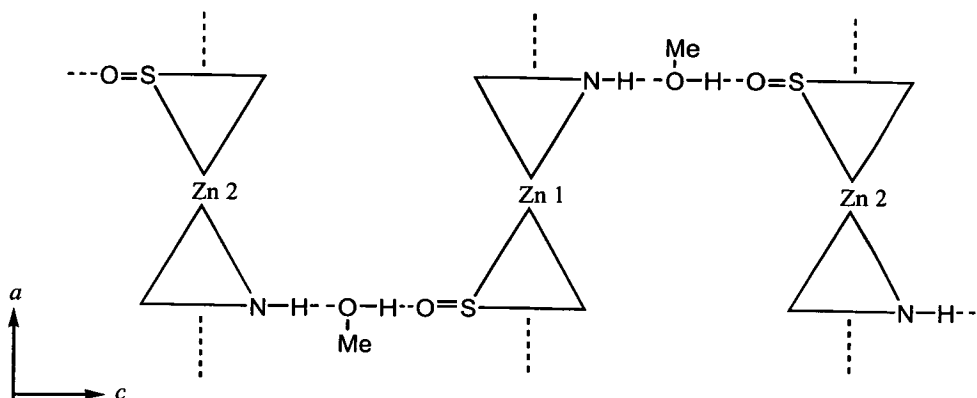
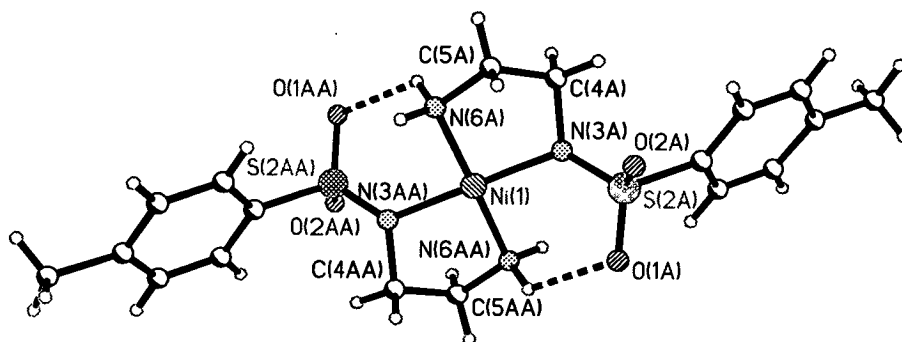


Figure 2.23: The two dimensional hydrogen-bonded sheet of **12**.

#### 2.4.3.2: Bis[N-(2-aminoethyl)-4-methylbenzenesulfonamidato]nickel(II) (**13**)

The asymmetric unit of **13** consists of half of the complex. The nickel(II) atom lies on an inversion centre and is coordinated by two amino and two sulfonamidato nitrogen atoms in a planar fashion with chelate, N(3)-Ni-N(6), angles of  $85.97(13)^\circ$ . This value is not far from the  $90^\circ$  expected for square-planar geometry. The smaller value of the angle than the ideal value may again be explained by the bite distance of  $2.61 \text{ \AA}$  which is restricted by the five-membered chelate ring. The sulfonamidato and amino nitrogen to nickel bond lengths are  $1.909(3)$  and  $1.918(3) \text{ \AA}$  respectively. Unlike the analogous zinc complex  $[\text{Zn}(\mathbf{1-H})_2]$  both nitrogen atoms appear to bind to the metal centre with similar strength.



**Figure 2.24:** The X-ray structure of bis[N-(2-aminoethyl)-4-methylbenzenesulfonamidato]nickel(II) (13).

Two *intra*-complex hydrogen-bonds between the sulfonamidato oxygen and amino hydrogen atoms [N(6A)-H---O(1AA), 2.797(5) Å; N-H-O, 123°] create a *pseudo*-macrocyclic ligand. Extensive *inter*-molecular hydrogen-bonding is also present.

The sulfonamidato oxygen and the amino hydrogen atoms involved in creating the *pseudo*-macrocycle are bifurcated and form N-H---O interactions along the *b* axis with two adjacent complexes to create a one dimensional chain of molecules. Further hydrogen-bonded N(6A)-H---O(2A) interactions between the sulfonamide oxygen and amino nitrogen atoms, not involved in the previous type of interaction, link the complex with four other complexes, two situated above and two below the chain of molecules to form a two dimensional hydrogen-bonded sheet in the *bc* plane. These hydrogen-bonding interactions are illustrated in Figure 2.25.

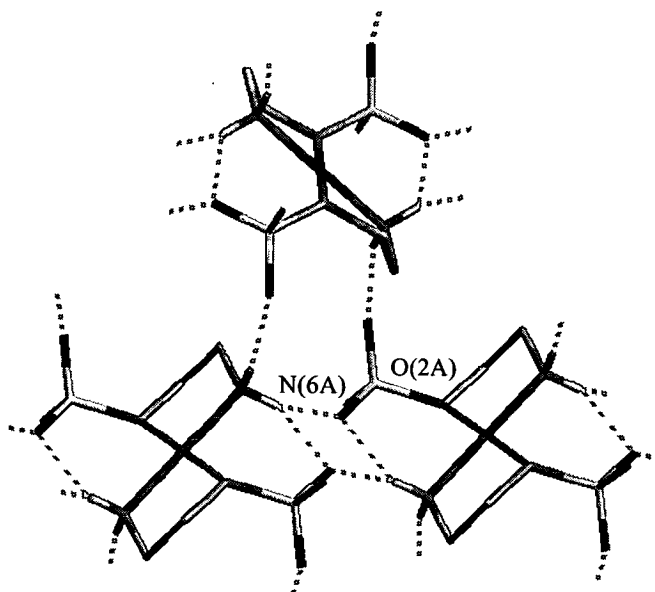


**Figure 2.25:** The secondary hydrogen-bonded structure of **13**. The tolyl groups and hydrogen atoms not involved in hydrogen-bonding are omitted for clarity.

#### 2.4.3.3 Bis[N-(2-aminoethyl)-4-*t*-butylbenzenesulfonamidato]copper(II) (**16**)

The asymmetric unit of [Cu(2-H)<sub>2</sub>] contains one complex (Figure 2.26), in which the copper(II) ion is slightly distorted from a planar geometry with a dihedral angle of 9.8° between the Cu(1), N(3A) and N(6A) plane and the Cu(1), N(3B) and N(6B) plane. The chelate angles are N(3A)-Cu-N(6A) 83.28(10)° and N(3B)-Cu-N(6B) 82.15(10)° which are smaller values than the 90° angle required for perfect square-planar coordination. These angles are less than in the analogous nickel complex (**13**) where a chelate angle of 86° is observed. This indicates the preference of d<sup>8</sup> nickel for a square-planar geometry because of the increase in ligand field stabilisation energy as the high energy *dx<sup>2</sup>-dy<sup>2</sup>* orbital is no longer occupied. The gain in ligand field stabilisation in d<sup>9</sup> copper complexes is less, due to the extra electron, therefore the metal centre is less likely to push the geometry towards perfect square planar despite the bite distances of 2.64 and 2.62 Å for the copper complex which are larger than the bite distance of 2.61 Å in the nickel complex. The copper to sulfonamidato nitrogen bond lengths are 1.975(2) and 1.987(2) Å and the copper to amino nitrogen bond lengths are 1.993(2) and 1.998(2) Å. The difference in these bond lengths is not

significant and suggests that the sulfonamido nitrogen atoms and the amino nitrogen atoms are of approximately equal strength as coordinating atoms.

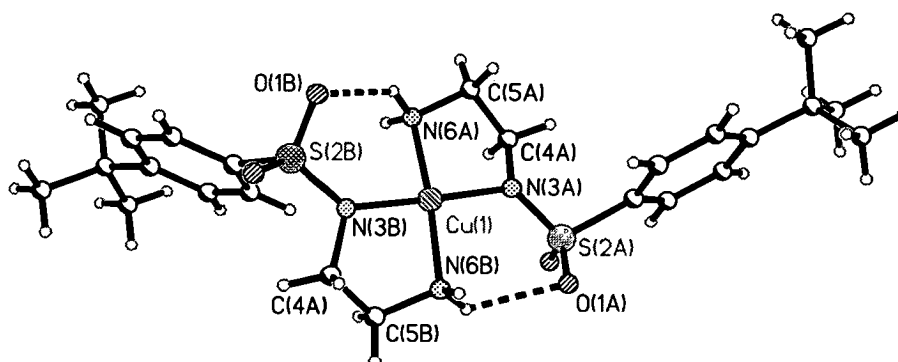


**Figure 2.26:** X-ray structure of Bis[N-(2-aminoethyl)-4-*tert*-butylbenzenesulfonamidato]copper(II) (**16**) showing *intra*-complex hydrogen-bonding.

In an analogous way to the nickel complex (**13**) a head-to-tail arrangement of the ligands around the metal is observed and two *intra*-complex hydrogen-bonds between the sulfonamido oxygen and amino hydrogen atoms [N(6A)-H---O(1B), 2.834(3) Å; N-H-O, 138° and N(6A)-H---O(1A), 2.785(3) Å; N-H-O, 120°] create a *pseudo*-macrocycle around the copper. This structure may be compared to the [Cu(**5-H**)<sub>2</sub>] complex of the propane bridged ligands.<sup>1</sup> Two crystalline forms of [Cu(**5-H**)<sub>2</sub>] were isolated<sup>1</sup> in which the copper(II) atom has either a highly distorted tetrahedral or highly distorted square-planar structure. The extra methylene unit in the backbone of ligand **5** *cf.* ligand **2**, results in such a distortion of the complex geometry. There is no *intra*-molecular hydrogen-bonding in the two polymorphs of [Cu(**5-H**)<sub>2</sub>] and it is thought<sup>1</sup> that extensive *inter*-molecular hydrogen-bonded networks are responsible for the unusual copper geometries.

The secondary hydrogen-bonded structure of **16** consists of a chain of molecules along the *a* axis of the unit cell (Figure 2.27). Each centrosymmetric complex is linked to two other complexes *via* four hydrogen-bonds between amino hydrogen atoms and

sulfonamidato oxygen atoms [N(6B)-H---O(2A), 2.970(3) Å; N-H-O, 165°] and [N(6A)-H---O(2B), 2.934(3) Å; N-H-O, 164°].

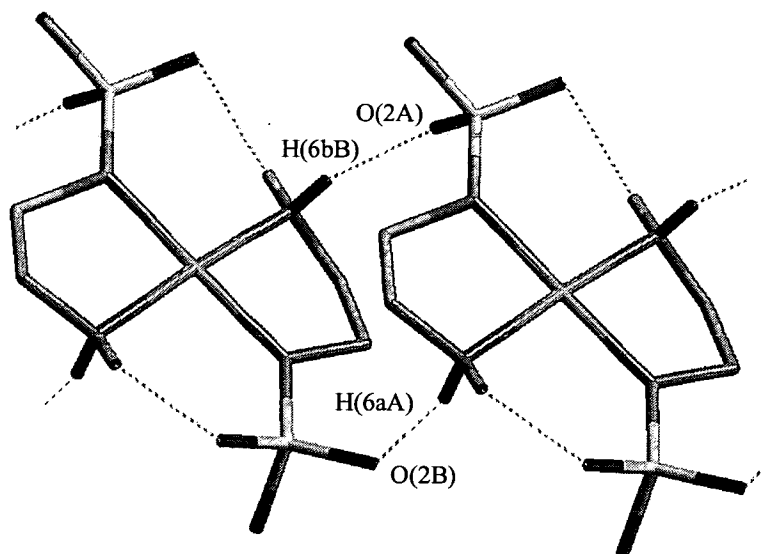


**Figure 2.27:** *Inter*-molecular hydrogen-bonding in [Cu(2-H)<sub>2</sub>] parallel to the *a* axis. The tolyl groups and hydrogen atoms not involved in hydrogen-bonding are omitted for clarity.

The nickel(II) complex of ligand **1** and the copper(II) complex of ligand **2** are both planar with *intra*-molecular hydrogen-bonds between one of the sulfonamidato oxygen atoms and one of the amino hydrogen atoms creating a *pseudo*-macrocycle around the metal centres. In contrast, the zinc(II) complex has a distorted tetrahedral geometry and no *intra*complex hydrogen-bonding. A CSD search (May 2001) showed that the metal to sulfonamidato nitrogen bond lengths for complexes **12**, **13** and **16** were comparable to the lengths of similar complexes in the data base (Cu-N<sub>(sulfonamidato)</sub> 1.922-2.003 Å, Zn-N<sub>(sulfonamidato)</sub> 1.925-1.969 Å, Ni-N<sub>(sulfonamidato)</sub> 1.904-1.916 Å).

#### 2.4.4 Hydrogen-bonding in sulfonamidodiamine complexes

All hydrogen-bonding interactions for each sulfonamidodiamine complex are summarised in Tables 2.6 and 2.7.



**Table 2.6:** Details of *intra*-complex hydrogen-bonds which form a *pseudo*-macrocyclic ligand around the nickel(II) and copper(II) centres in complexes [Ni(1-H)<sub>2</sub>](13) and [Cu(2-H)<sub>2</sub>](16).

Complex	Interaction	Number of interactions	Hydrogen-bond length / Å	Hydrogen-bond angle / °
[Ni(1-H) <sub>2</sub> ]	N(A)-H---O(S)	2	2.797(5)	122
[Cu(2-H) <sub>2</sub> ]	N(A)-H---O(S)	1	2.834(3)	138
	N(A)-H---O(S)	1	2.785(3)	119

**Table 2.7:** Details of *inter*-complex hydrogen-bonds in monosulfonamidodiamine complexes [Zn(1-H)<sub>2</sub>] (12), [Ni(1-H)<sub>2</sub>] (13) and [Cu(2-H)<sub>2</sub>] (16).

Complex	Interaction	Number of interactions	Hydrogen-bond length / Å	Hydrogen-bond angle / °
[Zn(1-H) <sub>2</sub> <sup>a</sup> ]				
Zn(1) complex	N(A)-H---O(S)	2	3.031(11)	144
	N(A)-H---O(S)	2	3.012(10)	156
	N(A)-H---O(S)	2	2.939(11)	125
	N(A)-H---O(M)	1	3.003(12)	163
	O(S)---H-O(M)	1	2.792(11)	140
Zn(2) complex	N(A)-H---O(S)	2	3.057(11)	155
	N(A)-H---O(S)	2	3.168(11)	157
	N(A)-H---O(S)	2	2.939(11)	141
	N(A)-H---O(M)	1	3.003(12)	163
	O(S)---H-O(M)	1	2.792(11)	140
[Ni(1-H) <sub>2</sub> ]	N(A)-H---O(S)	4	3.100(5)	143
	N(A)-H---O(S)	4	2.946(4)	156
[Cu(2-H) <sub>2</sub> ]	N(A)-H---O(S)	2	2.970(3)	163
	N(A)-H---O(S)	2	2.934(3)	165
[Cu(5-H) <sub>2</sub> <sup>b</sup> ] FODSIA <sup>1</sup>	N(A)-H---O(S)	2	2.93	153
	N(A)-H---O(S)	2	3.16	140
	N(A)-H---O(S)	2	3.11	141
	N(A)-H---O(S)	2	2.89	151
[Cu(5-H) <sub>2</sub> <sup>bc</sup> ] FODSIA01 <sup>1</sup>				
Cu(1) complex	O(S)---H-N(A)	1	2.93	163
	O(S)---H-N(A)	1	3.04	172
	N(A)-H---O(S)	1	3.08	172
	N(A)-H---O(S)	1	2.98	173
	N(A)-H---O(S)	2	2.97	170
	N(A)-H---O(S)	2	3.09	172
Cu(2) complex	N(A)-H---O(S)	1	2.93	163
	N(A)-H---O(S)	1	3.04	172
	O(S)---H-N(A)	1	3.08	172
	O(S)---H-N(A)	1	2.98	173
	N(A)-H---O(S)	2	3.08	168
	N(A)-H---O(S)	2	2.90	170

<sup>a</sup> This structure has two crystallographically independent metal complexes per asymmetric unit containing Zn(1) and Zn(2). <sup>b</sup> This complex exists in blue and green polymorphs. <sup>c</sup> The blue polymorph has two crystallographically independent complexes containing Cu(1) and Cu(2) per asymmetric unit. Atoms labelled *A* are contained in an amino group. Atoms labelled *S* are contained in a sulfonamido group. Atoms labelled *M* are contained in a methanol molecule.

Each complex is involved in between six and ten N(A)-H---O(S) hydrogen-bonding interactions. *Intra*-complex hydrogen-bonds have shorter lengths than *inter*-complex interactions but also have smaller bond angles, 2.80 and 3.01 Å and 126 and 157° respectively.

#### 2.4.5 Hole sizes, bite distances and torsion angles.

The “hole sizes”<sup>7</sup> in the free ligands, **5** and **9**, which show *pseudo*-macrocyclic structures *via inter*-molecular hydrogen-bonding in a dimer were calculated from their solid state structures (Figure 2.28). The centroid (X) of the four nitrogen atoms of the *pseudo*-macrocycle was determined. Its mean distance ( $R_m$ ) from the four nitrogen atoms is termed the hole size.

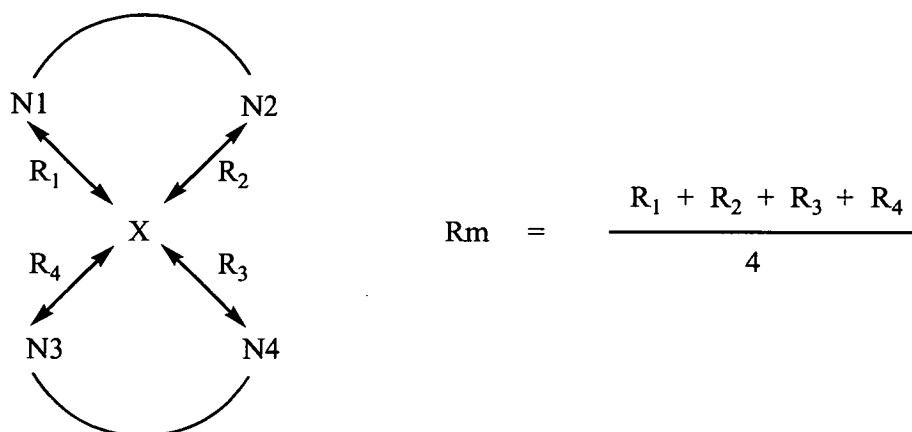


**Figure 2.28:** Calculation of the hole size of a hydrogen-bonded *pseudo*-macrocycle.

Values are recorded in Table 2.8 below of the hole size in the dimeric units of ligands **5** and **9** and in complexes **12**, **13**, **16**, **FODSIA (21)** and **FODSIA01 (22)**.

**Table 2.8:** The hole sizes of the *pseudo*-macrocyclic free ligands **5** and **9** and related metal(II) complexes.

Structure	Hole size / Å
<b>5</b>	3.14
<b>9</b>	3.50
[Zn(1-H) <sub>2</sub> ] <sup>a</sup> , ( <b>12</b> )	2.00
	2.00
[Ni(1-H) <sub>2</sub> ] <sub>2</sub> , ( <b>13</b> )	1.91
[Cu(2-H) <sub>2</sub> ] <sub>2</sub> , ( <b>16</b> )	1.99
[Cu(5-H) <sub>2</sub> ] <sub>2</sub> , <sup>b</sup> FODSIA <sup>1</sup> ( <b>21</b> )	1.98
[Cu(5-H) <sub>2</sub> ] <sub>2</sub> , <sup>bc</sup> FODSIA01 <sup>1</sup> ( <b>22</b> )	1.99
	1.99

<sup>a</sup> This structure has two crystallographically independent metal complexes per asymmetric unit containing Zn(1) and Zn(2). <sup>b</sup> This complex exists in blue and green polymorphs (**FODSIA** and **FODSIA01**). <sup>c</sup> The blue polymorph has two crystallographically independent complexes containing Cu(1) and Cu(2) per asymmetric unit.

A hydrogen-bonded dimeric *pseudo*-macrocyclic structure is not observed in the solid state of the two-carbon-bridged ligand (**1**) therefore we are unable to draw any conclusions here concerning the preorganisation of such ligands. However, two of the propane bridged ligands (**5** and **9**) show head-to-tail ligand dimerisation *via* hydrogen-bonding. The hole size in **5** may be compared with that in three crystallographically independent [Cu(**5**-H)<sub>2</sub>] complexes.<sup>1</sup> The hole size of the preorganised dimer is over 1 Å (> 50%) larger than that in the copper complexes. If a similar hydrogen-bonded dimer were to be found in the organic phase prior to complexation it would be interesting to compare the structures of the free ligand and the complexed ligand to gain information on the conformational changes required for the ligands to coordinate to the metal centre. In particular, it is informative to see how the ligand “bites” (the distances between the two nitrogen donors) in the complexes compared with those of the donor atoms in the free ligands (Table 2.9).

**Table 2.9:** Bite distances ( $N_{\text{amino}}\cdots N_{\text{sulfonamidato}}$ ) in monosulfonamidodiamine ligands and their complexes.

Ligand or Complex		Bite distance / Å
<b>1</b> <sup>a</sup>	molecule A	2.88
	molecule B	3.76
<b>5</b>		2.91
<b>7</b>		3.00
<b>9</b>		2.96
<b>10</b> <sup>a</sup>	molecule A	2.80
	molecule B	2.81
[Zn(1-H) <sub>2</sub> ] <sup>b</sup>	Zn(1) complex	2.72
		2.69
	Zn(2) complex	2.71
		2.70
[Ni(1-H) <sub>2</sub> ] <sup>c</sup>		2.61
[Cu(2-H) <sub>2</sub> ]		2.64
		2.62
[Cu(5-H) <sub>2</sub> ] <sup>d</sup>		2.87
<b>FODSIA</b> <sup>1</sup>		2.90
[Cu(5-H) <sub>2</sub> ] <sup>de</sup>	Cu(1) complex	2.85
	<b>FODSIA01</b> <sup>1</sup>	2.82
	Cu(2) complex	2.81
		2.84

<sup>a</sup> This structure has two crystallographically independent ligands per asymmetric unit. <sup>b</sup> This structure has two crystallographically independent metal complexes per asymmetric unit containing Zn(1) and Zn(2). <sup>c</sup> This complex is centrosymmetric. <sup>d</sup> This complex exists in blue and green polymorphs. <sup>e</sup> The blue polymorph has two crystallographically independent complexes containing Cu(1) and Cu(2) per asymmetric unit.

In each case the bite distance in the free ligand is greater than in the complex. However, the difference is usually less than 0.2 Å, with exception of type molecule B of ligand **1** which has an extended configuration (Figure 2.14) and does not have an *intra*-molecular hydrogen-bonding interaction between the sulfonamido nitrogen and the amino hydrogen. The shorter bite distances observed in the copper complex [Cu(2-H)<sub>2</sub>] in comparison with [Cu(5-H)<sub>2</sub>] may be explained by the shorter, two-carbon backbone of ligand **2** which leads to the formation of a five membered chelate ring upon complexation. As the observed copper-nitrogen distances are very similar in [Cu(2-H)<sub>2</sub>] and [Cu(5-H)<sub>2</sub>] and as the bite is constrained to be smaller in the five membered chelate ring in [Cu(2-H)<sub>2</sub>] it is inevitable that the chelate angle N-Cu-N will be smaller (mean 82.7°) than in the six-membered chelate ring of [Cu(5-H)<sub>2</sub>] (mean 91.6°).

To examine how the ligands change shape to reduce their bite distance and the hole size on complexation it is helpful to examine torsion angles in the chelate ring. A

torsion angle ( $\tau$ ) about a bond in a ring system is defined as the angle between the two adjacent bonds when projected into the plane perpendicular to the central bond (Figure 2.29).



**Figure 2.29:** Torsion angle  $c$ .

The torsion angles in the ligand backbone of **1** and **7**, in the inner great rings of the *pseudo*-macrocycles formed by ligands **5** and **9** and in the chelate rings of the metal complexes of ligands **1**, **2** and **5** are listed in Tables 2.10 and 2.11.

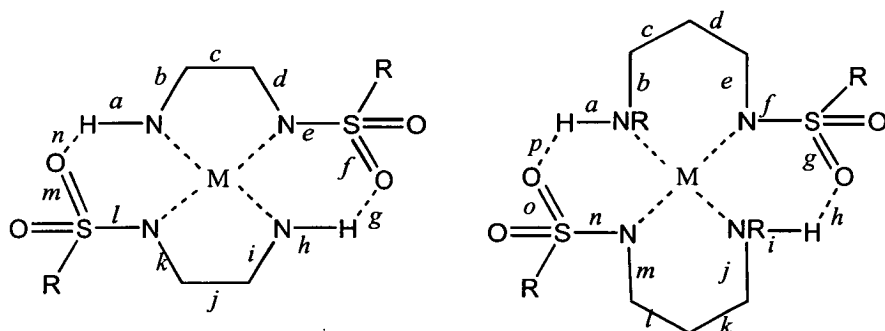


**Figure 2.30:** Labelling for the torsion angles of ligands and complexes with a two or three carbon atom bridge between the nitrogen donors.

**Table 2.10:** Torsion angles in the free ligand **1** and in chelate rings and pseudo-macrocycles of its zinc and nickel complex and the copper complex of **2**.

Bond	1(A) <sup>a</sup>	1(B) <sup>a</sup>	[Zn(1-H) <sub>2</sub> ] <sup>b</sup> (Zn1)	[Zn(1-H) <sub>2</sub> ] <sup>b</sup> (Zn2)	[Ni(1-H) <sub>2</sub> ]	[Cu(2-H) <sub>2</sub> ]
<i>a</i>					177.6	-167.2
<i>b</i>					86.6	159.6
<i>c</i>	59.7	173.5	49.9	-50.2	48.2	-49.9
<i>d</i>	100.4	96.4	171.5	-165.0	106.7	-169.2
<i>e</i>					-170.7	174.2
<i>f</i>					1.5	53.6
<i>g</i>					-25.0	-92.7
<i>h</i>					-177.6	-176.4
<i>i</i>					-86.6	-172.6
<i>j</i>			-47.3	45.0	-48.2	45.9
<i>k</i>			-147.1	158.3	106.7	159.9
<i>l</i>					170.7	163.8
<i>m</i>					-1.5	29.0
<i>n</i>					25.0	5.6

<sup>a</sup> This structure has two crystallographically independent molecules within the asymmetric unit (molecules A and B). <sup>b</sup> This structure has two crystallographically independent complexes in the asymmetric unit containing Zn(1) and Zn(2).

The two conformers of **1** observed in the X-ray structure differ principally as a result of the torsion angle *c* about the central C-C bond which has *trans* configuration (174°) in molecule B, leading to the extended conformation (Figure 2.14). Molecule A has a *gauche* configuration (torsion angle about *c* = 59.7°) providing an N---N bite (2.88 Å) similar to that in the metal complexes. Formation of a chelate ring on complex formation is associated with a flattening of the bridge with torsion angles about *c* or *j* falling between 45 and 50° in the Ni(II) and Zn(II) complexes and the Cu(II) complex of the similar ligand **2**. Whilst the chelate rings and the N<sub>4</sub><sup>2-</sup> donor set are most nearly planar in the nickel complex, the sulfonamidato group is displaced further from the plane as revealed by the torsion angles about bonds *d* and *k* of 106.7° compared with values between 147 to 171° in the Cu(II) and Zn(II) complexes. The amino hydrogen atom in [Ni(1-H)<sub>2</sub>] is displaced to the same side of the coordination plane as the adjacent sulfonamidato oxygen atom (torsion angles *b* and *c* of 87°), presumably to allow formation of a favourable hydrogen-bonding interaction. A much “flatter” configuration is observed for the N-H bond in [Cu(2-H)<sub>2</sub>] with torsion angles *b* and *c* of 160 and 173° respectively, again presumably to optimise the N-H---O=S hydrogen-bond because in this case the sulfonamidato group lies closer to the MN<sub>4</sub> coordinate plane (see above). Care needs to be taken not to over interpret results

based on parameters derived from the positions of hydrogen atoms because these are difficult to locate accurately in heavy atom structures.

**Table 2.11:** Torsion angles in the free ligands **5**, **7**, **9** and the copper complex  $[\text{Cu}(\mathbf{5}\text{-H})_2]^a$ .

Bond	<b>5</b>	<b>7</b>	<b>9</b>	$[\text{Cu}(\mathbf{5}\text{-H})_2]^a$ green form <sup>1</sup>	$[\text{Cu}(\mathbf{5}\text{-H})_2]^{ab}$ Cu(1) blue form <sup>1</sup>	$[\text{Cu}(\mathbf{5}\text{-H})_2]^{ab}$ Cu(2) blue form <sup>1</sup>
<i>a</i>	-21.5		70.2			
<i>b</i>	-58.5		67.3			
<i>c</i>	-173.2	-179.5	174.2	-71.2	-63.0	-67.4
<i>d</i>	64.2	-178.0	-176.9	62.0	53.3	61.0
<i>e</i>	152.3	-152.7	-153.0	132.8	105.5	97.7
<i>f</i>	45.5		43.1			
<i>g</i>	96.0		79.1			
<i>h</i>	-102.9		5.5			
<i>i</i>	21.5		-70.2			
<i>j</i>	58.5		-67.3			
<i>k</i>	173.2		-174.2	-73.0	-69.3	-66.4
<i>l</i>	64.2		176.9	64.2	62.0	56.4
<i>m</i>	152.3		155.0	133.0	105.0	109.5
<i>n</i>	-45.5		-43.1			
<i>o</i>	-96.0					
<i>p</i>	102.9					

<sup>a</sup> This complex exists in blue and green polymorphs. <sup>b</sup> The blue polymorph has two crystallographically independent  $[\text{Cu}(\mathbf{5}\text{-H})_2]$  complex units containing Cu(1) and Cu(2) per asymmetric unit.

The *gauche* configuration about bonds *c* and *d* in the  $[\text{Cu}(\mathbf{5}\text{-H})_2]$  complexes in comparison with the *trans* configuration about these bonds in ligands **5**, **7** and **9** is associated with the formation of a chelate ring on complex formation. The free ligands each have an extended conformation in the solid state (Figures 2.9 (**5**), 2.12 (**9**) and 2.17 (**7**)). The configuration of ligands **5** and **9** does not appear to have been directed by the formation of a hydrogen-bonded macrocycle and the values of torsion angles about the two macrocycles are not similar

#### 2.4.6 Geometry of amido and sulfonamido nitrogens

A number of studies may be found in the literature which investigate why the amido nitrogen is most commonly found to be planar in amides of carboxylic acids. The planarity of amides is associated with a resonance form in which, the lone pair of the nitrogen is also localised in the C-N bonding resulting in a partial N-C double bond, thus hindering rotation.<sup>8</sup> Figure 2.31 shows the two most important canonical forms.

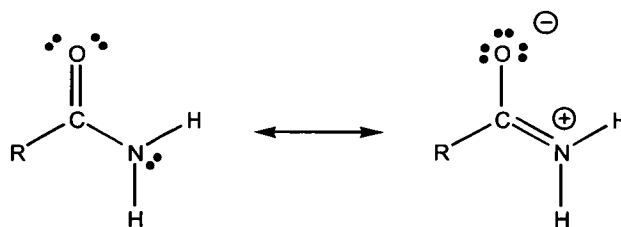


**Figure 2.31:** The resonance of the amides of carboxylic acids.

It is thought that the biological importance of the amide group as part of the peptide bond is due in part to the rigid planarity of the amido nitrogen<sup>9</sup> which, coupled with hydrogen-bonding, provides proteins with the ability to form secondary and tertiary structures, *e.g.* “protein folding”, which is fundamental to biological activity.

Similar studies on sulfonamido systems can also be found. Planar sulfonamides have been reported however most tend to exhibit nitrogen pyramidalization<sup>10</sup> and thus, the energy barrier to rotation around the N-S bond is supposed to be less than the analogous N-C bond in amides. An *ab initio* comparative study of the electronic properties of amides of sulfonic and carboxylic acids<sup>11</sup> concluded that the conjugation over the –OC-N fragment in amides does not exist for the –O<sub>2</sub>S-N fragment in amides of sulfonic acids. It was therefore concluded<sup>11</sup> that there is no electronic analogy between amides and sulfonamides.

#### 2.4.7 Geometry of the sulfonamido nitrogen in monosulfonamidodiamine ligands

The crystal structures obtained in this thesis of several sulfonamide ligands and their complexes allow us to look at the planarity of the sulfonamido nitrogen in relatively simple systems. Three parameters are used to evaluate the planarity of the sulfonamido nitrogen. The sum of the three angles around the nitrogen atom  $\theta$  is 360° when the unit is perfectly planar. The “out of plane angle” of the sulfur atom (the angle between the N-S bond and the bisector of the CNH or CNM angle) is zero when the unit is perfectly planar (Figure 2.32).



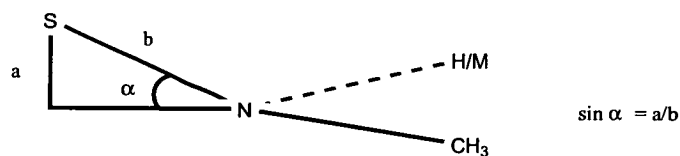


**Figure 2.32:** The out of plane angle ( $\alpha$ ) for the N-S bond is defined by the distance (a) of S from the HNC or MNC plane.

The distance of the nitrogen atom from the plane defined by its three bonded atoms is the simplest representation of the planarity of the sulfonamido nitrogen. These three parameters are given in Table 2.12.

**Table 2.12:** Parameters defining the planarity of the sulfonamido nitrogen atoms in the monosulfonamido ligands and their metal complexes.

Ligand or Complex	Distance of N from MCS or HCS plane (Å)	Sum of 3 angles (°) around N, $\theta$	Angle of S (°) from NCH/M plane, $\alpha$	
<b>1<sup>a</sup></b>	molecule A	0.236	350.3	32.0
	molecule B	0.223	351.3	27.6
<b>5</b>		0.194	343.6	39.9
<b>7</b>		0.303	352.6	25.7
<b>9</b>		0.271	344.9	37.9
<b>10<sup>a</sup></b>	molecule B	0.143	355.5	20.5
	molecule A	0.194	350.3	31.4
<b>[Zn(1-H)<sub>2</sub><sup>b</sup>]</b>	Zn(1) complex	0.245	353.5	23.1
		0.009	359.9	0.9
	Zn(2) complex	0.143	357.7	13.7
		0.069	359.5	6.6
<b>[Ni(1-H)<sub>2</sub><sup>c</sup>]</b>		0.301	350.0	28.8
<b>[Cu(2-H)<sub>2</sub>]</b>		0.292	352.2	25.7
		0.017	360.0	1.6
<b>[Cu(5-H)<sub>2</sub><sup>d</sup>]</b>		0.013	360.0	2.1
		0.019	359.9	1.4
<b>[Cu(5-H)<sub>2</sub><sup>d,e</sup>]</b>	Cu(1) complex	0.199	355.7	21.8
		0.158	357.1	17.1
	Cu(2) complex	0.236	353.7	25.7
		0.158	357.2	17.5

<sup>a</sup> These structures have two crystallographically independent molecules within the asymmetric unit (molecules A and B). <sup>b</sup> This structure has two crystallographically independent complexes in the asymmetric unit containing Zn(1) and Zn(2). <sup>c</sup> This complex is centrosymmetric. <sup>d</sup> This complex exists in blue and green polymorphs. <sup>e</sup> The blue polymorph has two crystallographically independent [Cu(5-H)<sub>2</sub>] complex units containing Cu(1) and Cu(2) per asymmetric unit.

If a resonance effect occurs in sulfonamides we would expect to see a shortening in the S-N bond and a lengthening of the S=O bond as the nitrogen geometry moves towards planarity. These bond lengths are listed in Table 2.13.

**Table 2.13:** S-N and S=O bond lengths of sulfonamido diamines and their complexes.

Ligand or complex		S=O(1) / Å	S=O(2) / Å	S=O <sup>f</sup> / Å	S-N / Å
1 <sup>a</sup>	molecule A	1.424	1.432	1.428	1.614
	molecule B	1.446	1.435	1.441	1.593
<b>5</b>		1.431	1.435	1.433	1.608
<b>7</b>		1.433	1.442	1.438	1.604
<b>9</b>		1.428	1.433	1.431	1.610
10 <sup>a</sup>	molecule A	1.433	1.442	1.438	1.612
	molecule B	1.444	1.426	1.435	1.627
[Zn(1-H) <sub>2</sub> ] <sup>b</sup>	Zn(1) complex	1.456	1.450	1.453	1.563
		1.457	1.433	1.445	1.572
	Zn(2) complex	1.462	1.445	1.454	1.552
		1.437	1.453	1.445	1.572
[Ni(1-H) <sub>2</sub> ] <sup>c</sup>		1.444	1.452	1.448	1.580
[Cu(2-H) <sub>2</sub> ]		1.442	1.447	1.445	1.585
[Cu(5-H) <sub>2</sub> ] <sup>d</sup>		1.449	1.452	1.451	1.563
[Cu(5-H) <sub>2</sub> ] <sup>d</sup>		1.445	1.463	1.454	1.554
[Cu(5-H) <sub>2</sub> ] <sup>d,e</sup>		1.445	1.456	1.451	1.572
[Cu(5-H) <sub>2</sub> ] <sup>d,e</sup>	Cu(1) complex	1.448	1.450	1.449	1.560
		1.456	1.446	1.451	1.576
	Cu(2) complex	1.464	1.446	1.455	1.575
		1.454	1.446	1.450	1.553

<sup>a</sup> These structures have two crystallographically independent molecules within the asymmetric unit (molecules A and B). <sup>b</sup> This structure has two crystallographically independent complexes in the asymmetric unit containing Zn(1) and Zn(2). <sup>c</sup> This complex is centrosymmetric. <sup>d</sup> This complex exists in blue and green polymorphs. <sup>e</sup> The blue polymorph has two crystallographically independent [Cu(5-H)<sub>2</sub>] complex units containing Cu(1) and Cu(2) per asymmetric unit. <sup>f</sup> Mean.

To analyse if there is a relationship between the parameters in Tables 2.12 and 2.13 the correlation coefficients were calculated using Equation 2.3.

$$\rho_{x,y} = \frac{Cov(X,Y)}{\sigma_x \cdot \sigma_y} \quad \text{Eq 2.3}$$

The covariance of the two data sets ( $Cov(X,Y)$ ) is divided by the product of their standard deviations. The definition of the covariance is illustrated in Equation 2.4 where  $\mu_{x/y}$  is the mean value of a set of values x or y.

$$\text{Cov}(X, Y) = \frac{1}{n} \sum_{i=1}^n (x_i - \mu_x)(y_i - \mu_y) \quad \text{Eq 2.4}$$

The derivation of the standard deviations ( $\sigma_{x/y}$ ) of data sets x and y is shown in Equations 2.5 and 2.6.

$$\sigma_x^2 = \frac{1}{n} \sum (X_i - \mu_x)^2 \quad \text{Eq 2.5}$$

$$\sigma_y^2 = \frac{1}{n} \sum (Y_i - \mu_y)^2 \quad \text{Eq 2.6}$$

The better the correlation between the two parameters the closer the coefficient is to 1 and conversely if the parameters are unrelated the coefficient is zero. A positive coefficient is observed when one parameter increases as the other increases and for a negative coefficient one parameter increases as the other decreases. Results for sulfonamide ligands and complexes are shown in Tables 2.14 and 2.15 respectively.

**Table 2.14:** The correlation coefficients of the parameters of nitrogen planarity in sulfonamide ligands **1, 5, 7, 9** and **10** with S=O and S-N bond length.

X	Y	Correlation coefficient
S-N length / Å	Average S=O length / Å	-0.49
Distance of N from HCS plane / Å	Average S=O length / Å	-0.16
Distance of N from HCS plane / Å	S-N bond length / Å	0.31
Sum of 3 angles around N, $\theta$	Average S=O length / Å	0.55
Sum of 3 angles around N, $\theta$	S-N length / Å	-0.03
Angle of S from NCH plane, $\alpha$	Average S=O length / Å	-0.65
Angle of S from NCH plane, $\alpha$	S-N bond length / Å	0.15

**Table 2.15:** The correlation coefficients of the parameters of nitrogen planarity in sulfonamide complexes [Zn(1-H)<sub>2</sub>], [Ni(1-H)<sub>2</sub>], [Cu(2-H)<sub>2</sub>] and [Cu(5-H)<sub>2</sub>] with S=O and S-N bond length.

X	Y	Correlation coefficient
S-N length / Å	Average S=O length / Å	-0.51
Distance of N from MCS plane / Å	Average S=O length / Å	-0.01
Distance of N from MCS plane / Å	S-N bond length / Å	0.36
Sum of 3 angles around N, $\theta$	Average S=O length / Å	0.05
Sum of 3 angles around N, $\theta$	S-N length / Å	-0.46
Angle of S from NCM plane, $\alpha$	Average S=O length / Å	0.05
Angle of S from NCM plane, $\alpha$	S-N bond length / Å	0.31

The free ligands and the metal complexes show a reasonable correlation (-0.49 and -0.51) between the S-N and S=O bond lengths. There is very poor correlation between

the distance of N from the H/MCS plane and the S=O length (-0.16 and -0.01). Better correlation is shown between the distance of N from the MCS plane and the S-N length (0.36). However, for the free ligands the opposite correlation is observed (-0.31). This is surprising as it is expected that the S-N bond would become shorter as the system became more planar due to electron delocalisation from the S=O bond over the S-N bond. For metal complexes there is a good correlation (-0.46) for  $\theta$  with the S-N length but not with the S=O length (-0.03), in contrast for the free ligands a good correlation (0.55) is observed between  $\theta$  and the S=O length but not with the S-N length (0.05). Finally, there is good correlation between  $\alpha$  and the S=O length for the free ligands (-0.65), whereas for complexes the correlation is close to zero (0.05) and a low correlation is observed in each case between  $\alpha$  and the S-N length (0.15 and 0.31).

#### **2.4.8 Geometry of amides of carboxylic and sulfonic acids in the Cambridge Structural Database (CSD)**

The geometry of amides of sulfinic and carboxylic acids in the CSD (July 2001) were compared to the nitrogen atom geometry of sulfonamide ligands and complexes discussed in this chapter. The values of the sum of the three angles around the nitrogen atom,  $\theta$ , for amides and their complexes are shown graphically in Figures 2.34 and 2.35. These show that the geometry of the nitrogen atom in free amides of carboxylic acids is more likely to be planar ( $\theta = 360^\circ$ ) than the nitrogen atom in amides of sulfonic acids.  $\theta$  values for free sulfonamides are spread over a wider range than  $\theta$  for amides of carboxylic acids, of which the majority are in the range 358-360°.

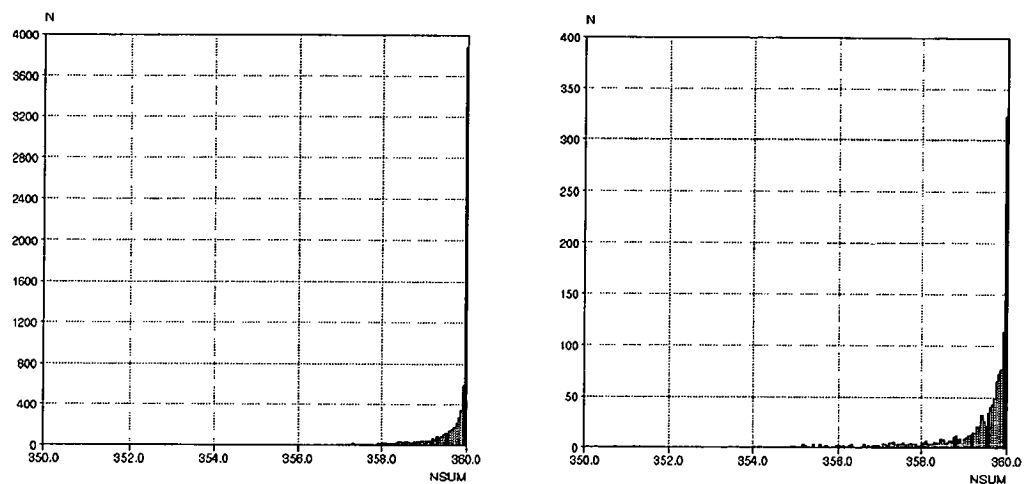


**Figure 2.34:**  $\theta$  values for amides of carboxylic acids and their complexes. ( $N$  = number of complexes and  $NSUM = \theta$ )

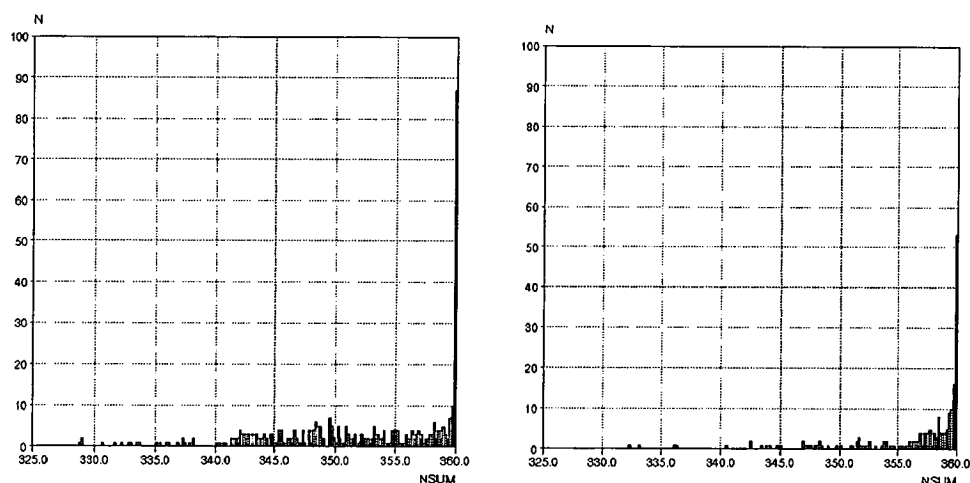


**Figure 2.35:**  $\theta$  values for amides of sulfonic acids and their complexes. ( $N$  = number of complexes and  $NSUM = \theta$ )

When the nitrogen atom is coordinated to a metal centre in amides of carboxylic acids the majority of  $\theta$  values are spread over a wider range ( $356\text{--}360^\circ$ ) than for free amides. In contrast when the nitrogen atom of amides of sulfonic acids is coordinated to a metal centre the nitrogen atom is more likely to be planar than the nitrogen of a free sulfonamide and the majority of  $\theta$  values are in the range  $355\text{--}360^\circ$  (*cf.*  $340\text{--}360^\circ$  for

free sulfonamides). This was also observed for the monosulfonamidodiamine ligands discussed in this chapter.

## 2.5 Equilibrium constants of monosulfonamidodiamines

Values of  $\log K_{LHn}$ ,  $\log K_{ML}$  and  $\log \beta_{ML2}$  for ligands **1**, **5** and **10** and their copper, nickel and zinc complexes were determined by Dr D. J. White.<sup>12</sup> The two stepwise deprotonation constants  $K_1$  and  $K_2$  are shown in Figure 2.36 below.

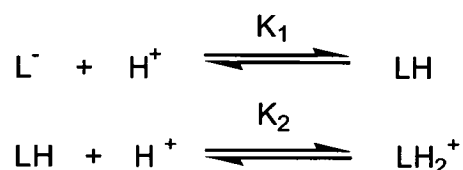


Figure 2.36: Equilibria for ligand protonation and deprotonation.

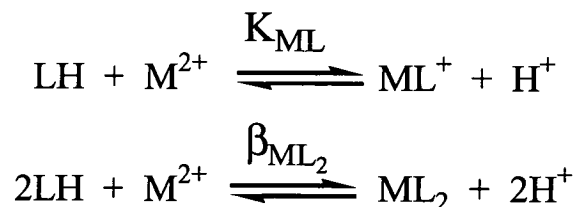
$\log K_n$  is equal to the  $pK_a$  value which measures the acidity of the protonated species. The results are given below in Table 2.16.

Table 2.16:  $pK_a$  values for ligands **1**, **5** and **10**.

Ligand	$pK_{a1}$	$pK_{a2}$
<b>1</b>	8.89	10.75
<b>5</b>	9.49	10.89
<b>10</b>	3.17	9.83

The  $pK_a$  values of the sulfonamido groups in ligands **1** and **5** fall close to the usual value for sulfonamides ( $\sim 9$ ) showing that the proton is lost relatively easily. The  $pK_a$  of **10** is much lower, indicating the higher acidity of the proton. This is due to the electron withdrawing effect of the aromatic ring and delocalisation of anionic charge causing the N-H bond to be weaker.

The formation constants  $K_{ML}$  and  $\beta_{ML2}$  for these ligands with divalent copper, nickel and zinc are listed in Table 2.17.



**Table 2.17:** The formation constants  $\log K_{\text{ML}}$  and  $\log \beta_{\text{ML}_2}$  of copper, nickel and zinc complexes of **1**, **5** and **10**.

Complex	Log $K_{\text{ML}}$	Log $\beta_{\text{ML}_2}$
[Cu(1-H) <sub>2</sub> ]	10.40	19.42
[Ni(1-H) <sub>2</sub> ]	5.70	9.84
[Zn(1-H) <sub>2</sub> ] <sup>a</sup>	5.78	—
[Cu(5-H) <sub>2</sub> ] <sup>a</sup>	9.99	—
[Ni(5-H) <sub>2</sub> ] <sup>b</sup>	—	—
[Zn(5-H) <sub>2</sub> ] <sup>a</sup>	6.29	—
[Cu(10-H) <sub>2</sub> ] <sup>b</sup>	—	—
[Ni(10-H) <sub>2</sub> ]	9.49	14.36
[Zn(10-H) <sub>2</sub> ]	9.75	14.70

<sup>a</sup> Measurement of  $\log \beta_{\text{ML}_2}$  was not possible due to precipitation of the complex. <sup>b</sup> Measurement of either formation constant was not possible due to precipitation of the complex.

### 2.5.1 Speciation of monosulfonamidamido diamines

The protonation constants measured for ligands **1**, **5** and **10** may be used to predict the species which will be present in solution at different pH values using the program Hyss2<sup>13</sup> (Figure 2.38).

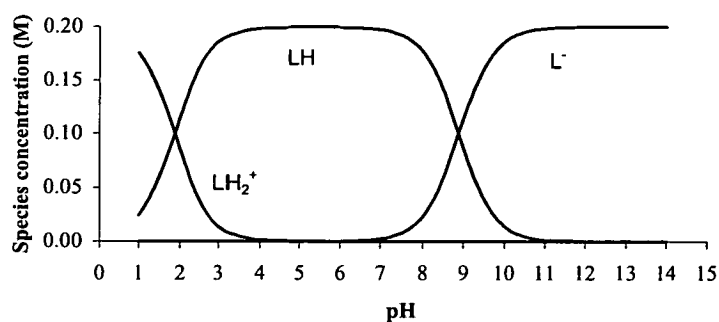


**Figure 2.38:** Calculated speciation distribution for ligand **1** as a function of pH for a 0.2 M 95% methanol solution.

The diagram shows that the ligand exists as a monocation only below pH 3 and that the ligand is deprotonated only above pH 8. Between pH 3 and pH 8 the dominant

species is the neutral free ligand. A very similar distribution is observed for ligand **5**. However, ligand **10** shows quite a different pattern (Figure 2.39).

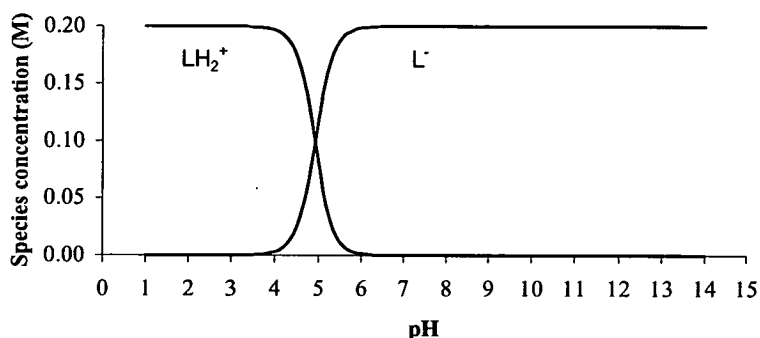


**Figure 2.39:** The calculated speciation distribution for ligand **10** as a function of pH for a 0.2M 95% methanol solution.

Only two species are predicted; below pH 5 most of the ligand is in the protonated form and above pH 5 the ligand is mostly present as its monoanion. These predictions suggest that ligand **10** would be the stronger complexing agent than **1** and **5** at neutral pH values

### 2.5.2 Prediction of the selectivity of monosulfonamidodiamines

If  $\beta_{ML_2}$  values for a series of metal ions are known for a ligand the Hyss2 program can be used to predict the selectivity of metal complexation. The equilibrium constants for the complexation of **1** with copper(II), nickel(II) and zinc(II) were used to generate the plot shown in Figure 2.40.

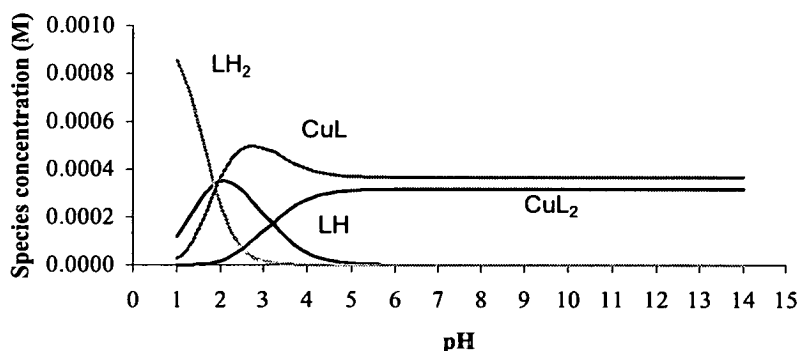




**Figure 2.40:** The selectivity of **1** over Cu(II), Ni(II) and Zn(II) at a ligand concentration of  $1 \times 10^{-3}$  M and a metal concentration of  $7 \times 10^{-4}$  M.

The diagram plainly indicates the selectivity of **1** for copper. There is no visible plot of nickel or zinc complexation as the predicted concentrations of the nickel and zinc complexes formed are close to zero. A similar prediction was done for ligand **5**, however only  $K_{ML}$  data are available for copper and zinc. As expected, selectivity for copper is predicted and concentrations of the  $Zn(5-H)_2$  species are close to zero. For ligand **10** data are only available for the nickel and zinc ML and  $ML_2$  complexes. A slight selectivity for zinc over nickel is predicted, (Figure 2.41).

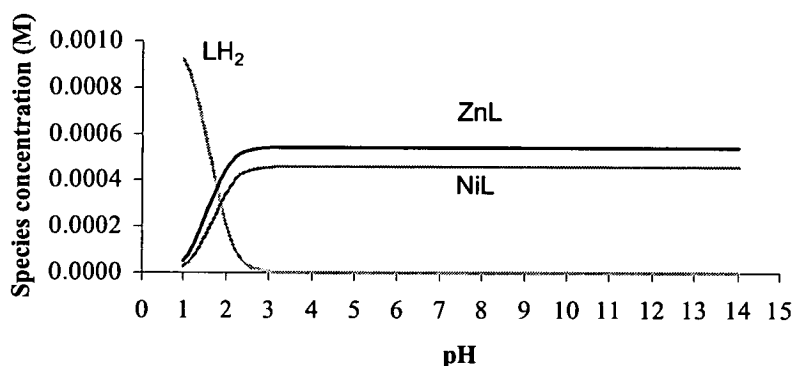


**Figure 2.41:** The speciation plot for ligand **10** with Ni(II) and Zn(II).

## 2.6 Solvent extraction

To establish the strength of monosulfonamido ligands as metal extractants the 'S' curves for copper extraction of ligands **4** and **8** were determined. The metal selectivity of these ligands was also investigated.

### 2.6.1 'S'-Curve determination

'S' curve determination was important to assess the strength of simple monosulfonamido ligands. Due to the low solubility of metal complexes of ligands **1** and **5**, even in solvents such as chloroform, the S curves for copper were determined for their more soluble N-2-ethylhexyl analogues **4** and **8**, (Figure 2.42).

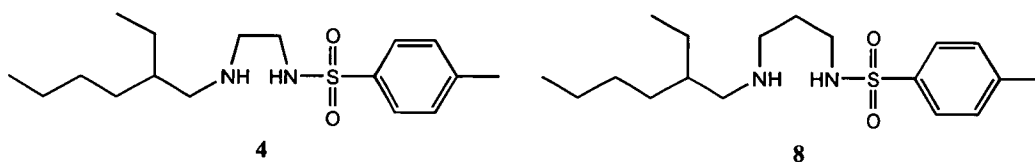


Figure 2.42: Soluble monosulfonamidodiamine ligands, 4 and 8.

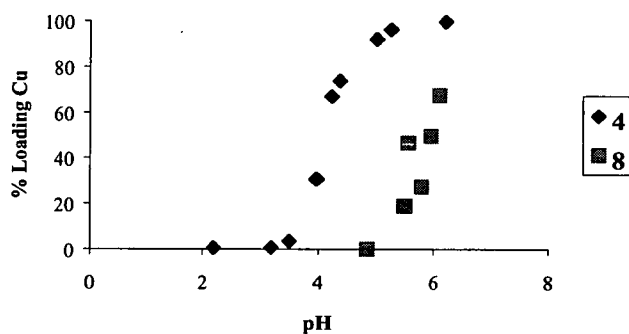


Figure 2.43: The S curve of 4 and 8 with copper. The copper was gradually stripped from a 0.1 M solution of  $[\text{Cu}(\text{L}-\text{H})_2]$  in dichloromethane using sulfuric acid.

The  $\text{pH}_{1/2}$  value is the pH at which the ligand is half loaded with metal.

Table 2.19:  $\text{pH}_{1/2}$  values of 4 and 8.

Ligand	$\text{pH}_{1/2}$ value
4	4.2
8	6

The  $\text{pH}_{1/2}$  values for ligands 4 and 8 are significantly higher than that of P50,  $< 2.0$  indicating that monosulfonamidodiamine ligands are much weaker extractants. Ligand 4 is a better extractant than ligand 8 and this is also illustrated in the following selectivity experiment.

### 2.6.2 Selectivity of monosulfonamidodiamine ligands

To establish the selectivities of the ethane- and propane- bridged sulfonamido extractants for divalent Co, Ni, Cu and Zn ions the more soluble ligands 4 and 8 were used. The results are given in Table 2.20.

**Table 2.20:** Selectivity of extraction of divalent metals shown by 0.1 M solutions of **4** and **8** in dichloromethane (DCM) after 1 hour contact at room temperature with an equal volume of an aqueous mixed metal(II) sulfate solution of 0.85 M of each of Co, Ni, Cu and Zn.

Ligand	M(II) concentration in dichloromethane / ppm			
	Co	Ni	Cu	Zn
<b>4</b>	2.0	31.4	400	1.5
<b>8</b>	9.4	7.6	70	0.6

Both extractants show a strong preference for copper. Neither gives 100% loading, (3177 ppm = 100% loading of copper). Ligand **4** is a stronger extractant than **8** which suggests that the ethyl bridge of ligand **4** is advantageous for metal complexation. This result is consistent with the stability constants (See Table 2.19) which showed that the 5-membered copper chelate is formed more readily than the 6-membered chelate. This may be rationalised from the solid state structures of the ligands. The ethane bridged ligand shows an N-H...N *intra*-molecular hydrogen-bond and is therefore closer to the rigid arrangement required in the complex *i.e.* the greater the preorganisation of ligand leads to a more favourable  $\Delta S$ . Also, the *inter*-donor repulsion energy term involved in bringing the N<sup>delta-</sup> donors close together is smaller for the more preorganised (ethane bridged) ligand, which would lead to a more negative value of  $\Delta G$  ( $\Delta G = \Delta H - T\Delta S$ ) for **4** than **8** and therefore complexation is more favourable.

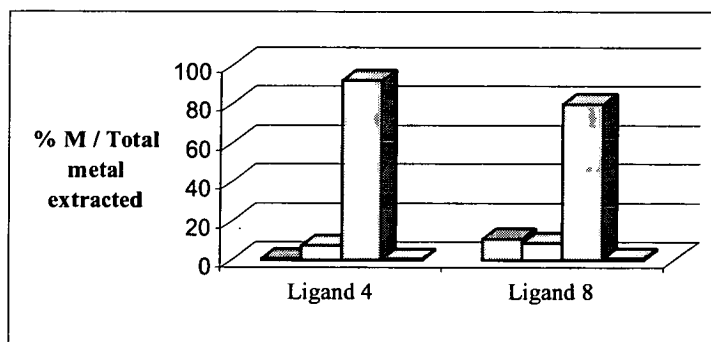


**Figure 2.44:** The selectivity of **4** and **8** for cobalt(II), nickel(II), copper(II) and zinc(II).

Metal(II) selectivities of ligands **4** and **8** are Cu>Ni>Co≈Zn and Cu>Co≈Ni>Zn respectively (Figure 2.44). Extractant **4**'s selectivity is similar to that for the Irving-Williams series.<sup>14</sup> However, we should not draw comparisons too closely as our species are 4-coordinate and not 6-coordinate. The main difference in selectivity

trends for the two extractants is the position of cobalt and nickel. The shorter backbone of **4** may result in preferential binding of nickel as a square planar geometry which will be more accessible than a tetrahedral geometry which a cobalt complex is likely to adopt. Following a similar argument for **8**, the longer backbone may prefer a tetrahedral geometry of the nitrogen atoms and a planar N-M-N conformation may be less favourable.

## 2.7 An electrochemical study of monosulfonamidodiamine complexes

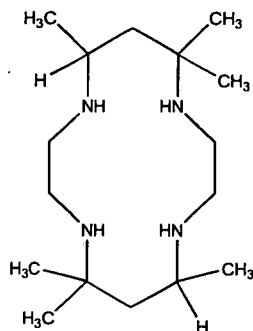
### 2.7.1 The stabilisation of metal(III) centres by deprotonated amide groups



Figure 2.45: The amide and sulfonamide groups.

The sulfonamide group can be compared to the amide group, (Figure 2.45). It is well known that amides are poor nucleophiles and therefore a poor coordinating atom.<sup>15</sup> This is due to the delocalisation of the nitrogen lone pair electrons through orbital overlap with the carbonyl group. However, upon deprotonation of the amide the nitrogen becomes a much better donor. This type of behaviour is also observed for the sulfonamido group.<sup>15</sup>

Some of the first evidence that deprotonated amide groups may stabilise Cu(III) and Ni(III) was the isolation of crystalline complexes of biuret  $K[M(NHCONHCONH)_2]$  where  $M = Cu(III)$  and  $Ni(III)$  by Bour and Steggerda.<sup>16</sup> Ni(III) complexes of macrocyclic tetra-aza ligands have been prepared and characterized in acetonitrile solution and as solids.<sup>17,18,19</sup> An example of such a ligand is shown in Figure 2.46.



**Figure 2.46:** 5,5,7,12,12,14-hexamethyl-(1,4,8,11-tetraaza-cyclotetradecane)<sup>19</sup> (**A**) which yields a Ni(III) complex.

The Ni(III) complex of **A** is stable in the absence of oxygen and water. Ni(III) cyclam complexes are very unstable and decompose in aqueous solution.<sup>20</sup> Cu(III) complexes of macrocyclic tetra-amines such as **A** have also been made in acetonitrile solution but the complexes are only stable on the time scale used in voltammetric measurements and undergo spontaneous reduction to Cu(II). In order to isolate samples work was done at  $-15$  to  $-20^{\circ}\text{C}$ .<sup>19</sup> Pulse radiolysis has also been used to generate transient Cu(III)-aquo and Cu(III)-amine complexes.<sup>21</sup>

### 2.7.2 Cu(III) and Ni(III) peptide complexes

Margerum has carried out an extensive study of polypeptide ligand stabilisation of Ni(III) and Cu(III) centres. Oligopeptides were deprotonated upon complexation resulting in strong in-plane donor ligands which stabilise the M(III) oxidation state relative to M(II). It was found that the Cu(III)/Cu(II) couple decreases with an increase in the number of deprotonated amide groups per ligand.<sup>22</sup>

Margerum first reported that relatively long lived Cu(III) peptide complexes could be formed in aqueous solution<sup>23</sup> and the similar Ni(III) peptide complexes were subsequently described.<sup>24</sup> The M(III) species (Figure 2.47) were formed by electrochemical or chemical oxidation of the relevant M(II) peptide complexes.

The tetraglycine ligand is involved in binding to the metal centre *via* three deprotonated amino peptide groups and one amine group.

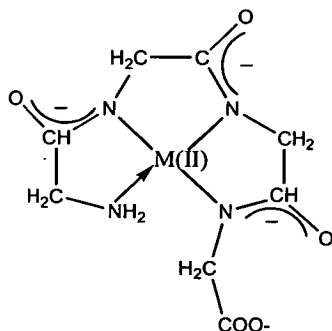


**Figure 2.47:** Dianionic Ni(II) and Cu(II) complexes  $[\text{Ni}(\text{B-4H})]^{2-}$  and  $[\text{Cu}(\text{B-4H})]^{2-}$  derived from tetraglycine (**B**).

Evidence that metal and not ligand-based oxidation is involved in forming these complexes was provided by studies of EPR and uv-visible spectra. The M(III)/M(II) redox potentials for such peptide complexes are lower than other complexes as a result of the very strong electron donor properties of the tetra-anionic ligand (Table 2.20).

**Table 2.20:** Comparison of M(III)/M(II) redox potentials for nickel and copper complexes of teraglycinate<sup>4-</sup> (**B**, see Figure 2.47) and the 14-membered N<sub>4</sub>-macrocycle tetra-amine (**A**, see Figure 2.46).

Electrochemical process	E°, V
$[\text{Ni}^{\text{III}}(\text{B-4H})] + e \rightleftharpoons [\text{Ni}^{\text{II}}(\text{B-4H})]^{2-}$	0.79
$[\text{Ni}^{\text{III}}(\text{A})]^{3+} + e \rightleftharpoons [\text{Ni}^{\text{II}}(\text{A})]^{2+}$	0.85
$[\text{Cu}^{\text{III}}(\text{B-4H})] + e \rightleftharpoons [\text{Cu}^{\text{II}}(\text{B-4H})]^{2-}$	0.63
$[\text{Cu}^{\text{III}}(\text{A})]^{3+} + e \rightleftharpoons [\text{Cu}^{\text{II}}(\text{A})]^{2+}$	1.12

The lower electrode potential for the copper tetraglycine species with relation to the nickel species may be explained in terms of the ligand field stabilisation energies involved.<sup>25,26</sup> The thermodynamic stability of the trivalent copper complex results from the ability of the peptide ligands to accommodate the square planar geometric preference of the d<sup>8</sup> complex with the consequent ligand field stabilisation energy. The oxidation of the Cu(II) centre from a d<sup>9</sup> configuration to a d<sup>8</sup> configuration is favourable for a square planar or tetragonal geometry which is observed for these

complexes as the high energy  $dx^2-dy^2$  orbital is no longer occupied in the  $d^8$  low spin complex.

### 2.7.3 Electrochemical studies of monosulfonamidodiamine complexes

The oligopeptide complexes investigated by Margerum<sup>23,24</sup> may be compared to the ethane-bridged monosulfonamidodiamine complexes which have been synthesised as part of this thesis. The ability of the sulfonamido group to stabilise metal oxidation in monosulfonamidodiamine complexes was investigated. Complexes of ligand **4** were used due to their higher solubility in DMF.

The cyclic voltammograms of the cobalt and nickel complexes in the range 2 to  $-2V$  showed peaks for one oxidation process and one reduction process. Both were electrochemically irreversible, *i.e.* the electron transfer process is followed rapidly by a chemical reaction. The cyclic voltammogram for the copper complex showed these two waves plus an additional oxidation and reduction wave. Table 2.21 lists the peak redox potential of the oxidation and reduction processes for the complexes and the free ligand. Note that the free ligand also gave rise to an irreversible oxidation and reduction.

**Table 2.21:** The oxidation and reduction potentials (V) of simple monosulfonamidodiamine complexes of ligand **4**.

Molecule	$E_p$ oxidation (V)	$E_p$ reduction (V)
[Co(II)(4-H) <sub>2</sub> ]	+1.40	-0.95
[Ni(II)(4-H) <sub>2</sub> ]	+1.50	-0.90
[Cu(II)(4-H) <sub>2</sub> ]	+1.45, +0.22	-0.95, -1.65
<b>4</b>	+1.45	-0.9

Cyclic voltammetry was performed at 25°C in dimethylformamide with a three-electrode system consisting of a platinum working electrode, a platinum auxiliary electrode, and a Ag/AgCl reference electrode.

A comparison of the values shown in Table 2.21 suggests that oxidation at *ca.* +1.45V and reduction at *ca.*  $-0.95V$  of the metal complexes is primarily ligand based because peaks are observed at very similar potentials in the free ligand. This leads us to conclude that sulfonamido ligands are unlikely to act in an analogous way to amide ligands in the stabilisation of a metal(III) centre and that the ligand is oxidised in

preference to the metal. Analysis of the decomposition products of the oligopeptide complexes investigated by Margerum found that oxidation of the ligand occurred at the methylene group and indeed this may be the case here.<sup>27</sup> The cyclic voltammogram for the copper complex is shown in Figure 2.48.

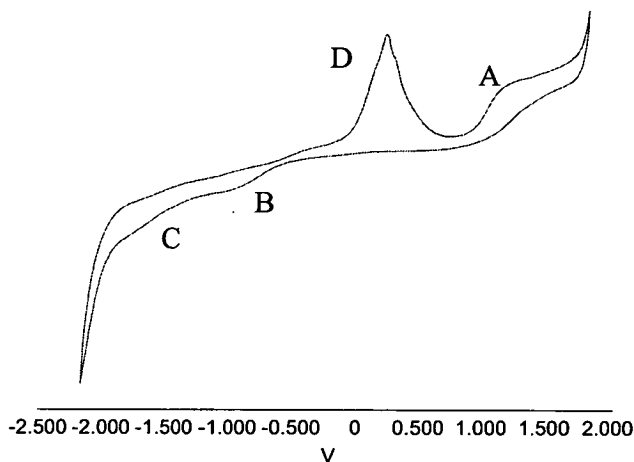


**Figure 2.48:** The cyclic voltammogram of  $[\text{Cu}(\text{II})(4\text{-H})_2]$  in DMF / 0.1M TBABF<sub>4</sub> at 298 K.

The ligand based oxidation and reduction peaks are found at points A and B and an additional oxidation and reduction process are found at point D and C. Oxidation peak D is a typical desorption peak<sup>28</sup> and may be ascribed to the oxidation of Cu(0) to Cu(II). This peak only appears if the applied potential is ramped beyond point C. Thus we conclude that the copper centre is reduced at potential C to copper metal which coats the working electrode and may be stripped off the electrode at potential D. Finally, no evidence that this class of ligands stabilises Cu(III), Ni(III) or Co(III) was found and it must be concluded that the deprotonated sulfonamido nitrogen does not have the same stabilising properties as peptide molecules.



## 2.8 Conclusions

This chapter has shown that monosulfonamidodiamine ligands are relatively simple to make and are versatile complexing agents. The ligands show selectivity for copper, but those derived from aliphatic diamines are much weaker copper extractants than the commercial phenolic oximes. Those derived from aromatic 1, 2-diamines show higher stability constants for their copper(II) complexes but have low solubilities, limiting their usefulness as solvent extractants. Secondary hydrogen-bonding in the ligands produced the desired *pseudo*-macrocyclic ligand in some cases, but the high number of hydrogen-bond donor and acceptor sites in the ligands made prediction of the hydrogen-bonded secondary structure difficult.

Chapter 3 deals with sulfonamide oxime ligands in which an oxime group is used to provide a single hydrogen-bond donor site with the intention of generating *pseudo*-macrocyclic secondary structures more analogous to that in P50.

## 2.9 Experimental

### 2.9.1 Instrumentation

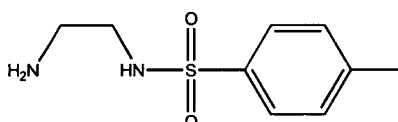
Melting points were determined with a Gallenkamp apparatus and are uncorrected. Elemental analysis was performed on a Perkin Elmer 2400 elemental analyser and a Carlo Erba 1108 Elemental analyser. IR spectra were obtained on a Perkin Elmer Paragon 1000 FT-IR spectrometer as potassium bromide discs or as thin films on NaCl plates.  $^1\text{H}$  and  $^{13}\text{C}$  NMR spectra were run on Bruker WP200, AC250 and AVANCE DPX360 spectrometers. Chemical shifts ( $\delta$ ) are reported in parts per million (ppm) relative to residual solvent protons as internal standards. Electron impact (EI) mass spectra were obtained either on a Finnigan MAT4600 quadrupole spectrometer or on a Kratos MS50TC spectrometer. Fast atom bombardment (FAB) mass spectra were obtained on a Kratos MS50TC spectrometer in acetonitrile/3-nitrobenzyl alcohol/thioglycerol matrices. Electrospray (ESI) mass spectra were obtained on a Thermoquest LCQ spectrometer in methanol. Inductively coupled plasma atomic emission spectroscopy (ICP-AES) analysis was performed on a Thermo Jarrell Ash Iris ICP-AES spectrometer. Potentiometric titrations were carried out in a sealed double jacket glass cell using a Metrohm 665 automated burette and a Corning 130 digital pH meter fitted with a Phillips glass electrode and a calomel electrode. All measurements were fully automated. Titrations were performed at  $25.0 \pm 0.1$  °C in constant ionic strength ( $I = 0.1$ ,  $[\text{Et}_4\text{N}][\text{ClO}_4]$ ) 95% methanol solution under purified nitrogen. Solutions of ligand (ca.  $1 \times 10^{-3}$  mol  $\text{dm}^{-3}$ ) alone and in the presence of 0.3, 0.8 and 1.5 equivalents of metal ion were titrated with 0.1 mol  $\text{dm}^{-3}$   $\text{Et}_4\text{NOH}$  respectively. Equilibrium constants were calculated from potentiometric data with the program MINQUAD.<sup>29</sup> Electrochemistry was carried out using a 0.1M  $[\text{TBA}][\text{BF}_4]$  (TBA = tetrabutylammonium) inert electrolyte and voltammograms were generated using an AUTOLAB PGSTAT 20 instrument.

### 2.9.2 Solvent and reagent pretreatment

Unless otherwise specified all reagents and solvents were obtained from commercial suppliers and were used as received. Solvents used for analytical purposes (NMR, MS, ICP) were of spectroscopic grade.

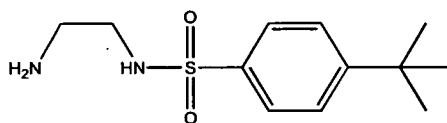
### 2.9.3 Ligands and their precursor

#### N-(2-amino-ethyl)-4-methylbenzenesulfonamide (1)



**1** was prepared by following the method of Kirsanov and Kirsanova.<sup>2</sup> A solution of 4-methylbenzenesulfonyl chloride (86 g, 0.45 mol) in toluene (400 cm<sup>3</sup>) was added dropwise over 8 hours to a solution of 1,2-diaminoethane (81 g, 1.35 mol) in toluene (300 cm<sup>3</sup>). The precipitate was isolated by filtration and washed with toluene (3 x 100 cm<sup>3</sup>). The solid was digested with methanol (600 cm<sup>3</sup>), filtered and the solvent removed *in vacuo* to give a white solid which was recrystallised from water (1 dm<sup>3</sup>) to yield a white crystalline product (50.91 g, 52%), mp 120-122 °C (Found: C, 50.37; H, 6.73; N, 12.84. Calc. for C<sub>9</sub>H<sub>14</sub>N<sub>2</sub>O<sub>2</sub>S: C, 50.45; H, 6.59; N, 13.07%).  $\delta_{\text{H}}$  (CDCl<sub>3</sub>, 200 MHz): 2.41 (s, 3 H, CH<sub>3</sub>), 2.85 (m, 2 H, CH<sub>2</sub>), 2.98 (m, 2 H, CH<sub>2</sub>), 7.29 (d, 2 H, J 7.9, Ar CH), 7.75 (d, 2 H, J 8.3, Ar CH).  $\delta_{\text{C}}$  (CDCl<sub>3</sub>, 50 MHz): 21 (CH<sub>3</sub>), 41 (CH<sub>2</sub>), 45 (CH<sub>2</sub>), 127 (2 C, Ar CH), 130 (2 C, Ar CH), 136 (Ar C), 143 (Ar C). IR (KBr disc)/cm<sup>-1</sup>: 3362s, 3049m, 2952m, 2862m, 1597m, 1495w, 1471w, 1440w, 1316s, 1297s, 1150s. FAB MS, *m/z* 215 (MH<sup>+</sup>, 100.0%).

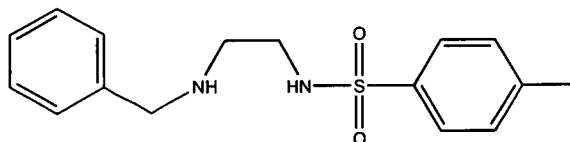
#### N-(2-aminoethyl)-4-*t*-butylbenzenesulfonamide (2)



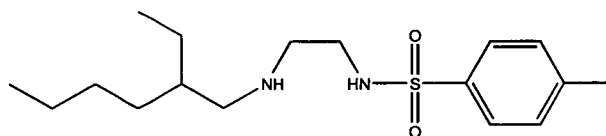
**2** was prepared by an adaptation of the method of Kirsanov and Kirsanova.<sup>2</sup> A solution of 4-*t*-butylbenzenesulfonyl chloride (12 g, 0.05 mol) in toluene (100 cm<sup>3</sup>) was added dropwise over 8 hours to a solution of 1,2-diaminoethane (9.34 g, 0.16 mol)

in toluene (100 cm<sup>3</sup>). The precipitate was isolated by filtration and washed with toluene (3 x 20 cm<sup>3</sup>). The product was recrystallised from toluene (250 cm<sup>3</sup>) and washed with diethylether (3 x 20 cm<sup>3</sup>). The white crystalline solid was dried *in vacuo* (5.39 g, 40%), decomposition temperature > 205 °C (Found: C, 55.93; H, 7.89; N, 11.03. Calc. For C<sub>12</sub>H<sub>20</sub>N<sub>2</sub>O<sub>2</sub>S: C, 56.22; H, 7.86; N, 10.93%).  $\delta_{\text{H}}$  (CDCl<sub>3</sub>, 250 MHz): 1.29 (s, 9H, CH<sub>3</sub>), 2.76 (m, 2 H, CH<sub>2</sub>), 2.48 (m, 2 H, CH<sub>2</sub>), 3.02 (s, 2 H, NH<sub>2</sub>), 7.47 (d, 2 H, J 7.5, Ar CH), 7.75 (d, 2 H, J 7.7, Ar CH).  $\delta_{\text{C}}$  (CDCl<sub>3</sub>, 63 MHz): 31 (3 C, CH<sub>3</sub>), 35 (Ar C), 41 (CH<sub>2</sub>), 45 (CH<sub>2</sub>), 126 (Ar CH), 127 (Ar CH), 137 (Ar C), 156 (Ar C). IR data (KBr disc)/cm<sup>-1</sup>: 2922s, 2677s, 1601s, 1511s, 1327m, 1161m. EI MS, *m/z* 256 (M<sup>+</sup>, 20.0%).

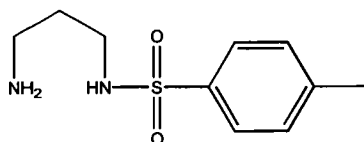
**N-(N-benzyl-2-aminoethyl)-4-methylbenzenesulfonamide (3)**



Benzaldehyde (7.43 g, 0.07 mol) was added to a solution of N-(2-amino-ethyl)-4-methylbenzenesulfonamide (**2**) (15 g, 0.07 mol) in ethanol (200 cm<sup>3</sup>) which was left to stir for one hour. A catalytic amount of anhydrous sodium tetraborate (0.2 g, 1 mmol) and sodium borohydride (10.59 g, 0.33 mol) were added and the solution was stirred for one hour. Distilled water (100 cm<sup>3</sup>) was added, the methanol removed *in vacuo*, and the product extracted into dichloromethane (200 cm<sup>3</sup>) which was washed with water (3 x 200 cm<sup>3</sup>), dried over anhydrous magnesium sulfate and filtered. The solvent was removed *in vacuo* to yield a white precipitate which was recrystallised from ethanol (100 cm<sup>3</sup>) to give a white crystalline solid (9.7 g, 46%), mp 78-80 °C (Found: C, 63.11; H, 6.55; N, 9.16. Calc. for C<sub>16</sub>H<sub>20</sub>N<sub>2</sub>O<sub>2</sub>S: C, 63.13; H, 6.62; N, 9.20%).  $\delta_{\text{H}}$  (CDCl<sub>3</sub>, 360 MHz): 2.44 (s, 3 H, CH<sub>3</sub>), 2.73 (m, 2 H, CH<sub>2</sub>), 3.03 (m, 2 H, CH<sub>2</sub>), 3.67 (s, 2 H, CH<sub>2</sub>), 7.29 (m, 7 H, Ar CH), 7.76 (d, 2 H, J 8.3, Ar CH).  $\delta_{\text{C}}$  (CDCl<sub>3</sub>, 90 MHz): 22 (CH<sub>3</sub>), 43 (CH<sub>2</sub>), 48(CH<sub>2</sub>), 53 (CH<sub>2</sub>), 128 (2 C, Ar CH), 128 (Ar CH), 129 (2 C, Ar CH), 129 (2 C, Ar CH), 130 (2 C, Ar CH), 137 (Ar C), 140 (Ar C), 144 (Ar C). IR data (KBr disc)/cm<sup>-1</sup>: 748m, 1162s, 1332s, 1598w, 2850m, 3060w, 3450m. FAB MS, *m/z* 305 (MH<sup>+</sup>, 100%).

**N-(N-2-ethylhexyl-2-aminoethyl)-4-methylbenzenesulfonamide (4)**

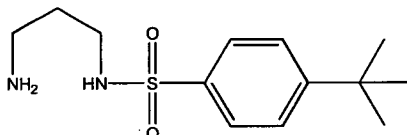
N-(2-aminoethyl)-4-methylbenzenesulfonamide (0.26 g, 2 mmol) was added to a solution of 2-ethylhexanal (0.43 g, 2 mmol) in methanol (30 cm<sup>3</sup>) over molecular sieves and stirred for one hour. A catalytic quantity of anhydrous sodium tetraborate (0.2 g, 1 mmol) and sodium borohydride (0.15 g, 4 mmol) was then added and the mixture was stirred for a further hour. Dichloromethane (30 cm<sup>3</sup>) was then added and the solution was washed with water (3 x 30 cm<sup>3</sup>) and dried over anhydrous magnesium sulfate which was removed by filtration. The solvent was then removed *in vacuo* to give an opaque yellow oil. The oil was dissolved in the minimum quantity of methanol and filtered. The solvent was then removed *in vacuo* to leave a colourless oil (0.4 g, 88%), (Found: C, 62.32; H, 9.97; N, 8.55. Calc. for C<sub>17</sub>H<sub>30</sub>N<sub>2</sub>O<sub>2</sub>S: C, 62.39; H, 9.47; N, 8.56).  $\delta_{\text{H}}$  (CDCl<sub>3</sub>, 360 MHz): 0.84 (t, 3 H, J 7.2, CH<sub>3</sub>), 0.92 (t, 3 H, J 7.0, CH<sub>3</sub>), 1.27 (m, 8 H, CH<sub>2</sub>), 2.35 (d, 2 H, J 5.6, CH<sub>2</sub>), 2.45 (s, 3 H, CH<sub>3</sub>), 2.69 (t, 2 H, J 5.6, CH<sub>2</sub>), 3.00 (t, 2 H, J 5.6, CH<sub>2</sub>), 7.32 (d, 2 H, J 7.9, Ar CH), 7.78 (d, 2 H, J 8.3, Ar CH).  $\delta_{\text{C}}$  (CDCl<sub>3</sub> 63 MHz): 11 (CH<sub>3</sub>), 14 (CH<sub>3</sub>), 21 (CH<sub>3</sub>), 23 (CH<sub>2</sub>), 24 (CH<sub>2</sub>), 29 (CH<sub>2</sub>), 31 (CH<sub>2</sub>), 39 (CH), 42 (CH<sub>2</sub>), 52 (CH<sub>2</sub>), 127 (2 C, Ar CH), 129 (2 C, Ar CH), 137 (Ar C), 143 (Ar C). IR data (KBr disc)/cm<sup>-1</sup>: 661s, 815s, 1034m, 1094s, 1158s, 1304s, 1458s, 1599m, 2873s, 2958s, 3286m. ESI MS, *m/z* 327 (MH<sup>+</sup>, 100.0%)

**N-(3-aminopropyl)-4-methylbenzenesulfonamide (5)**

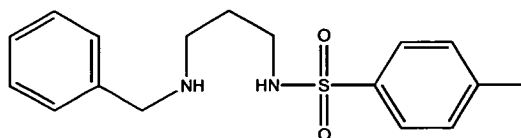
**5** was prepared by the method of Kirsanov and Kirsanova.<sup>2</sup> A solution of 4-methylbenzenesulfonyl chloride (42.3 g, 0.23 mol) in toluene (250 cm<sup>3</sup>) was added dropwise over 8 hours to a solution of 1,3-diaminopropane (50 g, 0.66 mol) in toluene (200 cm<sup>3</sup>). The solution was stirred for a further 4 hours then the precipitate was isolated by filtration and washed with toluene (3 x 50 cm<sup>3</sup>). The solid was digested

with methanol (300 cm<sup>3</sup>) at room temperature and filtered. The solvent was removed *in vacuo* to give a white solid which was recrystallised from water (250 cm<sup>3</sup>) to yield a white crystalline solid (35.4 g, 69%), mp 115-117°C (Found: C, 52.21; H, 7.21; N, 12.25. Calc. for C<sub>10</sub>H<sub>16</sub>N<sub>2</sub>O<sub>2</sub>S: C, 52.62; H, 7.06; N, 12.27).  $\delta_{\text{H}}$  (CDCl<sub>3</sub>, 200 MHz): 1.57 (tt, 2 H, J 6.2, CH<sub>2</sub>), 2.42 (s, 3 H, CH<sub>3</sub>), 2.78 (t, 2 H, J 6.1, CH<sub>2</sub>), 3.05 (t, 2 H, J 6.2, CH<sub>2</sub>), 7.28 (d, 2 H, J 8.4, Ar CH), 7.73 (d, 2 H, J 8.3, Ar CH).  $\delta_{\text{C}}$  (CDCl<sub>3</sub>, 50 MHz) 21 (CH<sub>3</sub>), 31 (CH<sub>2</sub>), 41 (CH<sub>2</sub>), 43 (CH<sub>2</sub>), 127 (2 C, Ar CH), 130 (2 C, Ar CH), 137 (Ar C), 143 (Ar C). IR data (KBr disc)/cm<sup>-1</sup>: 3063m, 2956m, 2919m, 2870m, 1598m, 1495m, 1457w, 1437w, 1321s, 1157s. FAB MS, *m/z* 229 (MH<sup>+</sup>, 100.0 %).

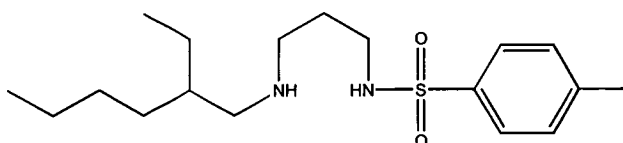
**N-(3-aminopropyl)-4-*t*-butylbenzenesulfonamide (6)**



6 was prepared by the adaptation of the method of Kirsanov and Kirsanova.<sup>2</sup> A solution of 4-*t*-butylbenzenesulfonyl chloride (12.10 g, 52 mmol) in toluene (100 cm<sup>3</sup>) was added dropwise over 8 hours to a solution of 1,3-diaminopropane (11.49 g, 0.16 mol) in toluene (100 cm<sup>3</sup>). The resulting white solid was isolated by filtration, washed with toluene (3 x 20 cm<sup>3</sup>), recrystallised from water (200 cm<sup>3</sup>) and washed with diethyl ether (3 x 20 cm<sup>3</sup>) to yield a white crystalline solid which was dried *in vacuo* (3.33 g, 24%), mp 226°C (Found: C, 50.37; H, 6.73; N, 12.84. Calc. for C<sub>13</sub>H<sub>22</sub>N<sub>2</sub>O<sub>2</sub>S: C, 50.45; H, 6.59; N, 13.07%).  $\delta_{\text{H}}$  (CDCl<sub>3</sub>, 200 MHz): 1.30 (s, 9 H, CH<sub>3</sub>), 1.59 (tt, 2 H, J 6.2, CH<sub>2</sub>), 2.80 (t, 2 H, J 6.1, CH<sub>2</sub>), 3.07 (t, 2 H, J 6.3, CH<sub>2</sub>), 7.50 (d, 2 H, J 8.8, Ar CH), 7.77 (d, 2 H, J 8.8, Ar CH).  $\delta_{\text{C}}$  (DMSO-*d*<sub>6</sub>, 63 MHz): 30 (CH<sub>2</sub>), 31 (3 C, CH<sub>3</sub>), 35 (q), 38 (CH<sub>2</sub>), 38 (CH<sub>2</sub>), 126 (2 C, Ar CH), 126 (2 C, Ar CH), 138 (Ar C), 155 (Ar C). IR data (KBr disc)/cm<sup>-1</sup>: 2961s, 1596m, 1542w, 1465m, 1329s, 1156s. FAB MS, *m/z* 271 (MH<sup>+</sup>, 100.0%).

**N-(N-benzyl-3-aminopropyl)-4-methylbenzenesulfonamide (7)**

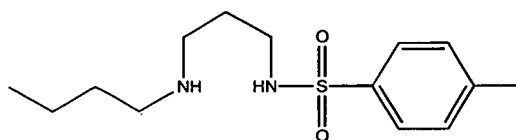
Benzaldehyde (1.86 g, 18 mmol) was added to a solution of N-(3-aminopropyl)-4-methylbenzenesulfonamide (4 g, 18 mmol) in ethanol (50 cm<sup>3</sup>) which was left to stir for one hour. A catalytic amount of anhydrous sodium tetraborate (0.2 g, 1 mmol) and sodium borohydride (2.65 g, 70 mmol) were added and the solution was again stirred for one hour. Distilled water (100 cm<sup>3</sup>) was added, ethanol was removed *in vacuo*, and the solid was recrystallised from ethanol (100 cm<sup>3</sup>) to give a white crystalline solid (2.12 g, 38%), mp 82-84°C (Found: C, 63.93; H, 6.84; N, 8.76. Calc. for C<sub>17</sub>H<sub>22</sub>N<sub>2</sub>O<sub>2</sub>S: C, 64.1; H, 6.96; N, 8.80%).  $\delta_{\text{H}}$  (CDCl<sub>3</sub>, 200 MHz) 1.61 (tt, 2 H, J 6.0, CH<sub>2</sub>), 2.40 (s, 3 H, CH<sub>3</sub>), 2.65 (t, 2 H, J 5.9, CH<sub>2</sub>), 3.03 (t, 2 H, J 6.0, CH<sub>2</sub>), 3.69 (s, 2 H, CH<sub>2</sub>), 7.27 (m, 7 H, Ar CH), 7.70 (d, 2 H, J 8.3, Ar CH).  $\delta_{\text{C}}$  (CDCl<sub>3</sub>, 50 MHz) 21 (CH<sub>3</sub>), 28 (CH<sub>2</sub>), 43 (CH<sub>2</sub>), 48 (CH<sub>2</sub>), 54 (CH<sub>2</sub>), 127 (2 C, Ar CH), 129 (2 C, Ar CH), 137 (Ar C), 140 (Ar C), 143 (Ar C). IR data (KBr disc)/cm<sup>-1</sup>: 1156s, 1185w, 1326s, 1454m, 1477m, 1497m, 1598m, 2832s, 2873w, 2933w, 2964w, 3059m, 3467w. FAB MS, *m/z* 319 (MH<sup>+</sup>, 100%).

**N-(N-2-ethylhexyl-3-aminopropyl)-4-methylbenzenesulfonamide (8)**

N-(3-aminopropyl)-4-methylbenzenesulfonamide (2.81 g, 22 mmol) was added to a solution of 2-ethylhexanal (5g, 22 mmol) in methanol (100 cm<sup>3</sup>) over molecular sieves. The solution was stirred for one hour. A catalytic quantity of anhydrous sodium tetraborate (0.2 g, 1 mmol) and sodium borohydride (0.15 g, 4 mmol) were added. The mixture was stirred overnight, filtered and the ethanol was removed *in vacuo*. Hexane (150 cm<sup>3</sup>) was added and the solution was washed with water (3 x 150 cm<sup>3</sup>) and dried over anhydrous magnesium sulfate. The hexane was removed *in vacuo* to yield a colourless oil (4.93 g, 66%), (Found: C, 63.54; H, 9.60; N, 8.24. Calc. for

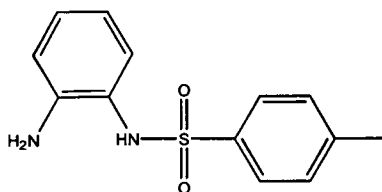
$C_{18}H_{32}N_2O_2S$ : C, 63.49; H, 9.47; N, 8.22%).  $\delta_H$  ( $CDCl_3$ , 360 MHz): 0.90 (t, 3 H, J 7.3,  $CH_3$ ), 0.93 (t, 3 H, J 6.7,  $CH_3$ ), 1.62 (t, 2 H, J 5.5,  $CH_2$ ), 2.67 (t, 2 H, J 5.6,  $CH_2$ ), 2.45 (s, 5 H,  $CH_2$ ,  $CH_3$ ), 3.08 (t, 2 H, J 5.7,  $CH_2$ ), 5.90 (m, 9 H,  $CH$ , 3 x  $CH_2$ ), 7.32 (d, 2 H, J 8.1, 2 H, Ar  $CH$ ), 7.76 (d, 2 H, J 8.1, Ar  $CH$ ).  $\delta_C$  ( $CDCl_3$ , 90 MHz): 11 ( $CH_3$ ), 14 ( $CH_3$ ), 21 ( $CH_3$ ), 23 ( $CH_2$ ), 24 ( $CH_2$ ), 29 ( $CH_2$ ), 31 ( $CH_2$ ), 39 ( $CH$ ), 42 ( $CH_2$ ), 52 ( $CH_2$ ), 127 (2 C, Ar  $CH$ ), 129 (2 C, Ar  $CH$ ), 137 (Ar C), 143 (Ar C). IR data (NaCl disc)/ $cm^{-1}$ : 515s, 659s, 1036m, 1095s, 1164s, 1328s, 1458s, 1496m, 1599m, 2362w, 2873s, 2928s, 3292m. ESI MS,  $m/z$  341 ( $MH^+$ , 100.0%).

**N-(N-butyl-3-aminopropyl)-4-methylbenzenesulfonamide (9)**

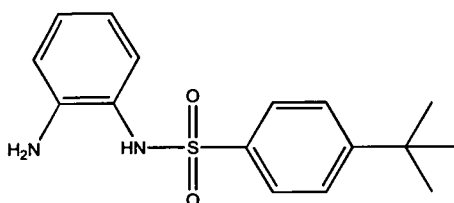


A solution of butanal (0.63 g, 8.76 mmol) in methanol (30  $cm^3$ ) was added to a solution of N-(3-aminopropyl)-4-methylbenzenesulfonamide in methanol (30  $cm^3$ ) and was stirred for 12 hours. A catalytic amount of anhydrous sodium tetraborate (0.2 g, 1 mmol) and sodium borohydride (1.33 g, 35 mmol) were added and the solution was stirred for one hour. Water (200  $cm^3$ ) was added and the methanol was removed *in vacuo*. The resulting yellow oil was extracted into dichloromethane (2 x 100  $cm^3$ ). Removal of solvent from the organic phase *in vacuo* gave a yellow oil which was triturated with hexane (3 x 100  $cm^3$ ) and diethylether (3 x 5  $cm^3$ ) to yield a sticky white solid. This proved extremely difficult to purify. However a few crystals suitable for x-ray crystallography separated from the yellow oil on standing for 5 days.  $\delta_H$  ( $CDCl_3$ , 250 MHz): 0.91 (t, 3 H, J 7.1,  $CH_3$ ), 1.46 (m, 6 H,  $CH_2$ ), 2.41 (s, 3 H,  $CH_3$ ), 2.53 (t, 2 H, J 7.0,  $CH_2$ ), 2.68 (t, 2 H, J 5.8, 2 H,  $CH_2$ ), 3.05 (t, 2 H, J 5.9,  $CH_2$ ), 7.29 (d, 2 H, J 8.0, Ar  $CH$ ), 7.73 (d, 2 H, J 8.3, Ar  $CH$ ). EI MS,  $m/z$  285 ( $MH^+$ , 100.0%).



**N-(2-aminophenyl)-4-methylbenzenesulfonamide (10)**

**10** was prepared by following the method of Cheng *et al.*<sup>3</sup> A solution of 4-methylbenzenesulfonyl chloride (4.3 g, 0.02 mol) in pyridine (50 cm<sup>3</sup>) was added dropwise to a solution of 1,2-diaminobenzene (7.25 g, 0.07 mol) in pyridine (100 cm<sup>3</sup>) over 8 hours. The mixture was quenched with hydrochloric acid (15% aq, 300 cm<sup>3</sup>) and poured into ice (500 g). The resulting pink/brown solid was isolated by filtration, dried *in vacuo* and recrystallised from ethanol (100 cm<sup>3</sup>) to give a crystalline white solid (1.74 g, 28%), mp 135-136°C (Found: C, 59.38; H, 5.32; N, 10.52. Calc. for C<sub>13</sub>H<sub>14</sub>N<sub>2</sub>O<sub>2</sub>S: C, 59.52; H, 5.38; N, 10.68%).  $\delta_{\text{H}}$  (CDCl<sub>3</sub>, 200 MHz): 2.41 (s, 1 H, CH<sub>3</sub>), 4.07 (s, 2 H, NH<sub>2</sub>), 5.93 (s, 1 H, NH), 6.42-6.54 (m, 2 H, Ar CH), 6.71-6.74 (dd, 1 H, J 8.0, Ar CH), 7.00-7.07 (m, 1 H, Ar CH), 7.23-7.27 (m, 2 H, Ar CH), 7.59-7.63 (m, 2 H, Ar CH).  $\delta_{\text{C}}$  (CDCl<sub>3</sub> 63 MHz): 21 (CH<sub>3</sub>), 117 (Ar CH), 118 (Ar CH), 121 (Ar CH), 127 (Ar CH), 128 (Ar CH), 129 (Ar CH), 143 (Ar C), 144 (Ar C). IR data (KBr disc)/cm<sup>-1</sup>: 3386m, 3209m, 1624s, 1464m, 1324s, 1151s, 726m. FAB MS, *m/z* 263 (MH<sup>+</sup>, 81.9%).

**N-(2-amino-phenyl)-4-*t*-butyl benzene-sulfonamide (11)**

**11** was prepared by an adaptation of the method of Cheng *et al.*<sup>3</sup> A solution of 4-*t*-butylbenzenesulfonyl chloride (5.35 g, 23 mmol) in pyridine (50 cm<sup>3</sup>) was added dropwise to a solution of 1, 2-diaminobenzene (7.25 g, 67 mmol) in pyridine (100 cm<sup>3</sup>) over 8 hours. The mixture was quenched with hydrochloric acid (15% aq, 300 cm<sup>3</sup>) and poured onto ice (500 g). The resulting pale brown precipitate was isolated by filtration, dried and recrystallised from ethanol (100 cm<sup>3</sup>) to give a crystalline white

solid (3.30 g, 47%), mp 135-136 °C (Found: C, 63.25; H, 6.62; N, 9.18. Calc. for  $C_{16}H_{20}N_2O_2S$ : C, 63.13; H, 6.62; N, 9.20 %).  $\delta_H$  ( $CDCl_3$ , 200 MHz): 1.31 (s, 9 H,  $CH_3$ ), 4.02 (s, 2 H,  $NH_2$ ), 6.49-6.52 (m, 2 H, Ar  $CH$ ), 6.69 (s, 1 H,  $NH$ ), 6.70-6.73 (m, 1 H, Ar  $CH$ ), 6.98-7.05 (m, 1 H, Ar  $CH$ ), 7.44 (d, 2 H, J 8.8, Ar  $CH$ ), 7.66 (d, 2 H, J 8.8, Ar  $CH$ ).  $\delta_C$  ( $CDCl_3$ , 63 MHz): 31 (3C,  $CH_3$ ), 35 (q, C), 117 (Ar, CH), 118 (Ar, CH), 121 (Ar C), 126 (Ar, CH), 127 (Ar, CH), 128 (Ar, CH), 129 (Ar, CH), 136 (Ar C), 144 (Ar C), 157 (Ar C). IR data (KBr disc)/ $cm^{-1}$ : 3465m, 3387s, 2965s, 2869m, 1625s, 1597s, 1464s, 1324s. FAB MS,  $m/z$  305 ( $MH^+$ , 100.0%).

#### 2.9.4 Monosulfonamidodiamine complex synthesis

##### **Bis[N-(2-aminoethyl)-4-methylbenzenesulfonamidato]zinc(II) (12)**

A solution of **1** (0.15 g, 0.7 mmol) and sodium hydroxide (0.7 mmol) in hot methanol (10  $cm^3$ ) was added to a solution of zinc(II) acetate dihydrate (77 mg, 0.35 mmol) also in methanol (10  $cm^3$ ). The solution was left in a sealed vessel until the product separated as a white crystalline solid after 3 days which was collected by filtration, washed with methanol (3 x 5  $cm^3$ ) and dried *in vacuo* (0.14 g, 81%), (Found: C, 41.67; H, 4.89; N, 12.19. Calc. for  $C_{18}H_{26}N_4O_4S_2Zn$ : C, 41.58; H, 5.4; N, 11.50%). IR data (KBr disc)/ $cm^{-1}$ : 710w, 1599m, 1636w, 2858w, 2940w, 3346m. FAB MS,  $m/z$  491 ( $M^+$ , 66.2%).

##### **Bis[N-(2-aminoethyl)-4-methylbenzenesulfonamidato]nickel(II) (13)**

The procedure described for **12** using nickel(II) acetate tetrahydrate yielded a beige crystalline solid (0.14 g, 83%), Crystals suitable for X-ray crystallography were obtained by the diffusion of toluene into a concentrated solution of **13** in dimethylformamide, (Found: C, 44.41; H, 4.87; N, 11.55. Calc. for  $C_{18}H_{26}N_4NiO_4S_2$ : C, 44.4; H, 5.4; N, 11.50%). IR data (KBr disc)/ $cm^{-1}$ : 1178m, 1148w, 1599m, 1654w, 3327m. FAB MS,  $m/z$  485 ( $M^+$ , 72.9%).

##### **Bis[N-(2-aminoethyl)-4-methylbenzenesulfonamidato]cobalt(II) (14)**

The procedure described for **12** using cobalt acetate tetrahydrate yielded a brown crystalline solid (0.08 g, 46%), (Found: C, 44.46; H, 5.40; N, 11.42. Calc. for

$C_{18}H_{26}N_4CoO_2S_2$ : C, 44.53; H, 5.40; N, 11.54%). IR (KBr disc)/ $cm^{-1}$ : 1158m, 1372w, 1583m, 1626m, 2966w, 292w, 3683w, 3289s, 3448m. FAB MS,  $m/z$  486 ( $MH^+$ , 54.1%).

**Bis[N-(2-aminoethyl)-4-methylbenzenesulfonamidato]copper(II) (15)**

A solution of **1** (0.15 g, 0.7 mmol) in hot methanol (10  $cm^3$ ) was added to copper acetate monohydrate (70 mg, 0.35 mmol) also in methanol (10  $cm^3$ ). The solution was left in a sealed vessel until the product separated as a purple crystalline solid overnight (0.13 g, 78%) (Found: C, 44.07; H, 5.18; N, 11.50. Calc. for  $C_{18}H_{26}N_4CuO_4S_2$ : C, 43.75; H, 5.30; N, 11.33%). IR data (KBr disc)/ $cm^{-1}$ : 710w 1178w 1348w 1603w 2946w 2819w 3316s. ESI MS,  $m/z$  490 ( $M^+$ , 82.5%).

**Bis[N-(2-aminoethyl)-4-*t*-butylbenzenesulfonamidato]copper(II) (16)**

A solution of **2** (0.15 g, 0.58 mmol) in hot methanol (10  $cm^3$ ) was added to a solution of copper(II) acetate monohydrate (58 mg, 0.29 mmol) also in methanol (10  $cm^3$ ). The solution was left in a sealed vessel until the product separated as a purple crystalline solid overnight (0.12 g, 59%). Crystals suitable for X-ray diffraction were prepared by the diffusion of diethyl ether into a concentrated solution of **16** in methanol, (Found: C, 50.19; H, 6.75; N, 9.60. Calc. for  $C_{24}H_{38}N_4CuO_4S_2$ : C, 50.02; H, 7.00; N, 9.72%). IR (KBr disc)/ $cm^{-1}$ : 835m, 981m, 1129m, 1252s, 1655m, 1686m, 2986m, 3632m. ESI MS,  $m/z$  574 ( $M^+$ , 65.0%).

**Bis[N-(N-2-ethylhexyl-2-aminoethyl)-4-methylbenzenesulfonamidato]nickel(II) (17)**

A solution of **4** (0.15 g, 0.46 mmol) in hot methanol (10  $cm^3$ ) was added to nickel(II) acetate tetrahydrate (57 mg, 0.23 mmol) in methanol (10  $cm^3$ ) and the mixture was stirred for 30 minutes before the solvent was removed *in vacuo* to yield an orange oil which was triturated with hexane to give an orange solid which was dried *in vacuo*. (0.19 g, 45%), (Found: C, 57.53; H, 8.17; N, 7.79. Calc. for  $C_{34}H_{58}N_4NiO_2S_2$ : C, 57.46; H, 8.22; N, 7.88%). IR data (KBr disc)/ $cm^{-1}$ : 669s, 971m, 1137m, 1279m, 1466w, 2343m, 2361m, 2929m, 3191m. FAB MS,  $m/z$  709 ( $M^+$ , 77.8%).

**Bis[N-(N-2-ethylhexyl-2-aminoethyl)-4-methylbenzenesulfonamidato]cobalt(II) (18)**

Using cobalt(II) acetate tetrahydrate in the procedure described for 17 yielded a purple solid which was dried *in vacuo*. (0.13 g, 32%). IR data (KBr disc)/cm<sup>-1</sup>: 668w, 1161w, 1332w, 1412w, 1560s, 2361w, 2961w, 3464m. FAB MS, *m/z* 709 (MH<sup>+</sup>, 96.0%), HRMS *m/z* calc. for 710.9322, found 710.3314.

**Bis[N-(N-2-ethylhexyl-2-aminoethyl)-4-methylbenzenesulfonamidato]copper(II) (19)**

Using copper(II) acetate monohydrate in the procedure described for 17 yielded a purple solid which was dried *in vacuo*. (0.22 g, 51%), (Found: C, 57.10; H, 8.14; N, 7.80. Calc. for C<sub>34</sub>H<sub>58</sub>N<sub>4</sub>CuO<sub>2</sub>S<sub>2</sub>: C, 57.15; H, 8.18; N, 7.84%). IR data (KBr disc)/cm<sup>-1</sup>: 667s, 1136s, 1274m, 1558s, 1685m, 2343m, 2362m, 2929m, 3447m. FAB MS, *m/z* 714 (MH<sup>+</sup>, 10.1%).

**Bis[N-(2-aminopropyl)-4-methylbenzenesulfonamidato]cobalt(II) (20)**

A solution of 5 (0.15 g, 0.66 mmol) in hot methanol (10 cm<sup>3</sup>) was added to cobalt acetate tetrahydrate (82 mg, 0.33 mmol) in methanol (10 cm<sup>3</sup>). The solution was left sealed until the product separated as a purple crystalline solid after 3 days which was collected by filtration, washed with methanol (3 x 5 cm<sup>3</sup>) and dried *in vacuo* (61 mg, 36%), (Found: C, 46.54; H, 6.13; N, 10.62. Calc. for C<sub>20</sub>H<sub>30</sub>N<sub>4</sub>CoO<sub>4</sub>S<sub>2</sub>: C, 46.78; H, 5.89; N, 10.91%). IR data (KBr disc)/cm<sup>-1</sup>: 709w, 1134s, 1684w, 3332m, 2929w, 2878w, 2846w. ESI MS, *m/z* 514 (M<sup>+</sup>, 6.3%).

**Bis[N-(2-aminopropyl)-4-methylbenzenesulfonamidato]copper(II)****(blue polymorph 21)<sup>1</sup>**

A solution of 5 (0.15 g, 0.66 mmol) in hot methanol (10 cm<sup>3</sup>) was added to a solution of copper acetate monohydrate (66 mg, 0.35 mmol) also in methanol (10 cm<sup>3</sup>). The solution was allowed to evaporate overnight to a volume of 10 cm<sup>3</sup> and yielded a blue crystalline solid which was collected by filtration, washed with methanol (3 x 5 cm<sup>3</sup>) and dried *in vacuo* (73 mg, 43%), (Found: C, 46.29; H, 5.62; N, 10.61. Calc. for C<sub>20</sub>H<sub>30</sub>N<sub>4</sub>CuO<sub>2</sub>S<sub>2</sub>: C, 46.33; H, 5.84; N, 10.81%). IR data (KBr disc)/cm<sup>-1</sup>: 1124s, 1195m, 1243s, 1274m, 1324w, 1608m, 2922m, 3166m, 3270s. FAB MS, *m/z* 519 (MH<sup>+</sup>, 62.0%).

**Bis[N-(2-aminopropyl)-4-methylbenzenesulfonamidato]copper(II)  
(green polymorph 22)<sup>1</sup>**

The procedure described for **20** using copper(II) acetate monohydrate yielded a green crystalline solid which was collected by filtration, washed with methanol (3 x 5 cm<sup>3</sup>) and dried *in vacuo*. (0.08 g, 47%), (Found: C, 46.12; H, 5.71; N, 10.79. Calc. for C<sub>20</sub>H<sub>30</sub>N<sub>4</sub>CuO<sub>2</sub>S<sub>2</sub>: C, 46.33; H, 5.84; N, 10.81%). IR data (KBr disc)/cm<sup>-1</sup>: 1028m, 1324m, 1358m, 1446m, 1576s, 1080m, 1340m, 1384m, 1478w, 1606s, 2894m, 3098m, 3179w. FAB MS, *m/z* 519 (M<sup>+</sup>, 43.0%).

**Bis[N-(2-aminopropyl)-4-methylbenzenesulfonamidato]zinc(II) (23)**

The procedure described for **20** using zinc(II) acetate dihydrate yielded a white crystalline solid which was collected by filtration, washed with methanol (3 x 5 cm<sup>3</sup>) and dried *in vacuo* (65 mg, 38%). (Found: C, 46.05; H, 5.42; N, 10.78. Calc. for C<sub>20</sub>H<sub>30</sub>N<sub>4</sub>O<sub>2</sub>S<sub>2</sub>Zn: C, 46.20; H, 5.82; N, 10.78%). IR data (KBr disc)/cm<sup>-1</sup>: 709w, 1173m, 1590m, 1653w 2848w, 2884w, 2934w, 3340m. ESI MS, *m/z* 519 (M<sup>+</sup>, 10.9%).

**Bis[N-(N-2-ethylhexyl-3-aminopropyl)-4-methylbenzenesulfonamidato]copper(II)  
(24)**

A solution of **8** (0.15 g, 44 μmol) in hot methanol (10 cm<sup>3</sup>) was added to a solution of copper acetate monohydrate (44 mg, 0.22 mmol) also in methanol (10 cm<sup>3</sup>). The solution was held at reflux for one hour and the solvent then removed *in vacuo* to yield a green oil (52 mg, 32%). IR data (CHCl<sub>3</sub>)/cm<sup>-1</sup>: 1173s, 1345s, 1683w, 2963m. ESI MS *m/z* 742 (MH<sup>+</sup>, 80.1%), HRMS *m/z* calc. for 743.5988, found 743.3561.

**Bis[N-(2-amino-phenyl)-4-methylbenzene-sulfonamidato]nickel(II) (25)**

A solution of **10** (0.15 g, 0.57 mmol) in hot methanol (10 cm<sup>3</sup>) was added to a solution of nickel(II) acetate tetrahydrate (71 mg, 0.29 mmol) also in methanol (10 cm<sup>3</sup>). The solution was left in a sealed vessel for three days until the product separated as a pale green solid which was collected by filtration (0.15 g, 93%), (Found: C, 53.71; H, 4.36; N, 9.61. Calc. for C<sub>26</sub>H<sub>26</sub>N<sub>4</sub>NiO<sub>2</sub>S<sub>2</sub>: C, 53.63; H, 4.50; N, 9.62%). IR data (KBr disc)/cm<sup>-1</sup>: 706w, 1163w, 1493s, 1599m, 3025w, 3448m. FAB MS, *m/z* 581 (MH<sup>+</sup>, 7.2%).

**Bis[N-(2-amino-phenyl)-4 methylbenzene-sulfonamidato]copper(II) (26)**

A solution of **10** (0.15 g, 0.58 mmol) in hot dimethylformamide (10 cm<sup>3</sup>) was added to a solution of copper acetate monohydrate (57 mg, 0.28 mmol) also in dimethylformamide (10 cm<sup>3</sup>). The solution was left sealed until product overnight until the product separated as a black crystalline solid which was collected by filtration, washed with dimethylformamide (3 x 5 cm<sup>3</sup>) and dried *in vacuo*. (0.15 g, 90%), (Found: C, 52.09; H, 5.91; N, 12.35. Calc. for C<sub>26</sub>H<sub>26</sub>N<sub>4</sub>CuO<sub>2</sub>S<sub>2</sub>: C, 52.19; H, 5.88; N, 12.17%). IR data (KBr disc)/cm<sup>-1</sup>: 707w, 1137m, 1390m, 1655s, 2927w, 3036w, 3448m. ESI MS *m/z* 587 (MH<sup>+</sup>, 100.0%).

**Bis[N-(2-amino-phenyl)-4 methylbenzene-sulfonamidato]zinc(II) (27)**

The procedure described for **25** using zinc(II) acetate dihydrate yielded a white crystalline solid which was collected by filtration, washed with methanol (3 x 5 cm<sup>3</sup>) and dried *in vacuo* (0.076g, 45%). (Found: C, 52.90; H, 4.46; N, 9.53. Calc. for C<sub>26</sub>H<sub>30</sub>N<sub>4</sub>O<sub>2</sub>S<sub>2</sub>Zn: C, 53.11; H, 4.46; N, 9.53%). IR data (KBr disc)/cm<sup>-1</sup>: 707w, 1160w, 1197w, 1264s, 1306s, 1542w, 1601m, 3035w, 3065w, 3259s, 3335s. FAB MS, *m/z* 589 (MH<sup>+</sup>, 5.7%).

**2.9.5 Solvent extraction experiments from sulfate media**S curve data

50 cm<sup>3</sup> of 0.1M Cu(II)L<sub>2</sub> (L = **4** or **8**) in dichloromethane was contacted with 50 cm<sup>3</sup> deionised water in a tightly sealed, screw top, glass jar, equipped with a magnetic stirrer. The two-phase system was stirred at 600 r.p.m. and at room temperature for ½ h, after which time the pH of the aqueous phase was measured and a 1 cm<sup>3</sup> sample was taken from the organic phase and the aqueous phase. A small amount of concentrated H<sub>2</sub>SO<sub>4</sub> was then added to the experiment which was stirred for a further ½ h, the pH was again recorded and 1 cm<sup>3</sup> samples were taken from the organic and the aqueous phases. This procedure was repeated until the organic phase was yellow or colourless. The samples were diluted by a factor of 1:10 with water (aqueous samples) or white spirit (organic samples) and their copper content analysed by ICP-AES. The data collected were plotted as a graph of pH versus % copper in the organic phase using Microsoft Excel.

### Selectivity data

20 cm<sup>3</sup> of 0.1 M ligand solution (ligand = **4** or **8**) were contacted with 20 cm<sup>3</sup> aqueous metal(II) sulfate solution (M = Co, Ni, Cu, Zn) and stirred for 1 h, after which time the two phases were separated by filtration. The samples were diluted by a factor of 1:10 and their metal content analysed by ICP-AES. The data were plotted as bar charts using Microsoft Excel.

### **2.9.6 X-ray crystallography**

Structures **1**, **5**, **7**, **10**, **12**, **13** and **16** were determined by Andrew Parkin and structure **9** was determined by Dr. Simon Parsons at the University of Edinburgh. In all cases data were collected at 220 K on a SMART or Stoe Stadi-4 diffractometer equipped with an Oxford Cryosystems low temperature device, using Cu-K $\alpha$  radiation for **13** and Mo-K $\alpha$  radiation for **1**, **5**, **7**, **9**, **10**, **12** and **16**. Reflections were scanned in  $\omega$ - $\theta$  mode. All structures were solved by direct methods (SHELXTL or SIR92<sup>30,31</sup>). All were completed by iterative cycles of least squares refinement against  $F^2$  and difference Fourier synthesis (SHELXTL<sup>32</sup>). H-atoms were idealised, being placed using geometric or difference maps and treated by riding or refall methods. Sulfonamido nitrogen atoms were placed using difference maps. In all cases non-H atoms were modelled with final anisotropic displacement parameters and final refinement statistics are presented in Tables 2.22 (**1**, **5** and **7**) 2.23 (**9** and **10**) and 2.24 (**12**, **13** and **16**).

Table 2.22: Crystallographic data for structures 1, 5 and 7.

Structure	1	5	7
Formula	C <sub>9</sub> H <sub>14</sub> N <sub>2</sub> O <sub>2</sub> S	C <sub>10</sub> H <sub>16</sub> N <sub>2</sub> O <sub>2</sub> S	C <sub>17</sub> H <sub>22</sub> N <sub>2</sub> O <sub>2</sub> S
M	214.28	228.31	318.43
Crystal system	Monoclinic	Monoclinic	Orthorhombic
Space group	Pn	P2 (1) / c	Pna2 (1)
a/Å	6.4295(17)	11.9460(8)	22.113
b/Å	7.0606(19)	7.8174(5)	8.4446(14)
c/Å	22.987(6)	13.1025(9)	8.9661(8)
α°	90	90	90
β°	90.097(5)	108.5310(10)	90
γ°	90	90	90
U/Å <sup>3</sup>	1043.5(5)	1160.16(13)	1674.3(4)
Crystal size/mm	0.36 x 0.05 x 0.05	0.50 x 0.40 x 0.27	0.89 x 0.27 x 0.21
D <sub>c</sub> /g cm <sup>-1</sup>	1.364	1.307	1.263
Z	4	4	4
μ/mm <sup>-1</sup>	0.287	0.262	0.202
Scan type	phi + omega	phi + omega	omega - theta
θ Limits/°	1.77-26.44	1.80-26.40	2.58-24.96
No. of unique data	3730	2371	1770
No. data with [F>4σ(F)]	3283	2002	1169
No. parameters	278	200	182
R1	0.0378	0.0333	0.0564
wR2	0.0795	0.0910	0.1094
Δρ <sub>max</sub> , Δρ <sub>min</sub> /e Å <sup>-3</sup>	0.290, -0.303	0.429, -0.299	0.259, -0.254

Table 2.23: Crystallographic data for 9 and 10.

Structure	9	10
Formula	C <sub>14</sub> H <sub>24</sub> N <sub>2</sub> O <sub>2</sub> S	C <sub>13</sub> H <sub>14</sub> N <sub>2</sub> O <sub>2</sub> S
M	284.41	262.32
Crystal system	Monoclinic	Monoclinic
Space group	P21 / c	P2 (1)
a/Å	15.891(3)	11.245(8)
b/Å	6.5484(12)	6.100(5)
c/Å	15.549(3)	18.916(17)
α°	90	90
β°	105.131(15)	98.50(8)
γ°	90	90
U/Å <sup>3</sup>	1561.9(5)	1283.4(18)
Crystal size/mm	0.70 x 0.43 x 0.19	0.86 x 0.51 x 0.35
D <sub>c</sub> /g cm <sup>-1</sup>	1.209	1.358
Z	4	4
μ/mm <sup>-1</sup>	0.208	0.248
Scan type	omega - theta	omega - theta
θ Limits/°	2.66-24.93	2.63-25.05
No. of unique data	2726	2503
No. data with [F>4σ(F)]	1654	2343



<b>No. parameters</b>	183	414
<b>R1</b>	0.0526	0.0287
<b>wR2</b>	0.1302	0.0773
$\Delta\rho_{\max}, \Delta\rho_{\min}/e \text{ \AA}^{-3}$	0.255, -0.308	0.209, -0.241

Table 2.24: Crystallographic data for structures 12, 13 and 16.

<b>Structure</b>	<b>12</b>	<b>13</b>	<b>16</b>
<b>Formula</b>	$C_{38}H_{60}N_8O_{10}S_4Zn_2$	$C_{18}H_{26}N_4NiO_4S_2$	$C_{24}H_{38}CuN_4O_4S_2$
<b>M</b>	1047.92	485.26	574.24
<b>Crystal system</b>	Monoclinic	Monoclinic	Monoclinic
<b>Space group</b>	$P 2(1) / a$	$P 2(1) / c$	$P2 (1)$
<b>a/Å</b>	11.784(6)	12.832(6)	6.2601(15)
<b>b/Å</b>	25.789(8)	6.912(3)	10.817(3)
<b>c/Å</b>	15.636(6)	12.253(5)	19.487(5)
$\alpha/^\circ$	90	90	90
$\beta/^\circ$	90.18(3)	108.68(3)	94.534(4)
$\gamma/^\circ$	90	90	90
<b>U/Å<sup>3</sup></b>	4752(3)	1029.5(7)	1315.5(5)
<b>Crystal size/mm</b>	0.62 x 0.10 x 0.08	0.47 x 0.16 x 0.10	0.40 x 0.30 x 0.03
<b>D<sub>c</sub>/g cm<sup>-3</sup></b>	1.465	1.565	1.450
<b>Z</b>	4	2	2
$\mu/\text{mm}^{-1}$	1.246	3.544	1.027
<b>Scan type</b>	omega - theta	omega - theta	phi + omega
<b><math>\theta</math> Limits/<math>^\circ</math></b>	1.30-23.52	3.64-60.01	1.05-26.40
<b>No. of unique data</b>	5435	1476	5178
<b>No. data with [F&gt;4<math>\sigma</math>(F)]</b>	3754	1305	4554
<b>No. parameters</b>	565	134	316
<b>R1</b>	0.0535	0.0528	0.0311
<b>wR2</b>	0.1408	0.1509	0.0648
$\Delta\rho_{\max}, \Delta\rho_{\min}/e \text{ \AA}^{-3}$	0.380, -0.654	0.620, -0.626	0.604, -0.352

## 2.10 References

- <sup>1</sup> D. J. White, L. Cronin, S. Parsons, N. Robertson, P. A. Tasker, A. P. Bisson, *J. Chem. Soc., Chem. Commun.*, 1999, 1107.
- <sup>2</sup> A. V. Kirsanov and N. A. Kirsanova, *Zhurnal Obshchei Khimii*, 1962, **32**, 887.
- <sup>3</sup> H.-Y. Cheng, C. -F. Lee , S. M. Peng, *Inorganica Chimica Acta*, 1991, **181**, 145.
- <sup>4</sup> A.D. Garnovskii, *Koord. Khim.*, (*Engl. Trans.*), 1992, **18**, 695.
- <sup>5</sup> D. H. Williams and I. Fleming, in *Spectroscopic Methods in Organic Chemistry*, McGraw-Hill Book Company, London, 5<sup>th</sup> edn., 1995, ch. 3, p. 118.
- <sup>6</sup> L. R. Hanton, C. A. Hunter and Duncan H. Purvis, *J. Chem. Soc., Chem. Commun.*, 1992, 1134.
- <sup>7</sup> K. Henrick, P. A. Tasker, L. F. Lindoy, *Progress in inorganic chemistry*, 1985, **33**, 1.
- <sup>8</sup> K. E. Laidig and L. M. Cameron, *J. Am. Chem. Soc.*, 1996, **118**, 1737.
- <sup>9</sup> C. J. Epstein, R. F. Goldberger, C. B. Anfinsen, *Cold Spring Harbor Symp. Quant. Biol.*, 1963, **28**, 439.
- <sup>10</sup> T. Ohwada, I. Okamoto, K. Shudo and K. Yamaguchi, *Tetrahedron Letters*, 1998, **39**, 7877.
- <sup>11</sup> J. Elguero, P. Goya, I. Rozas, J. Catalan and J. Luis, G. De Pas, *J. of Molecular Structure (Theochem)*, 1989, **184**, 115.
- <sup>12</sup> Dr D. J. White, work carried out at the University of Sydney, private communication.
- <sup>13</sup> L. Alderighi, P. Gans, A. Ienco, D. Peters, A. Sabatini and A. Vacca, *Coord. Chem. Rev.*, 1999, **184**, 311.
- <sup>14</sup> K. F. Purcell and J. C. Kotz, in *Inorganic Chemistry, Holt-Saunders International Editions*, Japan, 1985, ch. 13, pp. 694-755.
- <sup>15</sup> C.-F. Lee and S.-M. Peng, *Journal of the Chinese Chemical Society*, 1991, **38**, 559.
- <sup>16</sup> J. J. Bour and J. J. Steggerda, *J. Chem. Soc., Chem. Commun.*, 1967, 85.
- <sup>17</sup> D. C. Olson and J. Vasilevskis, *Inorg. Chem.*, 1969, **8**, 1611.

- <sup>18</sup> E. S. Gore and D. H. Busch, *Inorg. Chem.*, 1973, **12**, 1.
- <sup>19</sup> D. C. Olson and J. Vasilekskis, *Inorg. Chem.*, 1971, **10**, 463.
- <sup>20</sup> F. V. Lovecchio, E. S. Gore and D. H. Busch, *J. Am. Chem. Soc.*, 1974, **96**, 3109.
- <sup>21</sup> D. Mayerstein, *Inorg. Chem.*, 1971, **10**, 2244.
- <sup>22</sup> F. P. Bossu, K. L. Chellappa and D. W. Margerum, *J. Am. Chem. Soc.*, 1977, **99**, 2195.
- <sup>23</sup> D. W. Margerum, K. L. Chellappa, F. P. Bossu, G. L. Burce, *J. Am. Chem. Soc.*, 1975, **97**, 6894.
- <sup>24</sup> F. P. Bossu, D. W. Margerum, *J. Am. Chem. Soc.*, 1976, **98**, 4003.
- <sup>25</sup> F. P. Bossu, K. L. Chellappa and D. W. Margerum, *J. Am. Chem. Soc.*, 1977, **99**, 2195.
- <sup>26</sup> F. P. Bossu and D. W. Margerum, *Inorg. Chem.*, 1977, **16**, 1210.
- <sup>27</sup> S. T. Kirksey, Jr., T. A. Neubecker and D. W. Margerum, *J. Am. Chem. Soc.* 1979, **101**, 1631.
- <sup>28</sup> A. J. Bard and L. R. Faulkner, in *Electrochemical methods, Fundamentals and Applications*, ed. By D. Harris, C. Robey and E. Aiello, John Wiley and Sons Inc., New York, 2001, ch. 2, p. 44.
- <sup>29</sup> P. Gans, A. Sabatini and A. Vacca, *Inorg. Chim. Acta*, 1976, **18**, 237.
- <sup>30</sup> G. M. Sheldrick, SHELXTL version 5, Siemens Analytical X-ray Instrument, Madison, Wisc., USA, 1995.
- <sup>31</sup> A. Altomare, G. Cascarano, C. Giacovazzi and A. Guagliardi, *J. Appl. Cryst.*, 1994, **27**, 1045-1050.
- <sup>32</sup> P. T. Beurskens, G. Beurskens, W. P. Bosman, R. de Gelder, S. García-Granda, R. O. Gould, R. Israël and J. M. M. Smits, DIRDIF, Crystallography Laboratory, University of Nijmegen, The Netherlands.

**Chapter 3:**  
**Sulfonamido oxime ligands**

<b>Contents</b>	<b>Page</b>
3.1 Introduction .....	127
3.2 Synthesis of simple monosulfonamido oxime ligands and their metal complexes .....	128
3.2.1 Free Ligands .....	128
3.2.2 Metal complexes .....	129
3.3 Characterisation of sulfonamido oxime ligands .....	130
3.3.1 Nuclear magnetic resonance (NMR) spectroscopy .....	130
3.3.2 Mass spectrometry and IR spectroscopy .....	131
3.3.3 X-ray crystallography .....	132
3.4 Solid state structures of sulfonamido oxime ligands and their complexes .....	132
3.4.1 Free ligands .....	133
3.4.1.1 1-{2-[N-(4-methylbenzenesulfonamido)]phenyl} ethan-1-one oxime ( <b>28</b> ) .....	133
3.4.1.2 1-{2-[N-(4-t-butylbenzenesulfonamido)]phenyl} ethan-1-one oxime ( <b>29</b> ) .....	134
3.4.1.3 1-{2-[N-(4-methylbenzenesulfonamido)]phenyl} ethan-1-one O-methyloxime ( <b>32</b> ) .....	136
3.4.1.4 1-{2-[N-(4-methylbenzenesulfonamido)]-phenyl}(phenyl) methanone oxime ( <b>33</b> ) .....	137
3.4.2 Oxime stereochemistry .....	140
3.4.3 Hydrogen-bonding in sulfonamido oxime ligands .....	141
3.4.4 Sulfonamido oxime [ML <sub>2</sub> ] complexes .....	143
3.4.4.1 Bis[1-{2-[N-(4-methylbenzenesulfonamidato)]phenyl} ethan-1-one oxime] copper(II) ( <b>34</b> ) .....	144
3.4.4.2 Bis[1-{2-[N-(4-methylbenzenesulfonamidato)]phenyl} ethan-1-one oxime] nickel(II) ( <b>36</b> ) .....	145
3.4.5 Sulfonamido oxime cluster complexes .....	147
3.4.5.1 [Cu <sub>4</sub> ( <b>28</b> -H) <sub>2</sub> ( <b>28</b> -2H) <sub>2</sub> (CH <sub>3</sub> OH) <sub>2</sub> (CH <sub>3</sub> O) <sub>2</sub> ] ( <b>35</b> ) .....	147
3.4.5.2 [Ni <sub>2</sub> Na <sub>2</sub> ( <b>28</b> -H) <sub>2</sub> ( <b>28</b> -2H) <sub>2</sub> (CH <sub>3</sub> OH) <sub>4</sub> ] ( <b>38</b> ) .....	150

---

3.4.5.3 $[\text{Ni}_4(\mathbf{28-H})_2(\mathbf{28-2H})_2(\text{OH})_2(\text{MeO})_5]$ ( <b>39</b> ) .....	153
3.4.6 Coordination sites of sulfonamido oxime ligands .....	156
3.4.7 Hydrogen-bonding in sulfonamido oxime complexes .....	158
3.4.8 Hole size, bite distances and torsion angles .....	159
3.4.9 Geometry of the sulfonamido nitrogen .....	163
3.5 A study of the solution properties of <b>34</b> and <b>35</b> .....	166
3.6 Equilibrium constants .....	167
3.7 Conclusion .....	168
3.8 Experimental .....	169
3.8.1 Instrumentation .....	169
3.8.2 Solvent and reagent Pretreatment .....	170
3.8.3 Synthesis of sulfonamido intermediates .....	170
3.8.4 Synthesis of sulfonamide oximes .....	173
3.8.5 Synthesis of sulfonamido oxime complexes .....	177
3.8.6 X-ray crystallography .....	180
3.9 References .....	184

### 3.1 Introduction

Sulfonamido oxime ligands were investigated due to their similarity to P50 type phenolic oxime metal extractants (see chapter 1). The ligands have two nitrogen donor atoms (sulfonamido and oximic) for coordination to a metal centre. The sulfonamido proton is acidic ( $pK_a \sim 9$ ) and deprotonates on complexation to yield an anionic species, this also increases the nucleophilicity of the nitrogen donor atom. 2:1 complex formation with a divalent metal ion produces a charge neutral species which is essential for solubility in organic solvents. The sulfonamido oxygen lone pairs could act as hydrogen-bond acceptor sites to the hydrogen-bond donor atom of the oxime function in a head-to-tail interaction to create a *pseudo*-macrocyclic ligand (Figure 3.1).

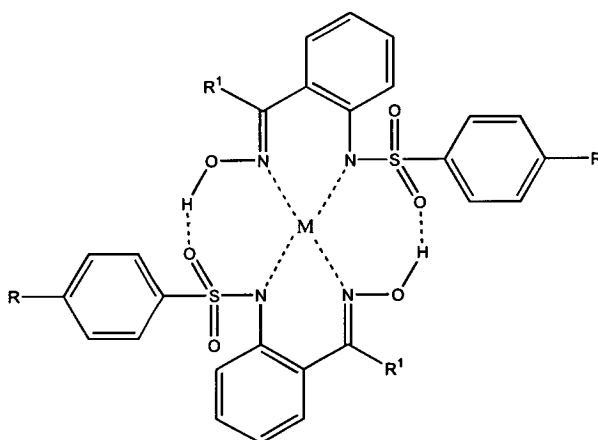
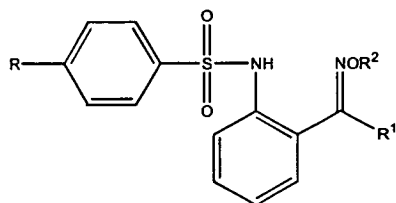


**Figure 3.1:** A *pseudo*-macrocyclic sulfonamido oxime ligand coordinated to a metal centre.

### 3.2 Synthesis of simple monosulfonamido oxime ligands and their metal complexes

The sulfonamido oxime ligands prepared in this thesis are shown in Figure 3.2.



	R	R <sup>1</sup>	R <sup>2</sup>
<b>28<sup>a</sup></b>	methyl	methyl	H
<b>29<sup>a</sup></b>	butyl	methyl	H
<b>30</b>	propyl	methyl	H
<b>31</b>	pentyl	methyl	H
<b>32<sup>a</sup></b>	methyl	methyl	methyl
<b>33<sup>a</sup></b>	methyl	phenyl	H

**Figure 3.2:** The sulfonamido oxime ligands discussed in this chapter. <sup>a</sup> Formula confirmed by X-ray crystallography.

The complexes which have been isolated of the above ligands are given in Table 3.1.

**Table 3.1:** Sulfonamido oxime complexes synthesised.

Abbreviation	Complex	Colour
<b>34<sup>a</sup></b>	[Cu(28-H) <sub>2</sub> ]	Brown
<b>35<sup>a</sup></b>	[Cu(28-H) <sub>2</sub> (28-2H) <sub>2</sub> (MeOH) <sub>2</sub> (MeO) <sub>2</sub> ]	Green
<b>36<sup>a</sup></b>	[Ni(28-H) <sub>2</sub> ]	Orange
<b>37</b>	[Ni(28-H) <sub>2</sub> ]	Purple
<b>38<sup>a</sup></b>	[Ni <sub>2</sub> Na <sub>2</sub> (28-H) <sub>2</sub> (28-2H) <sub>2</sub> (MeOH) <sub>4</sub> ]	Red
<b>39<sup>a</sup></b>	[Ni <sub>4</sub> (OH) <sub>2</sub> (28-H) <sub>2</sub> (28-2H) <sub>2</sub> (CH <sub>3</sub> OH) <sub>4</sub> ]	Green
<b>40</b>	[Ni(30-H) <sub>2</sub> ]	Orange
<b>41</b>	[Cu(33-H) <sub>2</sub> ]	Brown

<sup>a</sup> Formula confirmed by X-ray crystallography.

#### 3.2.1 Free Ligands

Two ligands were initially synthesised, 1-{2-[N-(4-methylbenzenesulfonamido)]-phenyl}ethan-1-one oxime (**28**) and 1-{2-[N-(4-methylbenzenesulfonamido)]-phenyl}(phenyl)methanone oxime (**33**) (Figure 3.3).



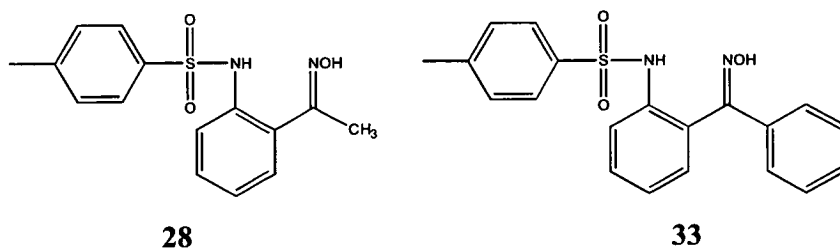


Figure 3.3: Ligands **28** and **33**.

The synthesis was achieved in two steps. The aminoketone was first converted to a sulfonamide by treatment with 4-methylbenzenesulfonyl chloride in pyridine which was then oximated in a 50:50, pyridine:ethanol medium (Figure 3.4).

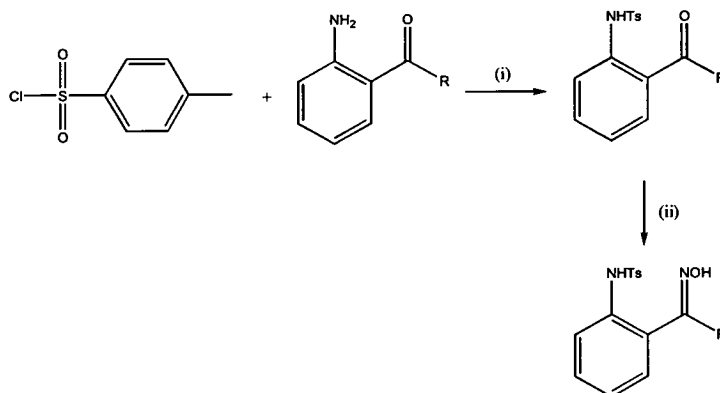


Figure 3.4: The preparation of the sulfonamido oxime ligands **28** (R = methyl) and **33** (R = phenyl).

(i) Pyridine, 298 K. (ii) 3 eq.  $\text{NH}_2\text{OH}\cdot\text{HCl}$ , 50:50, pyridine:ethanol, reflux for 4 hours. Ts =  $-\text{SO}_2(\text{C}_6\text{H}_4)\text{CH}_3$ .

As observed for the sulfonamido diamine ligands in chapter 2, the solubility of the prototype ligands, whilst sufficient for defining the coordination properties, was too low to enable their colligative properties and their ability to act as solvent extractants to be studied. The preparation and study of more soluble derivatives is described in chapter 4.

### 3.2.2 Metal complexes

Metal complexes **34**, **37**, **40** and **41** were synthesised by treating two equivalents of the appropriate ligand with one equivalent of the appropriate divalent metal acetate (Equation 3.1) in methanol or ethanol.<sup>1</sup>



When this method failed to yield the desired complex one equivalent of base (B) was added to facilitate deprotonation of the ligand (Equation 3.2). Formation of the complexes **36**, **38** and **39** required the addition of base; sodium, potassium or lithium hydroxide was used.



To study whether additional oxygen donors from the sulfonamido groups or from the oxime group can also be involved in complex formation, see Section 3.4.5, metal to ligand ratios of 1:1 were also tried. This resulted in the synthesis of **35**.

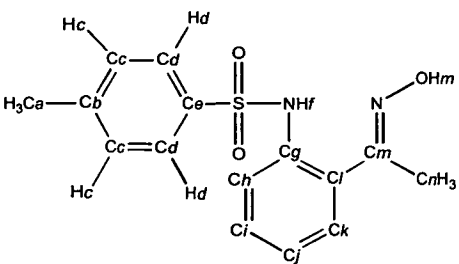
### 3.3 Characterisation of sulfonamido oxime ligands

#### 3.3.1 Nuclear magnetic resonance (NMR) spectroscopy

Sulfonamido oxime ligands **28-33** may be easily characterised by proton nmr. The set of two doublets arising from the protons, *c* and *d*, on the 4-methylbenzene group which were easily assigned in the sulfonamido-diamine ligands (chapter 2) are usually hidden in the oxime ligands by other signals in the aromatic region. However, other peaks are readily assigned, *e.g.* in ligands **28-32** a peak for the methyl group at position R<sup>1</sup> is observed between 1.95 and 2.38 ppm.

To characterise 1-{2-[N-(4-methylbenzenesulfonamido)]phenyl}ethan-1-one oxime (**28**) (Figure 3.5) as an example. A peak for the *p*-methylbenzene group is observed at 2.03 ppm and peaks for protons *f* (8.38 ppm) and *m* (10.85 ppm) are shifted to low field by the increasing electron withdrawing nature of the nitrogen and oxygen atoms respectively. The 1:1 ratio of the two methyl peaks (*a* and *n*) supported the characterisation and this was verified by the ratio of 3:8 between the methyl peak *a* and the aromatic region. <sup>13</sup>C nmr is also useful to confirm structures. The two methyl carbon signals *a* and *n* at 21 and 12 ppm are easily identified as is the signal for the imino carbon, *m*, which is shifted downfield past the aromatic signals at 157

ppm. The remaining signals were assigned using DEPT techniques<sup>2</sup> and are listed in Figure 3.5 along with assignments for the <sup>1</sup>H nmr spectrum.



label	<sup>13</sup> C NMR (ppm)	<sup>1</sup> H NMR (ppm)
<i>a</i>	12	2.03
<i>b</i>	125	—
<i>c'</i>	127	7.05-7.65
<i>d'</i>	129	7.05-7.65
<i>e</i>	143	—
<i>f</i>	—	8.38
<i>g and l</i>	136, 136	—
<i>h and k'</i>	128, 129	7.05-7.65
<i>i and j'</i>	122, 124	7.05-7.65
<i>m</i>	157	10.85
<i>n</i>	21	2.32

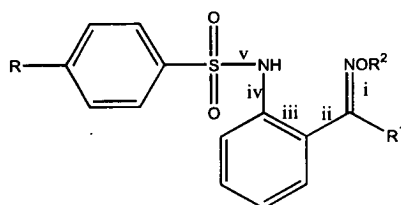
**Figure 3.5:** 1-{2-[N-(4-methylbenzenesulfonamido)]phenyl}ethan-1-one oxime (**28**) including the labelling scheme used for nmr assignments. *i* peaks for *c*, *d*, *h*, *i*, *j* and *k* all form a multiplet in the <sup>1</sup>H nmr spectrum between 7.05 and 7.65 ppm.

### 3.3.2 Mass spectrometry and IR spectroscopy

IR and mass spectrometry were used to support characterisation. IR confirming the presence of the sulfonamido group in the products. One strong band is expected in the 1370-1330 cm<sup>-1</sup> region and another in the 1180-1160 cm<sup>-1</sup> region for the -SO<sub>2</sub>-N group. A weak peak is also expected for the C=N bond of the oxime group between 1690 and 1640 cm<sup>-1</sup>. This was sometimes difficult to identify due to the proximity of C=C peaks. Electron impact (EI), fast atom bombardment (FAB) and electrospray ionisation mass spectrometry have all been used for analysis purposes. EI and FAB gave the expected molecular ion and ESI spectra gave peaks of higher molecular weight, suggesting that assembly is occurring in solution, the latter will be discussed further in chapter 4.

### 3.3.3 X-ray crystallography

Ligands **28**, **29**, **32** and **33** were also characterised by X-ray crystallography. This showed that the stereochemistry of the oxime is more commonly in an *E* configuration as ligands **28**, **29**, **32** and **33** were isolated in this form, however, ligand **33** was also isolated in the *Z* configuration as a second polymorph. The bond lengths of the central components are similar for each ligand and are listed in Figure 3.6. The structures are discussed fully in section 3.4.



Bond	<b>28</b>	<b>29</b>	<b>32</b>	<b>33<sup>a</sup> E isomer</b>	<b>33<sup>a</sup> Z isomer</b>
i	1.285(4)	1.280(5)	1.281(2)	1.294(5)	1.292(3)
ii	1.484(4)	1.478(5)	1.485(2)	1.460(6)	1.488(3)
iii	1.415(4)	1.407(5)	1.421(2)	1.409(6)	1.397(4)
iv	1.421(4)	1.431(5)	1.410(2)	1.433(6)	1.428(3)
v	1.614(2)	1.623(3)	1.6294(14)	1.632(4)	1.643(2)

Figure 3.6: Bond lengths (Å) for the central components of sulfonamido oxime ligands **28**, **29**, **32** and **33**.

## 3.4 Solid state structures of sulfonamido oxime ligands and their complexes

Sulfonamido oximes have significant numbers of hydrogen-bond donor and acceptor sites (Figure 3.7).

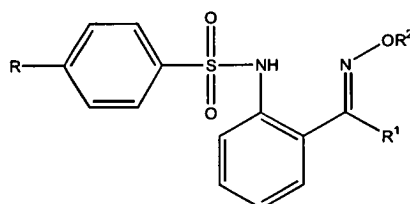


Figure 3.7: Hydrogen-bond donor (blue) and acceptor sites (red) of sulfonamido oximes.

Ligands **28**, **29**, **30**, **31** and **33** have eight hydrogen-bond acceptor sites, (three oxygen atoms, each with two lone pairs, and two nitrogen atoms) and two donor sites

(the oxime hydrogen atom and the sulfonamido hydrogen atom). Ligand **32** has the same number of acceptor sites but one less hydrogen-bond donor atom as the hydroxy hydrogen has been replaced with a methyl group. These numbers are greater than the one donor and the one acceptor site required for *pseudo*-macrocycle formation, but we assumed that these extra donors and acceptors would not interfere with ring formation.

### 3.4.1 Free ligands

#### 3.4.1.1 1-{2-[N-(4-methylbenzenesulfonamido)]phenyl}ethan-1-one oxime (**28**)

The asymmetric unit of **28** is a single molecule which is related by a centre of symmetry to a second molecule to form a hydrogen-bonded dimer *via* head-to-tail [O(8A)-H---O(1A), 2.795(4) Å; O-H-O, 159°] interactions between a sulfonamido oxygen atom and the hydrogen atom of the oxime (Figure 3.8).

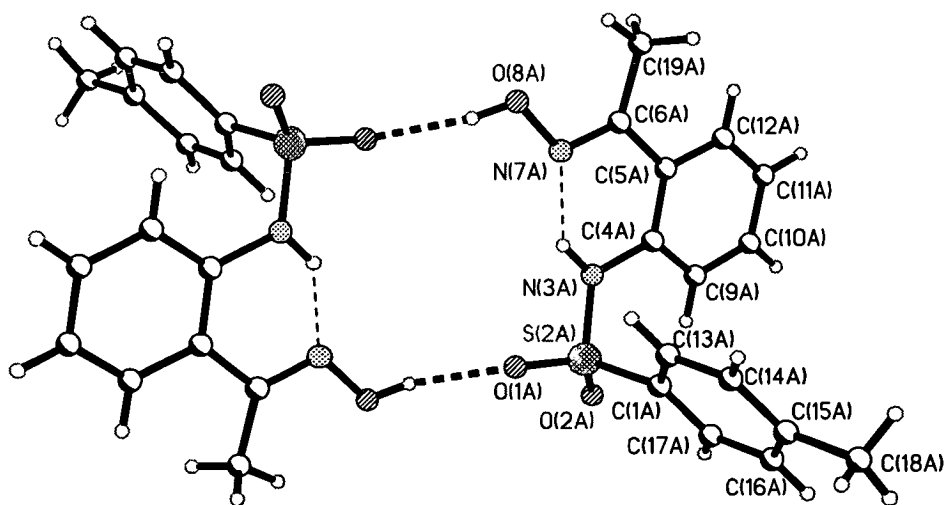


**Figure 3.8:** The dimeric hydrogen-bonded structure of 1-{2-[N-(4-methylbenzenesulfonamido)]phenyl}ethan-1-one oxime (**28**).

The hole size, as defined in chapter 2, of this *pseudo*-macrocycle is 2.94 Å. The configuration of the oxime is *E* and a single *intra*-molecular hydrogen-bond [N-(3A)-H---N(7A), 2.595(3) Å; N-H-N, 138°] between the sulfonamido hydrogen atom and the oximic nitrogen atom is observed. The six membered ring formed by this *intra*-molecular hydrogen-bond is almost planar. The greatest torsion angle is 6.4° along the N---H hydrogen-bond.

The sulfonamido nitrogen deviates slightly from planarity, bond angles for C-N-S, S-N-H and H-N-C are 126.0, 114.7 and 114.3° respectively, 355° in total, and the nitrogen atom is found 0.166 Å from the least squares plane.

The benzene ring of the sulfonamido is tilted at an angle of 99.8° to the phenyl ring. Finally, the sulfur atom of the ligand is chiral due to one oxygen being involved in hydrogen-bonding. Since the molecules in the dimer pair are related by inversion symmetry one *R* enantiomer and one *S* enantiomer form the *pseudo*-macrocycle.

#### 3.4.1.2 1-{2-[N-(4-*t*-butylbenzenesulfonamido)]phenyl}ethan-1-one oxime (29)

Molecule **29** has a very similar structure to **28**. There is one molecule in the unit cell which forms two hydrogen-bonds with a second molecule which is generated by symmetry to form a dimer (Figure 3.9). In an analogous way to **28**, hydrogen-bonds are formed between a sulfonamido oxygen atom and an oximic hydrogen atom [O(8AA)-H---O(1A), 2.73(4) Å; O-H-O, 146(5)°].

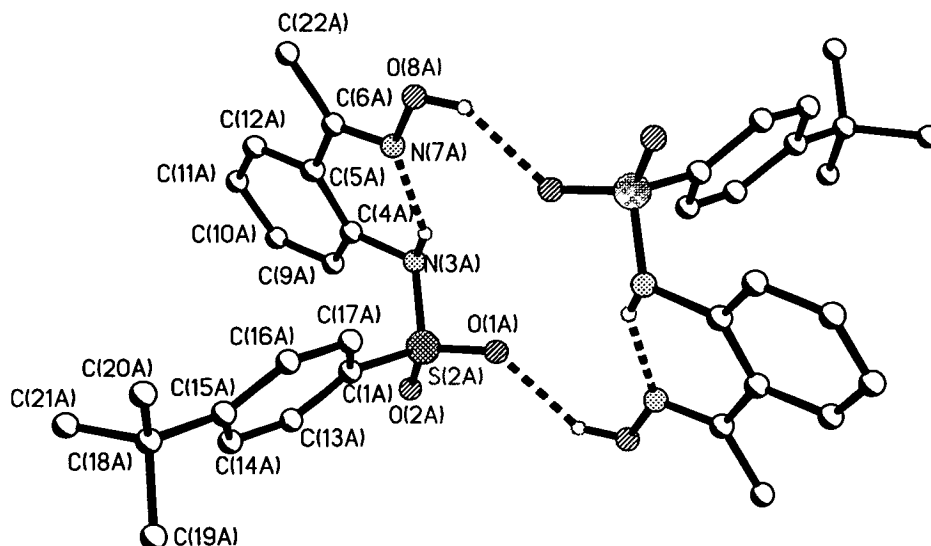


**Figure 3.9:** Hydrogen-bonded dimer of 1-[2-[N-(4-*t*-butylbenzenesulfonamido)]phenyl]ethan-1-one oxime (**29**). Hydrogen atoms not involved in hydrogen-bonding have been removed for clarity.

An *intra*-molecular hydrogen-bond is again present between the sulfonamido hydrogen atom and the oximic nitrogen atom [N(3A)-H---N(7A), 2.634(5) Å; N-H-N, 145(3)°]. The six membered ring formed by the *intra*-molecular hydrogen-bond deviates further from planarity than in **28**. The largest torsion angle is along the N-H bond at 11.3°, this may be a result of the optimisation of the *intra*-molecular hydrogen-bonding interaction.

The hole size of the hydrogen-bonded dimer is 2.91 Å, slightly smaller than in **28** *cf.* 2.94 Å. The sulfonamido nitrogen atom of **29** is less planar than in **28**. The sum of the angles around the nitrogen atom is 344.1°, and the nitrogen atom is found 0.278 Å from the SCH plane. Due to hydrogen-bonding the sulfur atom is again chiral with one *R* and one *S* isomer creating the *pseudo*-macrocycle.

### 3.4.1.3 1-{2-[N-(4-methylbenzenesulfonamido)]phenyl}ethan-1-one O-methyloxime (32)

In **32** R<sup>2</sup> is a methyl group and no longer a hydrogen atom. Removal of this hydrogen-bond donor atom prevented formation of a dimeric secondary hydrogen-bonded structure. The asymmetric unit is shown in Figure 3.10.

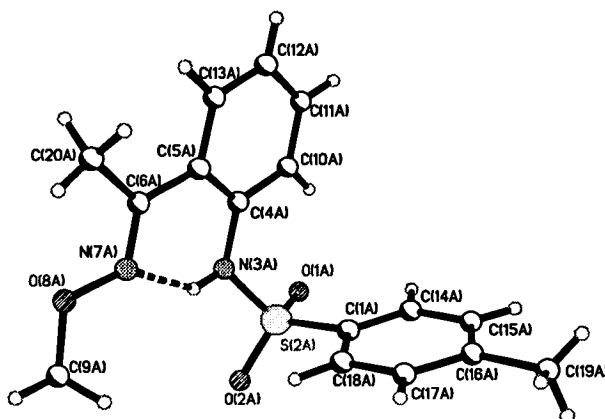


**Figure 3.10:** The X-ray structure of 1-{2-[N-(4-methylbenzenesulfonamido)]phenyl}ethan-1-one O-methyloxime (**32**).

Only *intra*-molecular hydrogen-bonding is observed between the sulfonamido hydrogen atom and the oximic nitrogen atom [N(3A)-H---N(7A), 2.620(2) Å; N-H-N, 138.1(18)°]. The geometry of the sulfonamido nitrogen is close to planar and the sum of the angles around the nitrogen, is 354.1° and the nitrogen atom is found at 0.172 Å from the SCH plane. The six membered ring formed by the *intra*-molecular hydrogen-bond is not planar as in **28** and **29**. This is probably due to the increased flexibility of **32** as it is not constrained by *inter*-molecular hydrogen-bonding. The only torsion angle close to zero is along the C(4A)-C(5A) bond at 1.7° where the two phenyl ring substituents are restricted by the aromatic bond.



### 3.4.1.4: 1-{2-[N-(4-methylbenzenesulfonamido)]-phenyl}(phenyl)methanone oxime (33)

Two crystalline forms of **33** have been isolated. One polymorph form is the *E* isomer of the oxime and has a dimeric secondary hydrogen-bonded structure closely related to those of **28** and **29** (Figure 3.11).

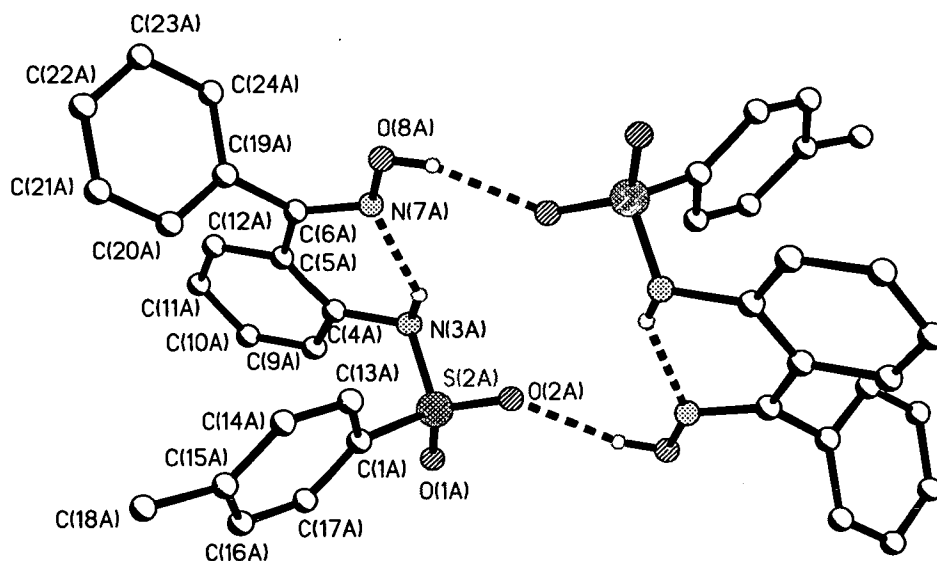


**Figure 3.11:** The dimeric secondary hydrogen-bonded structure of the *E* isomer of 1-{2-[N-(4-methylbenzenesulfonamido)]-phenyl}(phenyl)methanone oxime (**33**). Hydrogen atoms not involved in hydrogen bonding have been removed for clarity.

The asymmetric unit consists of one molecule which is symmetry related to a second molecule to form a dimer *via* hydrogen-bonds between the sulfonamido oxygen atom and the oximic hydrogen atom [O(8A)-H---O(2A), 2.754(5) Å; O-H-O, 151°]. The hole size of the dimer is 2.97 Å. As observed for the structures of **28**, **29** and **32** an *intra*-molecular hydrogen-bond between the sulfonamido hydrogen atom and the oximic nitrogen atom [N(3A)-H---N(7A), 2.673(6) Å; N-H-N, 141(5)°] forms a six membered ring. This ring is less planar than in **28** and **29** and the largest torsion angle is along the C(5A)-C(6A) bond at 19.7°.

The *Z* isomer of the oxime forms a second polymorph and a different hydrogen-bonded structure is observed. One molecule constitutes the asymmetric unit and instead of head-to-tail hydrogen-bonding, head-to-head and tail-to-tail hydrogen-bonding is observed. Each ligand forms six *inter*-molecular hydrogen-bonds to two adjacent ligands leading to an infinite one-dimensional zigzag chain along the *a* axis, illustrated schematically in Figure 3.12. Two *inter*-molecular hydrogen-bonds between the sulfonamido hydrogen atom H(3A) and the sulfonamido oxygen atom O(1A) are observed [N(3A)-H---O(1A), 3.104(3) Å; N-H-O, 156(2)°] and four interactions occur between the oxime moieties of the type [O(8A)-H---O(8AA), 3.231(3) Å; O-H-O, 133(3)° and O(8A)-H---N(7AA), 2.823(3) Å; O-H-N, 165(4)°].

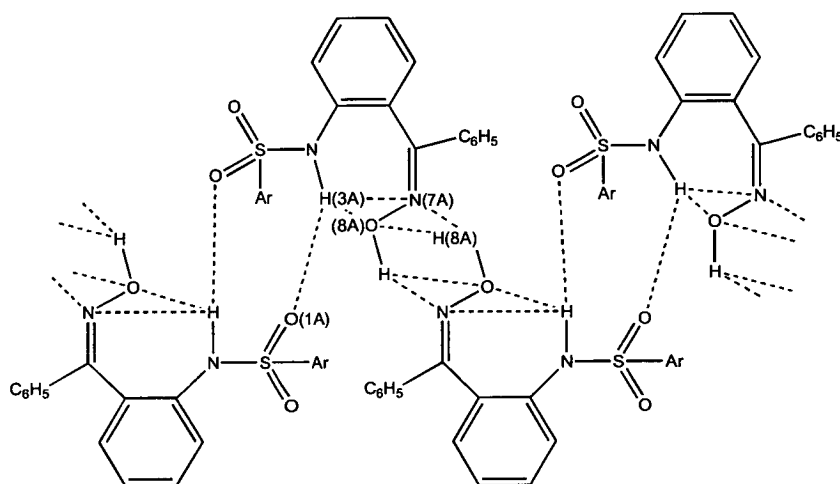


**Figure 3.12:** The hydrogen-bonded oligomeric structure of the *Z* isomer of **33**.

Two *intra*-molecular hydrogen-bonds are present between the sulfonamido hydrogen atom and the oximic nitrogen atom [N(3A)-H---N(7A), 3.22 Å; N-H-N, 127°] and a second interaction between the trifurcated sulfonamido hydrogen atom H(3A) and the hydroxy oxygen atom O(8A) [N(3A)-H---O(8A), 2.915(4) Å; N-H-O, 122(2)°] is possible because of the *cis*-stereochemistry of the oxime. The X-ray structure of the asymmetric unit of the *Z* isomer of **33** is shown in Figure 3.13.

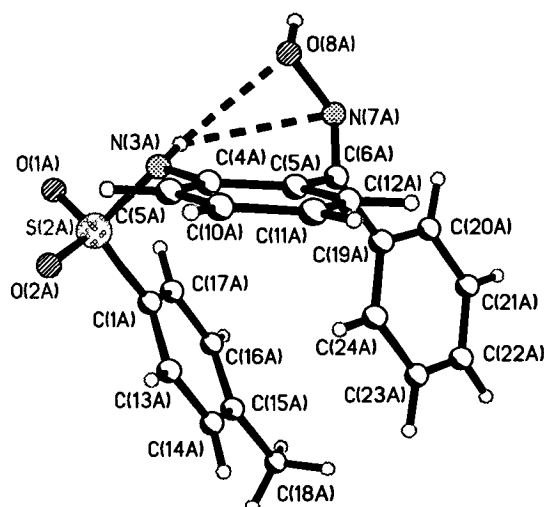


**Figure 3.13:** The X-ray structure of the *Z* isomer of 33.

The sulfonamido nitrogen atom deviates from planarity and the nitrogen atom is 0.229 Å from the least squares plane. Bond angles for C(4A)-N(3A)-S(2A), S(2A)-N(3A)-H and H-N(3A)-C(4A) are 117.0, 110.4 and 117.0° respectively, 344.4° in total.

One sulfonamido oxygen atom is involved in hydrogen-bonding and so the sulfur atom is chiral. Two symmetry related ligands are found in the unit cell, one is the *R* enantiomer and one the *S* enantiomer.

The sulfonamido tolyl ring and the benzene ring  $\alpha$  to the oximic carbon are not completely orthogonal to the central phenyl ring [122.3 and 109.1°], there is a dihedral angle between them of 28.7°. Weak  $\pi$  stacking interactions occur between the tolyl ring of the sulfonamido and the benzene ring  $\alpha$  to the oxime (Figure 3.14). The distance between centroid of the two rings is 4.15 Å in each case.

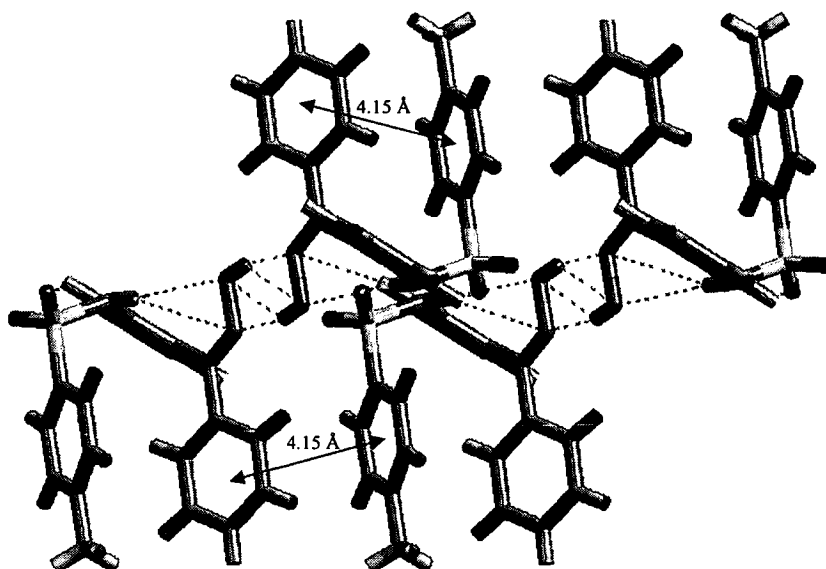


Figure 3.14:  $\pi$  stacking interactions in the oligomeric *Z* isomer of 33.

### 3.4.2 Oxime stereochemistry

The two stereoisomers of sulfonamido oxime ligands are shown in Figure 3.15.

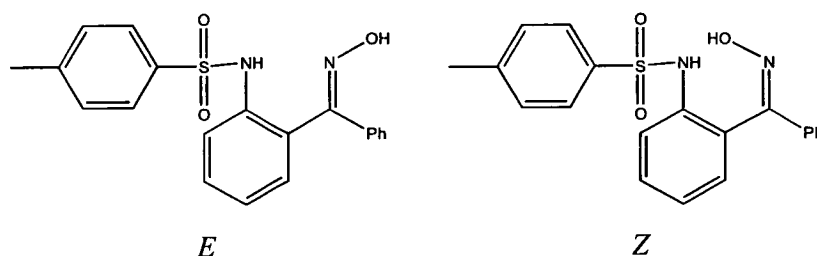


Figure 3.15: *E* and *Z* isomers of sulfonamido oxime ligands.

There has been considerable study of the conformational isomers of oximes. It is thought that steric effects make the *E* isomer predominate and aromatic *Z* aldehyde oximes have been shown to rearrange to the *trans E* isomer by hydrogen ion catalysis.<sup>3</sup> Oximes in the *Z* conformation have even been found to convert spontaneously albeit very slowly in the solid state.<sup>4</sup>

Results so far substantiate claims that the *E* isomer appears to predominate<sup>4</sup> as only one example of a sulfonamido oxime ligand (**33**) in the *cis*-conformation has been isolated when the group  $\alpha$  to the oxime is a bulky phenyl group.

A factor which might explain why it is possible to crystallise the less stable isomer comes from consideration of the lattice energies of the two structures. The higher density of hydrogen-bonds present in the structure of the polymer may mean that its lattice energy is higher than that of the dimeric structure. Therefore the free energy loss in adopting the less favourable stereoisomer has been offset by the increase in the lattice energy.

Each of the X-ray structures of metal complexes of sulfonamido oximes, which will be described in Sections 3.4.4 and 3.4.5, show that the oxime always exhibits *E* isomerism. This may be understood from the position of the hydroxy group in the two isomers. In the *E* isomer there is no obstruction to metal complexation, however in the *Z* isomer the hydroxy group precludes complexation. This has been observed in other ligand systems which include an oxime function,<sup>5</sup> *e.g.* only the *E* isomers of hydroxyoxime LIX reagents for metal extraction were found to be reactive towards copper.

### 3.4.3 Hydrogen-bonding in sulfonamido oxime ligands

Both the sulfonamido group and the oxime group have hydrogen-bond donor and acceptor functions. In molecules which contain either oxime or carboxyl functions such dual character often results in dimeric structures and functional groups from neighbouring molecules are linked with pairs of centrosymmetric hydrogen-bonds.<sup>6</sup> This arrangement is also possible for molecules containing a sulfonamido group (Figure 3.16).

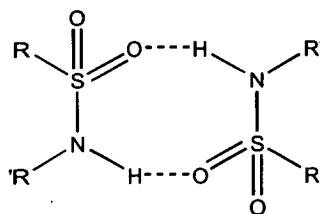


Figure 3.16: Centrosymmetric hydrogen-bonding of the sulfonamido group.

There are 110 entries in the CSD (August 2001) for centrosymmetric hydrogen-bonding in oximes (30% of all oxime entries) and 85 of sulfonamide molecules (17% of all sulfonamide entries). In molecules which incorporate both carboxylic and oxime groups,<sup>6,7</sup> head-to-tail interactions leading to a one dimensional chain structure are more commonly observed than the head-to-head, homologous binding, interactions which would lead to dimer formation. In fact only when bulky groups are incorporated into the ligands  $\alpha$  to the oxime or carboxyl functions is a dimer including head-to-head interactions observed. In comparison, the preferred head-to-tail interactions lead to a dimeric structure in sulfonamido oxime molecules involving only one and not two hydrogen-bonds. Homologous centrosymmetric binding of sulfonamido oximes as observed for **33**(*Z*) leads to a one dimensional chain structure.

The hydrogen-bonding interactions of sulfonamido oxime ligands are listed in Tables 3.2 and 3.3.

Table 3.2: The *intra*-molecular hydrogen-bond lengths ( $\text{\AA}$ ) and angles ( $^\circ$ ) of ligands **28**, **29**, **32** and **33**.

Ligand	Interaction type	Hydrogen-bond length / $\text{\AA}$	Hydrogen-bond angle / $^\circ$
<b>28</b>	N( <i>Ox</i> )---H-N( <i>S</i> )	2.595(3)	138
<b>29</b>	N( <i>Ox</i> )---H-N( <i>S</i> )	2.634(5)	145(3)
<b>32</b>	N( <i>Ox</i> )---H-N( <i>S</i> )	2.620(2)	138.1(18)
<b>33</b> <sup>a</sup> <i>E</i> isomer	N( <i>Ox</i> )---H-N( <i>S</i> )	2.673(6)	141(5)
<b>33</b> <sup>a</sup> <i>Z</i> isomer	N( <i>Ox</i> )---H-N( <i>S</i> )	3.22	127
	N( <i>Ox</i> )---H-N( <i>S</i> )	2.915(4)	122(2)

<sup>a</sup> Molecule **33** has been isolated as two polymorphs, the stereochemistry of the oxime is either *E* or *Z*. Atoms labelled *Ox* are contained in an oxime group. Atoms labelled *S* are contained in a sulfonamido group.

**Table 3.3:** The *inter*-molecular hydrogen-bond lengths (Å) and angles (°) of ligands **28**, **29**, and **33**.

Ligand	Interaction type	Number of interactions	Hydrogen-bond length / Å	Hydrogen-bond angle / °
<b>28</b> <sup>a</sup>	O(Ox)-H---O(S)	2	2.795(4)	159
<b>29</b> <sup>a</sup>	O(Ox)-H---O(S)	2	2.743(4)	146(5)
<b>33</b> <sup>ab</sup> <i>E</i> isomer	O(Ox)-H---O(S)	2	2.754(5)	151
<b>33</b> <sup>b</sup> <i>Z</i> isomer	O(S)---H-N(S)	2	3.104(3)	156(2)
	N(Ox)---H-O(Ox)	2	2.823(3)	165(4)
	O(Ox)-H---O(Ox)	2	3.231(3)	133(3)

<sup>a</sup> *Inter*-molecular hydrogen-bonding in these molecules forms a *pseudo*-macroyclic ligand structure. <sup>b</sup> Molecule **33** has been isolated as two polymorphs, the stereochemistry of the oxime is either *E* or *Z*.

The *intra*-molecular hydrogen-bonds of sulfonamido oxime ligands have similar lengths and angles. The small angles (122.4-146.0°) are probably due to the rigidity of the ligand backbone. The *inter*-molecular hydrogen-bonds of **28**, **29** and the *E* isomer of **33** are also very similar and are longer (mean 2.76 Å) in comparison with the *intra*-molecular hydrogen-bonds (mean 2.63 Å). The *inter*-molecular hydrogen-bonds of the *Z* isomer of **33** are even longer (mean 3.05 Å).

#### 3.4.4 Sulfonamido oxime [ML<sub>2</sub>] complexes

It is thought that the increased strength and selectivity of P50 over other similar phenolic oximes is due to the two *intra*-complex hydrogen-bonds which create a *pseudo*-macrocycle around the metal centre. It was hoped that the coordination chemistry of sulfonamido oxime ligands with divalent metal ions would be similar to phenolic oxime, P50 type, ligands and that a hydrogen-bonded *pseudo*-macroyclic ligand would be formed on complexation *via* the oxime hydrogen-bond donor atom and the sulfonamido oxygen acceptor sites. The proposed size of the *pseudo*-chelate ring formed by *intra*-complex hydrogen-bonding for sulfonamido oxime systems is seven membered in comparison with the five membered *pseudo*-chelate ring of phenolic oximes (Figure 3.17).

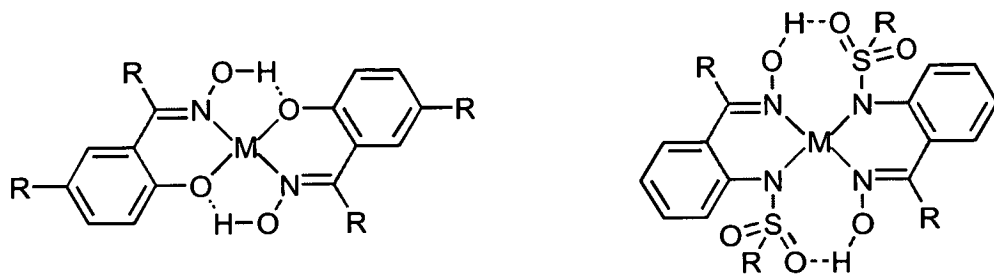


**Figure 3.17:** *Pseudo-macrocyclic ligand formation on complexation with divalent metal ions for phenolic oxime complexes and sulfonamido oxime complexes.*

#### 3.4.4.1 Bis[1-{2-[N-(4-methylbenzenesulfonamido)]phenyl}ethan-1-one oxime]copper(II) (34)

When two equivalents of **28** was reacted with one equivalent of copper acetate in methanol a brown complex (**34**) was obtained. The X-ray structure of **34** is shown in Figure 3.18.

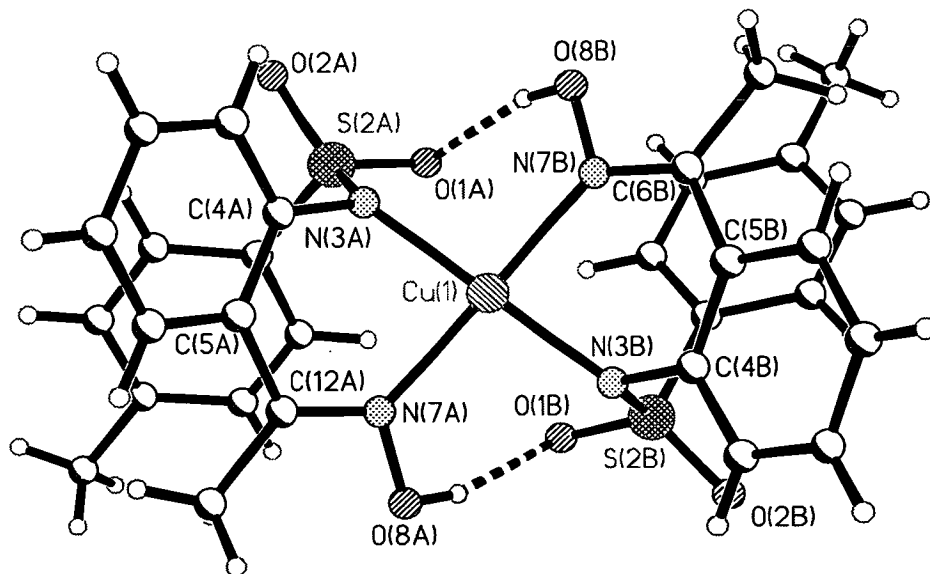


**Figure 3.18:** The X-ray structure of bis[1-{2-[N-(4-methylbenzenesulfonamido)]phenyl}ethan-1-one oxime]copper(II) (**34**).



The copper(II) atom has slightly distorted planar coordination geometry, the dihedral angle between the plane defined by the N(3A)-Cu-N(7A) chelate and the N(3B)-Cu-N(7B) chelate is  $5.9^\circ$  and the sum of the chelate angles is  $360.1^\circ$ . The copper to sulfonamido nitrogen bond lengths are at 1.947(3) and 1.952(3) Å and the copper to oximic nitrogen lengths are at 2.035(3) and 2.043(3) Å. The N(3)-Cu-N(7) bond angles are 85.46(11) and 88.95(11) $^\circ$ . The hole size of **34** is 1.99 Å, a smaller value than that observed for the free ligand *cf.* 2.94 Å.

The ligand arrangement around the copper(II) atom is similar to the solid state hydrogen-bonded structure of the free ligand (Figure 3.8) and *intra-complex* hydrogen-bonding between the sulfonamidato oxygen atom to the oximic hydrogen atom [O(8)-H---O(1), 2.725(4) and 2.706(4) Å; O-H-O, both at  $164^\circ$ ] creates a *pseudo-macrocycle* around the copper. The hydrogen-bond length is slightly longer than in the free ligand however the bonds are more linear *cf.* [O(8)-H---O(2), 2.80 Å; O-H-O,  $159^\circ$ ].

The sums of the angles around the sulfonamido nitrogen are 353.5 and 351.6 $^\circ$ . In each case the nitrogen atom is less planar than for the free ligand *cf.* (355.0 $^\circ$ ). This may be due to the constraints required for nitrogen coordination to the copper atom. The chirality of both ligands at the sulfur is *R* and the configuration of the oxime is *E* in both cases.

#### 3.4.4.2 Bis[1-{2-[N-(4-methylbenzenesulfonamidato)]phenyl}ethan-1-one oxime] nickel(II) (**36**)

When two equivalents of **28** and one equivalent of nickel acetate were combined in methanol and two equivalents of potassium hydroxide were added an orange complex was obtained with a nickel:ligand ratio of 1:2 (Figure 3.19).

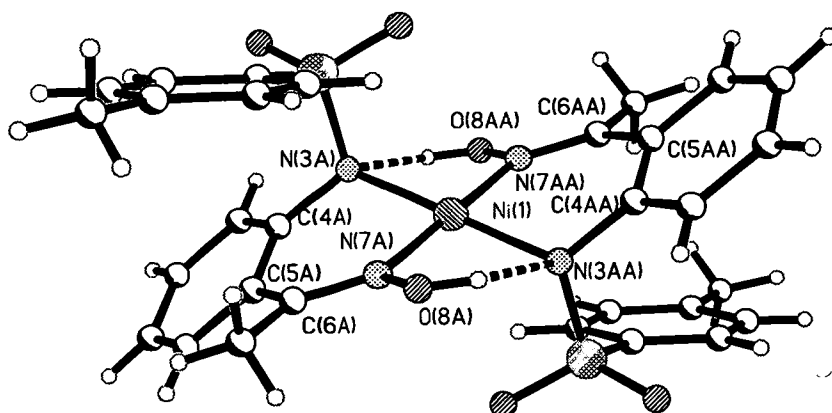


**Figure 3.19:** The X-ray structure of bis[1-{2-[N-(4-methylbenzenesulfonamido)]phenyl}ethan-1-one oxime] nickel(II) (**36**).

The asymmetric unit consists of half of the complex and the whole complex is generated through an inversion centre. The nickel(II) ion has square planar geometry. The N(3)-Ni(1)-N(7) angle is  $89.78(11)^\circ$  and the bond lengths are at Ni(1)-N(7A)  $1.881(3)$  Å and Ni(1)-N(3A)  $1.903(3)$  Å. The sulfonamido nitrogen is less planar than in the free ligand and the sum of the angles about the nitrogen atom in **36** is  $348.8^\circ$ .

The hydrogen-bonding in the nickel complex differs from that in copper complex **34** and *intra-complex* hydrogen-bonds between the hydroxy hydrogen atom and the sulfonamidato nitrogen atom [O(8A)-H---N(3A),  $2.704(4)$  Å; O-H-N,  $131^\circ$ ]. This may be a result of the preference of nickel(II) for perfect planar geometry, or the difference in the central radii of the planar Ni(II) and Cu(II) ions. The 14-membered *pseudo*-macrocyclic structure in the nickel complex **36** closely resembles that in the Cu-complexes of the phenolic oxime reagents used in copper recovery. The sulfonamidato group has been pushed away from the  $N_4^{2-}$  plane and the closest sulfonamidato oxygen atom is  $3.11$  Å from the hydroxy hydrogen atom. In order for a sulfonamidato oxygen atom to interact with the hydroxy hydrogen atom a deviation of the metal geometry away from planarity such as in the copper complex which has a dihedral angle of  $5.9^\circ$  between the chelate planes may be required.

### 3.4.5 Sulfonamido oxime cluster complexes

At the beginning of this project it was hoped that the coordination chemistry of sulfonamido oxime ligands would be similar to P50 type phenolic oxime molecules. The complexation studies in section 3.4.4 have shown that these ligands can complex divalent metal ions to form  $ML_2$  complexes. However, the complexation behaviour of **28** with copper(II) and nickel(II) varies with reaction conditions as the deprotonated oximic oxygen atom and the sulfonamido oxygen atoms are also able to coordinate to metal centres forming polynuclear species. The atoms available for metal coordination in sulfonamido oxime ligands are marked in red in Figure 3.20.

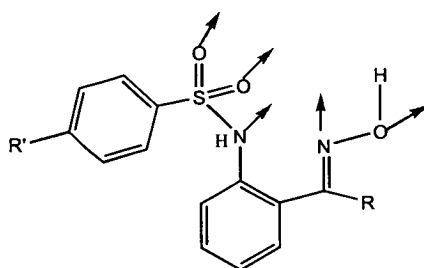


**Figure 3.20:** The donor atoms of sulfonamido oxime ligands.

#### 3.4.5.1 $[Cu_4(28-H)_2(28-2H)_2(CH_3OH)_2(CH_3O)_2]$ (**35**)

When **28** and copper acetate were combined in a 1:1 ratio in methanol a green crystalline solid was isolated with the formula  $[Cu_4(28-H)_2(28-2H)_2(CH_3OH)_2(CH_3O)_2]$  (**35**). The asymmetric unit consists of half of the tetranuclear species. There are two chemically different copper coordination spheres in **35**, type one (Cu(1)) and type two (Cu(2)). Each copper has a five-coordinate geometry and forms a distorted square based prismatic structure. Two ligands are singly deprotonated at the sulfonamido nitrogen atom and act as bidentate ligands (type B ligands) and two ligands are doubly deprotonated, at the sulfonamido nitrogen atom and the hydroxy oxygen atom and act as tetradentate ligands (type A ligands). Two methanol molecules complete the coordination sphere of the Cu(1) atom and two methoxide groups balance the charge to give a neutral species.

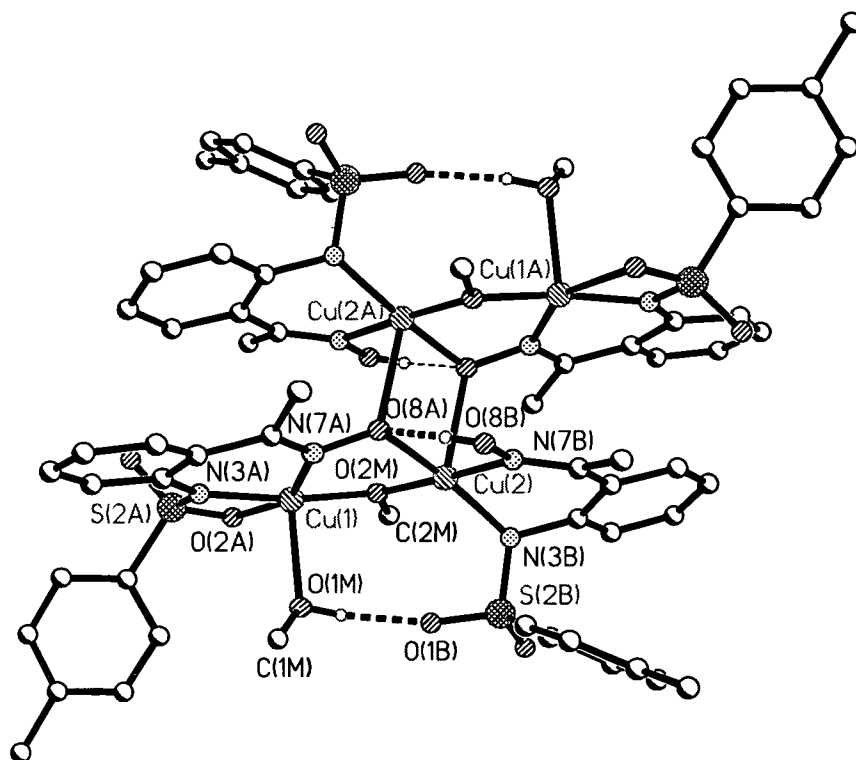


**Figure 3.21:** X-ray structure of the copper cluster  $[\text{Cu}_4(\mathbf{28-H})_2(\mathbf{28-2H})_2(\text{CH}_3\text{OH})_2(\text{CH}_3\text{O})_2]$  (**35**).

Type one copper(II) atoms are coordinated by two nitrogen atoms and a sulfonamido oxygen atom of a type A ligand [Cu(1)-N(3A) at 1.904(2) Å, Cu(1)-N(7A) at 1.958(2) Å and Cu(1)-O(2A) at 2.2766(19) Å], a methanol molecule [Cu(1)-O(1M) at 2.244(2) Å] and a bridging methoxide oxygen atom [Cu(1)-O(8A) at 1.8760(18) Å] completes the coordination sphere.

Type two copper(II) atoms are coordinated by the two nitrogen atoms of a type B ligand [Cu(2)-N(3B) at 1.952(2) and Cu(2)-N(7B) at 2.010(2) Å] and two deprotonated oximic oxygens of the type A ligands [Cu(2)-O(8A) 2.54 and 1.9759(19) Å]. The coordination sphere is completed by the oxygen atom of a bridging methoxide group [Cu(2)-O(2M) at 1.9199(18) Å] to a Cu(1) atom.

The deprotonated oximic oxygen atoms of type A ligands act as hydrogen-bond acceptor sites to the adjacent oximic hydrogens of type B ligands [O(8B)-H---O(8A), 2.61 Å; O-H-O, 155°]. Two further hydrogen-bonds between a sulfonamido oxygen atom of a type B ligand and a methanolic hydrogen atom are observed [O(1B)---H-O(1M), 2.63(3) Å; O-H-O, 163(4)°].

Weak  $\pi$  stacking interactions between the phenyl rings of the ligands occur (Figure 3.22). The distance between the centroid of the two phenyl rings is 3.957 Å and the angle between the planes of the two aromatic rings is 13.3°.

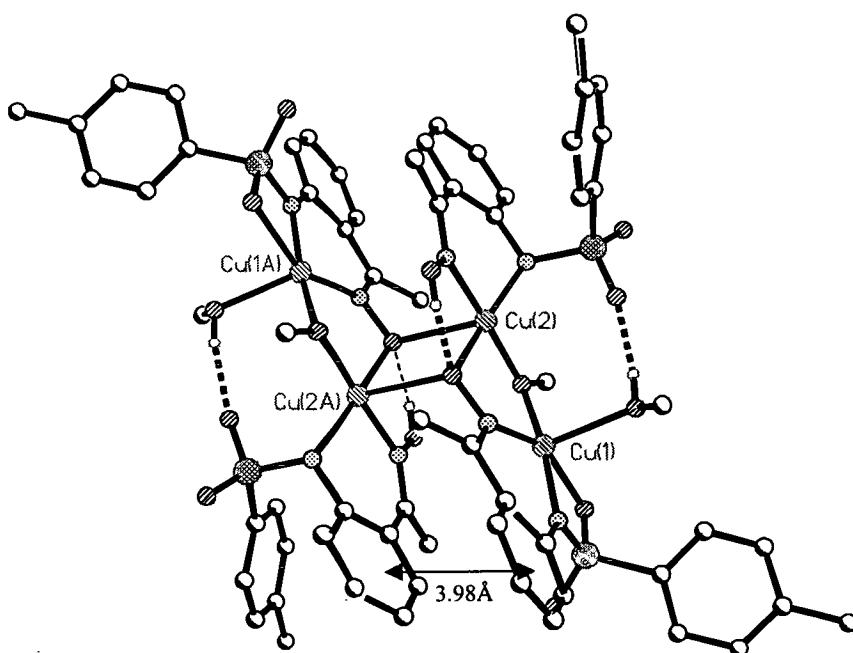


**Figure 3.22:**  $\pi$  stacking in **35**. The distance between the two phenyl rings is 3.98 Å.

The one to one, ligand to metal ratio in **35** is important from a metal extraction perspective. If this tetranuclear species were formed instead of a  $ML_2$  complex on extraction of copper from an aqueous phase into an organic phase and the metal could also be stripped back out of the complex this would mean that the efficiency of **28** as an extractant would increase two fold. This is unlikely as analogues of the

methanol and groups incorporated into the cluster to complete the copper coordination spheres and balance the overall charge would not be present in the hydrocarbon solvents used for metal extraction.

The binding of the sulfonamido oxygen atoms to copper and the formation of a four membered ring by the coordination of the sulfonamido nitrogen N(3A) and oxygen O(2A) to the same copper centre are unusual. The angles of this ring are at 67.2 to 102.4°.

#### 3.4.5.2 $[\text{Ni}_2\text{Na}_2(\text{28-H})_2(\text{28-2H})_2(\text{CH}_3\text{OH})_4]$ (**38**)

A red heterometallic cluster complex (**38**) was formed when two equivalents of sodium hydroxide were added to two equivalents of **28** and one equivalent of nickel acetate. The X-ray structure of this cluster is shown in Figure 3.23.

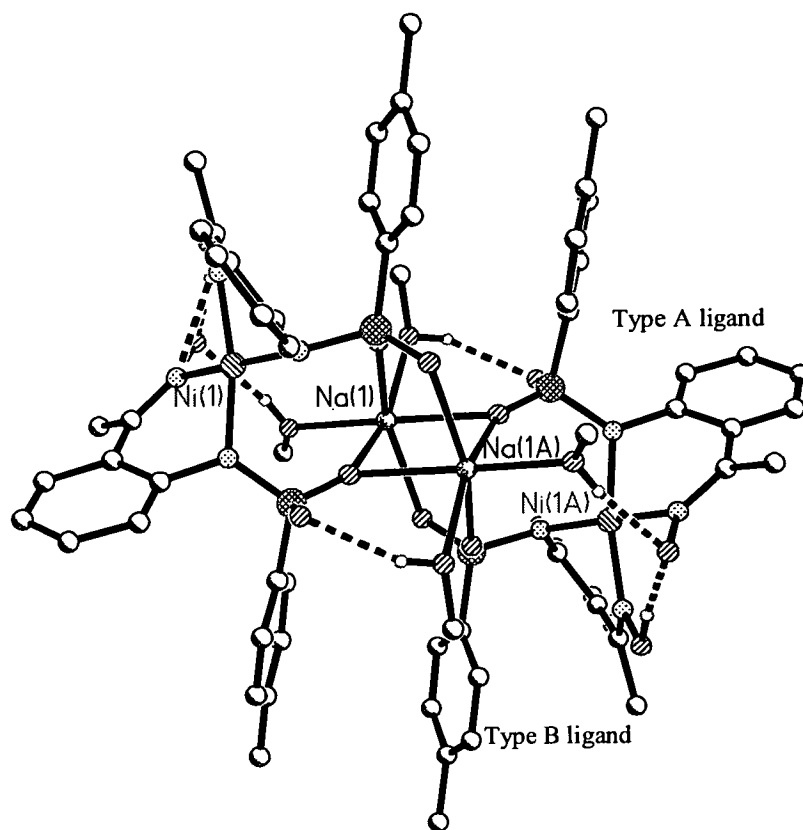


**Figure 3.23:** The X-ray structure of the nickel and sodium cluster (**38**).

The two halves of this cluster are related by an inversion centre lying between the sodium atoms. The entire complex is achieved *via* inversion of this fragment. The cluster consists of two tetracoordinate nickel(II) ions, two hexacoordinate sodium ions, two singly deprotonated (type B) molecules of **28**, two doubly deprotonated (type A) molecules of **28** and four methanol molecules. Each is a  $[\text{NiNa}(\text{C}_{15}\text{H}_{15}\text{N}_2\text{SO}_3)(\text{C}_{15}\text{H}_{14}\text{N}_2\text{SO}_3)(\text{CH}_3\text{OH})_2]$  moiety linked to the other half *via* hydrogen-bonding to methanol molecules and interactions to the two sodium ions. This can be seen schematically below in Figure 3.24.

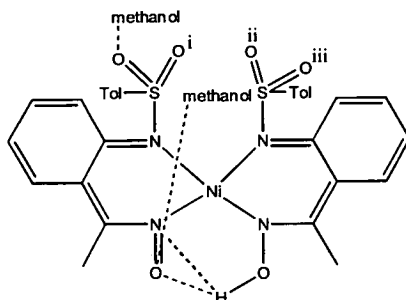


**Figure 3.24:** A schematic diagram of half of the nickel cluster. <sup>i</sup> Oxygen is bonded to sodium ions (1) and (1A). <sup>ii</sup> Oxygen is bonded to sodium (1). <sup>iii</sup> Oxygen is bonded to sodium (1A).

The nickel(II) atom is coordinated by two molecules of **28** in a distorted planar fashion with the N(3B)-Ni-N(7B) and N(3A)-Ni-N(7A) chelate angles at 86.7(2) and 86.4(2)° respectively. The nickel to sulfonamido nitrogen bond lengths are 1.883(5) and 1.900(5) Å and the nickel to oximic nitrogen bond lengths are 1.876(5) and 1.910(5) Å. The sum of the angles around the nickel is 361.4° and the dihedral angle between the chelate planes is 15.4°.

The oximic hydrogen atom of type B ligands forms two hydrogen-bonding interactions to the deprotonated oxime of a type A ligand *via* bifurcated [O(8B)-H---O(8A), 2.495(8) Å; O-H-O, 153°] and [O(8B)-H---N(7A), 2.88 Å; O-H-N, 117°] interactions. The oxygen atom of the deprotonated oxime group O(8A) and the uncoordinated sulfonamido oxygen O(1A) form strong *inter*-molecular interactions with two methanol molecules coordinated to the two sodium ions, [O(1M)-H---O(8A), 2.780(7) Å; O-H-O, 168°; O(2M)-H---O(1A), 2.887(7) Å; O-H-O, 149°].

The coordination sphere of the sodium atom consists of two methanolic oxygen atoms, [Na(1)-O(1M) at 2.312(5) Å and Na(1)-O(2M) at 2.403(6) Å], and four sulfonamido oxygen atoms, [Na(1)-O at 2.341(5), 2.419(4), 2.485(5) and 2.485(5) Å] complete the sphere to form an octahedral six coordinate geometry. The geometry of the sodium ions and the hydrogen-bonding described above can be seen in Figure 3.25.



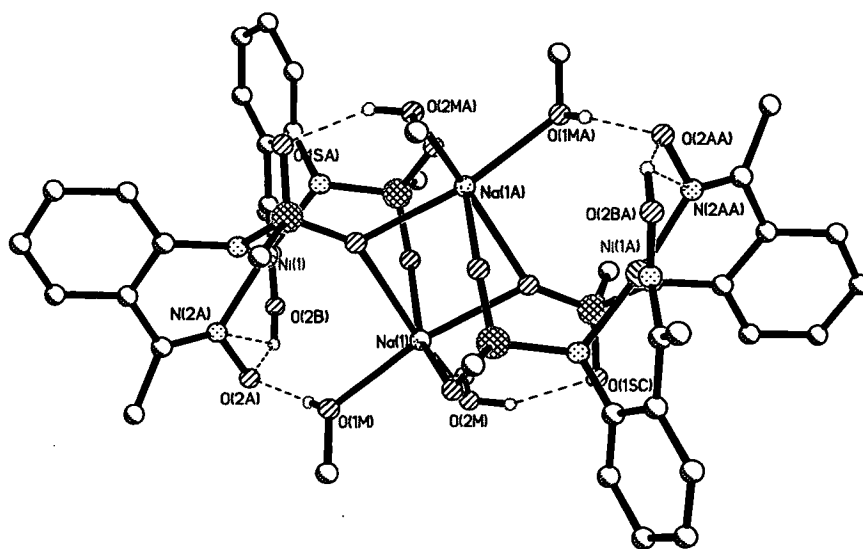


**Figure 3.25:** X-ray structure of the nickel cluster (38) showing the coordination sphere of the sodium ion and all hydrogen-bonding interactions. The sulfonamido aromatic rings and hydrogen atoms not involved in hydrogen bonding have been removed for clarity.

#### 3.4.5.3 $[\text{Ni}_4(\mathbf{28}\text{-H})_2(\mathbf{28}\text{-2H})_2(\text{OH})_2(\text{MeOH})_5]$ (39)

Complex 39 consists of four nickel(II) ions (Ni(1-4)), four molecules of **28**, two of which are singly deprotonated (ligands B and D) and two which are doubly deprotonated (ligand A and C), two hydroxy groups and five methanol groups. The X-ray structure can be seen in Figure 3.26.

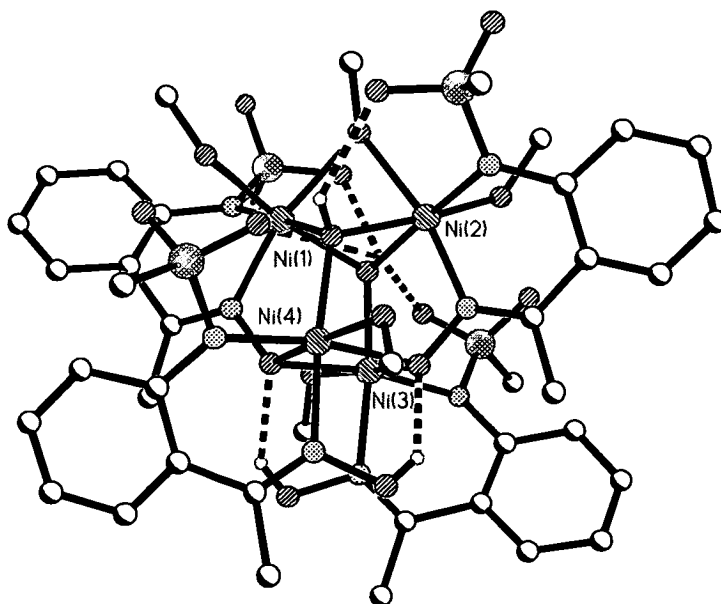


**Figure 3.26:** The X-ray structure of **39**. The aromatic sulfonamido group and hydrogen atoms not involved in hydrogen bonding have been removed for clarity.

The core of the nickel cluster consists of four six coordinate nickel(II) ions linked in a fused butterfly shape by two hydroxy oxygen atoms, O(124) and O(123), and the deprotonated oximic functions of ligands A and C (N(7C), O(8C) and N(7A), O(8A)). Ni(1) and Ni(2) are capped by a methanolic oxygen atom O(12) (Figure 3.27).

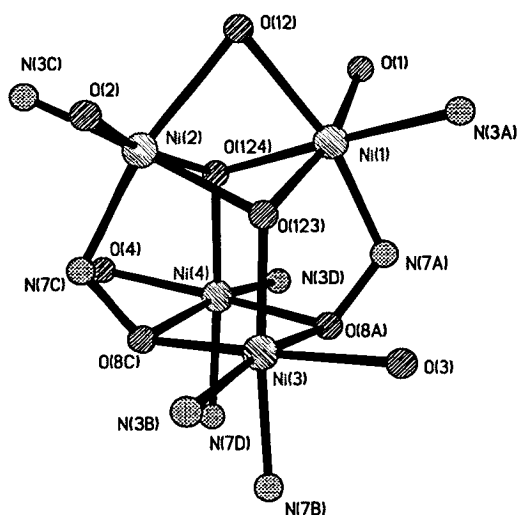


**Figure 3.27:** The coordination spheres of the four nickel(II) ions in the core of complex **39**.

The asymmetric unit of **39** consists of one whole cluster molecule and there are six hydrogen-bonds in the cluster. The coordination spheres of Ni(1)-Ni(4) are illustrated schematically below in Figures 3.28 and 3.29.

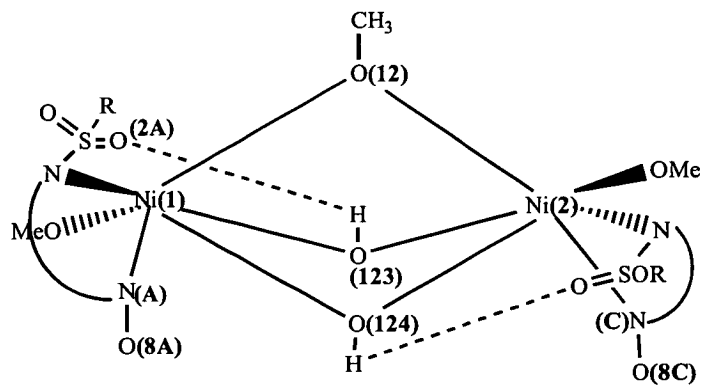


**Figure 3.28:** A schematic diagram of the coordination spheres of Ni(1) and Ni(2). Ni(1) is coordinated by the two nitrogen atoms of ligand A and the oxygen atom of a methanol group [Ni(1)-N(3A) at 2.073(18) Å; Ni(1)-N(7A) at 1.978(17) Å and Ni(1)-O(1) at 2.094(16) Å]. It is bridged to Ni(2) by one methanol group and two hydroxide groups [Ni(1)-O(12) at 2.248(18) Å; Ni(1)-O(123) at 2.060(15) Å and Ni(1)-O(124) at 2.037(16) Å]. Ni(2) has a similar coordination sphere, but with slightly different bond lengths.

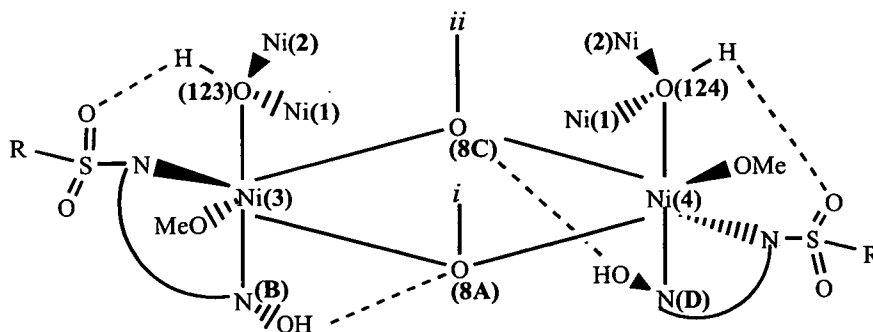


**Figure 3.29:** A schematic diagram of the coordination spheres of Ni(3) and Ni(4). <sup>i</sup> Bond is part of the deprotonated oxime group of ligand A. <sup>ii</sup> Bond is part of the deprotonated oxime group of ligand C. Ni(3) is coordinated to two nitrogen atoms of ligand B and the oxygen atom of a methanol group [Ni(3)-N(3B) at 2.155(18) Å; Ni(3)-N(7B) at 2.04(2) Å and Ni(3)-O(3) at 2.117(18) Å]. Ni(3) is linked to Ni(4) by the deprotonated hydroxide oxygen atoms of ligands A and C which act as bridging atoms [Ni(3)-O(8A) at 2.117(15) Å and Ni(3)-O(8C) at 2.117(14) Å].

### 3.4.6 Coordination sites of sulfonamido oxime ligands

The oxime function is more common than the sulfonamido group in transition metal complexes, it has only one atom (N) available for coordination to a metal centre in contrast with the sulfonamido group which has a possible three donor sites (N and 2 x O). There are 1066 entries in the Cambridge Structural Database (CSD), (July 2001), of an oximic nitrogen coordinating to a transition metal centre in contrast with 268 entries of transition metal complexes exhibiting coordination of the sulfonamido group through the nitrogen atom and 87 entries of coordination through an oxygen atom.

These 87 complexes in the CSD include 21 metal centres. The most common types of complex are tin (15 entries), sodium (14 entries) and silver and titanium (11 entries each). There are only 11 examples where the sulfonamido group binds through the sulfonamido nitrogen atom and an oxygen atom to the same metal centre in an analogous manner to the coordination of **28** in complex **35** (Figure 3.30), ten titanium complexes and one vanadium complex. Therefore, to date, the coordination

mode observed in complex **35** is novel in sulfonamido-copper coordination chemistry.

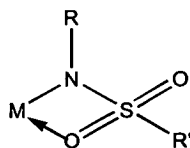


**Figure 3.30:** Coordination of the sulfonamido group by a chelating mode *via* the nitrogen and one oxygen atom.

Sulfonyl moieties are known to serve as electron donors capable of forming adducts with metal cations in either an *intra*- or *inter*-molecular fashion.<sup>8</sup> In sulfonamido-titanium chemistry it has been suggested that coordination of the sulfonamido oxygen atoms to Ti(IV) is due to the poor donor character of the amide substituted with the strongly electron withdrawing  $-\text{SO}_2\text{Ar}$  group.<sup>9</sup> The inductive effect of this group decreases the degree of  $\pi$  donation from the filled nitrogen  $p_z$  orbital to an empty titanium  $d_\pi$  orbital. It has also been reported that the hapticity of *bis*-sulfonamido ligands is highly dependent on crystal packing forces in titanium chemistry.<sup>10</sup> Depending on whether N-2-(4-methylbenzenesulfonylamino cyclohexyl)-4-methylbenzene -sulfonamido) (Figure 3.31) is resolved or a racemic mixture prior to complexation to Ti(IV) the coordination of either one or two sulfonamido oxygens to the titanium centre.<sup>10</sup>

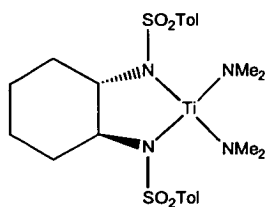


**Figure 3.31:** Bis[1, 2-Di(4-methylbenzenesulfonamidato)cyclohexane]] bis [dimethylaminato] titanium(IV). Tol =  $\text{C}_6\text{H}_4\text{CH}_3$ .

In rare earth metal disulfonamido complexes the interaction of the sulfonamido oxygen with the metal centre is stronger than in titanium complexes, and delocalisation of charge is observed.<sup>8</sup> This may be explained by the model in Figure 3.32. Delocalisation of charge may be occurring in complex **35** as the  $\text{S}=\text{O}$  bond lengths in type A ligands (where one sulfonamido oxygen atom is coordinated to the

copper centre) are 1.436(2) and 1.4664(19) Å in comparison with 1.446(2) and 1.440(2) Å in type B ligands (which do not coordinate to the metal centre through a sulfonamido oxygen atom). However the differences in bond lengths here are not large enough to be called significant. The S-N length is also shorter (1.593(2) Å) in type A ligands in comparison with 1.600(2) Å in type B ligands.

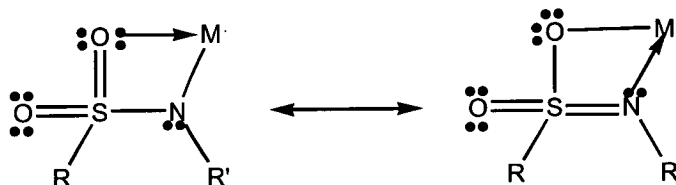


Figure 3.32: Charge delocalisation model of the  $\eta^2$ -coordinating sulfonamido group.<sup>8</sup>

### 3.4.7 Hydrogen-bonding in sulfonamido oxime complexes

The hydrogen-bond lengths (Å) and angles (°) of sulfonamido oxime  $ML_2$  complexes and cluster complexes are listed in Tables 3.4 and 3.5 respectively.

Table 3.4: The bond lengths (Å) and angles (°) of *intra*-complex hydrogen-bonds in  $ML_2$  complexes 34 and 36.

Complex	Interaction type	Hydrogen-bond length / Å	Hydrogen-bond angle / °
Cu(28-H) <sub>2</sub> (34)	O(S)---H-O(Ox)	2.725(4)	164
	O(Ox)-H---O(S)	2.706(4)	164
Ni(28-H) <sub>2</sub> (36) <sup>a</sup>	N(S)---H-O(Ox)	2.704(4)	131
	O(Ox)-H---N(S)	2.70	131

<sup>a</sup> Complex 36 is centrosymmetric. Atoms labelled Ox are contained in an oxime group. Atoms labelled S are contained in a sulfonamido group

**Table 3.5:** The bond lengths (Å) and angles (°) of *intra*-complex hydrogen-bonds in sulfonamido oxime cluster complexes **35**, **38** and **39**.

Complex	Interaction type	Number of interactions	Hydrogen-bond length / Å	Hydrogen-bond angle / °
<b>35<sup>a</sup></b>	O( <i>S</i> )---H-O( <i>M</i> )	2	2.653(3)	163(4)
	O( <i>Ox</i> )---H-O( <i>Ox</i> )	2	2.61	155
<b>38<sup>b</sup></b>	O( <i>S</i> )---H-O( <i>M</i> )	2	2.89	149
	O( <i>Ox</i> )---H-O( <i>M</i> )	2	2.780(7)	168
	O( <i>Ox</i> )---H-O( <i>Ox</i> )	2	2.495(8)	153
	N( <i>Ox</i> )---H-O( <i>Ox</i> )	2	2.87(7)	117
<b>39</b>	O( <i>H</i> )-H---O( <i>S</i> )	1	2.95(2)	128
	O( <i>H</i> )-H---O( <i>S</i> )	1	2.91(2)	129
	O( <i>H</i> )-H---O( <i>S</i> )	1	2.91(2)	126
	O( <i>H</i> )-H---O( <i>S</i> )	1	3.06(2)	125
	O( <i>Ox</i> )---H-O( <i>Ox</i> )	1	2.71(2)	139
	O( <i>Ox</i> )---H-O( <i>Ox</i> )	1	2.70(2)	123

<sup>a</sup> Complex **35** is centrosymmetric and half the molecule consists of a Cu<sub>2</sub>(**28-H**)(**28-2H**)(MeOH)(MeO) fragment.

<sup>b</sup> Complex **38** is centrosymmetric and half the molecule consists of a NiNa(**28-H**)(**28-2H**)(MeOH)<sub>2</sub> fragment. Atoms labelled *Ox* are contained in an oxime group. Atoms labelled *S* are contained in a sulfonamido group. Atoms labelled *M* are contained in a methanol group. Atoms labelled *H* are contained in a hydroxy group.

There are seven different kinds of hydrogen-bond listed in Tables 3.4 and 3.5. Of the total 22 interactions only two are between the sulfonamido oxygen and oximic hydrogen atoms. The oximic hydrogen atom is involved in over half of the total hydrogen-bonding interactions (12), the strongest of which are with another oximic oxygen atom (mean length 2.61 Å).

All the hydrogen bonds fall between 2.45-3.06 Å and most angles are greater than 140°. The two exceptions are in the nickel complexes **36** and **39**. In **36** the small angle (131°) could be a product of the constrained planar N<sub>4</sub><sup>2-</sup> donor set of the nickel geometry. The data from complex **39** however, should not be over interpreted due to the poor R factor of the structure (17%).

### 3.4.8 Hole size, bite distances and torsion angles

One of the aims of this thesis was to look at the importance of the hydrogen-bonded *pseudo*-macrocyclic around a metal centre. Even if the hydrogen-bonded ligand template exists in solution it would be improbable that this could be doubly deprotonated due to the close proximity of the anionic nitrogen atoms. Nevertheless, it is still helpful to compare the hole sizes of free ligands and ML<sub>2</sub> complexes. The

hole sizes (calculated as the mean distance from the nitrogen atoms to the centroid of the four donor atom) are given with the bite distances (the distance between the two nitrogen donor atoms) in Table 3.6.

**Table 3.6:** The hole size and bite distances of sulfonamido oxime ligands and complexes.

Ligand or complex	Hole size / Å	Bite distance / Å
<b>28</b>	2.94	2.60
<b>29</b>	2.91	2.63
<b>32</b>	—	2.62
<b>33<sup>a</sup> E isomer</b>	2.97	2.67
<b>33<sup>a</sup> Z isomer</b>	—	3.22
<b>34</b>	1.99	2.72 2.71
<b>35<sup>b</sup></b>	—	2.76 2.72
<b>36<sup>c</sup></b>	1.89	2.67
<b>38</b>	1.89	2.58 2.61
<b>39</b>	—	2.80 2.78 2.80 2.74

<sup>a</sup> Ligand **33** has been isolated as two different polymorphs. In one the oxime has *E* stereochemistry and in the other *Z* stereochemistry. <sup>b</sup> Complex **35** is centrosymmetric and half the molecule consists of a Cu<sub>2</sub>(**28-H**)(**28-2H**)(MeOH)(MeO) fragment. <sup>c</sup> Complex **36** is centrosymmetric. <sup>d</sup> Complex **38** is centrosymmetric and half the molecule consists of a NiNa(**28-H**)(**28-2H**)(MeOH)<sub>2</sub> fragment.

The hole sizes of ligands **28**, **29** and the *E* isomer of ligand **33** are all 1 Å larger than in the copper and nickel complexes (**34** and **36** respectively), this behaviour was also observed for monosulfonamidodiamine ligands (section 2.4.5). The bite distance of ligands **28**, **29**, **32** and the *E* isomer of **33** are very similar and fall in the range 2.60–2.67 Å. The *Z* isomer of **33** has a larger bite (3.22 Å) but it is known that *Z* isomers of oximes do not coordinate to metal centres,<sup>5</sup> and therefore this distance is of little relevance to an assessment of the preorganisation of the ligands. With the exception of **38** all the bites are larger in the complexes than in the free ligand and fall between 2.67 and 2.80 Å. To accommodate these changes in hole size and bite distance on complexation a change in the conformation of the ligand backbone must occur. To investigate this the torsion angles about the inner great ring of the *pseudo*-macrocyclic are listed in Tables 3.7, 3.8 and 3.9.



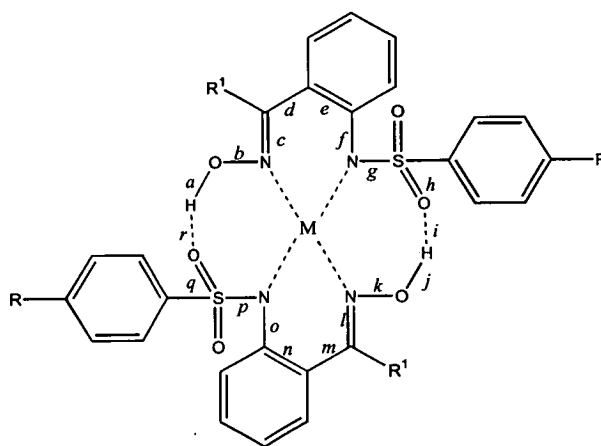


Figure 3.33: Labelling of the torsion angles around the inner great ring of sulfonamido oxime *pseudo*-macrocylic ligands.

Table 3.7: Torsion angles ( $^{\circ}$ ) for sulfonamido oxime ligands **28**, **29**, **32** and **33**.

Bond	Ligand				
	<b>28</b>	<b>29</b>	<b>32<sup>b</sup></b>	<b>33<sup>a</sup> E isomer</b>	<b>33<sup>a</sup> Z isomer</b>
<i>a</i>	-86.1	-23.3		4.7	
<i>b</i>	161.6	163.1	-177.6	165.8	179.9
<i>c</i>	179.8	177.8	179.8	-177.4	0.6
<i>d</i>	-3.0	1.3	1.1	19.7	-64.7
<i>e</i>	0	1.2	1.7	-2.8	1.7
<i>f</i>	-153.9	128.1	-153.1	119.6	-117.1
<i>g</i>	172.3	-178.1		-169.2	
<i>h</i>	93.3	-138.1		-121.9	
<i>i</i>	140.6	169.1		-166.8	
<i>j</i>	86.1	23.3		-4.7	
<i>k</i>	-161.6	-163.1		-165.8	
<i>l</i>	-179.8	-177.8		177.4	
<i>m</i>	3.0	-1.3		-19.7	
<i>n</i>	0	-1.2		2.8	
<i>o</i>	153.9	-128.1		-119.6	
<i>p</i>	-172.3	178.1		169.2	
<i>q</i>	-93.3	138.1		121.9	
<i>r</i>	-140.6	-169.1		166.8	

<sup>a</sup> Ligand **33** has been isolated as two different polymorphs. In one the oxime has *E* stereochemistry and in the other *Z* stereochemistry. <sup>b</sup> Free ligand **32** does not form a *pseudo*-macrocylic dimer (see 3.4.1.3).

**Table 3.8:** Torsion angles ( $^{\circ}$ ) for sulfonamido oxime  $ML_2$  complexes **34** and **36**. <sup>a</sup> Complex **36** is centrosymmetric.

Bond	Complex	
	<b>34</b>	<b>36<sup>a</sup></b>
<i>a</i>	13.6	
<i>b</i>	-163.4	168.9
<i>c</i>	179.2	-179.4
<i>d</i>	-29.2	-28.5
<i>e</i>	5.7	2.1
<i>f</i>	-104.1	-101.9
<i>g</i>	-172.3	
<i>h</i>	34.8	
<i>i</i>	-97.0	
<i>j</i>	25.2	
<i>k</i>	-162.7	-168.9
<i>l</i>	-179.2	179.4
<i>m</i>	-28.8	28.5
<i>n</i>	1.5	-2.1
<i>o</i>	-105.5	101.9
<i>p</i>	179.9	
<i>q</i>	159.9	
<i>r</i>	-93.0	

**Table 3.9:** Torsion angles ( $^{\circ}$ ) for sulfonamido oxime cluster complexes **35**, **38** and **39**.

Bond	Complex							
	<b>35<sup>a</sup></b>		<b>38<sup>b</sup></b>			<b>39</b>		
<i>b</i>	158.7	174.4	—	175.8	—	-166.6	—	162.9
<i>c</i>	178.2	179.6	-177.8	176.9	-179.1	-176.1	179.3	-176.9
<i>d</i>	-16.3	-29.1	34.4	-25.8	44.6	-26.7	37.4	-29.9
<i>e</i>	10.6	1.7	-0.7	3.0	-11.2	-6.3	-7.6	2.5
<i>f</i>	-169.2	-106.5	148.2	-98.4	160.4	-158.0	160.6	-157.8

<sup>a</sup> Complex **35** is centrosymmetric and half the molecule consists of a  $Cu_2(28-H)(28-2H)(MeOH)(MeO)$  fragment.

<sup>b</sup> Complex **38** is centrosymmetric and half the molecule consists of a  $NiNa(28-H)(28-2H)(MeOH)_2$  fragment.

Torsion angle *c* ( $0.6^{\circ}$ ) confirms the stereochemistry of the *Z* isomer of **33**. In all other structures *c* falls in the range  $176.1$ - $179.8^{\circ}$ . The values of *d*, *e*, *m* and *n* in the complexes are greater than those in the comparable ligands **28**, **29** and **32**. This twist around the ligand backbone will increase the bite distance on complexation. Twisting the imine bonds (torsion angles *c* and *l*) would not significantly increase the  $N\cdots N$  bite and accordingly no significant changes to these torsion angles was observed on complex formation. In general the value of the torsion angles about the amino bond (*f* and *o*) for the cluster complexes **35**, **38** and **39** are similar to those in the free ligands. However for complexes **34** and **36** *f* and *o* are smaller indicating a larger twist from planarity. This may be attributed to the displacement of the

sulfonamido group to approach the oxime function of the adjacent ligand to maximise the *intra*-complex hydrogen-bond between the sulfonamido and oxime functions in a 7-membered chelate ring of a *pseudo*-macrocyclic ligand around the metal centre.

### 3.4.9 Geometry of the sulfonamido nitrogen

A study similar to that described for monosulfonamido ligands (chapter 2, section 2.4.4.2) into the planarity of the sulfonamido nitrogen of sulfonamido oxime ligands was undertaken. Two angles,  $\theta$  and  $\alpha$  were measured ( $\theta$  is as the sum of the angles S-N-H/M, H/M-N-C and C-N-S and  $\alpha$  is the angle of the sulfur atom from the plane defined by the nitrogen, carbon and hydrogen or metal atoms) and the distance of the nitrogen from the plane of the carbon, sulfur and hydrogen or metal atoms was measured. The results are given in Tables 3.10 and 3.11.

**Table 3.10:** Values of the parameters  $\theta$ ,  $\alpha$  and the distance of the nitrogen atom from the HCS plane to show the planarity of the sulfonamido nitrogen atom in sulfonamido oxime ligands.

Ligand	Distance of N from HCS plane / Å	Sum of 3 angles, $\theta$ , around N / °	Angle of S, $\alpha$ , from NCH plane / °
<b>28</b>	0.166	355.0	21.2
<b>29</b>	0.278	344.1	36.4
<b>32</b>	0.172	354.1	23.4
<b>33<sup>a</sup> E isomer</b>	0.229	344.4	43.0
<b>33<sup>a</sup> Z isomer</b>	0.229	349.1	32.5

<sup>a</sup> Ligand 33 has been isolated as two different polymorphs. In one the oxime has *E* stereochemistry and in the other *Z* stereochemistry

**Table 3.11:** Values of the parameters  $\theta$ ,  $\alpha$  and the distance of the nitrogen atom from the MCS plane to show the planarity of the sulfonamido nitrogen atom in sulfonamido oxime complexes.

Complex	Distance of N from MCS plane / Å	Sum of 3 angles, $\theta$ , around N / °	Angle of S, $\alpha$ , from NCM plane / °
<b>34</b>	0.242	353.5	25.2
	0.276	351.6	28.6
<b>35<sup>a</sup></b>	0.020	360.0	2.4
	0.266	352.2	28.2
<b>36<sup>b</sup></b>	0.321	348.8	33.3
<b>38<sup>c</sup></b>	0.186	356.2	18.5
	0.291	350.6	29.7
<b>39</b>	0.191	356.0	19.1
	0.229	354.3	22.9
	0.182	356.4	18.1
	0.189	356.0	19.7

<sup>a</sup> Complex **35** is centrosymmetric and half the molecule consists of a  $\text{Cu}_2(\mathbf{28}\text{-H})(\mathbf{28}\text{-2H})(\text{MeOH})(\text{MeO})$  fragment.

<sup>b</sup> Complex **36** is centrosymmetric. <sup>c</sup> Complex **38** is centrosymmetric and half the molecule consists of a  $\text{NiNa}(\mathbf{28}\text{-H})(\mathbf{28}\text{-2H})(\text{MeOH})_2$  fragment.

In contrast to the behaviour of monosulfonamidodiamine ligands on complexation (chapter 2), the sulfonamido nitrogen atom of ligand **28** becomes less planar on complexation. As discussed in chapter 2, if the planarity of the amide is associated with a delocalisation of electronic density in the N-S=O unit then we might expect there to be a connection between the planarity of the nitrogen and the lengths of the sulfur to oxygen and sulfur to nitrogen bonds. S=O and S-N bond lengths are recorded in Tables 3.12 and 3.13. The correlation coefficients between bond lengths and parameters defining the planarity of the sulfonamido nitrogen atom (see also section 2.4.4.2) are recorded in Tables 3.14 and 3.15.

**Table 3.12:** S=O and S-N lengths for sulfonamido oxime ligands.

Ligand	S=O(1) / Å	S=O(2) / Å	Average S=O Length / Å	S-N bond / Å
<b>28</b>	1.445	1.426	1.436	1.614
<b>29</b>	1.438	1.431	1.435	1.625
<b>32</b>	1.432	1.428	1.43	1.629
<b>33<sup>a</sup> E isomer</b>	1.425	1.440	1.433	1.631
<b>33<sup>a</sup> Z isomer</b>	1.434	1.428	1.431	1.643

<sup>a</sup> Ligand **33** has been isolated as two different polymorphs. In one the oxime has *E* stereochemistry and in the other *Z* stereochemistry.

**Table 3.13:** S=O and S-N lengths of sulfonamido oxime complexes.

Complex	S=O(1) / Å	S=O(2) / Å	Average S=O Length / Å	S-N bond / Å
<b>34</b>	1.434	1.428	1.431	1.643
	1.451	1.433	1.442	1.594
<b>35<sup>a</sup></b>	1.436	1.466	1.451	1.593
	1.446	1.440	1.443	1.600
<b>36<sup>b</sup></b>	1.441	1.436	1.439	1.636
<b>38<sup>c</sup></b>	1.434	1.445	1.440	1.605
	1.453	1.441	1.447	1.607
<b>39</b>	1.420	1.495	1.458	1.569
	1.418	1.421	1.420	1.567
	1.441	1.443	1.442	1.598
	1.408	1.460	1.434	1.587

<sup>a</sup> Complex **35** is centrosymmetric and half the molecule consists of a Cu<sub>2</sub>(28-H)(28-2H)(MeOH)(MeO) fragment.

<sup>b</sup> Complex **36** is centrosymmetric. <sup>c</sup> Complex **38** is centrosymmetric and half the molecule consists of a NiNa(28-H)(28-2H)(MeOH)<sub>2</sub> fragment.

**Table 3.14:** The correlation coefficients of the parameters of nitrogen planarity in sulfonamido oxime ligands **28**, **29**, **32** and **33** with S=O and S-N bond lengths.

X	Y	Correlation coefficient
S-N length / Å	Average S=O length / Å	-0.76
Distance of N from HCS plane / Å	Average S=O length / Å	0.17
Distance of N from HCS plane / Å	S-N bond length / Å	-0.14
Sum of 3 angles around N, $\theta$	Average S=O length / Å	0.01
Sum of 3 angles around N, $\theta$ .	S-N length / Å	0.36
Angle of S from NCH plane, $\alpha$	Average S=O length / Å	-0.36
Angle of S from NCH plane, $\alpha$	S-N bond length / Å	0.45

**Table 3.15:** The correlation coefficients of the parameters of nitrogen planarity in sulfonamidooxime complexes **34**, **35**, **36**, **38** and **39** with S=O and S-N bond lengths.

X	Y	Correlation coefficient
S-N length / Å	Average S=O length / Å	-0.12
Distance of N from MCS plane / Å	Average S=O length / Å	-0.28
Distance of N from MCS plane / Å	S-N bond length / Å	0.20
Sum of 3 angles around N, $\theta$	Average S=O length / Å	-0.28
Sum of 3 angles around N, $\theta$	S-N length / Å	0.37
Angle of S from NCM plane, $\alpha$	Average S=O length / Å	-0.47
Angle of S from NCM plane, $\alpha$	S-N bond length / Å	0.39

Only one strong correlation (-0.76) is observed for sulfonamido oxime ligands with the S=O and the S-N lengths whereas analysis of the same data for sulfonamido oxime complexes shows poor correlation (-0.12). Correlation of the parameters of

nitrogen planarity with the S=O length is also weak and all values are less than 0.28. The complexes show the expected correlation (negative or positive values) however, the ligands show an opposite correlation to what is expected. Stronger correlation is observed with the S-N length and the parameters of nitrogen planarity and values fall above 0.36, the coefficients for the ligands and the complexes are similar.

### 3.5 A study of the solution properties of 34 and 35

Ratios of 1:1 and 1:2 of copper(II) acetate and 1-{2-[N-(4-methylbenzene sulfonamido)]phenyl}ethan-1-one oxime (**28**) in methanol both produced green solutions however a green tetranuclear species **35** was isolated from the 1:1 mixture and a brown ML<sub>2</sub> complex **34** was isolated from the 1:2 mixture. When complexes **34** and **35** were dissolved in methanol solution they each yielded a green solution, however, in chloroform a brown and a green solution were achieved. The solution structures of these species were investigated.

Vapour pressure osmometry (vpo) of the complexes in chloroform solution indicate that **34** retains its structure and that **35** exists as a larger aggregate. The average masses of the species in solution are in Table 3.16.

**Table 3.16:** Vpo measurements for **34** and **35** in chloroform solution at 25°C. *n* = measured osmolality/calculated osmolality.

Complex	Calculated osmolality (mmol)	Average mass in solution	<i>n</i>
<b>34</b>	20.16	678	1.02
<b>35</b>	18.54	1954	1.23

However, analysis by electrospray ionisation mass spectrometry of methanolic solution of **34** and **35** produce identical spectra. Both spectra have a strong peak at 691.9 (Cu(**28**-H)<sub>2</sub>Na)<sup>+</sup> and a smaller peak at 754.8 (Cu<sub>2</sub>(**28**-H)<sub>2</sub>Na)<sup>+</sup>.

Electron paramagnetic resonance (epr) was employed to try to define the copper coordination sphere of complexes **34** and **35** in chloroform solution. The spectra are plotted in Figure 3.33.

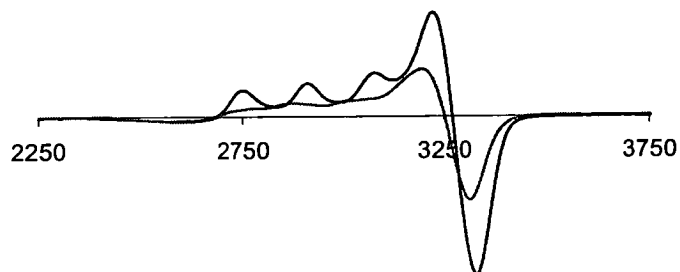


**Figure 3.33:** The EPR spectra of **34** and **35** in chloroform.

The profile of **34** ( $g_x = g_y \neq g_z$ ) in chloroform is characteristic of a Jahn-Teller-distorted tetragonal copper(II) coordination environment. The irregular slope of the  $g_{\perp}$  region of **35** possibly indicates the presence of more than one type of Cu(II) coordination environment in solution consistent with the two types of centre observed in the tetranuclear complex.

### 3.6 Equilibrium constants

The  $pK_{a1}$  (Equation 3.4) value of 9.81 for **28** was determined by Dr D. J. White.<sup>11</sup> This value is comparable to the  $pK_{a1}$  values for monosulfonamidodiamine ligands **1** and **5** in chapter 2, *cf.* 8.89 and 9.49.



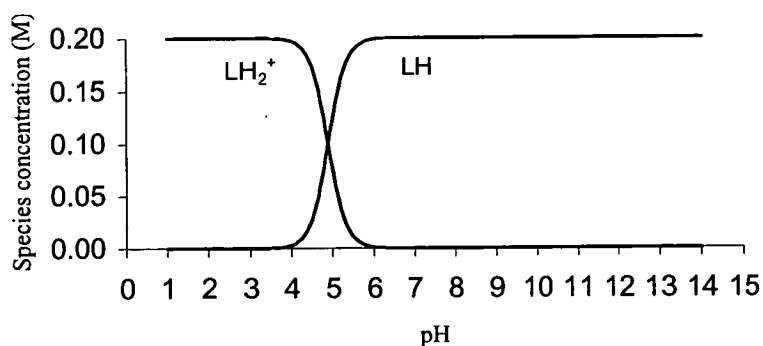


**Figure 3.32:** Calculated speciation distribution for ligand 28 as a function of pH for a 0.2 M solution in 95% methanol solution at 25°C.

The diagram shows that below pH 5 the ligand exists as a monocation and above this pH as the neutral free ligand.

### 3.7 Conclusion

The secondary hydrogen-bonded structures of the sulfonamido oxime free ligands have proved to be much more predictable than for monosulfonamido diamine ligands (chapter 2) and depend on the stereochemistry of the oxime function. The predicted sulfonamido oxygen atom to oximic hydrogen atom interaction does occur for the copper complex **35**. However the nickel complex **36** showed that an interaction between the oximic hydrogen atom and the sulfonamido nitrogen atom is also favourable.

The sulfonamido oxime ligands are relatively simple to make and have proved to have an interesting coordination chemistry. For a ligand to be suitable for solvent extraction it must form labile complexes because the metal must also be stripped back out of the complex and it is important that the coordination chemistry of a ligand is known and that simple complexes are formed. Simple mononuclear 2:1 complexation was predicted for sulfonamido oxime ligands. However, three complexes of 1-{2-[N-(4-methylbenzenesulfonamido)]phenyl}ethan-1-one oxime (**28**) have been isolated which show that these ligands can form clusters. Formation



of polynuclear complexes using doubly deprotonated ligands increases metal loading on the ligand but it is likely to be associated with slower loading and stripping processes.

## 3.8 Experimental

### 3.8.1 Instrumentation

Melting points were determined with a Gallenkamp apparatus and are uncorrected. Elemental analysis was performed on a Perkin Elmer 2400 elemental analyser or a Carlo Erba 1108 Elemental analyser. IR spectra were obtained on a Perkin Elmer Paragon 1000 FT-IR spectrometer as potassium bromide discs.  $^1\text{H}$  and  $^{13}\text{C}$  NMR spectra were run on Bruker WP200, AC250 and AVANCE DPX360 spectrometers. Chemical shifts ( $\delta$ ) are reported in parts per million (ppm) relative to residual solvent protons as internal standards. Electron impact (EI) mass spectra were obtained either on a Finnigan MAT4600 quadrupole spectrometer or on a Kratos MS50TC spectrometer. Fast atom bombardment (FAB) mass spectra were obtained on a Kratos MS50TC spectrometer in acetonitrile/3-nitrobenzyl alcohol/thioglycerol matrices. Electrospray ionisation (ESI) mass spectra were obtained on a Thermoquest LCQ spectrometer. Inductively coupled plasma atomic emission spectroscopy (ICP-AES) analysis was performed on a Thermo Jarrell Ash Iris ICP-AES spectrometer

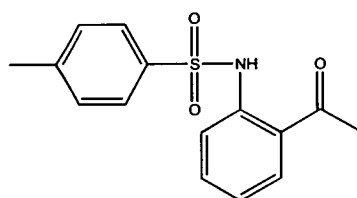
Potentiometric titrations were carried out in a sealed double jacket glass cell using a Metrohm 665 automated burette and a Corning 130 digital pH meter fitted with a Phillips glass electrode and a calomel electrode. All measurements were fully automated. Titrations were performed at  $25.0 \pm 0.1$  °C in constant ionic strength ( $I = 0.1$ ,  $[\text{Et}_4\text{N}][\text{ClO}_4]$ ) 95% methanol solution under purified nitrogen. Solutions of ligand (ca.  $1 \times 10^{-3}$  mol.dm $^{-3}$ ) alone and in the presence of 0.3, 0.8 and 1.5 equivalents of metal ion were titrated with 0.1 mol.dm $^{-3}$  Et $_4$ NOH respectively. Equilibrium constants were calculated from potentiometric data with the program MINIQUAD.<sup>12</sup> X-band EPR data for chloroform solutions were recorded on an X-band Bruker ER200D SCR spectrometer.

### 3.8.2 Solvent and reagent Pretreatment

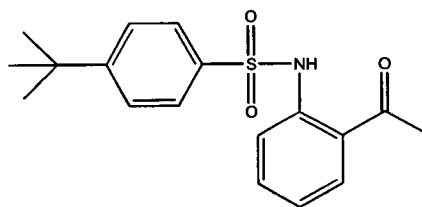
All reagents and solvents were commercially available (Acros or Aldrich) and were used as received. Solvents used for analytical purposes (NMR, MS, ICP) were of spectroscopic grade.

### 3.8.3 Synthesis of sulfonamido intermediates

#### 1-{2-[N-(4-methylbenzenesulfonamido)]phenyl}ethan-1-one

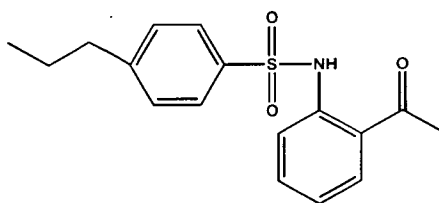


A solution of 1-(2-amino-phenyl)-ethanone (15 g, 0.11 mol) in pyridine (50 cm<sup>3</sup>) was added dropwise to a solution of 4-methylbenzenesulfonyl chloride (25 g, 0.13 mol) also in pyridine (50 cm<sup>3</sup>). The solution was stirred overnight after which time a white precipitate had formed. Full precipitation was achieved through the addition of diethylether (8 cm<sup>3</sup>). The solid was isolated by filtration and washed with diethyl ether (3 x 20 cm<sup>3</sup>). The product was recrystallised from ethanol (300 cm<sup>3</sup>) to give a crystalline solid (17.68 g, 55%), mp 147-149 °C (Found: C, 62.34; H, 5.23; N, 4.85. Calc. for C<sub>15</sub>H<sub>15</sub>NO<sub>3</sub>S: C, 61.79; H, 5.06; N, 4.65%).  $\delta_{\text{H}}$  (CDCl<sub>3</sub>, 200 MHz) 2.35 (s, 3 H, CH<sub>3</sub>), 2.55 (s, 3 H, CH<sub>3</sub>), 7.4 (m, 8 H, Ar CH).  $\delta_{\text{C}}$  (CDCl<sub>3</sub>, 90 MHz): 22 (CH<sub>3</sub>), 29 (CH<sub>3</sub>), 119 (Ar CH), 122 (Ar C), 123 (Ar CH), 128 (2C, Ar CH), 130 (2 C, Ar CH), 132 (Ar CH), 135 (Ar CH), 137 (Ar C), 140 (Ar C), 144 (Ar C), 203 (C=O). IR data (KBr disc)/cm<sup>-1</sup>: 3086m, 3054m, 3036m, 1652s, 1506w, 1359s, 1165s. EI MS, *m/z* 289 (M<sup>+</sup>, 37%).

1-{2-[N-(4-*t*-butylbenzenesulfonamido)]phenyl}ethan-1-one

A solution of 1-(2-amino-phenyl)-ethanone (9.06 g, 67 mmol) in pyridine (20 cm<sup>3</sup>) was added dropwise to a solution of 4-*t*-butylbenzenesulfonyl chloride (5.35 g, 23 mmol) also in pyridine (50 cm<sup>3</sup>) and the solution was stirred overnight. The solvent was then removed *in vacuo* leaving an orange solid which was recrystallised from ethanol (50 cm<sup>3</sup>) and washed with water (3 x 10 cm<sup>3</sup>) to give a yellow crystalline solid (5.32 g, 70%), mp 124-126°C (Found: C, 64.98; H, 6.46; N, 4.17. Calc. for C<sub>18</sub>H<sub>21</sub>NO<sub>3</sub>S: C, 65.23; H, 6.39; N, 4.23%).  $\delta_{\text{H}}$  (CDCl<sub>3</sub>, 250 MHz) 1.27 (s, 9 H, CH<sub>3</sub>), 2.53 (s, 3 H, CH<sub>3</sub>), 7.06 (m, 1 H, Ar CH), 7.44 (m, 3 H, Ar CH), 7.73 (m, 4 H, Ar CH), 11.45 (s, 1 H, NH).  $\delta_{\text{C}}$  (CDCl<sub>3</sub>, 63 MHz): 28 (CH<sub>3</sub>), 31 (3 C, CH<sub>3</sub>), 35 (C), 119 (Ar CH), 122 (Ar C), 122 (Ar CH), 126 (Ar CH), 127 (Ar CH), 132 (Ar CH), 135 (Ar CH), 136 (Ar C), 140 (Ar C), 157 (Ar C), 202 (-C=O). IR data (KBr disc)/cm<sup>-1</sup>: 2964m, 2874m, 1648s, 1593m, 1578m, 1467w, 1498m, 1341s, 1162s, 707s. EI MS, m/z 331 (M<sup>+</sup>, 38.4%).

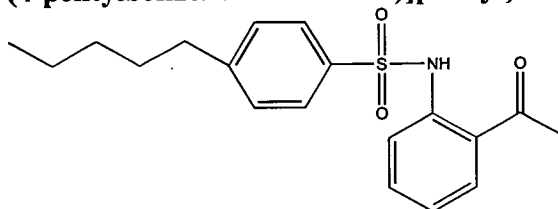
## 1-{2-[N-(4-propylbenzenesulfonamido)]phenyl}ethan-1-one



A solution of 1-(2-amino-phenyl)-ethanone (6.2 g, 46 mmol) in pyridine (30 cm<sup>3</sup>) was added dropwise to a solution of 4-propylbenzenesulfonyl chloride (10 g, 46 mmol) also in pyridine (20 cm<sup>3</sup>). The solution was stirred overnight after which time a white precipitate had formed. Full precipitation was achieved through the addition of diethyl ether (8 cm<sup>3</sup>). The solid was isolated by filtration and washed with diethyl ether (3 x 20 cm<sup>3</sup>). The product was recrystallised from ethanol (75 cm<sup>3</sup>) to give a crystalline solid (4.56 g, 31%), mp 112-114°C (Found: C, 64.53; H, 5.90; N, 4.36.

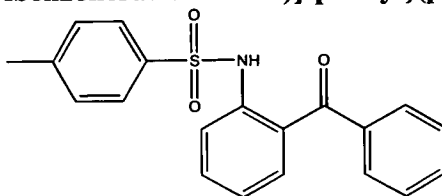
Calc. for  $C_{17}H_{19}NO_3S$ : C, 64.33; H, 6.03; N, 4.41%.  $\delta_H$  ( $CDCl_3$ , 250 MHz): 2.18 (t, 3 H, J 7.3,  $CH_3$ ), 1.56 (m, 2 H,  $CH_2$ ), 2.53 (s, 3 H,  $CH_3$ ), 2.56 (m, 2 H,  $CH_2$ ), 7.35 (m, 8 H, Ar CH), 11.43 (s, N-H).  $\delta_C$  ( $CDCl_3$ , 63 MHz): 13 ( $CH_3$ ), 23 ( $CH_2$ ), 28 ( $CH_3$ ), 38 ( $CH_2$ ), 119 (Ar CH), 122 (Ar C), 122 (Ar CH), 127 (2 C, Ar CH), 129 (2 C, Ar CH), 132 (Ar CH), 135 (Ar CH), 137 (Ar C), 139 (Ar C), 148 (Ar C), 202 (C=O). IR data (KBr disc)/ $cm^{-1}$ : 668m, 1162m, 1254m, 1456m, 1648m, 2342s, 2361s, 3649m. FAB MS:  $m/z$  318 ( $MH^+$ , 54.2%).

**1-{2-[N-(4-pentylbenzenesulfonamido)]phenyl}ethan-1-one**



A solution of 1-(2-amino-phenyl)-ethanone (3.93 g, 29 mmol) in pyridine (50  $cm^3$ ) was added dropwise to a solution of 4-*n*-pentyl benzene sulfonyl chloride (7.18 g, 29 mmol) also in pyridine (50  $cm^3$ ). The solution was stirred overnight after which time a small amount of white precipitate had formed. Full precipitation was achieved through the addition of water (8  $cm^3$ ). The solid was isolated by filtration and washed with water (3 x 20  $cm^3$ ) and hexane (3 x 20  $cm^3$ ). The product was recrystallised from hexane (300  $cm^3$ ) to give a crystalline solid (4.82 g, 48%), mp 90-92 °C (Found: C, 65.91; H, 6.73; N, 3.97. Calc. for  $C_{19}H_{23}NO_3S$ : C, 66.06; H, 6.71; N, 4.05%).  $\delta_H$  ( $CDCl_3$ , 360 MHz) 0.90 (m, 3 H,  $CH_3$ ), 1.32 (m, 4 H,  $CH_2$ ), 1.61 (m, 2 H,  $CH_2$ ), 2.59 (s, 3 H,  $CH_3$ ), 2.64 (m, 5 H,  $CH_2$ ), 7.10 (m, 1 H, Ar CH), 7.27 (m, 2 H, Ar CH), 7.49 (m, 1 H, Ar CH), 7.73 (d, 2 H, J 8.4, Ar CH), 7.80 (m, 2 H, Ar CH), 11.47 (s, C=O).  $\delta_C$  ( $CDCl_3$ , 90 MHz) 14  $CH_3$ ), 23 ( $CH_2$ ), 29 ( $CH_3$ ), 31 ( $CH_2$ ), 32 ( $CH_2$ ), 36 ( $CH_2$ ), 120 (Ar CH), 122 (Ar C), 123 (Ar CH), 128 (2 C, Ar CH), 129 (2 C, Ar CH), 132 (Ar CH), 135 (Ar CH), 137 (Ar C), 140 (Ar C), 149 (Ar C), 203 (C=O). IR data (KBr disc)/ $cm^{-1}$ : 680m, 760m, 931m, 1162s, 1342m, 1496m, 1648s, 2346w, 2867m, 2947m. FAB MS,  $m/z$  346 ( $MH^+$ , 62.8%)

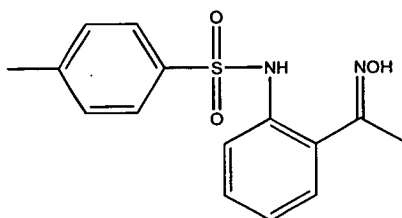
## 1-{2-[N-(4-methylbenzenesulfonamido)]-phenyl}(phenyl)methanone



A solution of (2-amino-phenyl)-phenyl-methanone (21.89 g, 0.11 mol) in pyridine (45 cm<sup>3</sup>) was added dropwise to a solution of 4-methylbenzene sulfonyl chloride (24.98 g, 0.131 mol) in pyridine (15 cm<sup>3</sup>) over 8 hours. Complete precipitation of the product was achieved by pouring the solution over an ice water mixture (500 cm<sup>3</sup>). The precipitate was then isolated by filtration and dried *in vacuo*. The product was recrystallised from ethanol (250 cm<sup>3</sup>) to give a yellow crystalline solid (26.39 g, 67%), mp 126-127°C (Found: C, 68.19; H, 4.81; N, 4.04. Calc. for C<sub>20</sub>H<sub>17</sub>NO<sub>3</sub>S: C, 68.36; H, 4.88; N, 3.99).  $\delta_{\text{H}}$  (CDCl<sub>3</sub>, 250 MHz): 2.21 (s, 3 H, CH<sub>3</sub>), 7.40 (m, 13 H, Ar CH), 9.97 (s, 2 H, NH).  $\delta_{\text{C}}$  (CDCl<sub>3</sub>, 63 MHz): 21 (CH<sub>3</sub>), 124 (Ar CH), 124.0 (Ar CH), 127 (Ar C), 128 (2 C, Ar CH), 129 (2 C, Ar CH), 130 (2 C Ar CH), 130 (2 C, Ar CH), 133 (Ar CH), 134 (Ar CH), 134 (Ar CH), 136 (Ar CH), 138 (Ar C), 139 (Ar C), 144 (Ar C), 198 (-C=O). IR data (KBr disc)/cm<sup>-1</sup>: 3246s, 3054w, 1968w, 1918w, 1649s, 1636s, 1596m, 1578w, 1395s, 1167s, 724s. EI MS, *m/z* 351 (M<sup>+</sup>, 70.3%).

## 3.8.4 Synthesis of sulfonamide oximes

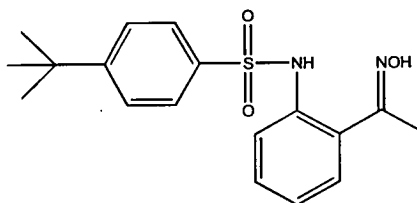
## 1-{2-[N-(4-methylbenzenesulfonamido)]phenyl}ethan-1-one oxime (28)



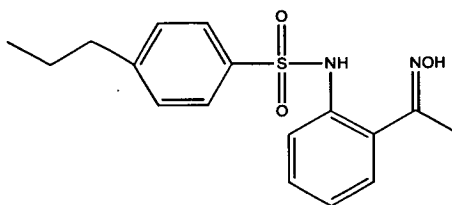
Hydroxylamine hydrochloride (7.15 g, 0.10 mol) was added to a solution of 1-{2-[N-(4-methylbenzenesulfonamido)]phenyl}ethan-1-one (10 g, 28 mmol) in a 50:50 pyridine:ethanol solution (350 cm<sup>3</sup>). This was heated at reflux for 4 hours and then cooled. The solvent was removed *in vacuo* to give a yellow oil. The oil was triturated with water (200 cm<sup>3</sup>) to produce a white solid which was isolated by

filtration. This solid was dried *in vacuo* then recrystallised from toluene (50 cm<sup>3</sup>) to give a white crystalline product (8.93 g, 84%), mp 149-150°C (Found: C, 58.92; H, 5.51; N, 9.37. Calc. for C<sub>15</sub>H<sub>16</sub>N<sub>2</sub>O<sub>3</sub>S: C, 59.39; H, 5.32; N, 9.23%).  $\delta_{\text{H}}$  (CDCl<sub>3</sub>, 200 MHz): 2.03 (s, 3 H, CH<sub>3</sub>), 2.32 (s, 3 H, CH<sub>3</sub>), 7.27 (m, 5 H, Ar CH), 7.62 (m, 3 H, Ar CH), 8.38 (s, NH), 10.85 (s, OH).  $\delta_{\text{C}}$  (CDCl<sub>3</sub>, 50 MHz) 12 (CH<sub>3</sub>), 21 (CH<sub>3</sub>), 122 (Ar CH), 124 (Ar CH), 125 (Ar C), 127 (2 C, Ar CH), 128 (Ar CH), 129 (2 C, Ar CH), 129 (Ar CH), 136 (Ar C), 136 (Ar C), 143 (Ar C), 157 (C=N-OH). IR data (KBr disc)/cm<sup>-1</sup>: 3423s, 2923m, 1654w, 1622s, 1576m, 1366m, 1329s, 1152s. EI MS, *m/z* 304 (M<sup>+</sup>, 47.0%).

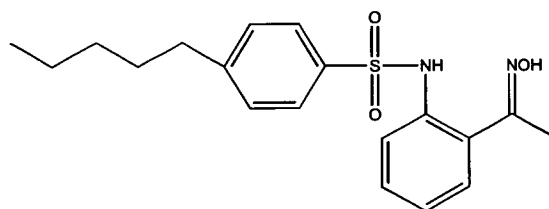
**1-{2-[N-(4-*t*-butylbenzenesulfonamido)]phenyl}ethan-1-one oxime (29)**



Hydroxylamine hydrochloride (3.49 g, 0.05 mol) was added to a solution of 1-{2-[N-(4-*t*-butylbenzenesulfonamido)]phenyl}ethan-1-one (5 g, 15 mmol) in a 50:50 pyridine:ethanol solution (150 cm<sup>3</sup>). This was heated at reflux for 4 hours and then cooled. The solvent was removed *in vacuo* to give a yellow oil which was triturated with water (200 cm<sup>3</sup>) hours to yield a white solid which was recrystallised from toluene (50 cm<sup>3</sup>) to give a white crystalline product (3.88 g, 74%), mp 192-193°C (Found: C, 62.32; H, 6.32; N, 8.02. Calc. for C<sub>18</sub>H<sub>22</sub>N<sub>2</sub>O<sub>3</sub>S: C, 62.40; H, 6.40; N, 8.09%).  $\delta_{\text{H}}$  (CDCl<sub>3</sub>, 250 MHz): 1.26 (s, 9 H, CH<sub>3</sub>), 1.95 (s, 3 H, CH<sub>3</sub>), 7.06-7.67 (m, 8 H, Ar CH), 8.39 (s, 1 H, NH), 10.76 (s, 1 H, OH).  $\delta_{\text{C}}$  (CDCl<sub>3</sub>, 63 MHz): 12 (CH<sub>3</sub>), 31 (3 C, CH<sub>3</sub>), 35 (C), 122 (Ar CH), 124 (Ar CH), 125 (C-NOH), 127 (Ar CH), 128 (Ar CH), 129 (Ar CH), 135 (Ar C). IR (KBr disc)/cm<sup>-1</sup>: 764m, 1013m, 1162s, 1329s, 1496m, 1593w, 2362w, 2870w, 2966m, 5387s. EI MS, *m/z* 346 (M<sup>+</sup>, 44.8%).

**1-{2-[N-(4-propylbenzenesulfonamido)]phenyl}ethan-1-one oxime (30)**

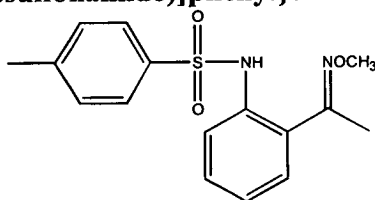
Hydroxylamine hydrochloride (2.7 g, 38 mmol) was added to a solution of 1-{2-[N-(4-propylbenzenesulfonamido)]phenyl}ethan-1-one (4 g, 13 mmol) in a 50:50 pyridine:ethanol solution (150 cm<sup>3</sup>). This was heated at reflux for 4 hours and then cooled. The solvent was removed *in vacuo* to give a white oil. The oil solidified over 72 hours to give a white solid which was washed with water (3.57g, 85%), mp 118-119°C (Found: C, 61.47; H, 5.85; N, 8.34. Calc. for C<sub>17</sub>H<sub>20</sub>N<sub>2</sub>O<sub>3</sub>S: C, 61.42; H, 6.06; N, 8.43%).  $\delta_{\text{H}}$  (CDCl<sub>3</sub>, 200 MHz): 0.88 (t, 3 H, J 7.3, CH<sub>3</sub>), 1.57 (s, 2 H, J 7.5, CH<sub>2</sub>), 2.01 (s, 3 H, CH<sub>3</sub>), 2.55 (t, 2 H, J 7.6, CH<sub>2</sub>), 7.12-7.33 (m, 5 H, Ar CH), 7.61 (m, 3 H, Ar CH), 8.41 (s, 1 H, NH), 10.83 (s, 1 H, N-OH).  $\delta_{\text{C}}$  (CDCl<sub>3</sub>, 90 MHz): 13 (CH<sub>3</sub>), 14 (CH<sub>3</sub>), 25 (CH<sub>2</sub>), 38 (CH<sub>2</sub>), 123 (Ar CH), 125 (Ar CH), 128 (2 C, Ar CH), 129 (Ar CH), 129 (2 C, Ar CH), 130 (Ar CH), 136 (Ar C), 137 (Ar C), 149 (Ar C), 157 (Ar C). IR data (KBr disc)/cm<sup>-1</sup>: 756m, 1012m, 1092m, 1155s, 1330s, 1498m, 1635w, 2876m, 2933m, 3391s. FAB MS: *m/z* 333 (MH<sup>+</sup>, 100.0%).

**1-{2-[N-(4-pentylbenzenesulfonamido)]phenyl}ethan-1-one oxime (31)**

Hydroxylamine hydrochloride (0.37 g, 5 mmol) was added to a solution of 1-{2-[N-(4-pentylbenzenesulfonamido)]phenyl}ethan-1-one (0.62 g, 2 mmol) in a 50:50 pyridine:ethanol solution (30 cm<sup>3</sup>). This was heated at reflux for 4 hours and then cooled. The solvent was removed *in vacuo* to give a colourless oil. The oil was triturated with water (5 cm<sup>3</sup>) and subsequently with hexane (5 cm<sup>3</sup>) to yield a white solid which was recrystallised from diethylether and hexane (20 cm<sup>3</sup>) and dried *in*

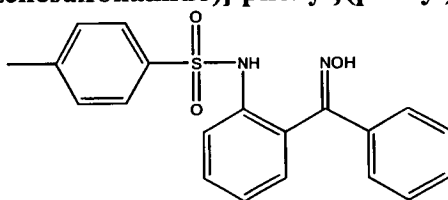
*vacuo*, (0.55g, 85%), mp 82-84° C (Found: C, 63.43; H, 6.75; N, 7.79. Calc. for C<sub>19</sub>H<sub>24</sub>N<sub>2</sub>O<sub>3</sub>S: C, 63.31; H, 6.71; N, 7.77%).  $\delta_{\text{H}}$  (CDCl<sub>3</sub>, 360 MHz): 0.90 (m, 3 H, CH<sub>3</sub>), 1.31 (m, 4 H, CH<sub>2</sub>), 1.59 (m, 2 H, CH<sub>2</sub>), 2.07 (s, CH<sub>3</sub>), 2.62 (m, 2 H, CH<sub>2</sub>), 7.13 (t, 1 H, J 6.9, Ar CH), 7.22 (d, 2 H, J 8.4, Ar CH), 7.31 (m, Ar CH), 7.36 (m, 1 H, Ar CH), 7.65 (m, 3 H, Ar CH).  $\delta_{\text{C}}$  (CDCl<sub>3</sub>, 90 MHz): 13 (CH<sub>3</sub>), 14 (CH<sub>3</sub>), 23 (CH<sub>2</sub>), 31 (CH<sub>2</sub>), 32 (CH<sub>2</sub>), 36 (CH<sub>2</sub>), 123 (Ar CH), 125 (Ar CH), 126 (q, Ar C), 127 (2 C, Ar CH), 128 (Ar CH), 129 (2 C, Ar CH), 130 (Ar CH), 136 (Ar C), 137 (Ar C), 149 (Ar C), 158 (>C=NOH). IR data (KBr disc)/cm<sup>-1</sup>: 659m, 1157s, 1332m, 1505m, 1628w, 2362w, 2859m, 2926m, 3401s. FAB MS, *m/z* 361 (MH<sup>+</sup>, 100.0%).

**1-{2-[N-(4-methylbenzenesulfonamido)]phenyl}ethan-1-one O-methyloxime (32)**



Hydroxylamine hydrochloride (1.95 g, 23 mmol) was added to a solution 1-(2-[N-(4-methylbenzenesulfonamido)]phenyl)ethan-1-one (2.02 g, 6.9 mmol) in a 50:50 pyridine:ethanol solution (60 cm<sup>3</sup>). This was heated at reflux for 4 hours and then cooled. The solvent was removed *in vacuo* to give a white solid. The solid was washed with water (3 x 10 cm<sup>3</sup>) and dried *in vacuo*. This was then recrystallised from toluene (20 cm<sup>3</sup>) to give a yellow crystalline product (1.19 g, 54%), mp 122-124° C (Found: C, 60.40; H, 5.59; N, 8.69. Calc. for C<sub>16</sub>H<sub>18</sub>N<sub>2</sub>O<sub>3</sub>S: C, 60.36; H, 5.70; N, 8.80%).  $\delta_{\text{H}}$  (CDCl<sub>3</sub>, 200 MHz): 2.03 (s, 3 H, CH<sub>3</sub>), 2.38 (s, 3 H, CH<sub>3</sub>), 4.09 (s, 3 H, OCH<sub>3</sub>), 7.23 (m, 5 H, Ar CH), 7.64 (m, 3 H, Ar CH), 10.79 (s, 1 H, NH).  $\delta_{\text{C}}$  (CDCl<sub>3</sub>, 50 MHz): 14 (CH<sub>3</sub>), 22 (CH<sub>3</sub>), 63 (OCH<sub>3</sub>), 122 (Ar CH), 124 (Ar CH), 125 (Ar C), 128 (2 C, Ar CH), 129 (Ar CH), 130 (2 C, Ar CH), 136 (Ar C), 137 (Ar C), 144 (Ar C), 156 (Ar C). IR data (KBr disc)/cm<sup>-1</sup>: 660s, 754s, 918s, 1052s, 1159s, 1293m, 1605m, 2364w, 2818m, 2936m, 2978m. FAB MS, *m/z* 319 (MH<sup>+</sup>, 100.0%).



**1-{2-[N-(4-methylbenzenesulfonamido)]-phenyl}(phenyl)methanone oxime (33)**

Hydroxylamine hydrochloride (6.49 g, 93 mmol) was added to a solution of 1-{2-[N-(4-methylbenzenesulfonamido)]-phenyl}(phenyl)methanone oxime (10 g, 28 mmol) in a 50:50 pyridine:ethanol solution (350 cm<sup>3</sup>). This was heated at reflux for 4 hours and then cooled. The solvent was removed in vacuo to give a yellow oil which was triturated with water (3 x 200 cm<sup>3</sup>) to yield a white solid which was recrystallised from toluene (50 cm<sup>3</sup>) to give a white crystalline product (3.55 g, 34%), mp 160°C (Found: C, 65.73; H, 4.93; N, 7.73. Calc. for C<sub>20</sub>H<sub>18</sub>N<sub>2</sub>O<sub>3</sub>S: C, 65.55; H, 4.95; N, 7.64 %). Two isomers of **6** were detected by <sup>1</sup>H nmr. δ<sub>H</sub> (CDCl<sub>3</sub>, 200 MHz): Major isomer, 2.20 (s, 3 H, CH<sub>3</sub>), 7.45 (m, 15 H, Ar CH), 10.60 (s, 1 H, N-OH), Minor isomer: 2.36 (s, 3 H, CH<sub>3</sub>), 6.88-8.03 (m, 15 H, Ar CH), 9.95 (s, 1 H, N-OH). Signals for the major isomer only were detected by <sup>13</sup>C nmr. δ<sub>C</sub> (CDCl<sub>3</sub> 50 MHz): 21 (CH<sub>3</sub>), 125 (Ar CH), 126 (Ar CH), 127 (Ar C), 127 (2 C, Ar CH), 128 (2 C, Ar CH), 128 (2 C, Ar CH), 129 (Ar CH), 129(2 C, Ar CH), 130 (Ar CH), 130 (Ar CH), 135 (Ar C), 135 (Ar C), 136 (Ar C), 143 (Ar C), 157 (C=N-OH). IR (KBr disc)/cm<sup>-1</sup>: 3276s, 1654w, 1600w, 1578w, 1492m, 1343m, 1169s. EI MS, m/z 366 (M<sup>+</sup>, 100.0%).

**3.8.5 Synthesis of sulfonamido oxime complexes****Bis[1-{2-[N-(4-methylbenzenesulfonamidato)]phenyl}ethan-1-one oxime] copper(II) (34)**

A solution of **28** (0.15 g, 0.49 mmol) in hot methanol (10 cm<sup>3</sup>) was added to a solution of copper acetate monohydrate (49 mg, 0.25 mmol) also in methanol (10 cm<sup>3</sup>). The solution was sealed until the product separated overnight as a brown crystalline solid which was collected by filtration, washed with methanol (3 x 5 cm<sup>3</sup>) and dried *in vacuo* (0.12 g, 75%), (Found: C, 53.77; H, 4.63; N, 8.72. Calc. for C<sub>30</sub>H<sub>30</sub>N<sub>4</sub>CuO<sub>6</sub>S<sub>2</sub>: C, 53.60;

H, 4.49; N, 8.33%). IR data (KBr disc)/cm<sup>-1</sup>: 708m, 1153m, 1367w, 1596m, 3423m. FAB MS *m/z* 672 (MH<sup>+</sup>, 18.0%).

**Cu<sub>4</sub>(C<sub>15</sub>H<sub>16</sub>N<sub>2</sub>SO<sub>3</sub>)<sub>2</sub>(C<sub>15</sub>H<sub>15</sub>N<sub>2</sub>SO<sub>3</sub>)<sub>2</sub>(CH<sub>3</sub>OH)<sub>2</sub>(CH<sub>3</sub>O)<sub>2</sub> (35)**

A solution of **28** (0.15 g, 0.49 mmol) in hot methanol (10 cm<sup>3</sup>) was added to a solution of copper acetate monohydrate (98 mg, 0.49 mmol) also in methanol (10 cm<sup>3</sup>). The solution was sealed until the product separated overnight as a green crystalline solid which was collected by filtration, washed with methanol (3 x 5 cm<sup>3</sup>) and dried *in vacuo* (0.19 g, 95%). (Found: C, 48.31; H, 4.67; N, 6.91. Calc. for: C<sub>64</sub>H<sub>76</sub>N<sub>8</sub>Cu<sub>4</sub>O<sub>16</sub>S<sub>2</sub>: C, 48.29; H, 4.56; N, 7.04 %). IR data (KBr disc)/cm<sup>-1</sup>: 1355w, 1446s, 1602s, 3375s, 3477s. ESI MS *m/z* 367 ([Cu(C<sub>15</sub>H<sub>16</sub>N<sub>2</sub>O<sub>3</sub>S)]<sup>+</sup>, 19.7%), 670 ([Cu(C<sub>15</sub>H<sub>15</sub>N<sub>2</sub>O<sub>3</sub>S)<sub>2</sub>]<sup>+</sup>, 12.6%).

**Bis[1-{2-[N-(4-methylbenzenesulfonamidato)]phenyl}ethan-1-one oxime]nickel(II) (orange, 36)**

A solution of **28** (0.15 g, 0.49 mmol) and potassium hydroxide (0.49 mmol) in hot methanol (10 cm<sup>3</sup>) was added to a solution of nickel acetate tetrahydrate (61 mg, 0.25 mmol) also in methanol (10 cm<sup>3</sup>). The solution was sealed until the product separated after 3 days as an orange crystalline solid which was collected by filtration, washed with methanol (3 x 5 cm<sup>3</sup>) and dried *in vacuo* (0.13 g, 38%). (Found: C, 53.74; H, 4.28; N, 8.14. Calc. for C<sub>30</sub>H<sub>30</sub>N<sub>4</sub>NiO<sub>6</sub>S<sub>2</sub>: C, 54.23; H, 4.55; N, 8.43%). IR data (KBr disc)/cm<sup>-1</sup>: 706w, 1151s, 1490m, 1560m, 3048w, 3423w. ESI MS *m/z* 663 (M<sup>+</sup>, 100.0%).

**Bis[1-{2-[N-(4-methylbenzenesulfonamidato)]phenyl}ethan-1-one oxime]nickel(II) (purple, 37)**

A solution of **28** (0.15 g, 0.49 mmol) in hot ethanol (10 cm<sup>3</sup>) was added to a solution of nickel acetate tetrahydrate (61 mg, 0.25 mmol) also in ethanol (10 cm<sup>3</sup>). The solution was sealed until the product separated after 3 days as a purple solid which was collected by filtration, washed with ethanol (3 x 5 cm<sup>3</sup>) and dried *in vacuo* (0.06 g, 37%), (Found: C, 54.21; H, 4.23; N, 8.74. Calc. for C<sub>30</sub>H<sub>30</sub>N<sub>4</sub>NiO<sub>6</sub>S<sub>2</sub>: C, 54.23; H, 4.55; N, 8.43%). IR data (KBr disc)/cm<sup>-1</sup>: 708m, 1133s, 1369w, 1597m, 1654w, 2871m, 2923m, 3422m. FAB MS *m/z* 664 ([Ni(C<sub>15</sub>H<sub>15</sub>N<sub>2</sub>O<sub>3</sub>S)<sub>2</sub>]<sup>-</sup>, 34.0%).

**Ni<sub>2</sub>Na<sub>2</sub>(C<sub>15</sub>H<sub>16</sub>N<sub>2</sub>SO<sub>3</sub>)<sub>2</sub>(C<sub>15</sub>H<sub>15</sub>N<sub>2</sub>SO<sub>3</sub>)<sub>2</sub>(CH<sub>3</sub>OH)<sub>2</sub>(CH<sub>3</sub>O)<sub>2</sub> (38)**

A solution of **28** (0.15 g, 0.49 mmol) and sodium hydroxide (0.49 mmol) in hot methanol (10 cm<sup>3</sup>) was added to a solution of nickel acetate tetrahydrate (61 mg, 0.25 mmol) also in methanol (10 cm<sup>3</sup>). The solution was sealed until the product separated after 3 days as red crystalline solid which was collected by filtration, washed with methanol (3 x 5 cm<sup>3</sup>) and dried *in vacuo* (84 mg, 45%). (Found: C, 51.03; H, 5.04; N, 7.33. Calc. for C<sub>64</sub>H<sub>76</sub>N<sub>8</sub>Na<sub>2</sub>Ni<sub>2</sub>O<sub>16</sub>S<sub>4</sub>: C, 51.08; H, 4.96; N, 7.45%). IR data (KBr disc)/cm<sup>-1</sup>: 1438m, 1560m, 1654m, 3448w. ESI MS *m/z* 666 ([Ni(C<sub>15</sub>H<sub>15</sub>N<sub>2</sub>O<sub>3</sub>S)<sub>2</sub>]<sup>+</sup>, 41.2%), 1460 ([Ni<sub>2</sub>(C<sub>15</sub>H<sub>16</sub>N<sub>2</sub>SO<sub>3</sub>)<sub>2</sub>(C<sub>15</sub>H<sub>15</sub>N<sub>2</sub>SO<sub>3</sub>)<sub>2</sub>(CH<sub>3</sub>OH)<sub>2</sub>(CH<sub>3</sub>O)<sub>2</sub>]<sup>+</sup>, 66.0%).

**Ni<sub>4</sub>(1-H)<sub>2</sub>(1-2H)<sub>2</sub>(OH)<sub>2</sub>(MeO)<sub>5</sub> (39)**

A solution of **28** (0.15 g, 0.49 mmol) and lithium hydroxide (0.49 mmol) in hot methanol (10 cm<sup>3</sup>) was added to a solution of nickel acetate tetrahydrate (61 mg, 0.25 mmol) also in methanol (10 cm<sup>3</sup>). The solution was sealed until product was observed. An orange crystalline solid was initially observed, however after 7 days a small number of green crystals were isolated (8 mg, 8%). Due to the small number of crystals formed microanalysis was not possible. IR data (KBr disc)/cm<sup>-1</sup>: 668m, 1087m, 1127m, 1235m, 1561w, 1655m, 2344s, 2363s, 3435s, 3856m. ESI MS *m/z* 1452 (Ni<sub>4</sub>(C<sub>15</sub>H<sub>15</sub>N<sub>2</sub>SO<sub>3</sub>)<sub>2</sub>(C<sub>15</sub>H<sub>14</sub>N<sub>2</sub>SO<sub>3</sub>)<sub>2</sub>(OH)<sub>2</sub>(MeOH)<sub>3</sub>)<sup>+</sup>, 43.0%), *m/z* 1484 (Ni<sub>4</sub>(C<sub>15</sub>H<sub>15</sub>N<sub>2</sub>SO<sub>3</sub>)<sub>2</sub>(C<sub>15</sub>H<sub>14</sub>N<sub>2</sub>SO<sub>3</sub>)<sub>2</sub>(OH)<sub>2</sub>(MeOH)<sub>4</sub>)<sup>+</sup>, 15.2%) *m/z* 1516 (Ni<sub>4</sub>(C<sub>15</sub>H<sub>15</sub>N<sub>2</sub>SO<sub>3</sub>)<sub>2</sub>(C<sub>15</sub>H<sub>14</sub>N<sub>2</sub>SO<sub>3</sub>)<sub>2</sub>(OH)<sub>2</sub>(MeOH)<sub>5</sub>)<sup>+</sup>, 7.6%).

**Bis[1-{2-[N-(4-propylbenzenesulfonamidato)]phenyl}ethan-1-one oxime] nickel(II) (40)**

A solution of **30** (0.15 g, 0.45 mmol) and potassium hydroxide (0.49 mmol) in hot methanol (10 cm<sup>3</sup>) was added to a solution of nickel acetate tetrahydrate (56 mg, 0.22 mmol) also in methanol (10 cm<sup>3</sup>). The solution was sealed until the product separated after 3 days as an orange crystalline solid which was collected by filtration, washed with methanol (3 x 5 cm<sup>3</sup>) and dried *in vacuo* (39 mg, 25%). (Found: C, 56.56; H, 5.38; N, 7.76. Calc. for C<sub>34</sub>H<sub>38</sub>N<sub>4</sub>NiO<sub>6</sub>S<sub>2</sub>: C, 56.52; H, 5.30; N, 7.75%). IR data (KBr disc)/cm<sup>-1</sup>: 1150s, 1309s, 1456m, 1636w, 2871m, 2931m, 2960m, 3042m. FAB MS *m/z* 665 (M<sup>+</sup>, 16.0%).

**Bis[{2-[N-(4-methylbenzenesulfonamido)]-phenyl}(phenyl)methanone oxime] copper(II) (41)**

A solution of **33** (0.15 g, 0.41 mmol) in hot methanol (10 cm<sup>3</sup>) was added to a solution of copper acetate monohydrate (41 mg, 0.21 mmol) also in methanol (10 cm<sup>3</sup>). The solution was sealed until the product separated overnight as a brown crystalline solid which was collected by filtration, washed with methanol (3 x 5 cm<sup>3</sup>) and dried *in vacuo* (0.11 g, 67%), (Found: C, 60.61; H, 4.43; N, 6.89. Calc. for C<sub>40</sub>H<sub>36</sub>N<sub>4</sub>CuO<sub>6</sub>S<sub>4</sub>: C, 60.48; H, 4.31; N, 7.05%). IR data (KBr disc)/cm<sup>-1</sup>: 668m, 1089s, 1167s, 1281m, 1328m, 1490m, 1597m, 3059m, 3275m, 3394m. ESI MS *m/z* 794 (MH<sup>+</sup>, 67.0%).

**3.8.6 X-ray crystallography**

Structures **28**, **33E**, **34** and **38** were determined by Dr. Simon Parsons and **29**, **32**, **33Z**, **36** and **39** were determined by Andrew Parkin at the University of Edinburgh. In all cases data were collected at 220 K on a SMART or Stoe Stadi-4 diffractometer equipped with an Oxford Cryosystems low temperature device, using Cu-K $\alpha$  radiation for **28**, and Mo-K $\alpha$  radiation for **29**, **32**, **33E**, **33Z**, **34**, **35**, **36**, **38** and **39**. Reflections were scanned in  $\omega$ - $\theta$  mode. Structures **28**, **29**, **32**, **33Z**, **34**, **35**, and **39** were solved by direct methods (SHELXTL<sup>13</sup>) and **36**, **38** and **33E** by Patterson methods (DIRDIF<sup>14</sup>). All were completed by iterative cycles of least squares refinement against  $F^2$  and difference Fourier synthesis (SHELXTL). H-atoms were idealised, being placed using geometric or difference maps and treated by riding or reffall methods. All sulfonamido hydrogen atoms were placed using difference maps. In all cases non-H atoms were modelled with final anisotropic displacement parameters and final refinement statistics are presented in Tables 3.17 (**28**, **29**, **32**), 3.18 (**33E** and **Z**), 3.19 (**34-36**) and 3.20 (**38** and **39**).

Table 3.17 : Crystallographic data for structures 28, 29 and 32.

Structure	28	29	32
Formula	C <sub>15</sub> H <sub>16</sub> N <sub>2</sub> O <sub>3</sub> S	C <sub>18</sub> H <sub>22</sub> N <sub>2</sub> O <sub>3</sub> S	C <sub>16</sub> H <sub>18</sub> N <sub>2</sub> O <sub>3</sub> S
M	304.36	346.44	318.38
Crystal system	Monoclinic	Monoclinic	Monoclinic
Space group	<i>P</i> 21 / <i>n</i>	<i>P</i> 2(1) / <i>c</i>	<i>P</i> 2 (1) / <i>n</i>
<i>a</i> /Å	8.2135(13)	10.2876(18)	11.332(2)
<i>b</i> /Å	8.2717(12)	15.182(3)	8.4432(14)
<i>c</i> /Å	21.717(3)	11.844(3)	16.599(3)
$\alpha^\circ$	90	90	90
$\beta^\circ$	94.061(9)	107.341(19)	100.381(15)
$\gamma^\circ$	90	90	90
<i>U</i> /Å <sup>3</sup>	1471.7(4)	1765.9(6)	1562.1(5)
Crystal size/mm	0.36 x 0.12 x 0.12	0.27 x 0.27 x 0.23	0.86 x 0.54 x 0.43
<i>D<sub>c</sub></i> /g cm <sup>-3</sup>	1.374	1.303	1.354
<i>Z</i>	4	4	4
$\mu$ /mm <sup>-1</sup>	2.062	0.201	0.221
Scan type	omega - theta	omega - theta	omega-2theta
$\theta$ Limits/ $^\circ$	4.08-60.13	2.67-25.06	2.72-25.00
No. of unique data	2172	3117	2735
No. data with [F>4 $\sigma$ (F)]	1788	1851	2361
No. parameters	195	273	272
R1	0.0452	0.0547	0.0304
wR2	0.1255	0.1302	0.0826
$\Delta\rho_{\max}, \Delta\rho_{\min}/e \text{ \AA}^{-3}$	0.245, -0.358	0.350, -0.259	0.221, -0.259

Table 3.18 : Crystallographic data for structures 33(E) and 33(Z).

Structure	33(E)	33(Z)
Formula	C <sub>20</sub> H <sub>18</sub> N <sub>2</sub> O <sub>3</sub> S	C <sub>20</sub> H <sub>18</sub> N <sub>2</sub> O <sub>3</sub> S
M	366.42	366.42
Crystal system	Monoclinic	Triclinic
Space group	<i>P</i> 21 / <i>c</i>	<i>P</i> - 1
<i>a</i> /Å	9.7368(16)	8.083(6)
<i>b</i> /Å	11.865(2)	9.772(7)
<i>c</i> /Å	16.242(3)	11.885(8)
$\alpha^\circ$	90	72.46(5)
$\beta^\circ$	101.523(17)	85.18(4)
$\gamma^\circ$	90	80.29(6)
<i>U</i> /Å <sup>3</sup>	1838.5(6)	881.8(11)
Crystal size/mm	0.51 x 0.19 x 0.16	0.47 x 0.23 x 0.23
<i>D<sub>c</sub></i> /g cm <sup>-3</sup>	1.324	1.380
<i>Z</i>	4	2
$\mu$ /mm <sup>-1</sup>	0.198	0.206
Scan type	omega-theta	omega-theta
$\theta$ Limits/ $^\circ$	2.56-25.09	2.56-25.11
No. of unique data	3267	3134
No. data with [F>4 $\sigma$ (F)]	1712	2577

No. parameters	242	308
R1	0.0677	0.0391
wR2	0.1609	0.0918
$\Delta\rho_{\max}, \Delta\rho_{\min}/e \text{ \AA}^{-3}$	0.249, -0.261	0.244, -0.355

Table 3.19 : Crystallographic data for structures 34-36.

Structure	34	35	36
Formula	$C_{30}H_{30}CuN_4O_6S_2$	$C_{64}H_{72}Cu_4N_8O_{16}S_4$	$C_{30}H_{30}Ni_4O_6S_2$
M	670.24	1591.70	665.41
Crystal system	Monoclinic	Triclinic	Triclinic
Space group	<i>P</i> 21 / <i>n</i>	<i>P</i> -1	<i>P</i> -1
<i>a</i> /Å	12.2008(14)	8.8883(4)	8.4754(15)
<i>b</i> /Å	15.258(2)	14.4574(7)	8.5995(15)
<i>c</i> /Å	17.329(2)	14.7591(5)	11.0123(19)
$\alpha^\circ$	90	62.487(3)	95.134(3)
$\beta^\circ$	108.704	82.793(3)	92.934(3)
$\gamma^\circ$	90	85.357(2)	114.367(2)
<i>U</i> /Å <sup>3</sup>	3055.6(6)	1668.22(12)	724.8(2)
Crystal size/mm	0.54 x 0.19 x 0.12	0.15 x 0.10 x 0.10	0.34 x 0.15 x 0.08
<i>D</i> <sub>c</sub> /g cm <sup>-1</sup>	1.457	1.584	1.525
Z	4	1	1
$\mu$ /mm <sup>-1</sup>	0.901	1.457	0.865
Scan type	omega + theta	phi + omega	Phi + omega
$\theta$ Limits/ $^\circ$	2.67-25.00	2.31-30.49	1.87-26.43
No. of unique data	5330	9467	2919
No. data with [ <i>F</i> >4 $\sigma$ ( <i>F</i> )]	4032	5640	2191
No. parameters	394	448	199
R1	0.0437	0.0479	0.0565
wR2	0.1059	0.1153	0.1288
$\Delta\rho_{\max}, \Delta\rho_{\min}/e \text{ \AA}^{-3}$	0.412, -0.339	0.616, -0.742	1.655, -1.045

Table 3.20 : Crystallographic data for structures 38 and 39.

Structure	38	39
Formula	$C_{64}H_{74}N_8Na_2Ni_2O_{16}S_4$	$C_{69}H_{98}N_8Ni_4O_{23}S_4$
M	1502.95	1770.63
Crystal system	Triclinic	Monoclinic
Space group	<i>P</i> -1	<i>P</i> 2 (1) / <i>n</i>
<i>a</i> /Å	10.236(6)	13.572(4)
<i>b</i> /Å	14.096(8)	27.576(7)
<i>c</i> /Å	14.395(8)	21.439(6)
$\alpha^\circ$	61.883(19)	90
$\beta^\circ$	73.43(3)	95.890(6)
$\gamma^\circ$	73.26(3)	90
<i>U</i> /Å <sup>3</sup>	1726.6(17)	7981(4)
Crystal size/mm	0.54 x 0.27 x 0.23	0.28 x 0.07 x 0.04
<i>D</i> <sub>c</sub> /g cm <sup>-1</sup>	1.445	1.474
Z	1	4
$\mu$ /mm <sup>-1</sup>	0.751	1.111

Scan type	omega-theta	phi + omega
<b><math>\theta</math> Limits/<math>^{\circ}</math></b>	2.78-25.09	1.21-21.16
<b>No. of unique data</b>	6127	8520
<b>No. data with <math>[F &gt; 4\sigma(F)]</math></b>	3881	5371
<b>No. parameters</b>	441	443
<b>R1</b>	0.0759	0.1785
<b>wR2</b>	0.1950	0.3613
<b><math>\Delta\rho_{\max}, \Delta\rho_{\min}/e \text{ \AA}^{-3}</math></b>	0.888, -1.421	1.128, -0.902

### 3.9 References

- <sup>1</sup> A. D. Garnovskii, *Koord. Khim.*, (Engl. Trans.), 1992, **18**, 695.
- <sup>2</sup> D. H. Williams and I. Fleming, in *Spectroscopic Methods in Organic Chemistry*, McGraw-Hill Book Company, London, 5<sup>th</sup> edn., 1995, ch. 3, p. 118.
- <sup>3</sup> H. Kessler, *Tetrahedron*, 1974, **30**, 184.
- <sup>4</sup> B. Jerslev and S. Larsen, *Acta Chemica Scandinavica*, 1991, **45**, 285.
- <sup>5</sup> A. W. Ashbrook, *Journal of Chromatography*, 1975, **105**, 141.
- <sup>6</sup> J. K. Maurin, *Acta Cryst.*, 1998, **B54**, 866-871.
- <sup>7</sup> C. H. Heathcock, M. A. Henderson, D. A. Oare and M. A. Sanner, *J. Org. Chem.*, 1985, **50**, 3022.
- <sup>8</sup> H. W. Görlitzer, M. Spiegler and R. Anwander, *Eur. J. Inorg. Chem.* 1998, 1009.
- <sup>9</sup> L. T. Armistead, P. S. White and M. R. Gagné, *Organometallics*, 1998, **17**, 216.
- <sup>10</sup> S. Pritchett, P. Gantzel, and P. J. Walsh, *Organometallics*, 1997, **16**, 5130.
- <sup>11</sup> Dr D. J. White, work carried out at the University of Sydney, private communication.
- <sup>12</sup> P. Gans, A. Sabatini and A. Vacca, *Inorg. Chim. Acta*, 1976, **18**, 237.
- <sup>13</sup> G. M. Sheldrick, SHELXTL version 5, Siemens Analytical X-ray Instrument, Madison, Wisc., USA, 1995.
- <sup>14</sup> P. T. Beurskens, G. Beurskens, W. P. Bosman, R. de Gelder, S. García-Granda, R.O. Gould, R. Israël and J. M. M. Smits, DIRDIF, Crystallography Laboratory, University of Nijmegen, The Netherlands.



## **Chapter 4:**

# **Solution studies on monosulfonamidodiamine and sulfonamido oxime ligands**

<b>Contents</b>	<b>Page</b>
4.1 Introduction .....	188
4.2 Improving ligand solubility .....	188
4.2.1 Reducing the number of hydrogen-bond donors and acceptors .....	189
4.2.1.1 An introduction to sulfinamides .....	189
4.2.1.2 Sulfinamide target molecules .....	192
4.2.1.3 Attempted synthesis of monosulfinamido diamine ligands .....	193
4.2.1.4 Attempted syntheses of sulfinamide oxime ligands .....	195
4.2.2 Ligand solubilisation by the introduction of a lipophilic group .....	197
4.2.2.1 The introduction of a lipophilic group into .....	
monosulfonamidodiamine ligands .....	197
4.2.2.2 The introduction of a lipophilic group into .....	
sulfonamido oxime ligands .....	199
4.2.3 Synthesis of sulfonyl chlorides .....	199
4.2.3.1 2-Ethylhexylsulfonyl chloride .....	202
4.2.3.2 Synthesis of aryl sulfonyl chlorides .....	204
4.3 Investigation of ligand association in solution .....	206
4.3.1 Electrospray ionisation mass spectrometry .....	206
4.3.2 Vapour pressure osmometry .....	207
4.3.3 NMR spectroscopy .....	207
4.3.4 Infrared spectroscopy .....	208
4.4 Solution studies of monosulfonamidodiamine ligands .....	208
4.4.1 ESI spectra of monosulfonamidodiamines .....	208
4.4.2 VPO of monosulfonamidodiamine ligands .....	211
4.4.3 Proton nmr of monosulfonamidodiamine ligands .....	213
4.4.4 IR of monosulfonamidodiamine ligands .....	214
4.5 Solution studies of sulfonamido oxime ligands .....	214
4.5.1 ESI spectra of sulfonamido oxime ligands .....	214
4.5.2 VPO of sulfonamido oxime ligands .....	216
4.5.3 Proton nmr of sulfonamido oxime ligands .....	217

4.5.3.1 Preliminary studies.....	217
4.5.3.2 Determination of equilibrium constants for the association ..... of sulfonamido oxime ligands.....	219
4.5.3.3 Thermodynamic data for the association of sulfonamido ..... oxime ligands.....	223
4.5.4.4 Speciation of sulfonamido oxime ligands.....	223
4.6 Conclusions .....	225
4.7 Experimental .....	226
4.7.1 Instrumentation.....	226
4.7.2 Solvent and reagent pretreatment.....	227
4.7.3 Synthesis of sulfinyl chlorides .....	227
4.7.4 Synthesis of sulfinamides and protected amines.....	228
4.7.5 Introduction of a lipophilic group into monosulfonamidodiamines.....	230
4.7.6 Synthesis of alkyl sulfonyl chlorides.....	231
4.7.7 Synthesis of alkyl-substituted arylsulfonyl chlorides.....	232
4.8 References .....	236

## 4.1 Introduction

The X-ray crystal structures of monosulfonamidodiamine ligands and sulfonamido oxime ligands and some of their metal complexes discussed in chapters 2 and 3 have provided very valuable insight into the secondary hydrogen-bonded structures of such ligands. It was the aim of this thesis to look at the importance of a head-to-tail hydrogen-bonded *pseudo*-macrocycle around a metal centre. It was also proposed to examine the importance of the self association of the free ligand in solution prior to complexation and establish whether a preorganised structure aids complexation. In certain cases a *pseudo*-macrocyclic ligand secondary structure was observed in the solid state and although such preorganisation of the ligand was not observed exclusively this does not rule out such interactions in solution. It was therefore considered important to investigate the solution structures of sulfonamido ligands.

## 4.2 Improving ligand solubility

In order to investigate the self assembly properties of monosulfonamidodiamine ligands and their strength and selectivity when used as metal extractants the ligands had to be soluble in a range of solvents. The very low solubility of the sulfonamido diamine and sulfonamido oxime ligands in organic solvents is thought to be due to the polar sulfonyl, amino and oxime groups and also to the extensive *inter*-molecular hydrogen-bonding networks which exist in the solid state. In order to increase ligand solubility in non-polar solvents either the number of hydrogen-bond donors or acceptors, marked in Figure 4.1, could be reduced by replacing the sulfonamido groups in **A** and **B** by the sulfinamido groups in **C** and **D**, or a bulky hydrocarbon group could be introduced into the molecule at R, R<sup>2</sup> or R<sup>3</sup>.

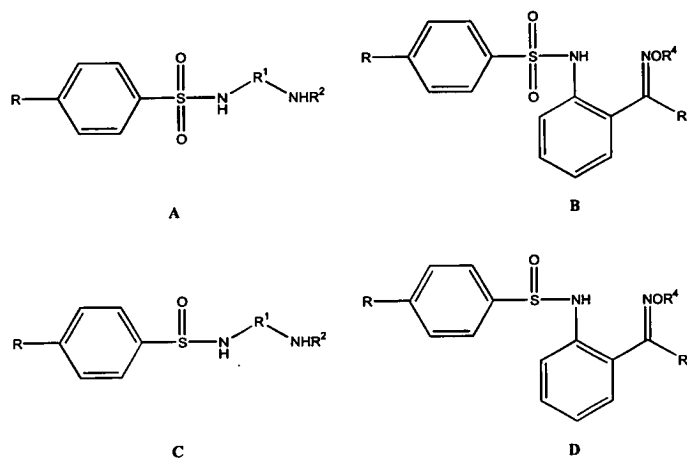
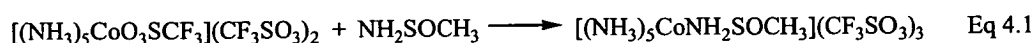


**Figure 4.1:** Hydrogen-bond donor (blue), and acceptor atoms (red), in monosulfonamidodiamine (A) and sulfonamido oxime (B) ligands, and their sulfinamide analogous (C) and (D).

## 4.2.1 Reducing the number of hydrogen-bond donors and acceptors

### 4.2.1.1 An introduction to sulfinamides

One approach to reduce the number of hydrogen-bond donors and acceptors would be to replace sulfonamido groups with sulfinamido groups (see Figure 4.1). It was hoped that this would encourage the formation of more selectively hydrogen-bonded structures and thus, *inter-complex* hydrogen-bonding may be reduced or even prevented leading to an improved solubility. Another reason for attempting the syntheses of such novel sulfinamide ligands was that the coordination chemistry of sulfinamides has been very little explored. Only three papers were found containing such studies.<sup>1,2,3</sup> The most recent paper describes a high yield route to nitrogen bonded sulfinamide complexes using the starting material  $[(\text{NH}_3)_5\text{CoO}_3\text{SCF}_3](\text{CF}_3\text{SO}_3)_2$  and the sulfinamide ligand  $\text{NH}_2\text{SOCH}_3$ .<sup>1</sup> It was found that the use of weakly coordinating solvents led to complexes in which the sulfinamide was coordinated to cobalt through the oxygen atom. In order to produce high yields of N bonded complexes (Equation 4.1) dry dipolar aprotic solvents and sterically hindered, non-coordinating bases had to be used. Uv-vis and  $^1\text{H}$  nmr spectroscopy were used to characterise the complexes formed.



Two earlier studies in the same laboratory were published in 1985.<sup>2,3</sup> In one paper<sup>2</sup> the ligands  $C_6H_5NHSOCH(CH_3)_2$  (**I**),  $C_6H_5NHSOCH_2COO^tBu$  (**II**) and  $C_6H_{11}NHSOCH_2COO^tBu$  (**III**) were complexed to zinc halides in an attempt to model the active site of zinc metalloproteins. The stoichiometry of the complexes was determined as one zinc to two ligands by nmr titration and was confirmed using atomic absorption spectroscopy. It was found that only the sulfinamido oxygen not the carboxyl groups in **II** and **III** are involved in binding to the zinc and that the complexes are tetrahedral with a  $2L : ZnX_2$  stoichiometry. A continuation<sup>3</sup> of this study used ligands of type (**II**), with a substituent, X, on the aromatic ring  $XC_6H_4NHSOCH_2COO^tBu$  where X is *o*-NH<sub>2</sub> (**IV**), *o*-OH (**V**), *m*-OH (**VI**) or *p*-OH (**VII**). <sup>1</sup>H nmr titrations were again used to determine complex stoichiometry and the Zn to L ratios were proved to be 1:1, 1:1, 2:1 and 1:2 for the complexes of ligands **IV** to **VII** respectively. IR techniques were again used to formulate the coordination spheres of the complexes.

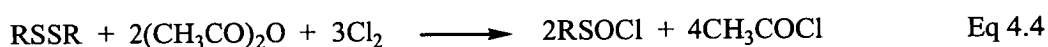
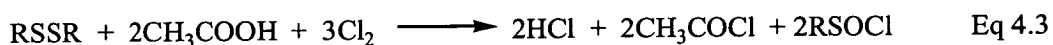
The preparation of sulfinamides is well documented in the literature. They are used as versatile synthetic intermediates,<sup>4</sup> for example in the preparation of racemic and chiral sulfinic acid esters *via* the reaction of sulfinamides with alcohols.<sup>5</sup> They are also an important class of compounds due to their biological activity,<sup>6</sup> the sulfinamide group may be used to replace the amide bond in peptide transition state analogues, as potential peptidase inhibitors or as substrates for the development of catalytic antibodies.<sup>7,8</sup>

Several methods for sulfinamide preparation are published including the use of Grignard reagents,<sup>9,10</sup> azides,<sup>11</sup> and the sulfination of amines with sulfinic acids in the presence of activating reagents such as diphenylphosphorochloridate.<sup>12</sup> However, the majority of papers treat an amine with the relevant sulfinyl chloride, in an anhydrous diethylether medium at 0°C.<sup>13,14,15,5</sup> The latter method was chosen in this project.

Sulfinyl chlorides are not available commercially due to their instability at room temperature. Their synthesis has been widely explored due to their extensive use in the preparation of racemic and optically active sulfinyl derivatives such as sulfinates, thiosulfinates, sulfinamides and sulfoxides.<sup>16</sup> The original preparation was based on the solvolysis of organosulfur trichloride using a hydroxylic solvent such as water (Equation 4.2).<sup>16</sup>



Problems associated with this method such as the isolation of the labile organosulfur trichlorides and the large quantity of HCl produced led to further work by Douglass *et al.*<sup>17,18,19</sup> From 1958 Douglass developed what became the most common procedure of sulfinyl chloride preparation, oxidative chlorination of sulfenyl derivatives (disulfides) in the presence of acetic acid (Equation 4.3) and subsequently in the presence of acetic anhydride (Equation 4.4).<sup>17,18,19</sup> In Equation 4.3 the isolation of the organosulfur trichloride is avoided and it is assumed that it is formed as an intermediate in the reaction. The second reaction, in Equation 4.4, avoids both these problems as no hydrogen chloride gas is formed.



In 1978 an important modification was reported by Schenk and Muller<sup>20</sup> in which chlorine was replaced by sulfuryl chloride. In this thesis sulfinyl chloride precursors were prepared from the related thiols by reaction with sulfuryl chloride in acetic acid at low temperature (Equation 4.5).<sup>21</sup>



This method generates sulfinyl chlorides in quantitative yields from both aliphatic and aromatic thiols whereas the success of the other methods mentioned depends on the nature of the R groups. Taking the starting materials, in the ratios close to those required by Equation 4.5, leads only to a sulfinyl derivative and avoids any possible sulfonamide formation. The thiol starting materials are either commercially available or can be easily synthesised.

Since only low boiling by-products are formed in the reaction (Equation 4.5) the sulfinyl chlorides are easily obtained in high purity. Alkanesulfinyl chlorides can be distilled to give a final pure product. However, aromatic sulfinyl chlorides should not be distilled due to the danger of explosion.<sup>22</sup> This was first reported by Douglass *et al*<sup>22</sup> after the attempted distillation of *p*-toluenesulfinyl chloride. Alkanesulfinyl chlorides should also not be stored in sealed containers at room temperature.<sup>23</sup> Sulfinyl chlorides can disproportionate to the sulfonyl chloride and the sulfenyl chloride. The subsequent self condensation of alkanesulfenyl chloride generates hydrogen chloride gas, among a variety of products, and thus high pressure can develop within the container which can lead to an explosion.

#### 4.2.1.2 Sulfinamide target molecules

The sulfinyl chlorides prepared using the method of Yoon *et al*<sup>21</sup> were 2-methyl-1-propanesulfinyl chloride (42) and 4-methylbenzenesulfinyl chloride (43) (Figure 4.2).

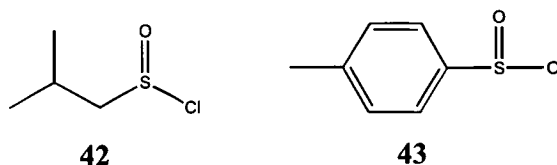


Figure 4.2: 2-methyl-1-propanesulfinyl chloride (42) and 4-methylbenzenesulfinyl chloride (43).

42 and 43 were used in the attempted synthesis of the target molecules shown in Figure 4.3.

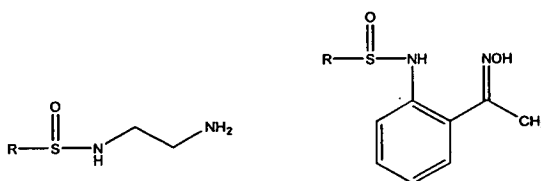
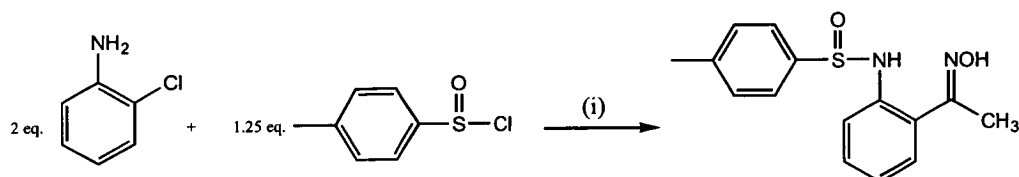


Figure 4.3: Sulfinamide target ligands. R =  $-\text{CH}_2\text{CH}(\text{CH}_3)_2$  or  $-\text{C}_6\text{H}_4\text{CH}_3$ .



### 4.2.1.3 Attempted synthesis of monosulfinamido diamine ligands.

The method of Raiford *et al*<sup>13</sup> was initially followed for the sulfinamide preparation due to the large number of sulfinamides which this paper includes. Reaction of a range of aryl amines were reported of which *o*-chloroaniline (Figure 4.4) is one example.<sup>13</sup> The method involves the treatment of a solution of two equivalents of amine dissolved in three volumes of dry diethylether with 1.25 portions of sulfinyl chloride in two volumes of dry diethylether, with continuous agitation at 0°C (Figure 4.4).<sup>13</sup>



**Figure 4.4:** The method of sulfinamide preparation of Raiford *et al*.<sup>13</sup> (i) Et<sub>2</sub>O, 0°C.

The extra equivalent of the amine is used as a base to mop up the HCl produced. The use of a second equivalent of the amine is also quoted in a paper by van der Marel and Liskamp.<sup>7</sup> When one equivalent of the amine is replaced by pyridine or diisopropylethylamine lower yields resulted.<sup>7</sup>

Following this procedure exactly with 1,2-diaminoethane and 2-methyl-1-propanesulfinyl chloride (Figure 4.5), yielded a mixture of monosubstituted and disubstituted (**44**) sulfinamide products.

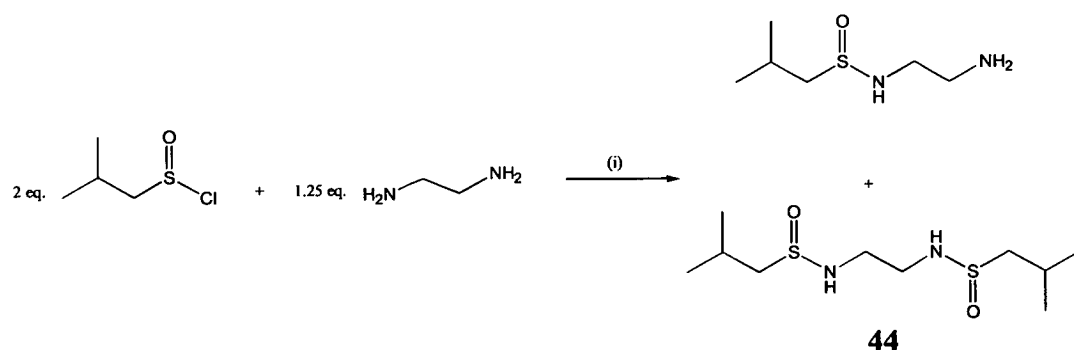


**Figure 4.5:** The reaction of 1,2-diaminoethane and 2-methyl-1-propanesulfinyl chloride. (i) Et<sub>2</sub>O, 0°C.

Isolation of the symmetrical disubstituted sulfonamide was achieved. However, it did not prove possible to isolate the monosubstituted species. A modification of the sulfinyl chloride to amine ratio from 1.25:2, to 3:1 used by Kirsanov *et al*<sup>24</sup> to produce monosubstituted sulfonamidodiamines failed to produce a monosubstituted product. Also, attempts made to replace one mole of the amine with triethylamine or Hunig's base (N,N-diisopropylethylamine) in the attempted synthesis of monosulfonamidodiamine ligands yielded only an intractable oil.

As monosubstitution did not prove possible for 1,2-diaminoethane it was decided to use N-acyl-1,2-diaminoethane as a starting material on the grounds that the acyl group should make the substituted nitrogen less nucleophilic, encouraging formation of the monosulfonamido product. However, the acyl group failed to have the desired effect and <sup>1</sup>H nmr analysis of the product indicated that a mixture of both mono- and di-substituted products were present (Figure 4.6).

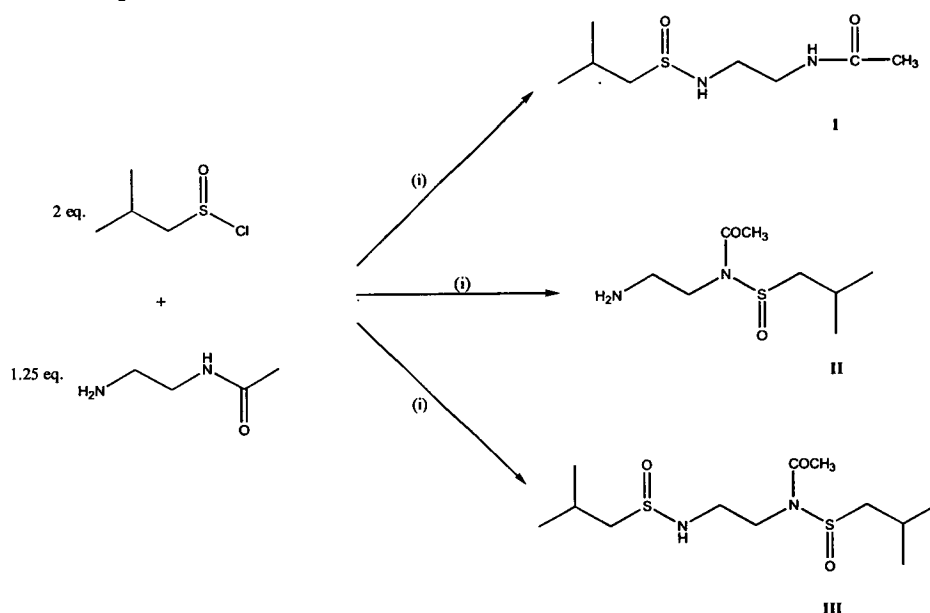


**Figure 4.6:** The attempted synthesis of N-[2-(2-methyl-propane-1-sulfinylamino)-ethyl]-acetamide (I) resulted in a mixture of products I, II and III. (I) Et<sub>2</sub>O, 0°C.

A di-amino starting material with only one amino hydrogen available for substitution was then prepared. The N-acyl-1,2-diaminoethane used previously was treated with phthalic acid anhydride to form the phthalimide, **45** (Figure 4.7).

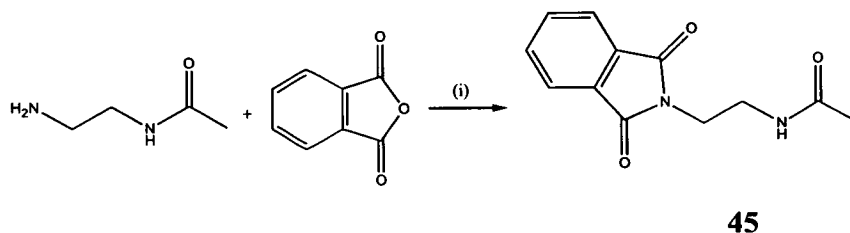


**Figure 4.7:** Protection of the  $\text{NH}_2$  group of the N-acyl-1, 2-diaminoethane. (i) *n*-butyl acetate, 5 hr. reflux.

Phthalimide **45** failed to react with the sulfinyl chloride. This result was surprising as N-acylated sulfonamido systems have been reported to stabilise the sulfonamide group.<sup>8</sup>

The reaction of 1,2-diaminoethane was also tried with 4-methylbenzenesulfinyl chloride, but again only a disubstituted product (**46**) could be isolated. There was very little evidence for the presence of a monosubstituted species. Due to the difficulties encountered in the attempted synthesis of a monosubstituted diaminoalkane ligand the investigation into sulfonamido derivatives of simple diamino ligands was abandoned.

#### 4.2.1.4 Attempted syntheses of sulfonamide oxime ligands

The reaction of one equivalent of 2-methyl-1-propanesulfinyl chloride with one equivalent of 1-(2-aminophenyl)ethanone in diethylether in the presence of one equivalent of triethylamine (Figure 4.8) yielded an intractable brown oil.

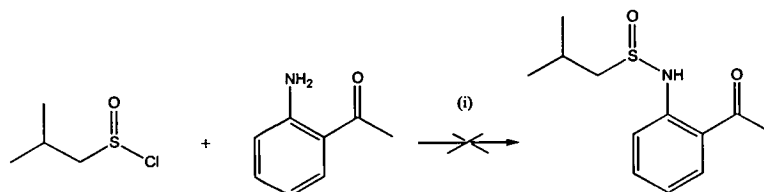


**Figure 4.8:** The failed reaction of one equivalent of 2-methyl-1-propanesulfinyl chloride with one equivalent of 1-(2-aminophenyl)ethanone. (i)  $\text{Et}_2\text{O}$ ,  $0^\circ\text{C}$ , 1 eq.  $\text{Net}_3$ .

The sulfonamide preparation of Raiford *et al*<sup>13</sup> was then applied, using 4-methylbenzenesulfinyl chloride. This resulted in successful synthesis of, **47**.

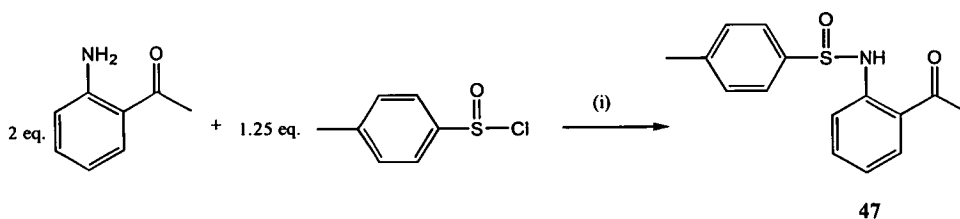


**Figure 4.9:** Synthesis of 1-(2-[N-(4-methylbenzenesulfinamido)]phenyl)ethan-1-one (**47**) (i) Et<sub>2</sub>O, 0°C.

One equivalent of 1-(2-amino-phenyl)-ethanone may be replaced with either triethylamine or potassium carbonate, however this did reduce the yield and purity of the product.

Oximation of the ketone group was attempted using the same method used for sulfonamido oxime ligands described in chapter 3, using the conditions outlined in Figure 4.10.

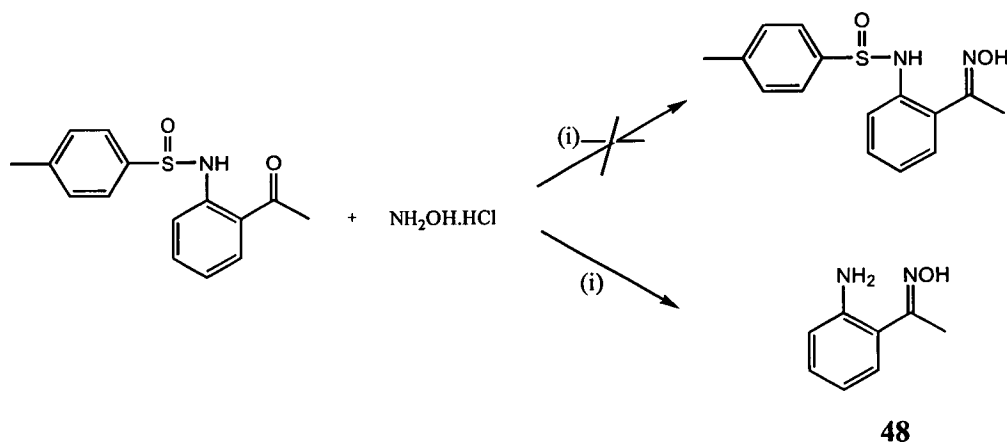


**Figure 4.10:** The attempted oximation of 1-(2-[N-(4-methylbenzenesulfinamido)]phenyl)ethan-1-one, (**47**) results in the formation of 1-(2-aminophenyl)ethan-1-one oxime (**48**). (i) 50:50 pyridine:ethanol, 4 hr. reflux.

The order of sulfonylation and oximation was then reversed but the reaction of 1-(2-aminophenyl)ethanone (**48**) with 4-methylbenzenesulfinyl chloride (Figure 4.11) failed to give the desired material. So too did the comparable methoxy oxime **49**. One of the problems associated with carrying out the reaction of **49** was its low solubility in diethylether.

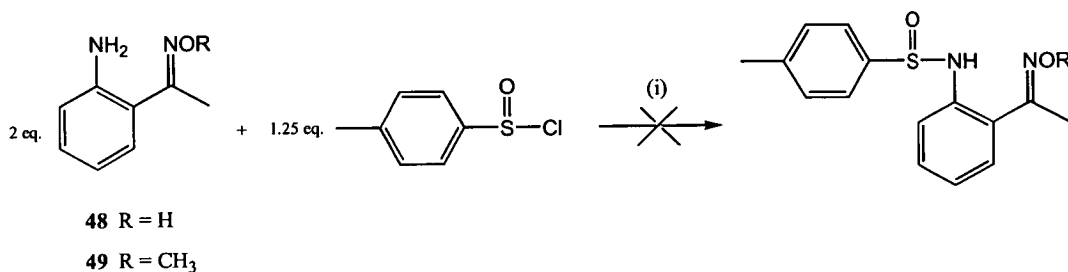


**Figure 4.11:** The attempted reaction of 1-(2-amino-phenyl)-ethanone (**48**) and with 1-(2-amino-phenyl)ethan-1-one O-methyl-oxime (**49**) with 4-methylbenzenesulfonyl chloride. (i) Et<sub>2</sub>O, 0°C.

The attempted syntheses of the sulfonamide oxime target molecule was stopped at this point as the ketosulfonamide **47** had proved to be unstable at ambient temperature, even under a nitrogen atmosphere. Even if the preparation of the target oximes had been achieved it is very likely that these would also be unstable. Consequently, it would have been very difficult to study their coordination chemistry or the hydrogen-bonded secondary structure of the molecules. The propensity of sulfonamides to hydrolyse<sup>25,26</sup> in the presence of acid or base would also have caused problems, making it very difficult to assess the “strength” of sulfonamide extractants by determining “S-curves” [plots of % loading against pH, see section 2.6.1].

#### 4.2.2 Ligand solubilisation by the introduction of a lipophilic group

As the attempted reduction of the number of hydrogen-bond acceptor sites by the replacement of the sulfonamido group by a sulfonamide group proved unsuccessful a second option to increase ligand solubility by the introduction of a lipophilic group was pursued.

##### 4.2.2.1 The introduction of a lipophilic group into monosulfonamidodiamine ligands

The first approach was to modify R, the group at position 4 on the benzenesulfonyl ring. Selected sulfonyl chlorides which have larger R groups than methyl are commercially available and *p-t*-butylbenzenesulfonyl chloride was used to prepare

2. However the solubility of the resulting ligand was very little different from the methyl analogue (Figure 4.12).

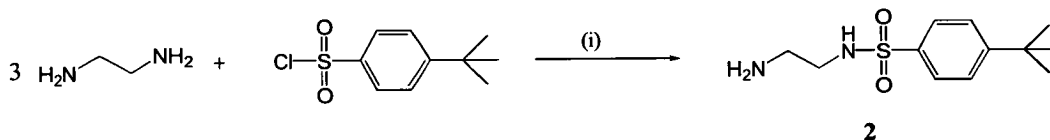


**Figure 4.12:** Synthesis of N-(2-aminoethyl)-4-*t*-butylbenzenesulfonamide (**2**). (i) Toluene, 25°C.

The second approach was to replace one amino hydrogen on the unsulfonated nitrogen atom *via* imination<sup>27</sup> and reduction (Figure 4.13).

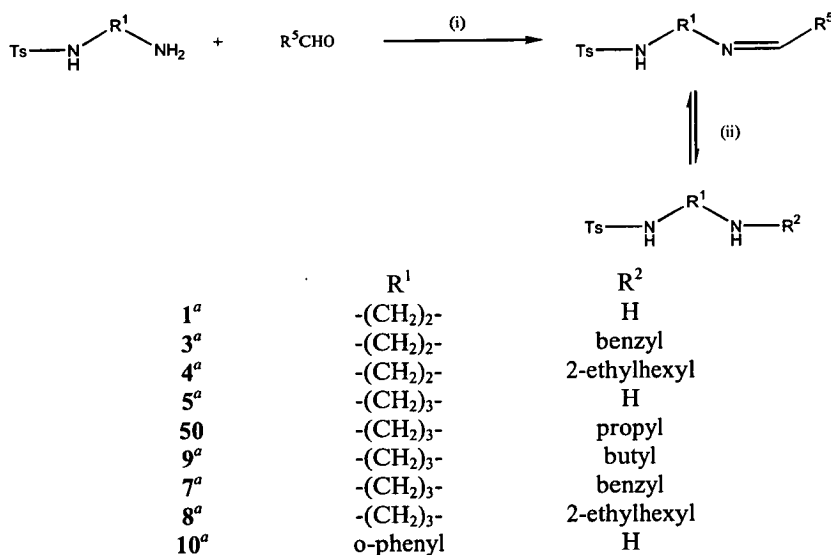


**Figure 4.13:** N-alkylation of the monosulfonamidodiamines *via* imine formation and reduction of the derivatives formed. (i) Ethanol, 25°C. (ii) XS NaBH<sub>4</sub>, catalytic quantity of NaB<sub>4</sub>O<sub>7</sub>. Ts = -SO<sub>2</sub>C<sub>6</sub>H<sub>4</sub>CH<sub>3</sub>. <sup>a</sup> Experimental details of these ligands may be found in experimental section 2.10.3.

The N-propyl (**50**) and N-butyl (**9**) derivatives proved very difficult to purify as they are oily solids which cannot be recrystallised. The N-benzyl derivatives **3** and **7** are crystalline solids but have only marginally greater solubility than the unsubstituted compounds **1** and **5**. Fortunately the addition of the 2-ethylhexyl group, afforded pure products **4** and **8** and also increased the ligand solubility dramatically affording ligands which were soluble in non polar solvents.

### 4.2.2.2 The introduction of a lipophilic group into sulfonamido oxime ligands

Ligands synthesised using commercially available benzenesulfonyl chlorides with large alkyl groups in the *para* position are listed in Figure 4.14.

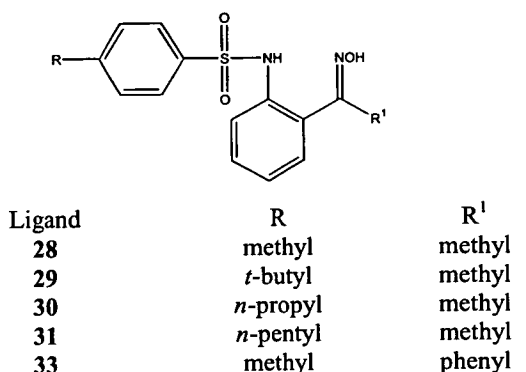


**Figure 4.14:** Sulfonamido oxime ligands synthesised using commercially available sulfonyl chlorides.

Ligands **29-31** have increased solubility over the methyl analogue, **28**. However, they are still insoluble in non polar solvents such as hexane.

### 4.2.3 Synthesis of sulfonyl chlorides

As the commercially available benzenesulfonyl chlorides did not afford sulfonamido oxime ligands of the required solubility the preparation of a sulfonyl chloride with a more lipophilic hydrocarbon group was attempted. Sulfonyl chlorides can be synthesised by a variety of routes.<sup>28</sup>

There are three types of reaction: C-S(VI) bond formation

oxidation

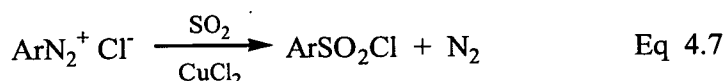
formation from other S(VI) containing compounds.

**Formation of carbon to hexavalent sulfur bonds.** Aryl sulfonyl chlorides may be prepared by reaction of chlorosulfonic acids with aromatic compounds which are activated toward electrophilic attack (Equation 4.6).<sup>29</sup> Low temperatures are necessary to avoid di- and tri- sulfonation of the aromatic ring.

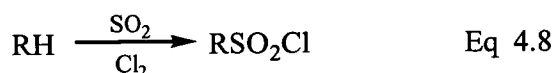


The analogous reactions of aliphatic compounds give lower yields.<sup>30</sup>

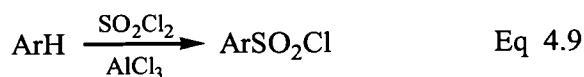
Aromatic diazonium salts on treatment with sulfur dioxide in the presence of copper(II) chloride (Equation 4.7) give arylsulfonyl chlorides.<sup>31</sup>



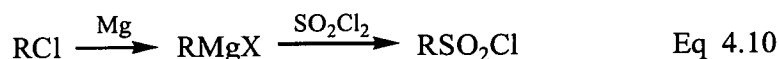
Sulfur dioxide also reacts with aliphatic compounds with the addition of chlorine (Equation 4.8) under conditions which permit formation of radicals.<sup>32</sup> However, a mixture of compounds is achieved.



Sulfonyl chloride may be used to prepare both aromatic and aliphatic sulfonyl chlorides. Aromatic hydrocarbons are treated in the presence of  $\text{AlCl}_3$  (Equation 4.9). Ring chlorination may also occur.<sup>33</sup>



For aliphatic halide molecules, high yields of alkylsulfonyl chlorides are claimed when they are converted into alkyllithium or Grignard reagents (Equation 4.10) and subsequently treated with sulfonyl chloride.<sup>34,35</sup>



The following reactions lead to **sulfonyl chlorides via oxidation**. Alkane sulfinyl chlorides may be oxidised using nitric acid to give the sulfonyl chloride in high yield (Equation 4.11).<sup>36</sup>

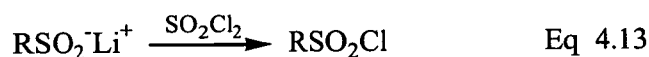


Alternatively arene sulfinic acids and their alkali metal salts may be oxidised using chlorine or copper halides, in water or aqueous acetic acid (Equation 4.12). However, ring chlorination may occur.<sup>37,38</sup>





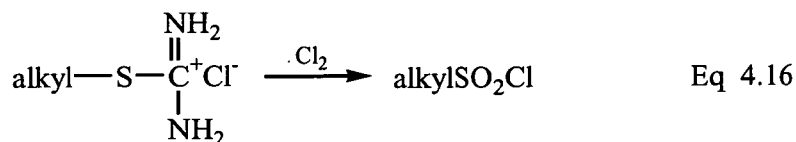
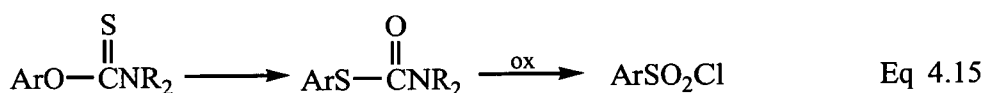
Alkylsulfinate salts, obtained by the reaction of sulfur dioxide with either alkyllithiums or Grignard reagents are converted into sulfonyl chlorides upon reaction with sulfuryl chloride (Equation 4.13).<sup>39</sup> A mixture of thionyl chloride and DMF may also be used.<sup>40</sup>



A classical method is by the oxidation of thiols or disulfides with chlorine in the presence of water, acetic acid or nitric acid (Equation 4.14).<sup>41,42</sup>



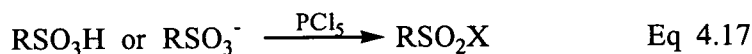
Aromatic and aliphatic sulfonyl chlorides may be prepared by oxidation of a thiocarbamic ester, after Newman-Kwart rearrangement (Equation 4.15)<sup>43</sup> or by treatment of S-alkyl isothiuronium salts with aqueous chlorine (Equation 4.16).<sup>44</sup>



There is some risk of explosion when salts are directly chlorinated<sup>45</sup> and a safer method involves the reduction of the salt to the thiol prior to chlorination.<sup>46</sup>

The oxidation of sulfides, sulfoxides and sulfones to give sulfonyl chlorides is also possible. However, forcing conditions may be required.<sup>47,48,49</sup>

Finally **sulfonyl chlorides** may be prepared from **other S(VI) containing compounds**, most commonly from sulfonic acids and their salts. When  $\text{PCl}_5$  is used side reactions may occur as it is a strong chlorinating agent (Equation 4.17).<sup>50</sup>



$\text{POCl}_3$  may also be used as the chlorinating agent where fewer side reactions occur.<sup>51</sup>

### 4.2.3.1 2-Ethylhexylsulfonyl chloride

It was hoped that the 2-ethylhexyl group, used to solubilise monosulfonamidodiamines *via* N-substitution, would improve the solubility of sulfonamido oximes and the synthesis of 2-ethylhexylsulfonyl chloride (**51**) was attempted (Figure 4.15).

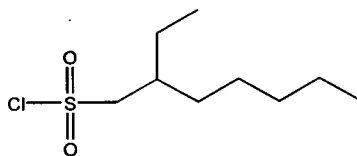


Figure 4.15: 2-Ethylhexylsulfonyl chloride (**51**)

It was decided to prepare the 2-ethylhexane sulfonate salt which would then be chlorinated. The Strecker<sup>52</sup> method to prepare the sodium salt of 2-ethylhexane sulfonic acid from 1-bromo-2-ethylhexane proved unsuccessful (Figure 4.16).

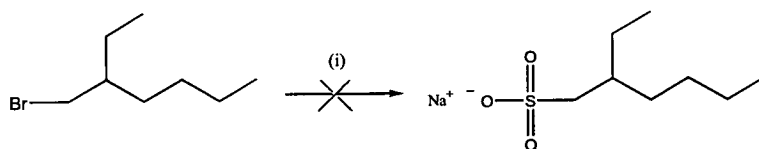
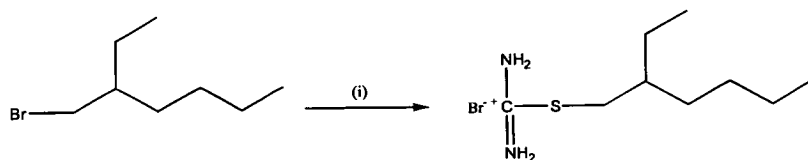


Figure 4.16: Attempted preparation of 2-ethylhexyl sodium sulfonate by the Strecker synthesis. (i)  $\text{Na}_2\text{SO}_3$ ,  $\text{H}_2\text{O}$ , reflux.

The failure of this reaction was probably due to the insolubility of 2-ethylhexyl bromide in water. However, the reaction did not succeed even when a 3:1 water:ethanol medium was used. It has been reported that poor yields are obtained in the preparation of sulfonate salts from alkyl halides with chains containing more than five carbon atoms<sup>53,54</sup> *via* the Hemilian method in which the sodium sulfate is replaced by ammonium sulfate.

Due to the limited commercial availability of alkyl sulfonic acids Ziegler *et al* developed a route to alkylsulfonyl chlorides *via* the chlorination of thiols prepared from alkylisothiuronium salts.<sup>46</sup> Alkylisothiuronium salts may be easily obtained from the reaction of alkylhalides with thiourea (Figure 4.17).<sup>46</sup>



**Figure 4.17:** Synthesis of 2-ethylhexylisothiuronium bromide. (i)  $\text{NH}_2\text{CSNH}_2$ , EtOH, 12 hr. reflux.

Alkylisothiuronium salts may be directly chlorinated, but this can be hazardous due to the explosive nitrogen trichloride which can be produced.<sup>55</sup> Ziegler avoided this problem by the reducing of the alkylisothiuronium salt to a thiol prior to chlorination, as shown in Figure 4.18.<sup>46</sup>

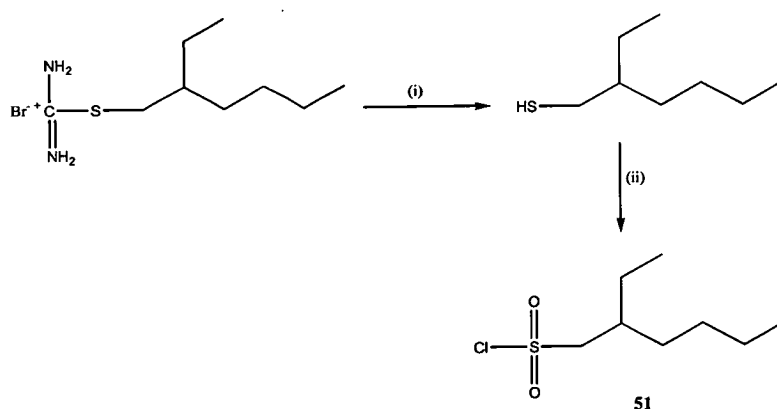


**Figure 4.18:** The preparation of 2-ethylhexylsulfonyl chloride (**51**) based on the method of Ziegler.<sup>46</sup>  
(i)  $\text{H}_2\text{O}$ , NaOH. (ii) ice,  $\text{CH}_3\text{COOH}$ ,  $\text{Cl}_{2(\text{g})}$ .

The desired sulfonyl chloride was obtained in good yield, 54%, and purified by distillation. Reaction with 1-(2-aminophenyl)ethanone produced the sulfonamide 1-{2-[N-(2-ethylhexanesulfonamido)]phenyl}ethan-1-one. This intermediate could not be isolated in a pure form and was used crude in the oximation reaction to yield the target molecule as an impure yellow oil (Figure 4.19).

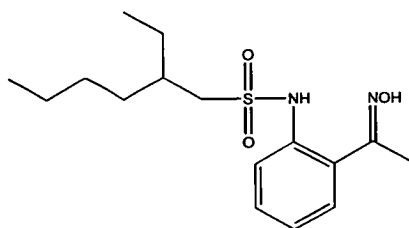


**Figure 4.19:** 1-{2-[N-(2-ethylhexanesulfonamido)]phenyl}ethan-1-one oxime.

1-{2-[N-(2-ethylhexanesulfonamido)]phenyl}ethan-1-one oxime proved very difficult to purify and also discoloured from pale yellow to red overnight suggesting

that the compound was unstable. For these reasons it was decided to investigate the synthesis of aromatic sulfonyl chlorides which were known to afford stable sulfonamido oxime products.

#### 4.2.3.2 Synthesis of aryl sulfonyl chlorides

The development of a convenient method for the synthesis of aryl sulfonyl chlorides with a chosen length of alkyl chain at the *para* position to the sulfonyl group was attempted. The first step was to attach an appropriate alkyl group to a benzene ring. The well known Friedel Crafts alkylation reaction is known to produce a mixture of products.<sup>56</sup> A recent publication by Taylor *et al*<sup>57</sup> covers the addition of organolithium reagents to styrene to produce pure alkylbenzene derivatives of higher yield than analogous reported Friedel Craft reactions. This procedure was followed. The first target molecule was tetradecylbenzene (**52**). Dodecyl lithium was prepared and then added to a solution of styrene (Figure 4.20).

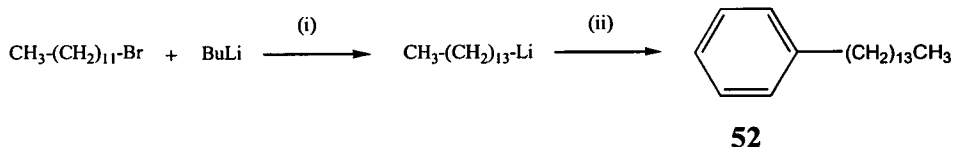


**Figure 4.20:** The synthesis of tetradecylbenzene (**52**). (i) Et<sub>2</sub>O, -78°C, N<sub>2</sub>. (ii) Styrene, -25°C.

Addition of the sulfonyl chloride group was achieved using chlorosulfonic acid (Figure 4.21).<sup>58</sup>

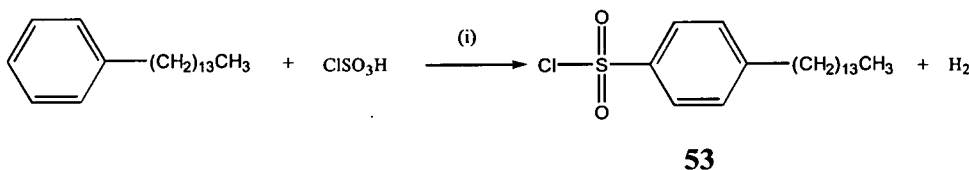


**Figure 4.21:** The preparation of 4-tetradecylbenzenesulfonyl chloride (**53**). (i) Chloroform, 25°C.

The chloride was purified using Kugelrohr techniques before it was reacted with 1-(2-amino-phenyl)-ethanone to produce 1-{2-[N-(4-tetradecylbenzenesulfonamido)]phenyl}ethan-1-one. This could not be isolated as a pure form and the crude product was oximated to produce the target molecule 1-{2-[N-(4-tetradecylbenzene sulfonamido)]phenyl}ethan-1-one oxime (Figure 4.22).

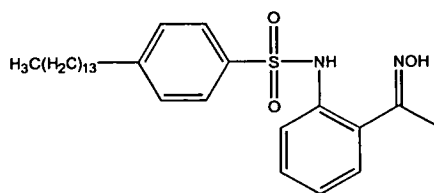
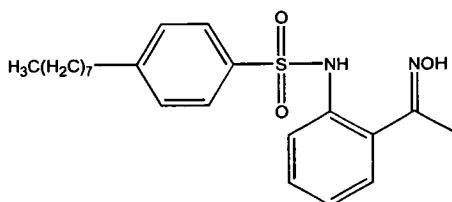


**Figure 4.22:** 1-{2-[N-(4-tetradecylbenzenesulfonamido)]phenyl}ethan-1-one oxime.

Again the sulfonamido oxime proved extremely difficult to purify. The boiling point of the molecule was too high for purification by distillation and chromatography techniques proved unsuccessful.

Preparation of the *n*-octyl analogue, 1-{2-[N-(4-octylbenzenesulfonamido)]phenyl}ethan-1-one oxime (**54**) was then attempted (Figure 4.23).



**54**

**Figure 4.23:** Target molecule 1-{2-[N-(4-octylbenzenesulfonamido)]phenyl}ethan-1-one oxime (**54**).

Commercially available sodium 4-octylsulfonate was used as the precursor. Alkyl sulfonate salts may be chlorinated by a variety of methods (see 4.2.2.3). Phosphoryl chloride was chosen to yield 4-octylbenzenesulfonyl chloride (**55**) (Figure 4.24).<sup>59</sup>

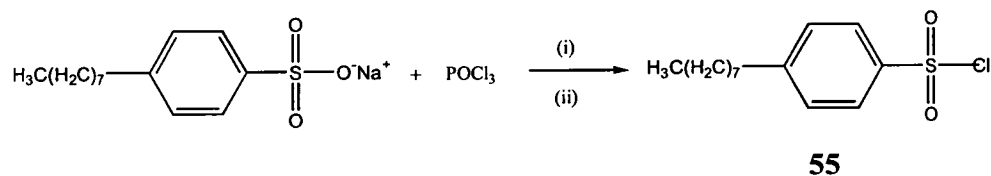
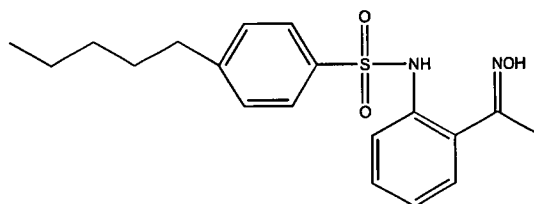


**Figure 4.24:** Synthesis of 4-octylbenzenesulfonyl chloride (**55**). (i) 170°C, 1 hr. (ii) Dichloroethane, 30 min. reflux.

A clean product was obtained and used without purification in the reaction with 1-(2-aminophenyl)ethanone to produce the sulfonamido intermediate 1-{2-[N-(4-octylbenzenesulfonamido)]phenyl}ethan-1-one (**56**). Oximation of **56** yielded target molecule **54**. Again, however, the product proved very difficult to purify.

At this stage the situation was reviewed. It was apparent that ligands with sufficiently large alkyl substituents to ensure solubility in hexane and related hydrocarbons could not be obtained readily in a purity which would make colligative property measurement reliable. Consequently it was decided to investigate association phenomena in solution in other types of solvent. The pure ligand **31** was used in these studies (Figure 4.25).



**31**

**Figure 4.25:** 1-(2-[N-(4-pentylbenzenesulfonamido)]phenyl)ethan-1-one oxime (**31**)

### 4.3 Investigation of ligand association in solution.

There are several ways in which association of molecules in solution may be explored. The methods below allowed a study of the behaviour of both monosulfonamidodiamine and sulfonamido oxime ligands.

#### 4.3.1 Electrospray ionisation mass spectrometry

Electrospray ionisation spectrometry has emerged as a very useful technique<sup>60</sup> which allows detection of supramolecular species which are held together only by non covalent interactions.<sup>61</sup> The sensitivity of the technique allows analysis of very dilute samples, the mild nature of the ionisation process also minimises fragmentation of the parent species and even allows the analysis of ionic transition-metal complexes which often undergo reduction during the ionisation.<sup>62</sup> Due to its ability to produce multiply-charged species it can be applied to the characterisation of very high molecular weight compounds.<sup>63</sup>

### 4.3.2 Vapour pressure osmometry

The association of molecules in solution causes the vapour pressure to increase. By measuring this change using “vapour pressure osmometry” the average mass of the species in solution may be determined indicating the degree of aggregation. The technique may be used simply to find the average mass in solution or if, several readings at different concentrations and at different temperatures are taken, both equilibrium constants and thermodynamic information may be achieved. Vapour pressure osmometry (VPO) has been used to study the solution structure of commercial metal extractants.<sup>64,65</sup> A knowledge of the processes taking place in solution and the stoichiometry of the extracted species is very important in solvent extraction processes in order to define optimal conditions for the unit operations of separation and concentration.<sup>64</sup> For example, VPO was used to establish whether Cyanex 272, 302 and 301 extractants (Figure 4.26) exist as dimers or monomers in toluene.<sup>65</sup>

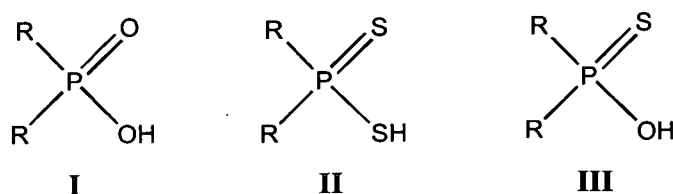


Figure 4.26: The commercial reagents cyanex 272 (I), 302 (II) and 301 (III).

It was found that while **I** and **III** exist as dimers, **II** is a monomer presumably due to the poor hydrogen-bond donor and acceptor properties of the thiol and thiophosphoryl groups. The solution behaviour of additives used in solvent extraction have also been studied by VPO.<sup>66</sup> Vapour pressure osmometry may also be applied to study molecules of biological importance such as cholesterol<sup>67</sup> and inorganic materials.<sup>68</sup>

### 4.3.3 NMR spectroscopy

Variable concentration and variable temperature proton nmr have been widely used to look at the association of species in solution.<sup>69,70,71,72</sup> The technique has been used to study a variety of systems such as cyclodextrins<sup>69</sup> or more drug molecules and nucleotides.<sup>70</sup> A proton involved in hydrogen-bonding will exhibit a downfield shift

due to deshielding by the hydrogen-bond acceptor and proton nmr may be applied to systems where two or more species are present in addition to studying the self association of molecules.<sup>71</sup> Two dimensional correlation spectroscopy and nuclear Overhauser effect spectroscopy may also be used to study interactions based on the combination of  $\pi$  stacking and hydrogen-bonding *e.g.* in model systems for nucleotides.<sup>72</sup>

#### 4.3.4 Infrared spectroscopy

Infrared spectroscopy is also a useful tool to study the association of molecules, both in the solid state and in solution. A shift in a peak in an IR spectrum with a change in concentration or the addition of a second species to the solution indicates a change in the strength of the bond which can be interpreted in terms of the atoms being involved in more or less hydrogen-bonding interactions. Most studies reported have used organic solutions,<sup>73,74</sup> usually carbon tetrachloride, as a convenient medium however the technique may also be applied to study molecules in such solvents as supercritical carbon dioxide.<sup>75</sup>

### 4.4 Solution studies of monosulfonamidodiamine ligands

#### 4.4.1 ESI spectra of monosulfonamidodiamines

ESI spectra were recorded using  $1 \times 10^{-6}$  M samples of ligands **1**, **5**, **4** and **8** in methanol (Figures 4.27-4.30).



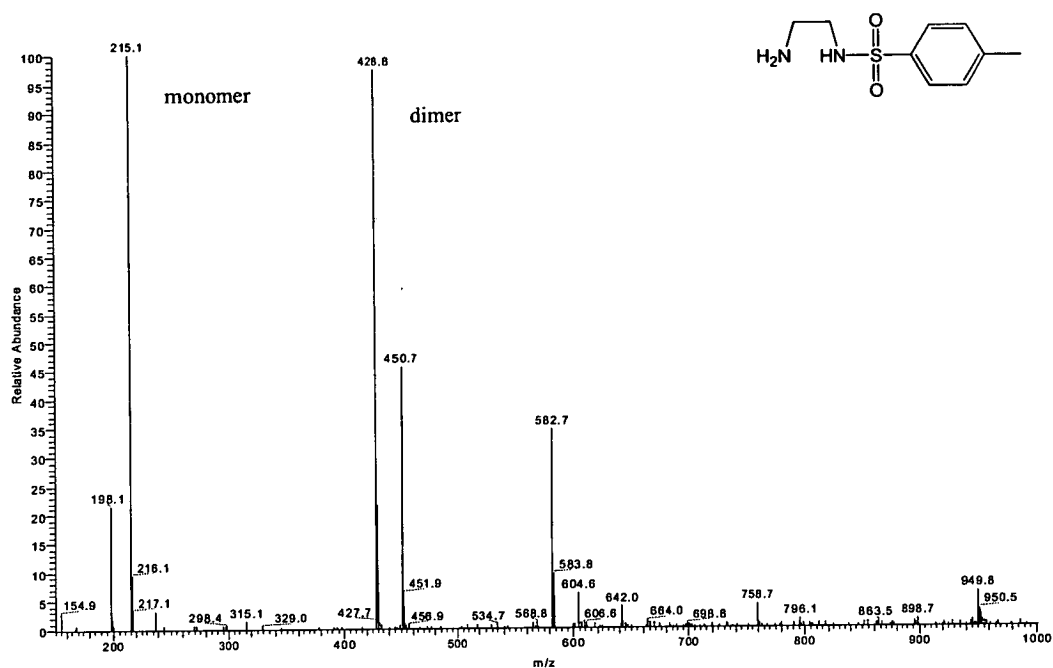


Figure 4.27: ESI spectrum of a  $1 \times 10^{-6}$  M methanolic solution of (N-(2-amino-ethyl)-4-methylbenzenesulfonamide) (1).

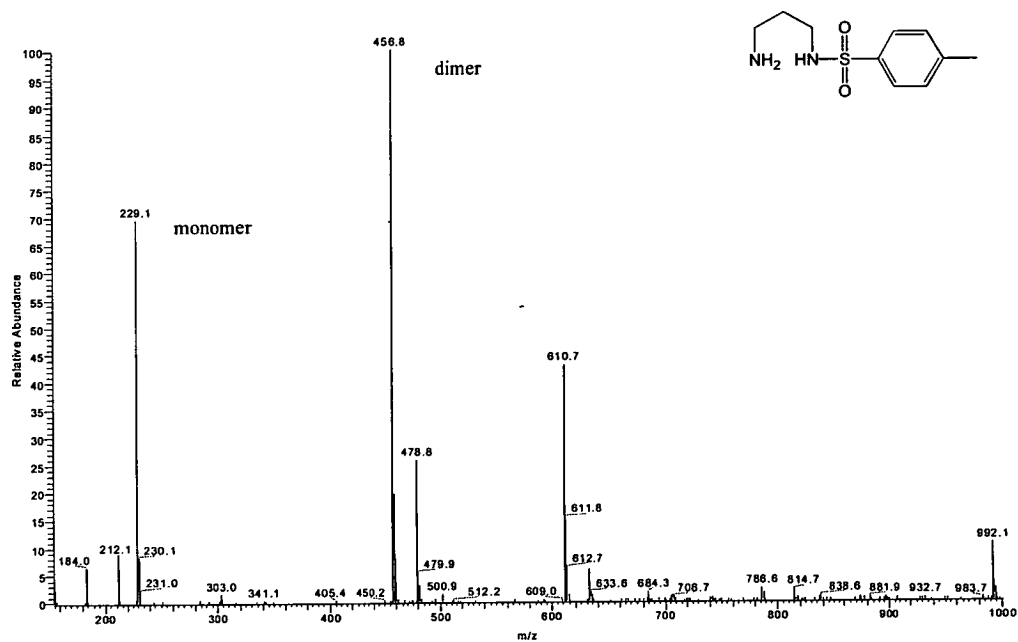


Figure 4.28: ESI spectrum of a  $1 \times 10^{-6}$  M methanolic solution N-(3-aminopropyl)-4-methylbenzenesulfonamide (5).

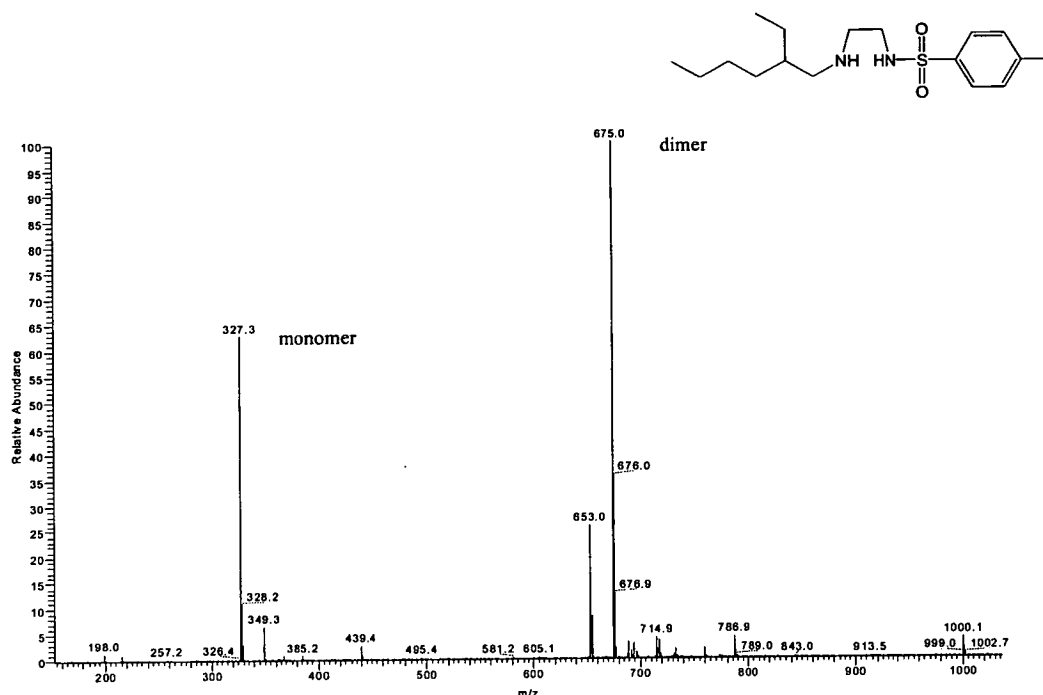


Figure 4.29: ESI spectrum of a  $1 \times 10^{-6}$  M methanolic solution N-(N-2-ethylhexyl-2-aminoethyl)-4-methylbenzenesulfonamide (4).

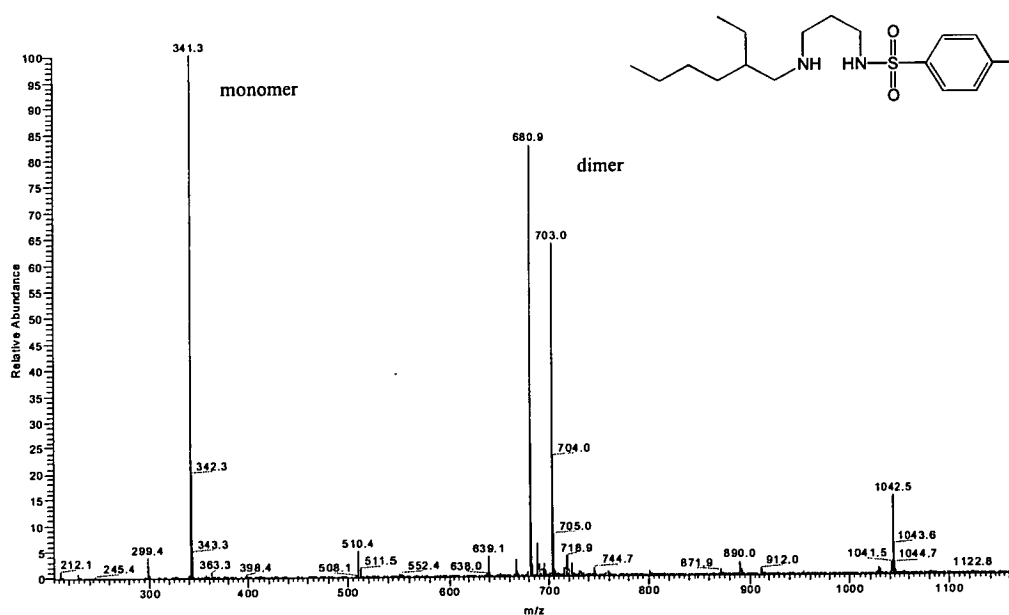


Figure 4.30: ESI spectrum of a  $1 \times 10^{-6}$  M methanolic N-(N-2-ethylhexyl-3-aminopropyl)-4-methylbenzenesulfonamide (8).

Each spectrum displays peaks for a monomer and a dimer species in solution. These results are encouraging, however at best they are qualitative. Although the

concentration of the initial ligand solution was known, molecular ions are produced by evaporation of the solvent until the droplets are reduced in size (Figure 4.31) to the point at which desolvation may be aided by repulsive Coulombic forces overcoming the cohesive forces of the droplet.<sup>76</sup> Therefore the concentration of ligand is much higher prior to detection and it must be remembered that such dimer peaks may be a product of the ESI technique only.

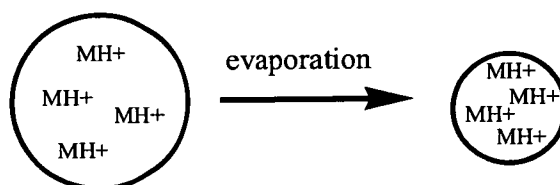


Figure 4.31: Reduction in droplet size using the ESI technique.

#### 4.4.2 VPO of monosulfonamidodiamine ligands

Preliminary VPO studies on ligands **1**, **5** and **10** were carried out in chloroform due to their limited solubility in other solvents (Figure 4.32). These preliminary studies were carried out to confirm that VPO could be used to follow association phenomenon before undertaking the preparation of ligands with solubility in a range of organic solvents. Results for all VPO measurements in this chapter are tabulated in Appendix I.

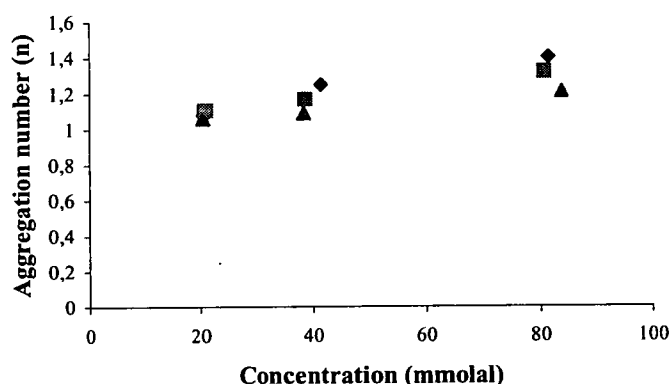
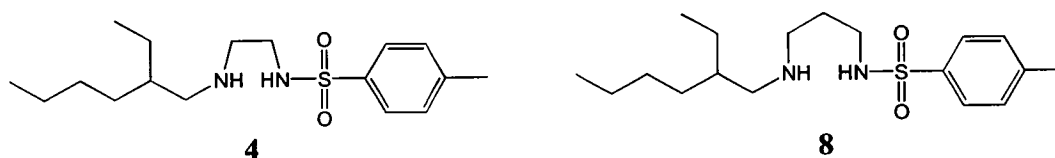


Figure 4.32: The aggregation number ( $n$ ), determined by VPO as a function of concentration for ligands (N-(2-aminoethyl)-4-methylbenzenesulfonamide)  $\blacklozenge$  (**1**), N-(3-aminopropyl)-4-methylbenzenesulfonamide  $\blacksquare$  (**5**), and N-(2-aminophenyl)-4-methylbenzenesulfonamide  $\blacktriangle$  (**10**). [ $n$  is determined by the division of the experimentally determined value for the average mass in solution by the relative molecular mass.]

At a concentration of 20 mmolal the aggregation number of each species is very similar. As the concentration increases the value of  $n$  also increases indicating more aggregation in solution. Aggregation of ligand **1** increases with concentration slightly more rapidly than **5** or **10**.

Measurement of monosulfonamido diamines in solvents of different polarity was made possible by the introduction of a 2-ethylhexane group into ligands **1** and **5** (Figure 4.33).



**Figure 4.33:** Monosulfonamidodiamino ligands N-(N-(2-ethylhexyl-2-aminoethyl)-4-methylbenzenesulfonamide (**4**) and N-(N-(2-ethylhexyl-3-aminopropyl)-4-methylbenzenesulfonamide (**8**).

Measurements were made in cyclohexane, toluene, chloroform, acetone and acetonitrile (dielectric constants are 2.0, 2.4, 4.8, 20.7 and 37.5 respectively<sup>77</sup>). It was expected that as the dielectric constant of the solvent increased a lower ligand-aggregation would be observed, however it must be remembered that this is not always the case. Results are plotted in Figures 4.34 and 4.35.

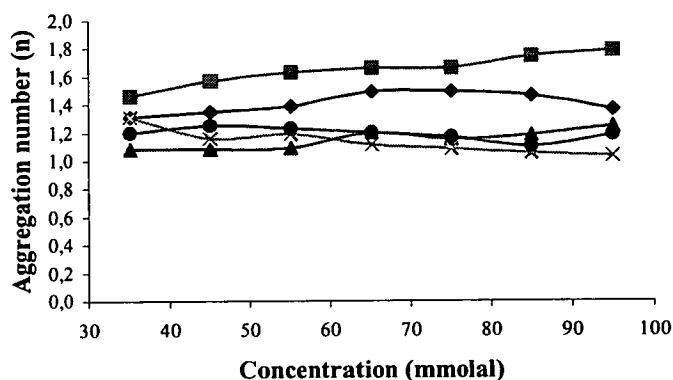


**Figure 4.34:** The aggregation number ( $n$ ), determined by VPO, of N-(N-(2-ethylhexyl-2-aminoethyl)-4-methylbenzenesulfonamide (**4**) in cyclohexane ■, toluene ◆, acetone ●, chloroform ▲ and acetonitrile x.

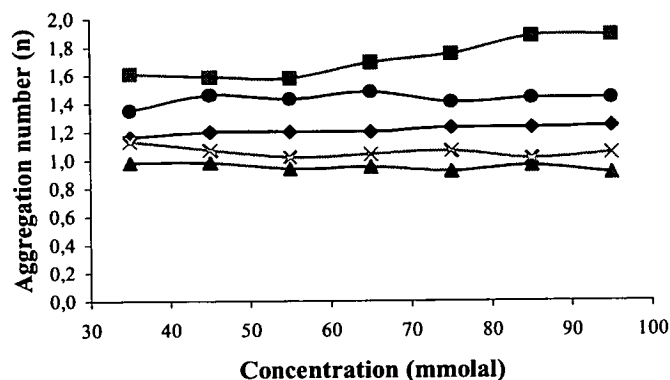


**Figure 4.35:** The aggregation number ( $n$ ), determined by VPO, of *N*-(*N*-2-ethylhexyl-3-aminopropyl)-4-methylbenzenesulfonamide (**8**) in cyclohexane ■, toluene ◆, acetone ●, chloroform ▲ and acetonitrile x.

The highest aggregation numbers for both **4** and **8** are observed in cyclohexane solution. Ligand **4** shows the expected trend in aggregation with solvent at high concentration and significantly higher aggregation numbers are observed for the non polar cyclohexane and toluene solutions. However at low concentration it is surprising to see more aggregation in acetone and acetonitrile over chloroform considering their much higher dielectric constants. Ligand **8** shows a different picture and aggregation cannot be explained by a change in dielectric constant. The lower aggregation in toluene than acetone found for **8** has been observed before at Edinburgh with 2-hydroxyphenyl oxime ligands.<sup>78</sup>

#### 4.4.3 Proton nmr of monosulfonamidodiamine ligands

Analysis of the behaviour of monosulfonamidodiamines in solution by proton nmr did not prove possible because the peak for the amino protons is not observed in chloroform- $d_1$  or toluene- $d_8$  and only a very broad peak is observed in acetonitrile- $d_3$ . The position of amino hydrogen atoms is unpredictable as it depends on the extent to which the hydrogen atoms are involved in hydrogen-bonding.<sup>79</sup>

#### 4.4.4 IR of monosulfonamidodiamine ligands

IR spectra of ligands **4** and **8** were recorded at a concentration of  $5 \times 10^{-1}$  M in dimethylsulfoxide, acetonitrile, acetone, chloroform, toluene and cyclohexane. The wave numbers of the N-H peak were recorded and are listed in Table 4.1.

**Table 4.1:** Amino peaks ( $\text{cm}^{-1}$ ) for 0.5 M solutions of ligands **4** and **8** in different solvents. <sup>a</sup> In some solvents the amino peak was not clearly observed for **8**.

Solvent & dielectric constant	DMSO	Acetonitrile	Acetone	Chloroform	Toluene	Cyclohexane
<b>4</b>	45.0	37.5	20.7	4.8	2.4	2.0
<b>8<sup>a</sup></b>	—	—	3271.6	—	3288.0	3290.9

As the amino proton becomes more involved in hydrogen-bonding the N-H bond is expected to become weaker and will be seen at lower  $\nu$  in the IR spectrum. As the dielectric constant of a solvent is reduced it is expected that more inter-ligand hydrogen-bonding will be observed. For **4** this appears to be the case as moving from left to right along the table energy associated with the wave number for the N-H stretch decreases. The high degree of hydrogen-bonding in these solvents may be attributed to the solvents themselves being involved in hydrogen-bonding with the amino group. Trends are less clear for **8** because the N-H stretching band could not be observed in several solvents.

### 4.5 Solution studies of sulfonamido oxime ligands

#### 4.5.1 ESI spectra of sulfonamido oxime ligands

ESI spectra were recorded using  $1 \times 10^{-6}$  M samples of ligands **28**, **33** and **32** in methanol (Figures 4.36-4.38).

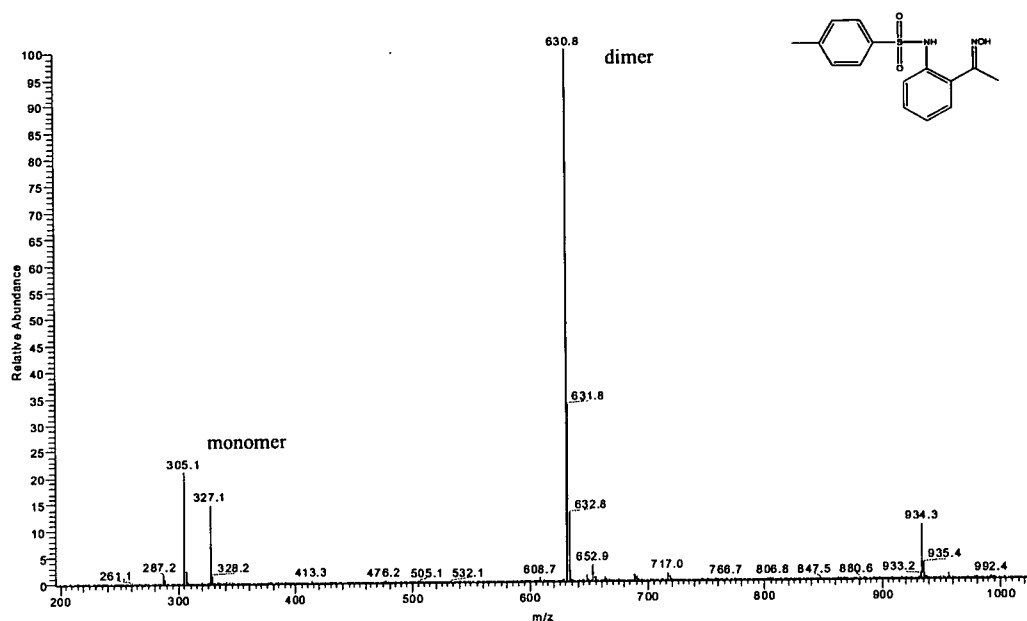


Figure 4.36: ESI spectrum of a  $1 \times 10^{-6}$  M methanolic solution of 1-{2-[N-(4-methylbenzenesulfonamido)]phenyl}ethan-1-one oxime (28).

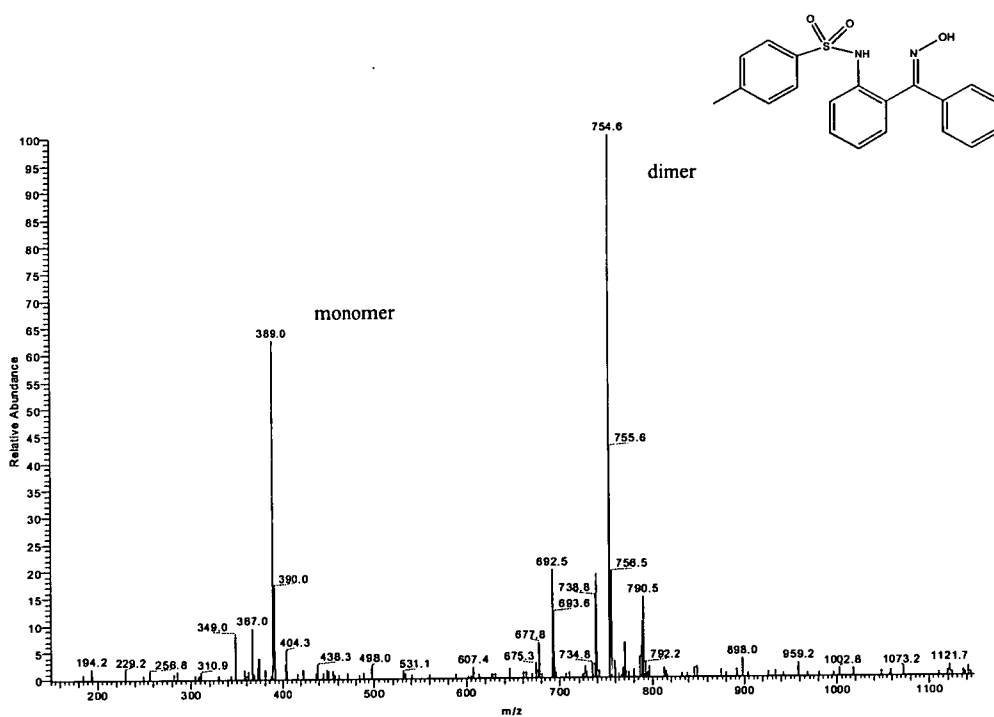
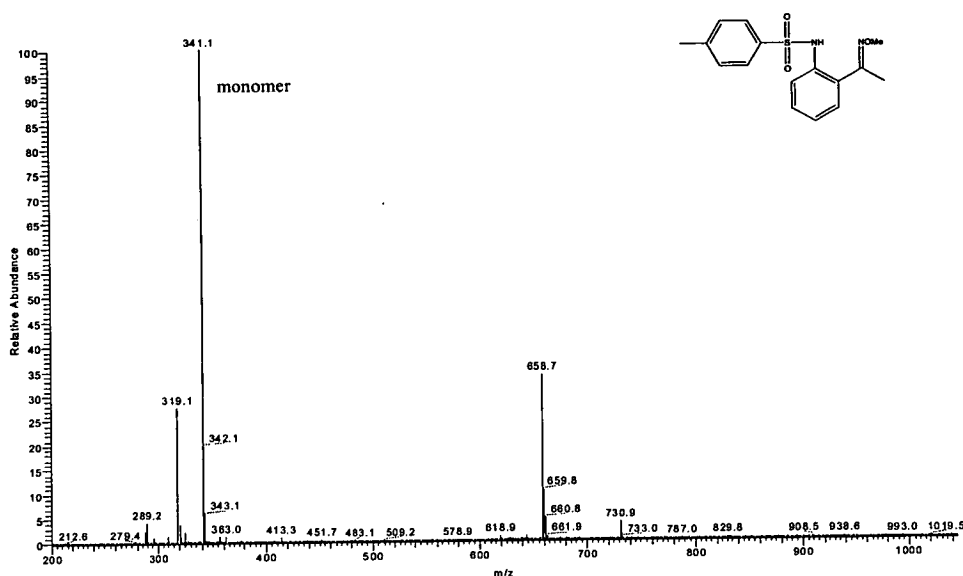


Figure 4.37: ESI spectrum of a  $1 \times 10^{-6}$  M methanolic solution of 1-{2-[N-(4-methylbenzenesulfonamido)]phenyl}(phenyl)methanone oxime (33).



**Figure 4.38:** ESI spectrum of a  $1 \times 10^{-6}$  M methanolic solution of 1-(2-[N-(4-methylbenzenesulfamido)]phenyl)ethan-1-one O-methyl oxime (**32**)

ESI spectra of sulfonamido oxime ligands show evidence for the formation of a dimer species. It is interesting to note that a peak for a species with a mass slightly higher than the value expected for a dimer is observed for **32**. These results are again consistent with the formation of associated species but given the nature of the technique do not prove that such behaviour occurs in solvents and under conditions of use which relate to extraction.

#### 4.5.2 VPO of sulfonamido oxime ligands

Only sulfonamido oxime ligands **28** and **33** were studied using VPO. Due to their limited solubility results were recorded at only three different osmolalities in chloroform solution, (Figure 4.39).



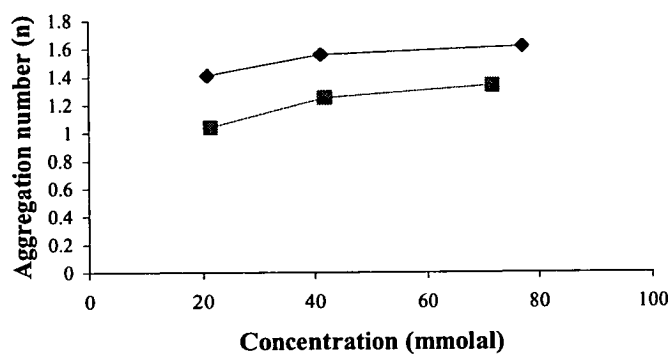


**Figure 4.38:** The aggregation number ( $n$ ), [where  $n$  is the average mass determined in solution divided by the relative molecular mass of the molecule] determined by VPO for 1-{2-[N-(4-methylbenzenesulfonamido)]phenyl}ethan-1-one oxime (**28**) ■ and 1-{2-[N-(4-methylbenzenesulfonamido)]phenyl}(phenyl)methanone oxime (**33**) ◆ in chloroform.

Ligand **33** is shown to have a higher aggregation number than **28**. This may be due to the second (*Z*) isomer of **33** which is also present in solution (Figure 4.40).

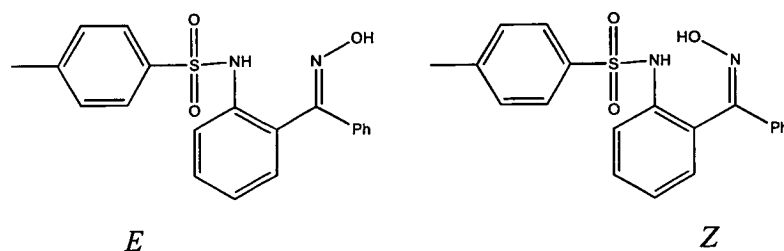


**Figure 4.40:** *E* and *Z* isomers of **33**.

In **28** the oxime has *E* configuration and the X-ray structures of each sulfonamido oxime ligand of this configuration show only hydrogen-bonded dimerisation in the solid state (chapter 3). However, for **33** the X-ray structure of a *Z* isomer was also obtained and here the oxime is involved in a hydrogen-bonded oligomeric secondary structure. If this is also occurring in solution a higher value of  $n$  would be expected for **33** in comparison with **28**.

### 4.5.3 Proton nmr of sulfonamido oxime ligands

#### 4.5.3.1 Preliminary studies

A preliminary nmr study on sulfonamido oxime ligands was undertaken using 1-{2-[N-(4-methylbenzenesulfonamido)]phenyl}ethan-1-one oxime (**28**) and 1-{2-[N-(4-

methylbenzenesulfonamido)phenyl}}(phenyl)methanone oxime (**33**) in chloroform. [All data for the nmr experiments in this chapter may be found in Appendix II.] Peaks for the oximic proton and the sulfonamido proton were easily identified and spectra were recorded at different concentrations (Figure 4.41). Spectra were also run on ligand **32** in which the hydroxy oxime group has been replaced by a methoxy oxime group, however no change was observed in the spectra with concentration.

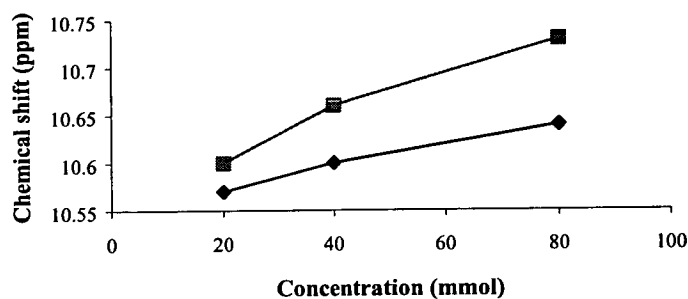
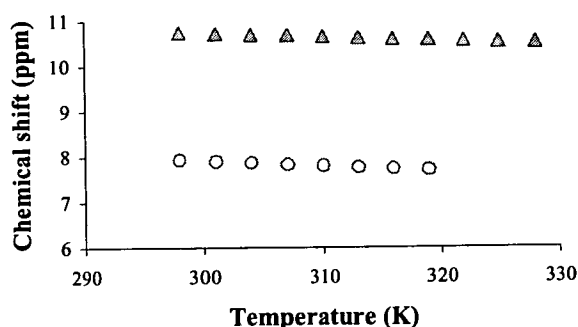


Figure 4.41: Change in chemical shift of the oximic proton of 1-{2-[N-(4-methylbenzenesulfonamido)] phenyl}ethan-1-one oxime (**28**) ■ and 1-{2-[N-(4-methylbenzenesulfonamido)phenyl}}(phenyl)methanone oxime (**33**) ◆ in chloroform.

The data plotted in Figure 4.41 for 1-{2-[N-(4-methylbenzenesulfonamido)]phenyl} (phenyl)methanone oxime (**33**) are for the predominant *E* isomer. Because pure samples of the *E* and *Z* isomers of **33** were not available no further studies of **33** were done as the other isomer present could lead to complex association behaviour.

It was expected that the chemical shifts of protons involved in hydrogen-bonding would move to higher field with increasing temperature, indicating that they are less involved in hydrogen-bonding. This was shown to be the case for 1-{2-[N-(4-methylbenzenesulfonamido)]phenyl}ethan-1-one oxime (**28**) (Figure 4.42).



**Figure 4.42:** The change in chemical shift of the oximic proton  $\blacktriangle$  and the sulfonamido proton  $\circ$  of 1-{2-[N-(4-methylbenzenesulfonamido)] phenyl}ethan-1-one oxime (**28**) with temperature of a 70 mM chloroform solution.

#### 4.5.3.2 Determination of equilibrium constants for the association of sulfonamido oxime ligands

Following the success of these preliminary experiments, more comprehensive studies on the behaviour of 1-{2-[N-(4-methylbenzenesulfonamido)]phenyl}ethan-1-one oxime (**28**) in chloroform and of 1-{2-[N-(4-pentylbenzenesulfonamido)]phenyl}ethan-1-one oxime (**31**) in deuterated chloroform, toluene and acetonitrile were carried out. The plot in Figure 4.43 shows the very similar behaviours in chloroform solution of ligand **28** and its more soluble analogue **31**.

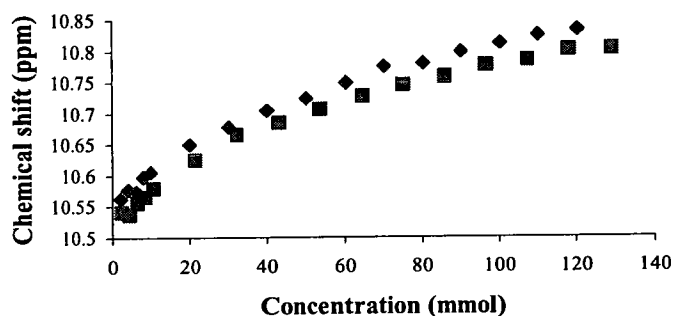


**Figure 4.43:** Chemical shifts of 1-{2-[N-(4-methylbenzenesulfonamido)]phenyl}ethan-1-one oxime (**28**)  $\blacksquare$ , and of 1-{2-[N-(4-pentylbenzenesulfonamido)]phenyl}ethan-1-one oxime (**31**)  $\blacklozenge$ , in chloroform at 297K.

The results for **31** in different solvents and at different temperatures are shown in Figure 4.44.

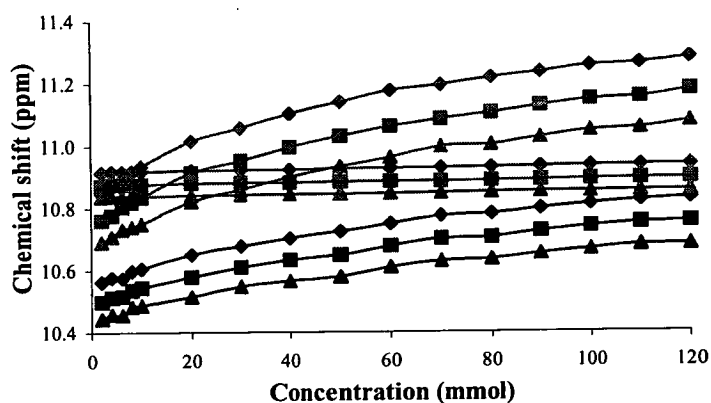


**Figure 4.44:** The effect of temperature on the chemical shift of the oxime proton of 1-{2-[N-(4-pentyl-benzenesulfonamido)]phenyl}ethan-1-one oxime (31) in chloroform, acetonitrile and toluene at 297K  $\blacklozenge$ , 307K  $\blacksquare$ , and 317K  $\blacktriangle$ .

Figure 4.44 clearly indicates that the chemical shift of the oximic proton is very dependent on the nature of the solvent. The signals in toluene are at lower field than those for solutions of identical concentration and at the same temperature in  $\text{CDCl}_3$  indicating that more hydrogen-bonding is taking place. The higher values for the chemical shifts of the oximic proton in acetonitrile solution can be attributed to the involvement of the solvent molecules in hydrogen-bonding to the oximic proton. This would also explain the very small changes in chemical shift of the oximic proton with concentration. The chemical shift of the sulfonamido proton also changes with solvent, concentration and temperature.

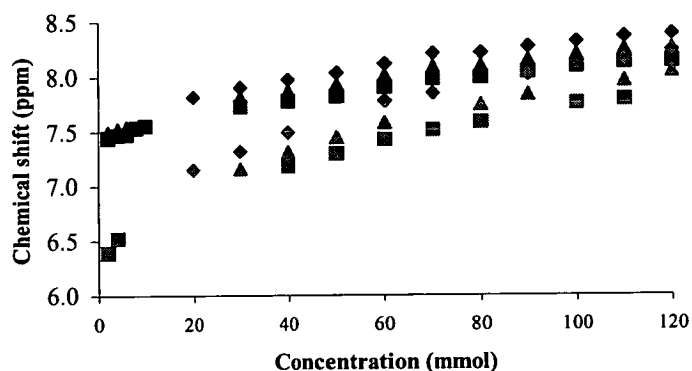


**Figure 4.45:** The effect of temperature on the chemical shift of the sulfonamido proton of 1-{2-[N-(4-pentylbenzenesulfonamido)]phenyl}ethan-1-one oxime (31) in chloroform and toluene at 297K  $\blacklozenge$ , 307K  $\blacktriangle$ , and 317K  $\blacksquare$ .

X-ray crystallography studies of sulfonamido oxime ligands (section 3.4) showed that the sulfonamido NH of ligands **28**, **29** and **33** is involved in *intra*-molecular hydrogen-bonding. The solution structure of these ligands may not be the same as the solid state structure. However, if this *intra*-molecular hydrogen-bond is present in solution it should become stronger upon the association of the ligands by hydrogen-bonding thus changing the chemical shift of the proton. This would be a result of the oximic nitrogen becoming more electronegative due to the hydrogen-bonding interaction of the oximic proton and of the sulfonamido proton becoming more electropositive due to the inductive effect of a hydrogen-bond on the sulfonamido oxygen atom.

Figure 4.46 shows that the data for ligand **31** in chloroform at 297K may be fitted to two different models.<sup>80</sup> In one, a monomer-dimer equilibrium is assumed and in the second a monomer-N-mer equilibrium is assumed.

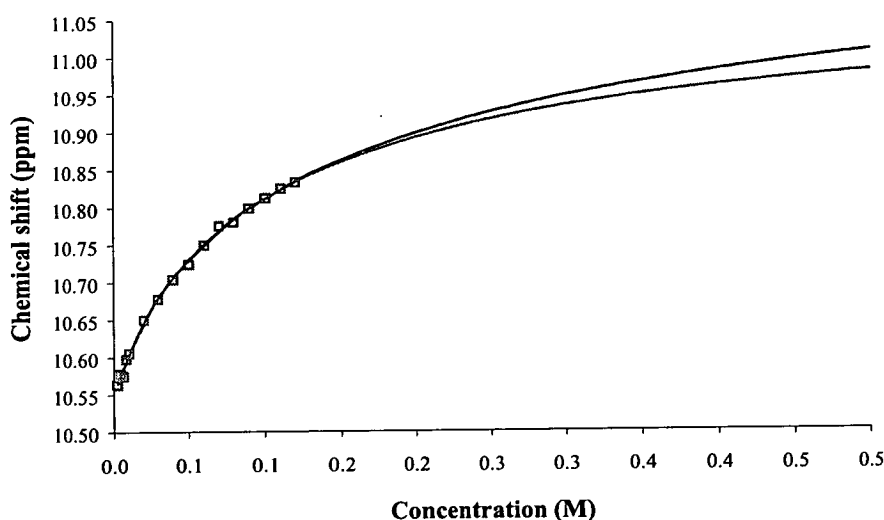
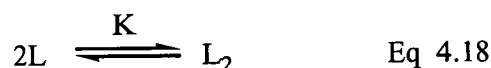


**Figure 4.46:** Curve fits for dimerisation equilibrium and N-merisation equilibrium of nmr data for **31** in chloroform  $\square$  at 297K.

In order to determine which type of equilibrium applies in our systems, a study of the concentration dependence of nmr signals of (**31**) should be carried out. This was not possible due to the limited solubility of this ligand. From the ESI spectra which indicate the presence of dimer species and from VPO measurements for **28** and **33**

which suggest that aggregation numbers do not exceed 2 it was assumed that the equilibria are monomer-dimer for **28** and **31**. Similar problems in the identification of equilibrium systems by nmr have been previously reported by others, *e.g.* Neumann who used  $^{19}\text{F}$  nmr to investigate the aggregation behaviour of acid red 266 dye in aqueous solution.<sup>81</sup>

Nmr data were used to calculate the equilibrium constant (K) (Equation 4.18) for the self association of these ligands using the programme WinEQNMR.<sup>82</sup>



Equilibrium constants calculated for ligands **28** in chloroform- $d_1$  and **31** in chloroform- $d_1$  and toluene- $d_8$  are given in Table 4.2. The data collected for **31** in acetonitrile solution could not be fitted by the programme WinEQNMR to calculate the association constants. This may be due to the very small changes in chemical shift observed with concentration which indicate that very little association of molecules of **31** is taking place in acetonitrile.

**Table 4.2:** The equilibrium constant (K) for the dimerisation of 1-{2-[N-(4-methylbenzenesulfonamido)]phenyl}ethan-1-one oxime (**28**) in chloroform- $d_1$  and 1-{2-[N-(4-pentylbenzenesulfonamido)]phenyl}ethan-1-one oxime (**31**) in chloroform- $d_1$  and toluene- $d_8$  at 297, 307 and 317K.

Ligand	Solvent	K at 297K	K at 307K	K at 317K
<b>28</b>	Chloroform- $d_1$	$5.3 \pm 0.5$	$4.7 \pm 0.5$	$3.7 \pm 0.3$
<b>31</b>	Chloroform- $d_1$	$4.2 \pm 0.4$	$3.8 \pm 0.5$	$3.3 \pm 0.5$
<b>31</b>	Toluene- $d_8$	$7.8 \pm 0.4$	$6.4 \pm 0.4$	$5.1 \pm 0.5$

The observed equilibrium constants show that a higher level of aggregation of sulfonamido oxime ligands is observed in the less polar toluene solution. The pentyl-substituted ligand **31** shows a smaller degree of association than the methyl-substituted ligand **28** in chloroform solution.

### 4.5.3.3 Thermodynamic data for the association of sulfonamido oxime ligands

When similar data are collected at different temperatures  $\Delta G$  may be calculated at each temperature from the equilibrium constant  $K$  (Equation 4.19) and  $\Delta H$  and  $\Delta S$  may be determined using Equation 4.20.

$$\Delta G = -RT \ln K \quad \text{Eq 4.19}$$

$$\Delta G = \Delta H - T\Delta S \quad \text{Eq 4.20}$$

**Table 4.3:** Thermodynamic data for the dimerisation of 1-{2-[N-(4-methylbenzenesulfonamido)] phenyl}ethan-1-one oxime (**28**) in chloroform at 298K and for the dimerisation of 1-{2-[N-(4-pentylbenzenesulfonamido)]phenyl}ethan-1-one oxime (**31**) in chloroform and toluene at 298K.

Ligand	Solvent	$\Delta G$ kJ mol <sup>-1</sup>	$\Delta H$ kJ mol <sup>-1</sup>	$\Delta S$ J mol <sup>-1</sup> K <sup>-1</sup>
<b>28</b>	Chloroform- <i>d</i> <sub>1</sub>	-4.2 ± 2.9	-14.5 ± 2.9	-34.7 ± 9.4
<b>31</b>	Chloroform- <i>d</i> <sub>1</sub>	-6.1 ± 2.1	-9.7 ± 2.1	-20.7 ± 6.8
<b>31</b>	Toluene- <i>d</i> <sub>8</sub>	-5.1 ± 3.3	-21.0 ± 3.3	-53.3 ± 10.6

As might be anticipated for a reaction where bonds are formed the  $\Delta H$  values are negative indicating an exothermic process. The negative sign of  $\Delta G$  indicates that the association of sulfonamido oxime molecules is a favourable process and the loss in entropy of the systems is attributed to the organisation of the ligands by hydrogen-bonding. The dielectric constant of chloroform (4.8) is roughly twice the value of toluene (2.4), this shows strong negative correlation with the magnitude of the equilibrium constants of dimerisation of **31** at different temperatures which are approximately double in toluene. This illustrates the effect of solvent polarity on hydrogen-bonding.

### 4.5.4.4 Speciation of sulfonamido oxime ligands

The working concentration of P50, Avecia's copper extractant, depends on the pH and the amount of copper in the aqueous feed and can range between 0.2-0.45 M.<sup>83</sup> Using the computer package 'HySS2'<sup>84</sup> and the equilibrium constants determined for ligands **28** and **31** the percentage of sulfonamido oxime dimer present at various

ligand concentrations for may be predicted. The percentage of dimer and monomer present relative to the total molar concentration of the ligand as the monomer are shown in Figures 4.47, 4.48 and 4.49.

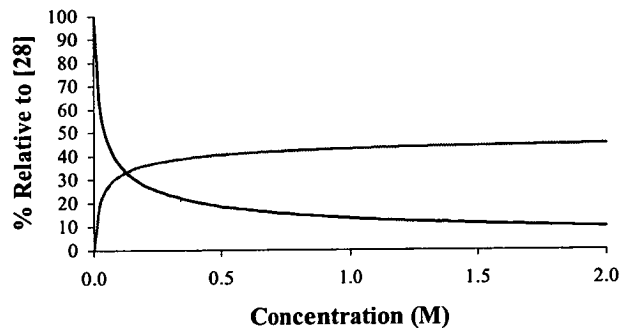


**Figure 4.47:** The variation in the % of dimer and monomer of ligand 28 in chloroform with ligand concentration.

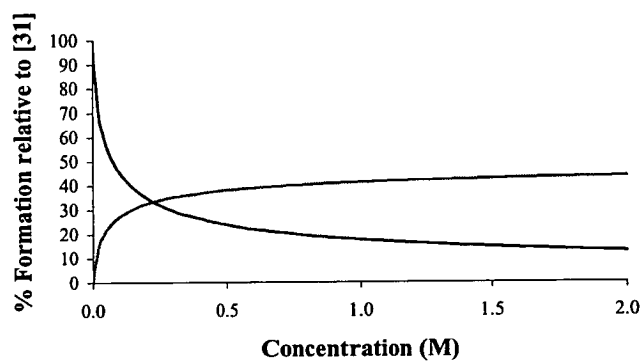


**Figure 4.48:** The variation in the % of dimer and monomer of ligand 31 in chloroform with ligand concentration.



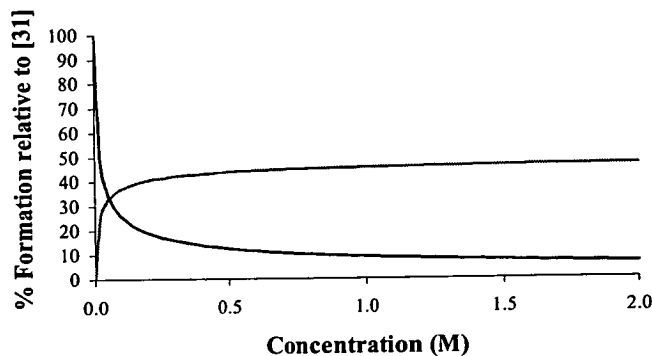


Figure 4.49: The variation in the % of dimer and monomer of ligand **31** in toluene with ligand concentration.

Figures 4.47, 4.48 and 4.49 show the similar behaviour of **28** and **31**. The gradient of the curve showing the % of dimer depends on the different equilibrium constants. In each case, at concentrations above 0.5 M the ligand exists almost completely as a dimer (Figure 4.50).

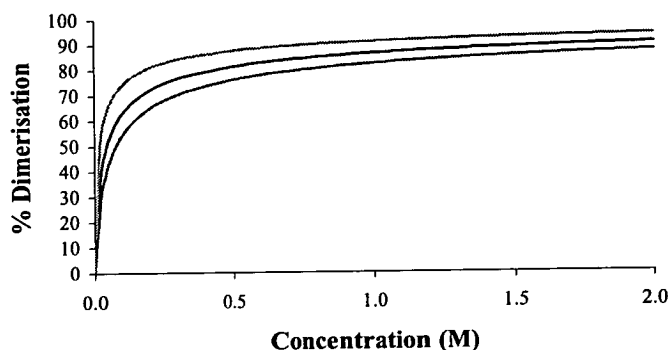


Figure 4.50: The predicted % of ligand dimerisation for ligands **28** (—) and **31** (---) in chloroform and ligand **31** (—) in toluene.

## 4.6 Conclusions

This chapter has ruled out the use of sulfinamido molecules to replace sulfonamido ligands as extractants on practical grounds. They have proved to be unstable and their preparations are difficult. In general terms the sulfonamido-ligands have low solubilities in non-polar solvents and this may limit their usefulness in any commercial application. The solubility of the monosulfonamidodiamine ligands was

improved by the introduction of a 2-ethylhexyl group and the solubility of sulfonamido oxime ligand **28** was enhanced by the use of 4-pentylbenzenesulfonyl chloride as the sulfonating component. Studies of the more soluble oxime ligands indicate that dimerisation to give pre-organised dimer set may occur in a similar manner to that proposed for the commercial oxime extractants for copper. However, the equilibrium constants for these dimerisation processes, as measured by nmr experiments, are relatively small and the importance of preorganisation in enhancing the “strength” of extractants in metal-recovery processes is not clear. Ligand-ligand association is also revealed in the studies on the monosulfonamidodiamine ligands but it has not proved possible to estimate the equilibrium constants for these processes because the signals associated with the N-H groups cannot be assigned in their proton nmr spectra. The following chapter expands the original aim to look at the development of ligands to form ternary complexes in an extraction process using the information on hydrogen-bonding gathered in chapters 2, 3 and 4.

## 4.7 Experimental

### 4.7.1 Instrumentation

Melting points were determined with a Gallenkamp apparatus and are uncorrected. Elemental analysis was performed on a Perkin Elmer 2400 elemental analyser and a Carlo Erba 1108 Elemental analyser. IR spectra were obtained on a Perkin Elmer Paragon 1000 FT-IR spectrometer as potassium bromide discs or as thin films on NaCl plates.  $^1\text{H}$  and  $^{13}\text{C}$  NMR spectra were run on Bruker WP200, AC250 and AVANCE DPX360 spectrometers. Chemical shifts ( $\delta$ ) are reported in parts per million (ppm) relative to residual solvent protons as internal standards. Electron impact (EI) mass spectra were obtained either on a Finnigan MAT4600 quadrupole spectrometer or on a Kratos MS50TC spectrometer. Fast atom bombardment (FAB) mass spectra were obtained on a Kratos MS50TC spectrometer in acetonitrile/3-nitrobenzyl alcohol/thioglycerol matrices. Electrospray ionisation (ESI) mass spectra were obtained on a Thermoquest LCQ spectrometer. Inductively coupled plasma atomic emission spectroscopy (ICP-AES) analysis was performed on a Thermo

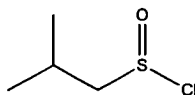
Jarrell Ash Iris ICP-AES spectrometer. Vapour pressure osmometry (VPO) measurements were performed on a Wescor 5500 apparatus.

#### 4.7.2 Solvent and reagent pretreatment

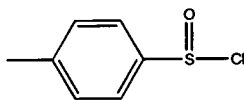
All reagents and solvents were commercially available (Acros or Aldrich) and were used as received. Solvents used for analytical purposes (NMR, MS, ICP, VPO, IR) were of spectroscopic grade.

#### 4.7.3 Synthesis of sulfinyl chlorides

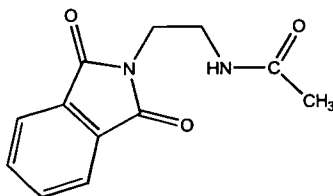
##### 2-Methyl-propane-1-sulfinyl chloride (42)



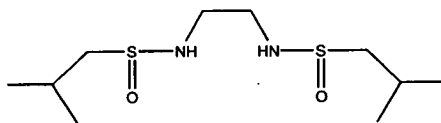
**42** was prepared by the method of Yoon *et al*<sup>21</sup>. A well stirred mixture of 2-methyl-1-propanethiol (45.1 g, 0.5 mol) and acetic acid (30.0 g, 0.5 mol) was cooled to -40°C. Sulfuryl chloride (141.8 g, 1.05 mol) was added dropwise over a period of 30 minutes. Gas evolution was observed during the addition of the first quarter of the sulfuryl chloride, and the colour changed to yellow. Stirring was continued for 30 minutes at -40°C, and the mixture was then allowed to reach room temperature over a period of 2h. Gas evolution commenced again and the colour changed to red. The mixture was warmed at 30°C until gas evolution ceased (~4h), while the pale yellow colour of the sulfinyl chloride appeared. Acetyl chloride was distilled off under vacuum to leave the crude sulfinyl chloride. The product was purified by distillation at 20 mm Hg, bp 94-98°C (55.15 g, 78%), (Found: C, 34.29; H, 6.43. Calc. for C<sub>4</sub>H<sub>9</sub>ClOS: C, 34.16; H, 6.45%).  $\delta_{\text{H}}$  (CDCl<sub>3</sub>, 200 MHz): 1.09 (d, 6 H, J 8.3, CH<sub>3</sub>), 2.29 (m, 1 H, CH), 3.29 (m, 2 H, CH<sub>2</sub>).  $\delta_{\text{C}}$  (CDCl<sub>3</sub>, 50 MHz): 21 (CH<sub>3</sub>), 22 (CH<sub>3</sub>), 25 (CH), 74 (CH<sub>2</sub>). IR data (NaCl plate)/cm<sup>-1</sup>: 722w, 1147s, 1371m, 1387w, 1400w, 1466m, 2875w, 2932w, 2964s.

**4-Methylbenzenesulfinyl chloride (43)<sup>21</sup>**

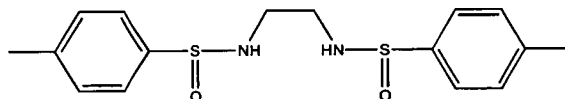
Using 4-methylbenzenethiol (62.11 g, 0.5 moles) in the procedure described for **42** yielded **43** (58.46 g, 67%). This was characterised by nmr and IR spectroscopy and was not purified before use due to the risk of explosion.<sup>22</sup>  $\delta_{\text{H}}$  ( $\text{CDCl}_3$ , 360 MHz): 2.49 (s, 3 H,  $\text{CH}_3$ ), 7.43 (d, 2 H, J 8.0, Ar CH), 7.80 (d, 2 H, J 8.3, Ar CH).  $\delta_{\text{C}}$  ( $\text{CDCl}_3$ , 90 MHz): 22 ( $\text{CH}_3$ ), 124 (2 C, Ar CH), 131 (2 C, Ar CH). IR data (NaCl plate)/ $\text{cm}^{-1}$ : 810w, 1161m, 1377s.

**4.7.4 Synthesis of sulfinamides and protected amines****2-(2-Acetamido-ethyl)-isoindole-1,3-dione (45)**

n-Butyl acetate (200  $\text{cm}^3$ ) was added to phthalic acid anhydride (5.26 g, 36 mmol) and N-acetyleneethylenediamine (3.3 g, 32mmol). The mixture was heated at reflux for five hours and then left to cool. The resulting yellow solid was collected by filtration and recrystallised from ethanol (50  $\text{cm}^3$ ) to yield a white crystalline solid, (5.08 g, 68%), mp 184°C (Found: C, 62.18; H, 5.00; N, 11.94. Calc. for  $\text{C}_{12}\text{H}_{12}\text{N}_2\text{O}_3$ : C, 62.06; H, 5.21; N, 12.06%).  $\delta_{\text{H}}$  ( $\text{CDCl}_3$ , 200 MHz) 1.90 (s, 3 H,  $\text{CH}_3$ ), 3.46-3.54 (m, 2 H,  $\text{CH}_2$ ), 3.81-3.86 (m, 2 H,  $\text{CH}_2$ ), 6.09 (s, NH).  $\delta_{\text{C}}$  ( $\text{CDCl}_3$ , 63 MHz) 23 ( $\text{CH}_3$ ), 37 ( $\text{CH}_2$ ), 39 ( $\text{CH}_2$ ), 123 (2 C, Ar CH), 132 (2 C, Ar C), 134 (2 C, Ar CH), 168 (C=O), 170 (2 C, C=O). IR data (KBr disc)/ $\text{cm}^{-1}$ : 714w, 1027w, 1159w, 1400m, 1382m, 1657s, 1705s, 2361w, 3286m, 3461w. FAB MS,  $m/z$  233 ( $\text{MH}^+$ , 100.0%)

**1, 2-Di(2-methylpropane-1-sulfinylamino)ethane (44)**

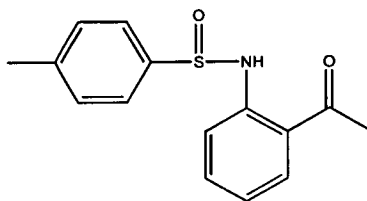
A solution of 2-methylpropane-1-sulfinyl chloride (5 g, 0.036 mol) in dry diethylether (50 cm<sup>3</sup>) was added dropwise to a solution of 1,2-diaminoethane (12.8 g, 0.21 mol) in diethylether (150 cm<sup>3</sup>) at -10°C over a period of two hours. A white precipitate and a yellow oil are observed. The diethylether was then removed in vacuo and tetrahydrofuran (100 cm<sup>3</sup>) was added. The tetrahydrofuran was then decanted, filtered and the solvent removed in vacuo to yield a white powder. Analysis proved this to be a disubstituted product (44) (1.11 g, 23%), mp 109-111°C (Found: C, 44.57; H, 8.55; N, 10.45. Calc. for C<sub>10</sub>H<sub>24</sub>N<sub>2</sub>O<sub>2</sub>S<sub>2</sub>: C, 44.74; H, 9.01; N, 10.44%).  $\delta_{\text{H}}$  (CDCl<sub>3</sub>, 200 MHz): 1.04 (d, 6 H, J 6.6, CH<sub>3</sub>), 2.06 (m, 2 H, CH), 2.63 (m, 2 H, CH<sub>2</sub>), 3.31 (m, 4 H, CH<sub>2</sub>), 4.83 (m, 2 H, NH).  $\delta_{\text{C}}$  (CDCl<sub>3</sub>, 50 MHz): 21 (2 C, CH<sub>3</sub>), 22 (2 C, CH<sub>3</sub>), 24 (2 C, CH), 44 (2 C, CH<sub>2</sub>), 63 (2 C, CH<sub>2</sub>). IR data (KBr disc)/cm<sup>-1</sup>: 1035s, 1078m, 1509m, 2960m, 3218m, 3434w. FAB MS, *m/z* 269 (MH<sup>+</sup>, 100.0%)

**1, 2-Di(4-methylbenzene-1-sulfinylamino)ethane (46)**

A solution of 4-methylbenzenesulfinyl chloride (5 g, 29 mmol) in dry diethylether (50 cm<sup>3</sup>) was added dropwise to a solution of 1,2-diaminoethane (5.16 g, 86 mmol) in diethylether (150 cm<sup>3</sup>) at -10°C over a period of two hours. A white precipitate and a yellow oil are observed. The diethylether was then removed *in vacuo* and tetrahydrofuran (100 cm<sup>3</sup>) was added. The tetrahydrofuran was then decanted, filtered and the solvent removed *in vacuo* to yield a white powder. Analysis proved this to be the disubstituted product (1.32 g, 27%), mp 104-106°C (Found: C, 56.74; H, 5.69; N, 8.31. Calc. for C<sub>16</sub>H<sub>20</sub>N<sub>2</sub>O<sub>2</sub>S<sub>2</sub>: C, 57.11; H, 5.99; N, 8.33%).  $\delta_{\text{H}}$  (CDCl<sub>3</sub>, 360 MHz): 2.43 (s, 6 H, CH<sub>3</sub>), 3.02 (m, 4 H, CH<sub>2</sub>), 7.31 (d, 4 H, J 7.9, Ar CH), 7.58 (d, 4 H, J 8.3, Ar CH).  $\delta_{\text{C}}$  (CDCl<sub>3</sub>, 91 MHz): 22 (2 C, CH<sub>3</sub>), 41 (CH<sub>2</sub>), 42 (CH<sub>2</sub>), 126

(4C, Ar CH), 130 (4 C, Ar CH), 141 (2 C, Ar C), 142 (2 C, Ar C). IR data (KBr disc)/cm<sup>-1</sup>: 1047s, 1087m, 1490w, 2872m, 2918m, 31965s, 3448w. FAB MS, *m/z* 337 (MH<sup>+</sup>, 58.6%).

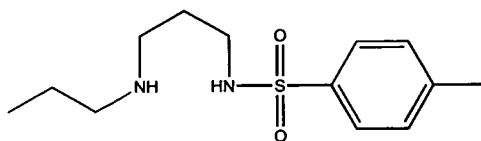
#### 1-{2-[N-(4-methylbenzenesulfinamido)]phenyl}ethan-1-one (47)



A solution of 4-methylbenzenesulfinyl chloride (0.32 g, 1.8 mmol) in dry diethylether (10 cm<sup>3</sup>) was added dropwise to a solution of 1-(2-amino-phenyl)-ethanone (0.5 g, 3.7 mmol) in dry diethylether (10 cm<sup>3</sup>). The mixture was then stirred for one hour. At the end of this time a yellow precipitate had formed and this was isolated by filtration. The yellow precipitate was washed with water (3 x 5 cm<sup>3</sup>) to yield a white powder. (0.56 g, 55%).  $\delta_{\text{H}}$  (CDCl<sub>3</sub>, 360 MHz): 2.45 (s, 3 H, CH<sub>3</sub>), 2.61 (s, 3 H, CH<sub>2</sub>), 7.03 (t, 1 H, J 7.1, Ar CH), 7.37 (d, 2 H, J 8.5, Ar CH), 7.50 (t, 1 H, J 7.8, Ar CH), 7.65 (d, 1 H, J 8.4, Ar CH), 7.71 (d, 2 H, J 8.2, Ar CH), 7.87 (d, 1 H, J 8.0, Ar CH), 10.88 (NH).  $\delta_{\text{C}}$  (CDCl<sub>3</sub>, 91 MHz): 22 (CH<sub>3</sub>), 29 (CH<sub>3</sub>), 117 (Ar CH), 121 (Ar CH), 122 (Ar C), 126 (2 C, Ar CH), 130 (2 C, Ar CH), 133 (Ar CH), 135 (Ar CH), 141 (Ar C), 142 (Ar C), 145 (Ar C), 202 (C=O). IR data (KBr disc)/cm<sup>-1</sup>: 1054m, 1070m, 1363s, 1488s, 1618m, 1648s, 2797m, 3435m. FAB MS, *m/z* 274 (MH<sup>+</sup>, 41.8%)

#### 4.7.5 Introduction of a lipophilic group into monosulfonamidodiamines

##### N-(N-propyl-3-aminopropyl)-4-methylbenzenesulfonamide (50)

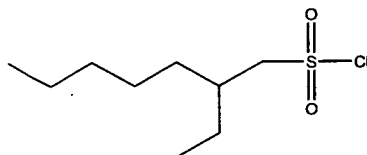


A solution of propanal (1.53 g, 26.3 mmol) in methanol (30 cm<sup>3</sup>) was added to a solution of N-(3-aminopropyl)-4-methylbenzenesulfonamide (4 g, 17.5 mmol) in

methanol (30 cm<sup>3</sup>) and was stirred for 12 hours. A catalytic amount of anhydrous sodium tetraborate (0.2 g, 1 mmol) and sodium borohydride (2.65 g, 70 mmol) were added and the solution was stirred for one hour. Water (200 cm<sup>3</sup>) was added and the methanol was removed *in vacuo*. The resulting yellow oil was extracted into dichloromethane (2 x 100 cm<sup>3</sup>). Removal of solvent from the organic phase *in vacuo* gave a yellow oil which was triturated with hexane (3 x 100 cm<sup>3</sup>) and diethylether (3 x 5 cm<sup>3</sup>) to yield a sticky white solid (2.61 g, 55%). This proved difficult to purify.  $\delta_{\text{H}}$  (CDCl<sub>3</sub>, 200 MHz): 0.84 (t, 3 H, J 7.2, CH<sub>3</sub>), 1.48 (m, 4 H, CH<sub>2</sub>), 2.36 (s, 3 H, CH<sub>3</sub>), 2.41 (t, 2 H, J 7.0, CH<sub>2</sub>), 2.57 (t, 2 H, J 5.9, CH<sub>2</sub>), 2.96 (t, 2 H, J 5.0, CH<sub>2</sub>), 7.23 (d, 2 H, J 8.5, Ar CH), 7.67 (d, 2 H, J 8.3, Ar CH). FAB MS, m/z 271 (MH<sup>+</sup>, 100.0%).

#### 4.7.6 Synthesis of alkyl sulfonyl chlorides

##### 2-Ethylhexanesulfonyl chloride (51)

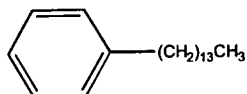


**51** was prepared by an adaptation of the method of Zeigler and Sprague.<sup>46</sup> 1-Bromo-2-ethylhexane (38.63 g, 0.2 mol) and thiourea (15.22 g, 0.2 mol) in 50 cm<sup>3</sup> of ethanol were refluxed overnight. The ethanol was then removed *in vacuo* to leave a white solid. The crude *isothiuronium* salt was dissolved in 250 cm<sup>3</sup> warm water and 40% sodium hydroxide was added until no more cloudiness developed. The crude 2-ethylhexane thiol was separated, washed with water, and dissolved in 50 cm<sup>3</sup> of acetic acid. About 25 g of crushed ice was added to the solution and the mixture was saturated with chlorine at 0-15°C. The oily product was extracted with diethylether. The extract was washed with 5% sodium bisulfite solution (100 cm<sup>3</sup>), and water (2 x 100 cm<sup>3</sup>) then and dried over magnesium sulfate. The extract was filtered and the diethylether evaporated. A yellow liquid was obtained by distillation at 0.75 mm Hg, bp 92-96°C (14.89 g, 35%).  $\delta_{\text{H}}$  (CDCl<sub>3</sub>, 360 MHz): 0.95 (m, 6 H, CH<sub>3</sub>), 1.36 (m, 4 H, CH<sub>2</sub>), 1.60 (m, 4 H, CH<sub>2</sub>), 2.24 (m, 1 H, CH), 3.71 (d, 2 H, J 6.0, CH<sub>2</sub>).  $\delta_{\text{C}}$

(CDCl<sub>3</sub>, 90 MHz): 11 (CH<sub>3</sub>), 14 (CH<sub>3</sub>), 23 (CH<sub>2</sub>), 26 (CH<sub>2</sub>), 29 (CH<sub>2</sub>), 32 (CH<sub>2</sub>), 37 (CH), 70 (CH<sub>2</sub>). FAB MS, *m/z* (MH<sup>+</sup>, 21.6%).

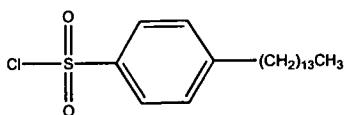
#### 4.7.7 Synthesis of alkyl-substituted arylsulfonyl chlorides

##### Tetradecylbenzene (52)

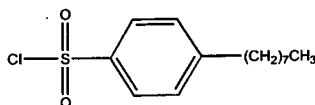


**52** was prepared by an adaptation of the method of Wei *et al.*<sup>57</sup> 1-bromododecane (5 g, 20 mmol) in dry diethylether (20 cm<sup>3</sup>) was cooled to -78°C in an acetone/dry ice bath. Butyllithium (20 mmol) was then added and the mixture was allowed to stir for 30 minutes. A solution of styrene (1.9 g, 18 mmol) in dry diethylether (20 cm<sup>3</sup>) was then cooled to -25°C using an *o*-xylene/dry ice bath. The dodecylolithium solution was then added to the styrene solution *via* a canula, care was taken to maintain the temperature below -25°C. A colour change was then observed to deep orange. The solution was left to stir at -25°C for two hours. Methanol (1 cm<sup>3</sup>) was then added and the solution became an opaque white. The mixture was allowed to stir for 10 minutes before it was washed with water (3 x 50 cm<sup>3</sup>). The ethereal solution was then dried over anhydrous magnesium sulfate. The colourless oil was then purified by kugelrohr (3.20 g, 58%), (Found: C, 86.84; H, 12.97. Calc. for C<sub>20</sub>H<sub>34</sub> C, 87.51; H, 12.48%). δ<sub>H</sub> (CDCl<sub>3</sub>, 360 MHz): 0.86 (t, 3 H, J 6.9, CH<sub>3</sub>), 1.28 (m, 26 H, CH<sub>2</sub>), 7.20 (m, 5 H, Ar CH). δ<sub>C</sub> (CDCl<sub>3</sub>, 91 MHz): 14 (CH<sub>3</sub>), 14 (CH<sub>2</sub>), 23 (CH<sub>2</sub>), 23 (CH<sub>2</sub>), 28 (CH<sub>2</sub>), 28 (CH<sub>2</sub>), 30 (CH<sub>2</sub>), 30 (CH<sub>2</sub>), 30 (CH<sub>2</sub>), 30 (CH<sub>2</sub>), 32 (CH<sub>2</sub>), 33 (CH<sub>2</sub>), 37 (CH<sub>2</sub>), 47 (CH<sub>2</sub>), 126 (Ar CH), 128 (2 C, Ar CH), 129 (2 C, Ar CH), 147 (Ar C). IR data (KBr disc)/cm<sup>-1</sup>: 1603w, 2854s, 2924s, 3027m.



**4-Tetradecylbenzenesulfonyl chloride (53)**

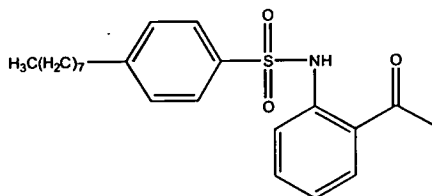
**53** was prepared by the adaptation of the method of Buckel *et al.*<sup>58</sup> To a solution of tetradecylbenzene (2.5 g, 9 mmol) in chloroform (30 cm<sup>3</sup>), chlorosulfonic acid (3.18 g, 27 mmol) was added and the mixture was stirred at room temperature for 20 hours. The solution was then poured on ice, and the aqueous layer was then extracted with dichloromethane (2 x 50 cm<sup>3</sup>). The combined extracts were washed with water (100 cm<sup>3</sup>), a 10% aqueous solution of NaHCO<sub>3</sub> (100 cm<sup>3</sup>) and water (2 x 100 cm<sup>3</sup>) before being treated with activated charcoal and dried over anhydrous MgSO<sub>4</sub>. The residue was purified by kugelrohr (3.00 g, 89%).  $\delta_{\text{H}}$  (CDCl<sub>3</sub>, 360 MHz): 0.90 (m, 3 H, CH<sub>3</sub>), 1.27 (m, 26 H, CH<sub>2</sub>), 7.40 (d, 2 H, J 8.5, Ar CH), 7.98 (d, 2 H, J 8.6, Ar CH).  $\delta_{\text{C}}$  (CDCl<sub>3</sub>, 91 MHz): 14.4 (CH<sub>3</sub>), 15 (CH<sub>2</sub>), 23 (CH<sub>2</sub>), 23 (CH<sub>2</sub>), 28 (CH<sub>2</sub>), 28 (CH<sub>2</sub>), 30 (CH<sub>2</sub>), 30 (CH<sub>2</sub>), 30 (CH<sub>2</sub>), 32 (CH<sub>2</sub>), 32 (CH<sub>2</sub>), 37 (CH<sub>2</sub>), 37 (CH<sub>2</sub>), 49 (CH<sub>2</sub>), 128 (2 C, Ar CH), 129 (2 C, Ar CH), 142 (Ar C), 156 (Ar C). IR data (neat, NaCl plate)/cm<sup>-1</sup>: 1083m, 1175m, 1306w, 1381m, 2854s, 2926s.

**4-Octylbenzenesulfonyl chloride (55)**

4-Octylbenzenesulfonyl chloride was prepared by the adaptation of the method of Yamaguchi *et al.*<sup>59</sup> A mixture of sodium 4-octylsulfonate (6.14 g, 21 mmol) and phosphoryl chloride (4.83 g, 32 mmol) was stirred at 170°C for two hours. The mixture was cooled to 60°C before dichloromethane (100 cm<sup>3</sup>) was added and the solution was heated at reflux for 30 minutes. The solution was then cooled and poured into water (100 cm<sup>3</sup>), the sulfonyl chloride was then extracted with chloroform, washed with aqueous sodium chloride solution (2 x 100 cm<sup>3</sup>) and dried with anhydrous magnesium sulfate (5.56 g, 92%).  $\delta_{\text{H}}$  (CDCl<sub>3</sub>, 360 MHz): 0.92 (t, 3 H, J 6.7, CH<sub>3</sub>), 1.33 (m, 10 H, CH<sub>2</sub>), 1.69 (t, 2 H, J 7.3, CH<sub>2</sub>), 2.76 (t, 2 H, J 7.7, CH<sub>2</sub>), 7.44 (d, 2 H, J 8.5, Ar CH), 7.98 (d, 2 H, J 8.5, Ar CH).  $\delta_{\text{C}}$  (CDCl<sub>3</sub>, 90 MHz):

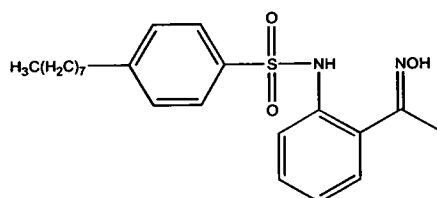
14 (CH<sub>3</sub>), 23 (CH<sub>2</sub>), 30 (CH<sub>2</sub>), 30 (CH<sub>2</sub>), 31 (CH<sub>2</sub>), 32 (CH<sub>2</sub>), 37 (CH<sub>2</sub>), 54 (CH<sub>2</sub>), 128 (2 C, Ar CH), 130 (2 C, Ar CH), 142 (Ar C), 152 (Ar C). IR data (NaCl plate, neat)/cm<sup>-1</sup>: 1175m, 1379m, 2856s, 2927s. FAB MS, *m/z* 289 (MH<sup>+</sup>, 28.6%)

**1-{2-[N-(4-octylbenzenesulfonamido)]phenyl}ethan-1-one (56)**



A solution of 1-(2-amino-phenyl)-ethanone (2.11 g, 15.6 mmol) in pyridine (30 cm<sup>3</sup>) was added dropwise to a solution of 4-octylbenzenesulfonyl chloride (4.5 g, 15.6 mmol) in pyridine (30 cm<sup>3</sup>) at 0°C over one hour. The mixture was then allowed to stir overnight. The pyridine was then removed in vacuo to produce a pink oil. Hexane (100 cm<sup>3</sup>) was then added to give a pink solid which was recrystallised from hexane (150 cm<sup>3</sup>) to yield a white crystalline solid (2 g, 35%), mp 63-64°C (%), (Found: C, 68.19; H, 7.60; N, 3.60. Calc. for C<sub>22</sub>H<sub>29</sub>NO<sub>3</sub>S C, 68.18; H, 7.54; N, 3.61%). δ<sub>H</sub> (CDCl<sub>3</sub>, 360 MHz): 0.90 (t, 3 H, J 6.8, CH<sub>3</sub>), 1.28 (s, 10 H, CH<sub>2</sub>), 1.59 (m, 2 H, CH<sub>2</sub>), 2.58 (s, 3 H, CH<sub>3</sub>), 2.63 (t, 2 H, J 7.8, CH<sub>2</sub>), 7.09 (t, 1 H, J 7.0, Ar CH), 7.26 (d, 2 H, J 8.3, Ar CH), 7.48 (t, 1 H, J 7.2, Ar CH), 7.73 (d, 1 H, J 7.8, Ar CH), 7.77 (d, 2 H, J 8.3, Ar CH), 7.82 (d, 1 H, J 8.0, Ar CH). δ<sub>C</sub> (CDCl<sub>3</sub>, 90 MHz): 14 (CH<sub>3</sub>), 23 (CH<sub>2</sub>), 29 (CH<sub>3</sub>), 30 (2 C, CH<sub>2</sub>), 30 (CH<sub>2</sub>), 32 (CH<sub>2</sub>), 32 (CH<sub>2</sub>), 36 (CH<sub>2</sub>), 120 (Ar CH), 123 (Ar C), 123 (Ar CH), 128 (2 C, Ar CH), 129 (2 C, Ar CH), 132 (Ar CH), 135 (Ar CH), 137 (Ar C), 141 (Ar C), 149 (Ar C), 203 (C=O). IR data (KBr disc)/cm<sup>-1</sup>: 760m, 1162s, 1226m, 1342m, 1498m, 1648s, 2928s. FAB MS, *m/z* 388 (MH<sup>+</sup>, 100.0%), HRMS *m/z* calc. for 388.5511, found 388.1952.

**1-{2-[N-(4-octylbenzenesulfonamido)]phenyl}ethan-1-one oxime (54)**



Hydroxylamine hydrochloride (1.08 g, 16 mmol) was added to a solution of 1-{2-[N-(4-octylbenzenesulfonamido)]phenyl}ethan-1-one (2 g, 5.2 mmol) in a 50:50 pyridine:ethanol solution (30 cm<sup>3</sup>). This was heated at reflux for 4 hours and then cooled. The mixture was poured into water (100 cm<sup>3</sup>), the product was then extracted into diethylether (2 x 50 cm<sup>3</sup>) and washed with water (6 x 100 cm<sup>3</sup>). The ethereal solution was then dried over anhydrous magnesium sulfate, filtered and the diethylether removed in vacuo to yield a yellow oil (1.77 g, 85%).  $\delta_{\text{H}}$  (CDCl<sub>3</sub>, 360 MHz): 0.90 (s, 3 H, CH<sub>3</sub>), 1.29 (m, 10 H, CH<sub>2</sub>), 1.51 (m, 2 H, CH<sub>2</sub>), 2.11 (s, 3 H, CH<sub>3</sub>), 2.63 (m, 2 H, CH<sub>2</sub>), 1.51 (m, 2 H, CH<sub>2</sub>), 2.11 (s, 3 H, CH<sub>3</sub>), 2.63 (m, 2 H, CH<sub>2</sub>), 7.25 (m, 6 H, Ar CH), 7.60 (d, J 8.4, 2 H, Ar CH).  $\delta_{\text{C}}$  (CDCl<sub>3</sub>, 90 MHz): 13 (CH<sub>3</sub>), 15 (CH<sub>3</sub>), 23 (CH<sub>2</sub>), 30 (CH<sub>2</sub>), 30 (CH<sub>2</sub>), 31 (CH<sub>2</sub>), 32 (CH<sub>2</sub>), 32 (CH<sub>2</sub>), 36 (CH<sub>2</sub>), 122 (Ar CH), 126 (Ar CH), 128 (2 C, Ar CH), 129 (2 C, Ar CH), 136 (Ar C), 137 (Ar C), 137 (Ar CH), 137 (Ar C), 137 (Ar C), 149 (Ar C), 150 (Ar CH), 157 (C=NOH). IR data (nujol, NaCl plate)/cm<sup>-1</sup>: 1159w, 1377m, 1625w, 3392w. FAB MS, *m/z* 403 (MH<sup>+</sup>, 71.3%).

## 4.8 References

- <sup>1</sup> D. P. Fairlie and W. G. Jackson, *Inorganica Chimica Acta*, 1990, **175**, 203.
- <sup>2</sup> M. Baltas, J. D. Bastide, A. Deblic, L. Cazaux, L. Gorrichonguigon, P. Maroni, M. Perry, P. Tisnes, *Spectrochimica Acta-Part A-Molecular and biomolecular Spectroscopy*, 1985, **41A**, 789.
- <sup>3</sup> M. Baltas, J. D. Bastide, L. Cazaux, L. Gorrichonguigon, P. Maroni, P. Tisnes, *Spectrochimica Acta Part A-Molecular and biomolecular Spectroscopy*, 1985, **41A**, 793.
- <sup>4</sup> L. Field, *Synthesis*, 1972, 101.
- <sup>5</sup> B. Bujnicki, J. Drabowicz, M. Mikolajczyk, A. Kolbe, and L. Stefaniak, *J. Org. Chem.*, 1996, **61**, 7593.
- <sup>6</sup> P. Ruostesuo, A. M Hakkinen, T. Mattila, *Magnetic Resonance in Chemistry*, 1987, **25**, 189.
- <sup>7</sup> W. J. Moree, G. A. van der Marel and R. M. J. Liskamp, *Tetrahedron Letters*, 1991, **32**, 409.
- <sup>8</sup> D. Merricks, P. G. Sammes, E. R. H. Walker, K. Henrick and M. M. McPartlin, *J. Chem. Soc. Perkin Trans*, 1991, 2169.
- <sup>9</sup> A. Sonn and E. Schmidt, *Ber*, 1924, **57**, 1355.
- <sup>10</sup> H. Gilman and H. L. Morris, *J. Amer. Chem. Soc.*, 1926, **48**, 2399.
- <sup>11</sup> T. J. Maricichi and C. N. Angeletakis, *J. Org. Chem*, 1984, **49**, 1931.
- <sup>12</sup> Y. Noguchi, I. Masanobu, K. Kuroki and M. Furukawa, *Chem. pharm. Bull.*, 1982, **30**, 1644.
- <sup>13</sup> L. C. Raiford and S. E. Hazlet, *J. Amer. Chem. Soc.*, 1935, **57**, 2172.
- <sup>14</sup> Y. Miura and Y. Nakamura, *Bull. Chem. Soc. Jpn.*, 1990, **63**, 1154.
- <sup>15</sup> P. Ruostesuo, A.-M. Hakkinen and T. Mattila, *Magnetic Resonance in Chemistry*, 1987, **25**, 189.
- <sup>16</sup> I. B. Douglass and D. R. Poole, *J. Org. Chem.*, 1957, **22**, 536.
- <sup>17</sup> I. B. Douglass and B. S. Farah, *J. Org. Chem.*, 1958, **23**, 330.

- 18 I. B. Douglass and B. S. Farah, *Org. Syntheses*, 1961, **40**, 62.
- 19 I. B. Douglass and R.V. Norton, *J. Org. Chem.*, 1968, **33**, 2104.
- 20 W. Muller and K. Schenk, *Chem. Ber*, **III**, 1978, 2870.
- 21 J. -H. Yoon and R. Herrmann, *Synthesis*, 1987, **1**, 72.
- 22 I. B. Douglass and R. V. Norton, *J. Org. Chem.*, 1968, **33**, 2104.
- 23 I. B. Douglass and D. A. Koop, *J. Org. Chem.*, 1964, **29**, 951.
- 24 A. V. Kirsanov and N. A. Kirsanova, *Zhurnal Obshchei Khimii*, 1962, **32**, 887.
- 25 B. J. Wagner, J. T. Doi and W. K. Musker, *J. Org. Chem.*, 1990, **55**, 5941.
- 26 C. K. Kim and I. Lee, *Bull. Korean Chem. Soc.*, 1997, **18**, 880.
- 27 J. March, in *Advanced Organic Chemistry, Reactions, Mechanisms and Structure*, Wiley-Interscience, New York, 4<sup>th</sup> edn., 1992, ch. 6, p. 896.
- 28 J. Hoyle, in *The Chemistry of Sulfonic Acids, Esters and their Derivatives*, ed. S. Patai and Z. Rappoport, John Wiley and Sons Ltd, 1991, ch 10, pp. 379-386.
- 29 R. Cremlyn and R. Nunes, *Phosphorus Sulfur*, 1987, **31**, 245.
- 30 E. E. Gilbert, *Sulfonation and Related Reactions*, Interscience, New York, 1965.
- 31 H. Meerwein, E. Buchner and E. Emster, *J. Prakt. Chem.*, 1939, **260**, 238.
- 32 F. Asinger, W. Schmidt and F. Ebeneder, *Chem. Ber.*, 1942, **75**, 34.
- 33 J. Boeseken, *Recl. Trav. Chim. Pays-Bas*, 1911, **30**, 382.
- 34 S. N. Bhattacharya, C. Eaborn and D. R. M. Walton, *J. Chem. Soc. (C)*, 1968, 1265.
- 35 R. B. Scott and R. E. Lutz, *J. Org. Chem.*, 1954, **19**, 830.
- 36 M. S. Schechter and H. L. Haller, *J. Am. Chem. Soc.*, 1941, **63**, 1764.
- 37 S. W. Lee and G. Dougherty, *J. Org. Chem.*, 1942, **5**, 81.
- 38 R. Otto and O. von Gruber, *Ann. Chem.*, 1867, **142**, 96.
- 39 T. Hamada and O. Yonemitsu, *Synthesis*, 1986, 852.
- 40 B. Z. Yakovlev, L. F. Kotlova, O. P. Koninskaya, N. A. Lodygin, R. D. Erlikh and K. M. Dyumaev, *Chem. Abstr.*, 1981, **96**, 34766b.
- 41 R. N. Haszeldine and J. M. Kidd, *J. Chem. Soc.*, 1955, 2901.

- 42 T. Zincke and W. Frohneberg, *Chem. Ber.*, 1909, **42**, 2728.
- 43 A. Wagenaar and J. B. F. N. Engberts, *Recl. Trav. Chim. Pays-bas*, 1982, **101**, 91.
- 44 J. F. King and M. Aslam, *Synthesis*, 1980, 285.
- 45 K. Folkers, A. Russell and R. W. Bost, *J. Am. Chem. Soc.*, 1941, **63**, 3530.
- 46 C. Ziegler and J. M. Sprague, *J. Org. Chem.*, 1951, **16**, 621.
- 47 G. G. I. Moore, *J. Org. Chem.*, 1979, **44**, 1708.
- 48 C. F. Bennett, D. W. Goheen and W. S. MacGregor. *J. Org. Chem.*, 1963, **28**, 2485.
- 49 M. Wechsberg, *Chem. Abstr.*, 1979, **90**, 84603.
- 50 C. R. Noller and P. J. Hearst, *J. Am. Chem. Soc.*, 1948, **70**, 3955.
- 51 G. Cignarella and U. Tetino, *J. Am. Chem. Soc.*, 1960, **82**, 1594.
- 52 A. Strecker, *Ann.*, 1868, **90**, 148.
- 53 P. H. Latimer and R. W. Bost, *J. Org. Chem.*, 1940, **5**, 24.
- 54 W. Hemilian, *Ann.*, 1873, **145**, 168.
- 55 K. Folkers, A. Russell and R. W. Bost, *J. Am. Chem. Soc.*, 1941, **63**, 3530.
- 56 H. Gilman and R. N. Meals, *J. Org. Chem.*, 1943, **8**, 126-148.
- 57 X. Wei, P. Johnson and R. J. K. Taylor, *J. Chem. Soc., Perkin Trans.*, 2000, **1**, 1109.
- 58 F. Buckel, P. Persson, F. Effenberger, *Synthesis*, 1999, **6**, 953.
- 59 T. Yamaguchi, T. Seki, T. Tamaki and K. Ichimura, *Bull. Chem. Soc. Jpn.*, 1992, **65**, 649.
- 60 J. B. Fenn, M. Mann, C. K. Meng, S. F. Wong, *Mass Spectrometry Reviews*, 1990, **9**, 37.
- 61 N. Yoshida, N. Ito and K. Ichikawa, *J. Chem. Soc., Perkin Trans.*, 1997, **2**, 2387.
- 62 V. Katta, S. K. Chowdhury and B. T. Chait, *J. Am. Chem. Soc.*, 1990, **112**, 5348.

- <sup>63</sup> F. Bitsch, C. O. Dietrich-Buchecker, A. -K. Khemiss, J.-P. Sauvage, A. Van Dorsselaer, *J. Am. Chem. Soc.*, 1991, **113**, 4023.
- <sup>64</sup> A.-M. Sastre, N. Miralles, and M. Martinez., *Monatshefte für Chemie*, 1995, **126**, 401.
- <sup>65</sup> B. K. Tait, *Hydrometallurgy*, 1993, **32**, 365.
- <sup>66</sup> A. Almela, M. P. Elizalde, and R. Benito, *Journal of Solution Chemistry*, 1993, **22**, 231.
- <sup>67</sup> C. Klofutar, S. Paljk and V. Abram, *J. Chem. Soc. Faraday Trans.*, 1993, **89**, 3065.
- <sup>68</sup> O. F. Schall, K. Robinson, J. L. Atwood and G. W. Gokel, *J. Am. Chem. Soc.*, 1993, **115**, 5962.
- <sup>69</sup> B. Hamelin, L. Jullien, A. Laschewsky, C. Hervé du Penhoat, *Chem. Eur. J.*, 1999, **5**, 2546.
- <sup>70</sup> D. B. Davies, L. N. Djimant, A. N. Vesselkov, *J. Chem. Soc., Faraday Trans.*, 1996, **92**, 383.
- <sup>71</sup> A. P. Bisson, F. J. Carver, C. A. Hunter, J. P. Waltho, *J. Am. Chem. Soc.*, 1994, **116**, 10292.
- <sup>72</sup> O. F. Schall and G. W. Gokel, *J. Org. Chem.* 1996, **61**, 1449.
- <sup>73</sup> C. Bruyneel, T. Zeegers-Huyskens, *Journal of Molecular Structure*, 1999, **508**, 163.
- <sup>74</sup> L. K. Patterson and R. M. Hammaker, *Spectrochimica Acta*, 1967, **23A**, 2333.
- <sup>75</sup> M. Yamamoto, Y. Iwai, T. Nakajima and Y. Arai, *J. Phys. Chem. A*, 1999, **103**, 3525.
- <sup>76</sup> D. H. Williams and I. Flemming, in *Spectroscopic Methods in Organic Chemistry*, McGraw-Hill Book Company, London, 5<sup>th</sup> edn., 1995, ch. 4, p. 179.
- <sup>77</sup> The Merk Index, 11<sup>th</sup> ed., 1989.
- <sup>78</sup> Lucy Emeleus, PhD Thesis.

- <sup>79</sup> D. H. Williams and I. Flemming, in *Spectroscopic Methods in Organic Chemistry*, McGraw-Hill Book Company, London, 5<sup>th</sup> edn., 1995, ch 3, p. 76.
- <sup>80</sup> Calculations done by Dr. P. Camp, University of Edinburgh.
- <sup>81</sup> B. Neumann, *Langmuir*, 2001, **17**, 2675.
- <sup>82</sup> M. J. Hynes, *J. Chem. Soc., Dalton Trans.*, 1993, 311.
- <sup>83</sup> J. Campbell, Avecia, private communication.
- <sup>84</sup> L. Alderighi, P. Gans, A. Ienco, D. Peters, A. Sabatini, A. Vacca, *Coord. Chem. Rev.*, 1999, **184**, 311.



**Chapter 5:**  
**Ternary sulfonamido ligand complexes**

<b>Contents</b>	<b>Page</b>
5.1 Introduction .....	244
5.2 Bidentate bis-sulfonamidodiamine ligand systems .....	245
5.2.1 Synthesis of bis-sulfonamidodiamine ligands.....	245
5.2.2 Characterisation of bis-sulfonamidodiamine ligands .....	245
5.2.2.1 NMR spectroscopy.....	245
5.2.2.2 Mass spectrometry, IR spectroscopy and micro-analysis .....	246
5.2.2.3 X-ray crystallography .....	247
5.2.3 Solid state structures of bis-sulfonamidodiamine ligands.....	247
5.2.3.1 1, 2-Di(4-methylbenzenesulfonamido)ethane ( <b>57</b> ).....	247
5.2.3.2 1, 2-Di(4-methylbenzenesulfonamido)cyclohexane ( <b>58</b> ) .....	249
5.2.3.3 1,2-Di(4-methylbenzenesulfonamido)benzene ( <b>59</b> ) .....	250
5.2.4 Hydrogen-bonding in bis-sulfonamidodiamine ligands .....	252
5.2.5 Attempted formation of transition metal complexes of.....	
bis-sulfonamidodiamine ligands .....	252
5.3 Tridentate tris-sulfonamidotriamino ligand systems.....	253
5.3.1 Synthesis of tridentate tris-sulfonamidotriamine ligands.....	253
5.3.2 Characterisation of tris-sulfonamidotriamine ligands .....	256
5.3.2.1 NMR spectroscopy.....	256
5.3.2.2 Mass spectrometry, IR spectroscopy, X-ray crystallography .....	
and micro-analysis .....	257
5.3.3 Solid state structures of tris-sulfonamidotriamine ligands .....	258
5.3.3.1 Tris-(2-(4-methylbenzenesulfonamido)ethyl)amine ( <b>60</b> ) .....	258
5.3.3.2 Cis-cis-1,3,5, tris-(4-methylbenzenesulfonamido)- .....	
cyclohexane ( <b>61</b> ) .....	260
5.3.3.3 N,N',N''-tris-(4-methylbenzenesulfonyl)-2-aminomethyl- .....	
2- methylpropane-1, 3-diamine ( <b>62</b> ) .....	263
5.3.4 Hydrogen-bonding in tris-sulfonamidotriamine ligands .....	264
5.3.5 Coordination chemistry of tris-sulfonamidotriamine ligands .....	265
5.3.5.1 Attempted formation of transition metal complexes of.....	

tris-sulfonamidotriamine ligands .....	265
5.3.5.2 N,N',N'',N'''[Tris-(2-(4-methylbenzenesulfonylamino)ethyl) .. aminato] copper(II) potassium(I) (70) .....	266
5.3.6 Attempted methylation of tris-[2-(4-methylbenzenesulfonylamino)..... ethyl]amine (60).....	267
5.3.7 Nitrogen geometry of bis- and tris-sulfonamide ligands.....	268
5.4 Conclusion .....	271
5.5 Experimental .....	272
5.5.1 Instrumentation.....	272
5.5.2 Solvent and reagent pretreatment.....	272
5.5.3 Synthesis of bis-sulfonamidodiamine ligands.....	273
5.5.4 Synthesis of tris-sulfonamidotriamine ligands .....	275
5.5.5 Complexes of tris-sulfonamidotriamine ligands .....	282
5.5.6 X-ray crystallography.....	282
5.6 References .....	286

## 5.1 Introduction

Chapters 2 and 3 dealt with ligand systems in which a hydrogen-bond donor atom and a hydrogen-bond acceptor site were built into one ligand system. *Pseudo*-macrocyclic ligand formation of these ligands occurred through a head-to-tail arrangement of the ligands. Progression from such  $ML_2$  systems led to the attempted development of  $ML^1L^2$  complexes in which one ligand ( $L^1$ ) contains two acceptor sites and the second ligand ( $L^2$ ) contains two donor sites. Such a system could also be applied to tridentate ligand systems to create ligands which form a *pseudo*-cage structure. A schematic representation of such 4-coordinate and 6-coordinate  $ML^1L^2$  systems is given in Figure 5.1.

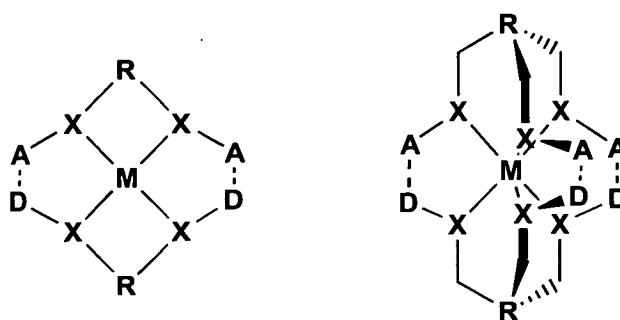


**Figure 5.1:** Target  $ML^1L^2$  systems where X are the donor atoms, A are the hydrogen-bond acceptor sites and D are the hydrogen-bond donor sites.

Such systems could be very versatile as metal extractants because different hydrogen-bond donor and acceptor ligand types could be combined to tune the properties of the systems to bind selectively to one target metal.

Bis- and tris-sulfonamido ligands ( $L^1$ ) were synthesised. The two oxygen atoms of each sulfonamide group provide hydrogen-bond acceptor sites. The sulfonamido nitrogen atoms should be relatively easily deprotonated to give di- or tri-anionic ligands  $[L^1-2H]^{2-}$  or  $[L^1-3H]^{3-}$ . Simple, di- or tri- amines were envisaged as the complementary ( $L^2$ ) ligands because of their N-H hydrogen-bond donor groups.

## 5.2 Bidentate bis-sulfonamidodiamine ligand systems

### 5.2.1 Synthesis of bis-sulfonamidodiamine ligands

The generic form of the disulfonamidodiamine ligands synthesised is shown in Figure 5.2.

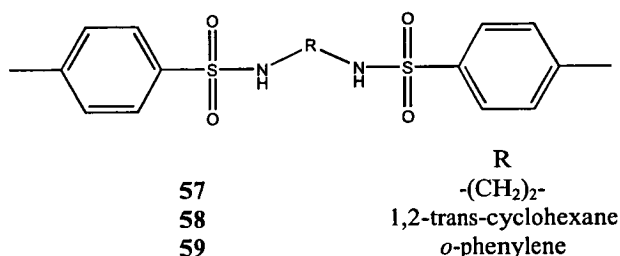


**Figure 5.2:** The generic form of a disulfonamidodiamine ligand, and ligands synthesised in this work.

**57** and **58** were readily prepared by the addition of two equivalents of 4-methylbenzenesulfonyl chloride in toluene to one equivalent of the relevant diamine in toluene (Figure 5.3).

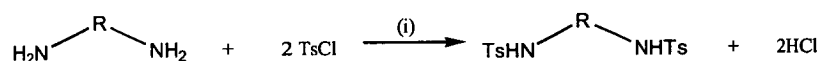


**Figure 5.3:** The synthesis of ligands **57** (R = -(CH<sub>2</sub>)<sub>2</sub>-) and **58** (R = 1,2-C<sub>6</sub>H<sub>10</sub>). (i) toluene, 25°C.

**59**, was prepared following the method of Cheng *et al.*<sup>1</sup> The same reagent stoichiometries were used but pyridine was used as the solvent instead of toluene.

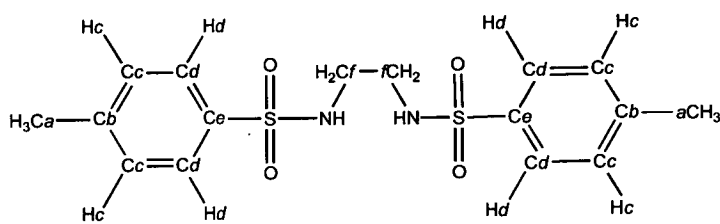
### 5.2.2 Characterisation of bis-sulfonamidodiamine ligands

#### 5.2.2.1 NMR spectroscopy

The characteristic resonances in the aromatic region, used to identify the monosulfonamido diamine ligands, shown by *p*-alkylarylsulfonamides were again useful for the identification of bis-sulfonamidodiamine ligands. The four aromatic protons fall into two magnetically equivalent sets in *c* and *d* (Figure 5.4) which have sufficiently different chemical shifts to give rise to two doublets, observed between 7.2 and 7.7 ppm depending on the exact structure, and with a coupling constant <sup>3</sup>J<sub>HH</sub> of typically 8 Hz. The *d* protons were shifted to lower field with respect to the *c*

protons due to the deshielding effect of the sulfonyl group. The 4-methylbenzene groups also give rise to a further characteristic singlet at around 2.4 ppm for the methyl group.

As an example, 1,2-di(4-methylbenzenesulfonamido)ethane (**57**), shows a further multiplet at 2.70 ppm assigned to the methylene hydrogens of the ethane linkage group (Figure 5.4).  $^{13}\text{C}$  NMR is also useful in confirming the structures. Assignments for 1,2-di(4-methylbenzenesulfonamido)ethane (**57**) are given in Figure 5.4. The methyl signal of the *p*-methylbenzene group is usually found around 20 ppm and two equivalent sets of four aromatic C-H groups are found around 130 ppm. The remaining signals are easily assigned using DEPT techniques.<sup>2</sup>



	$^{13}\text{C}$ NMR (ppm)	$^1\text{H}$ NMR (ppm)
<i>a</i>	21	2.38
<i>b</i>	143	—
<i>c</i>	127	7.38
<i>d</i>	130	7.61
<i>e</i>	143	—
<i>f</i>	42	2.70

Figure 5.4: NMR assignments for 1, 2-di(4-methylbenzenesulfonamido)ethane (**57**).

### 5.2.2.2 Mass spectrometry, IR spectroscopy and micro-analysis

IR and mass spectrometry were routinely used for characterisation. One strong band was found in the  $1370\text{--}1330\text{ cm}^{-1}$  region and another in the  $1180\text{--}1160\text{ cm}^{-1}$  region for the  $-\text{SO}_2\text{--N}$  group. Of the mass spectrometry techniques available (EI, FAB and ESI) fast atom bombardment has been used primarily for analysis purposes. The composition of each compound was supported by elemental analysis.

### 5.2.2.3 X-ray crystallography

Ligands **57**, **58**, and **59** were all characterised by X-ray crystallography. The bond lengths of the central components of each ligand are listed in Figure 5.5.

Bond	57 <sup>a</sup>	58 <sup>a</sup>	59
i	1.622(3)	1.6113(19)	1.621(3)
ii	1.467(5)	1.465(3)	1.414(5)
iii	1.509(7)	1.531(4)	1.414(5)
iv	1.467(5)	1.465(3)	1.429(5)
v	1.622(3)	1.6113(19)	1.624(3)

<sup>a</sup> Molecules **57** and **58** are centrosymmetric.

**Figure 5.5:** Bond lengths (Å) for the central components of bis-sulfonamidodiamine ligands **57**, **58**, and **59**.

The S-N lengths are similar in each case. The C-N lengths in **57** and **58** are similar however they are shorter in **59** due to the delocalisation of the  $\pi$  electrons over the C-N bond. The C-C length in **59** is also shorter due to the aromatic nature of the bond.

## 5.2.3 Solid state structures of bis-sulfonamidodiamine ligands

### 5.2.3.1 1, 2-Di(4-methylbenzenesulfonamido)ethane (**57**)

The asymmetric unit of **57** consists of half of the molecule, the whole molecule is generated by a centre of symmetry (Figure 5.6).

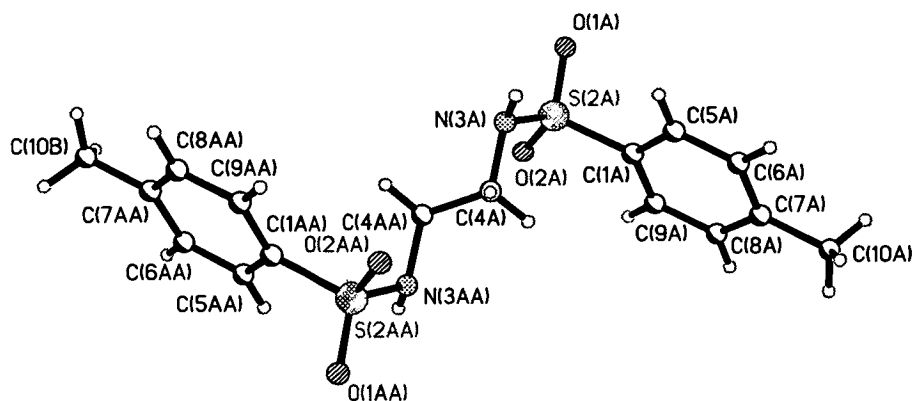


**Figure 5.6:** The X-ray structure 1, 2-di(4-methylbenzenesulfonamido)ethane (**57**).

There is no *intra*-molecular hydrogen-bonding in **57**, however molecules are linked along the *b* axis by four hydrogen-bonds between the sulfonamido oxygen atom (O(1A)) and the sulfonamido hydrogen atoms (H(3A)), [N(3A)-H---O(1A), 2.958(4) Å; N-H-O, 165(4)°] (Figure 5.7).

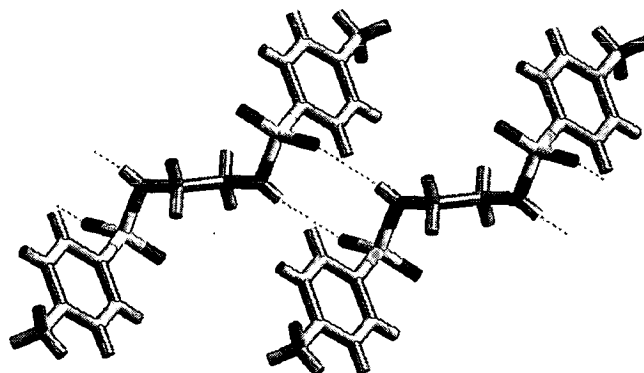


**Figure 5.7:** The hydrogen-bonded chain of molecules of **57** along the *b* axis.



5.2.3.2 1, 2-Di(4-methylbenzenesulfonamido)cyclohexane (**58**)

The asymmetric unit of **58** consists of half of the molecule and the whole molecule is generated by a  $C_2$  axis passing through the cyclohexane ring (Figure 5.8).

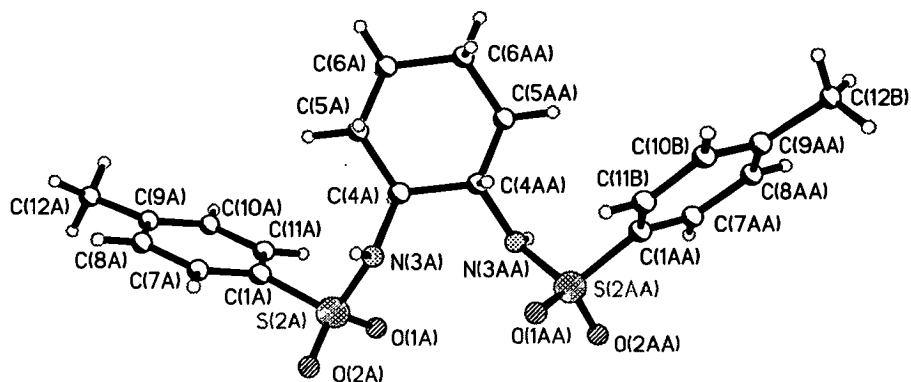


**Figure 5.8:** The X-ray structure 1, 2-di(4-methylbenzenesulfonamido)cyclohexane (**58**).

The secondary hydrogen-bonded structure is very similar to **57** and the sulfonamido groups assemble across inversion centres to form a chain along the  $c$  axis. In total, there are four hydrogen-bonds per molecule involving the sulfonamido oxygen (O(2A)) and hydrogen atom (H(3A)), [N(3A)-H---O(2A), 2.956(2) Å; N-H-O, 172(2)°] (Figure 5.9).

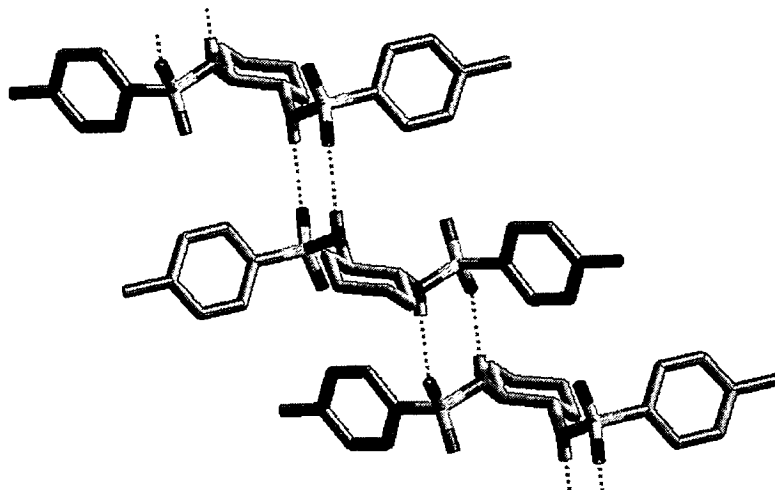
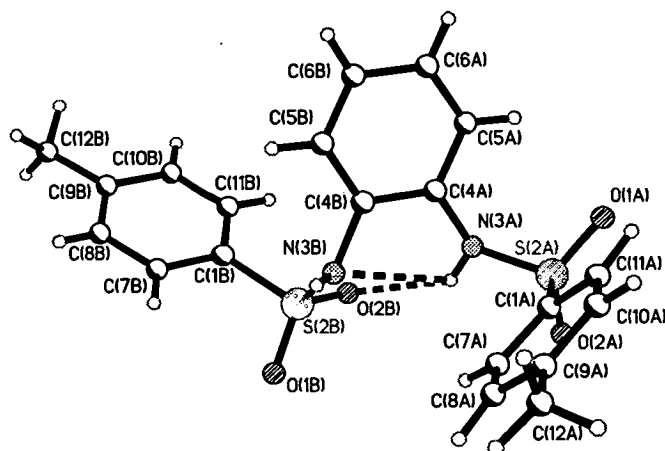


Figure 5.9: *Inter*-molecular hydrogen-bonded chain of molecules of **58** along the *c* axis.

### 5.2.3.3 1,2-Di(4-methylbenzenesulfonamido)benzene (**59**)

The asymmetric unit of **59** is shown in Figure 5.10. There are two *intra*-molecular hydrogen-bonds per molecule. Similar hydrogen-bonds were observed for the monosubstituted molecule (**10**) discussed in section 2.4.1.5. One sulfonamido hydrogen atom (H(3A)) is bifurcated and forms hydrogen-bonds with the sulfonamido nitrogen atom (N(3B)) and the sulfonamido oxygen atom (O(2B)) of the second sulfonamido group [N(3A)-H---N(3B), 2.809(4) Å; N-H-N, 101(3)°] and [N(3A)-H---O(2B), 2.877(4) Å; N-H-O, 134(4)°] respectively.



**Figure 5.10:** The asymmetric unit of 1, 2-di(4-methylbenzenesulfonamido)benzene (**59**).

Molecules of **59** are linked along the *c* axis by two *inter*-molecular hydrogen-bonds between the sulfonamido hydrogen atom (H(3B)) not involved in *intra*-molecular hydrogen-bonding and a sulfonamido oxygen atom (O(2A)) [N(3A)-H---O(2A), 2.975(4) Å; N-H-O, 170(5)°] (Figure 5.11).

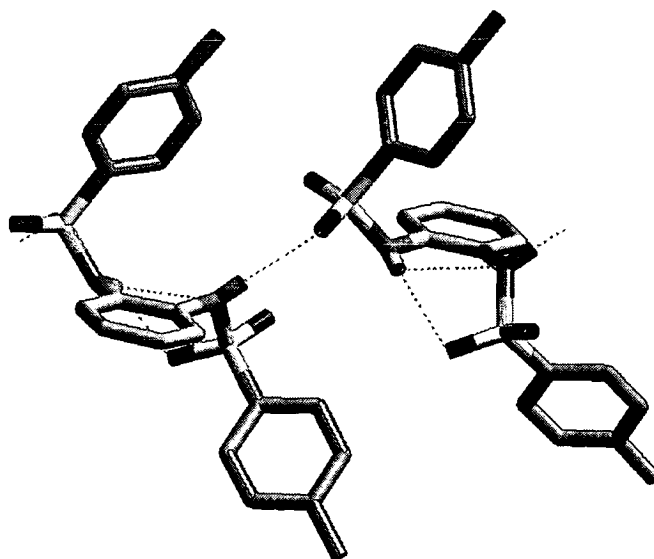


**Figure 5.11:** The hydrogen-bonded chain of molecules of **59** along the *c* axis.

### 5.2.4 Hydrogen-bonding in bis-sulfonamidodiamine ligands

The *intra*- and *inter*-molecular hydrogen-bonding interactions in bis-sulfonamidodiamine ligands are summarised in Tables 5.1 and 5.2.

**Table 5.1:** The *intra*-molecular hydrogen-bond lengths (Å) and angles (°) of bis-sulfonamido ligand **59**.

Ligand	Interaction type	Hydrogen-bond length / Å	Hydrogen-bond angle / °
<b>59</b>	N( <i>S</i> )-H---O( <i>S</i> )	2.809(4)	101(3)
	N( <i>S</i> )-H---N( <i>S</i> )	2.877(4)	134(4)

Atoms labelled *S* are contained in a sulfonamido group.

**Table 5.2:** The *inter*-molecular hydrogen-bond lengths (Å) and angles (°) of bis-sulfonamido ligands **57**, **58** and **59**.

Ligand	Interaction type	Number of interactions	Hydrogen-bond length / Å	Hydrogen-bond angle / °
<b>57</b>	N( <i>S</i> )-H---O( <i>S</i> )	4	2.958(4)	165(4)
<b>58</b>	N( <i>S</i> )-H---O( <i>S</i> )	4	2.956(2)	172(2)
<b>59</b>	N( <i>S</i> )-H---O( <i>S</i> )	2	2.975(4)	170(5)

Atoms labelled *S* are contained in a sulfonamido group.

The average *intra*-molecular hydrogen-bond length (2.85 Å) is shorter than the mean *inter*-molecular length (2.96 Å). However, the *inter*-molecular bonds are closer to linearity (mean bond angle= 168°) than the *intra*-molecular bonds (mean bond angle = 118°).

### 5.2.5 Attempted formation of transition metal complexes of bis-sulfonamidodiamine ligands

The reaction of equimolar mixtures of bis-sulfonamido ligands **57-59** and a diamine with an identical hydrocarbon backbone with metal(II) acetate salts in methanolic solution did not generate metal complexes containing deprotonated sulfonamides. Colour changes for the reaction of copper, nickel and cobalt acetates were consistent with the formation of diamine complexes. The complexation of **57** with copper(II) and N,N'-dibutyl-1,2-diaminoethane or N,N'-dibenzyl-1,2-diaminoethane was also tried in addition to reaction mixtures where pyridine or 1,2-diaminoethane were used as the amine and the solvent. However, the only product of these reactions identified was the tris(1,2-diaminoethane)copper(II) complex with two acetate counteranions.

### 5.3 Tridentate tris-sulfonamidotriamino ligand systems

#### 5.3.1 Synthesis of tridentate tris-sulfonamidotriamine ligands

The three target molecules are illustrated in Figure 5.12.

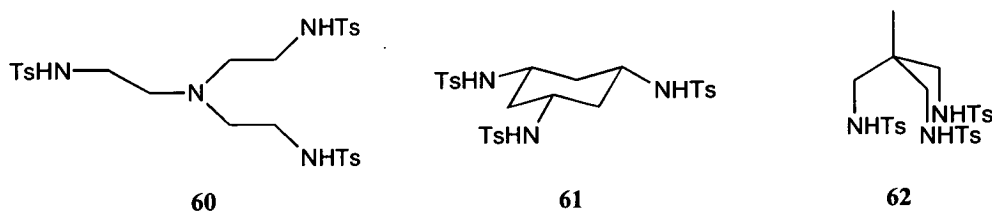


**Figure 5.12:** Target ligands tris-[2-(4-methylbenzenesulfonylamido)ethyl]amine (**60**), *cis-cis*-1,3,5-tris-(4-methylbenzenesulfonylamido)cyclohexane (**61**) and N,N',N''-tris-(4-methylbenzenesulfonyl)-2-aminomethyl-2-methylpropane-1,3-diamine (**62**). Ts =  $-\text{SO}_2\text{C}_6\text{H}_4\text{CH}_3$ .

The tri-amine precursor of **60** is commercially available and the method of Chen *et al*<sup>3</sup> was used to synthesise **60** according to the scheme in Figure 5.13. 4-Methylbenzenesulfonyl chloride in diethylether was added dropwise to tris-(2-aminoethyl)amine and sodium hydroxide in water. This led to the formation of **60** in good yield (79%).

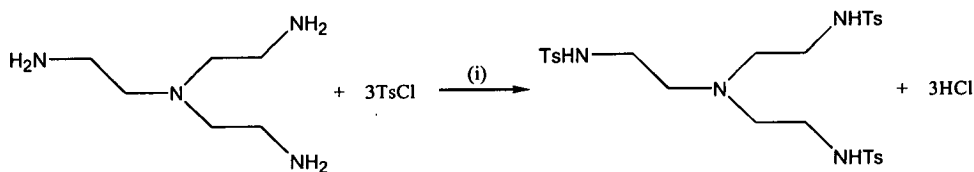


**Figure 5.13:** The synthesis of tris-(2-(4-methylbenzenesulfonylamido)ethyl)amine (**60**). (i) 1. Diethylether, 2. NaOH, H<sub>2</sub>O.

The *cis-cis*-1, 3, 5-triaminocyclohexane required for the synthesis of **61** was not commercially available and was prepared by the method of Bowen *et al*<sup>4</sup> (Figure 5.14).

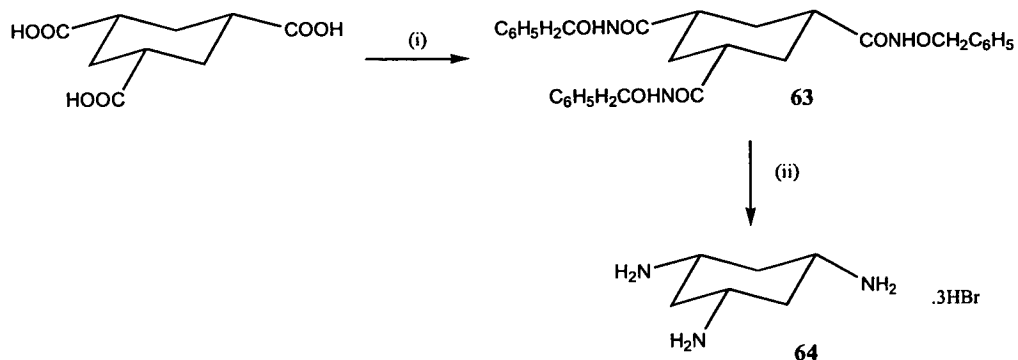


**Figure 5.14:** The synthesis of the hydrobromide salt of *cis*-1,3,5-triaminocyclohexane (**64**) via cyclohexane-1,3,5-tricarboxylic acid tris-(benzyloxy-amide) (**63**). (i) 1. Benzene,  $\text{NEt}_3$ , diphenylphosphoryl azide. 2. Benzyl alcohol, 18 hour reflux. (ii) 1. 30% v/v HBr in acetic acid, stir for 3 hours. 2. Ethanol.

The tris-sulfonamide **61** was prepared by the reaction of 4-methylbenzenesulfonyl chloride with **64** using a similar method<sup>5</sup> for the synthesis of **60**.

The preparation of the triamine precursor of ligand **62** was attempted by the route used by Fleischer *et al.*<sup>6</sup> This involved three steps (Figure 5.15).

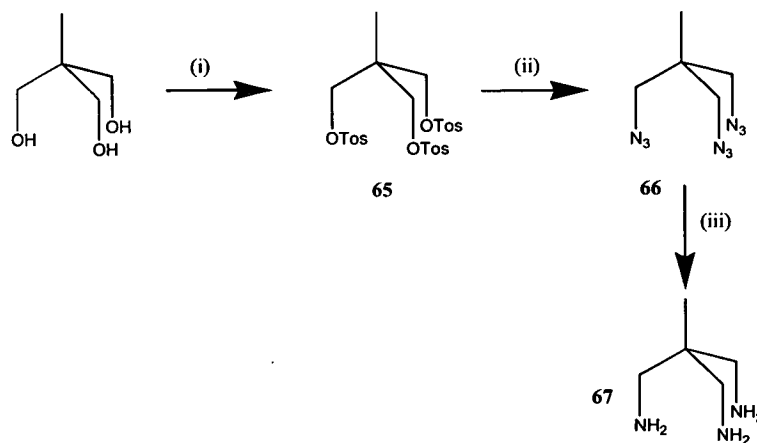


**Figure 5.15:** The synthesis of 1,1,1-tris(aminomethyl)ethane (**67**). (i) 3 eq. 4-methylsulfonyl chloride, pyridine,  $0^\circ\text{C}$ . (ii) Sodium azide, ethylene glycol, 16 hours at  $135^\circ\text{C}$ . (iii) Ethanol,  $\text{H}_2$ , PdC, 3.4 atm.

1,1,1-Tris(hydroxymethyl) ethane was reacted with 4-methylbenzenesulfonyl chloride to yield 1,1,1-tris(benzenesulfonyloxymethyl)ethane (**65**)<sup>7</sup> which was subsequently treated with sodium azide to yield 1,1,1-tris(azidomethyl)ethane (**66**).<sup>6</sup> The third step, involving the reduction of **66** using lithium aluminium hydride,<sup>6</sup> proved to be difficult and resulted in low yields. Reduction of the azide by hydrogenation<sup>8</sup> proved to be a much simpler and quicker route to **67** and resulted in higher yields.

The tris-sulfonamide **62** was prepared by the reaction of 4-methylbenzenesulfonyl chloride with **67** using the method of Crank and Eastwood.<sup>9</sup> Conditions were again similar to those used for the synthesis of **60** and **61**.

Aliphatic azides are known to be potentially explosive and other routes to **67** and **62**, avoiding azide formation, were explored. None of the experiments mentioned below proved successful. However it may be useful to others to note that such routes were tried. Figure 5.16 shows the attempted displacement of methylsulfonate groups from **68** or bromide groups from **69**, by sodium amide. Reaction of **68** failed and <sup>1</sup>H nmr analysis of the product formed upon reaction of **69** suggested the formation of a polymeric material.

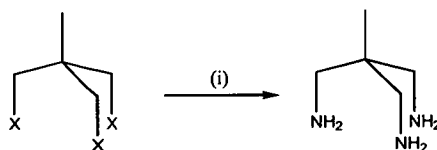


**Figure 5.16:** Attempted synthesis of salt of **67** by the displacement of X by sodium amide.

X = -OSO<sub>2</sub>CH<sub>3</sub> (**68**) or Br (**69**). (i) Na, NH<sub>3</sub>(liquid).

The direct synthesis of **62** by the nucleophilic substitution of a methylsulfonate group by a 4-methylbenzenesulfonamide group was also tried (Figure 5.17). However, experiments where 4-methylbenzenesulfonamide was generated *in situ* using sodium methoxide or butyllithium and where it was first prepared using sodium all proved unsuccessful.

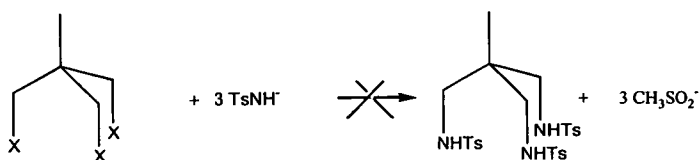


**Figure 5.17:** The reaction of 2-methyl-1,3-bis(methylsulfonyloxy)-2-(methylsulfonyloxy-methyl)propane (**68**) with 4-methylbenzenesulfonamide. X =  $-\text{OSO}_2\text{CH}_3$ .

### 5.3.2 Characterisation of tris-sulfonamidotriamine ligands

#### 5.3.2.1 NMR spectroscopy

Characterisation was accomplished using nmr assignments for the sulfonamido units as outlined in 5.2.2.1.

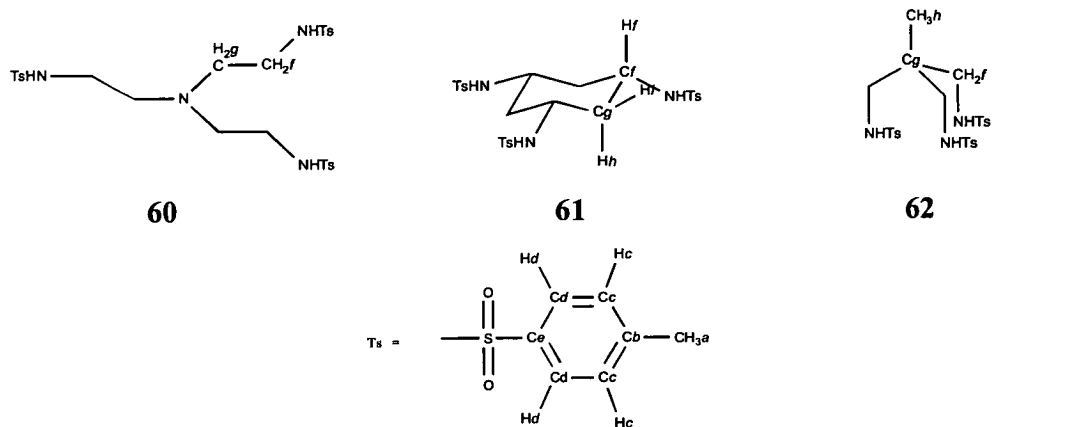
Each of the tris-sulfonamido ligands have significantly different backbones and the  $^1\text{H}$  and  $^{13}\text{C}$  nmr assignments for each ligand are listed in Figure 5.18. In ligand **60**, two additional multiplet signals are observed for the methylene groups at 2.42 and 2.86 ppm. The protons of methylene groups *f* are shifted further downfield than in group *g* due to the electron withdrawing sulfonyl group.

The hydrogen atoms of the cyclohexyl ring in **61** are in three different environments. Atoms *h* and *i* are different as they are positioned *trans* to either another proton or a sulfonamido group. Although signals *h* and *i* are multiplets, and the coupling constants cannot be measured for the splitting pattern, the signals may be assigned due to the width of the signal. Protons *h* and *i* are coupled resulting in a large geminal coupling. Each proton would also be coupled to proton *f*, in *h* this results in a large axial-axial coupling and in *i* a smaller axial-equatorial coupling is observed. Therefore it is expected that a broader signal is observed for *h* than for *i*.

A singlet for the methylene groups of **62** is observed at 2.58 ppm and for the methyl group *h* at 0.77 ppm.



$^{13}\text{C}$  NMR spectra were readily assigned. The methyl signal of the 4-methylbenzene group is usually found at 20 ppm and two equivalent sets of six aromatic C-H groups are found around 130 ppm. The remaining signals are easily assigned using DEPT techniques.<sup>2</sup>



		<i>a</i>	<i>b</i>	<i>c</i>	<i>d</i>	<i>e</i>	<i>f</i>	<i>g</i>	<i>h</i>	<i>i</i>
<b>60</b>	$^1\text{H}$ nmr	2.38	—	7.25	7.76	—	2.86	2.42	—	—
	$^{13}\text{C}$ nmr	22	137	128	130	144	55	41	—	—
<b>61</b>	$^1\text{H}$ nmr	2.42	—	7.35	7.58	—	2.97	—	0.88	1.50
	$^{13}\text{C}$ nmr	22	140	127	130	143	49	41	—	—
<b>62</b>	$^1\text{H}$ nmr	2.40	—	7.41	7.66	—	2.58	—	0.77	—
	$^{13}\text{C}$ nmr	22	138	127	131	144	48	—	19	—

Figure 5.18:  $^1\text{H}$  and  $^{13}\text{C}$  nmr assignments for **60**, **61** and **62**.

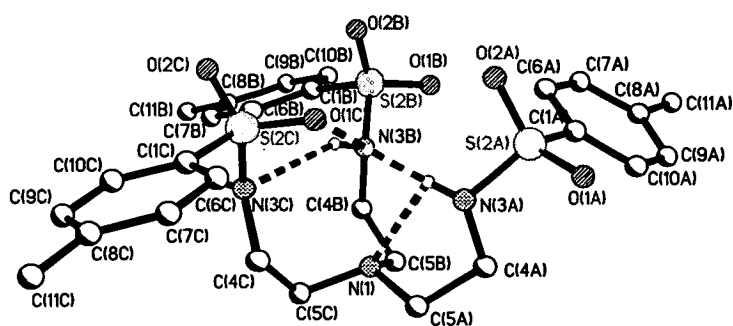
### 5.3.2.2 Mass spectrometry, IR spectroscopy, X-ray crystallography and micro-analysis

IR and mass spectrometry were routinely used for characterisation. IR spectroscopy confirmed the presence of the sulfonamide group in the products. One strong band was expected in the  $1370\text{--}1330\text{ cm}^{-1}$  region and another in the  $1180\text{--}1160\text{ cm}^{-1}$  region for the  $-\text{SO}_2\text{-N}$  group. Of the mass spectrometry techniques available (EI, FAB and ESI) fast atom bombardment has been used primarily for analysis. Each ligand was analysed by X-ray crystallography and the composition of the bulk sample was determined by elemental analysis to support the structure.

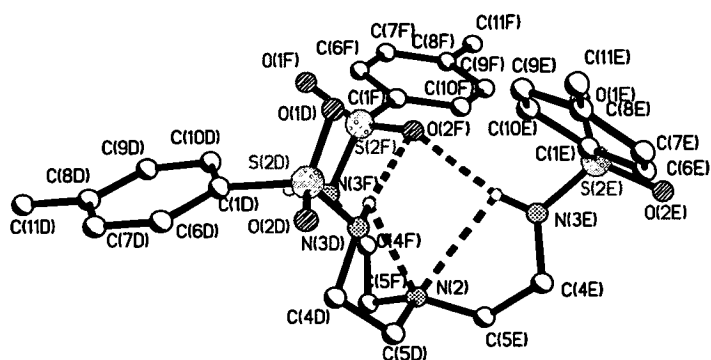
### 5.3.3 Solid state structures of tris-sulfonamidotriamine ligands

#### 5.3.3.1 Tris-(2-(4-methylbenzenesulfonamido)ethyl)amine (60)

There are two crystallographically independent molecules of **60** in the asymmetric unit, type 1 and type 2, (Figure 5.19). Each shows extensive *intra*-molecular hydrogen-bonding. Type 1 molecules (containing arms A, B and C) have two interactions from the bifurcated sulfonamido hydrogen atom of arm A to the central nitrogen atom and to a sulfonamido oxygen atom of arm C [N(3A)-H---N(1), 2.849(4) Å; N-H-N, 110(4)°; N(3A)-H---O(1C), 3.187(4) Å; N-H-O, 129(4)°] and one interaction from the sulfonamido hydrogen atom of arm B to the sulfonamido nitrogen atom of arm C [N(3B)-H---N(3C), 3.321(5) Å; N-H-N, 155(5)°]. There are four *intra*-molecular interactions in type 2 molecules (containing arms D, E and F). The bifurcated sulfonamido hydrogen atom of arm E bonds to the bifurcated sulfonamido oxygen of arm F and to the central nitrogen atom [N(3E)-H---O(2F), 2.956(4) Å; N-H-O, 163(5)°; N(3E)-H---N(2), 2.91 Å; N-H-N, 102°]. The sulfonamido hydrogen atom of arm D is also bifurcated and forms interactions with the bifurcated sulfonamido oxygen atom of arm F and the central nitrogen atom [N(3D)-H---O(2F), 3.306(5) Å; N-H-O, 170(5)°; N(3D)-H---N(2), 2.90 Å; N-H-N, 100°].



1



2

**Figure 5.19:** The two crystallographically independent molecules, type 1 and type 2, of tris-(2-(4-methylbenzenesulfonamido)ethyl)amine (**60**) in the unit cell.

Extensive *inter*-molecular hydrogen-bonding is also observed in **60**. Each crystallographically independent molecule forms separate hydrogen-bonded chains. Type 1 molecules are linked to two other molecules *via* two hydrogen-bonds between the sulfonamido hydrogen atom of arm C and a sulfonamido oxygen atom of arm A [N(3C)-H---O(2A), 2.793(4) Å; N-H-N, 154(5)°] (Figure 5.20). Very similar interactions between the sulfonamido hydrogen atom of arm F and a sulfonamido oxygen atom of arm E link type 2 molecules [N(3F)-H---O(1E), 2.900(5) Å; N-H-O, 165(5)°].

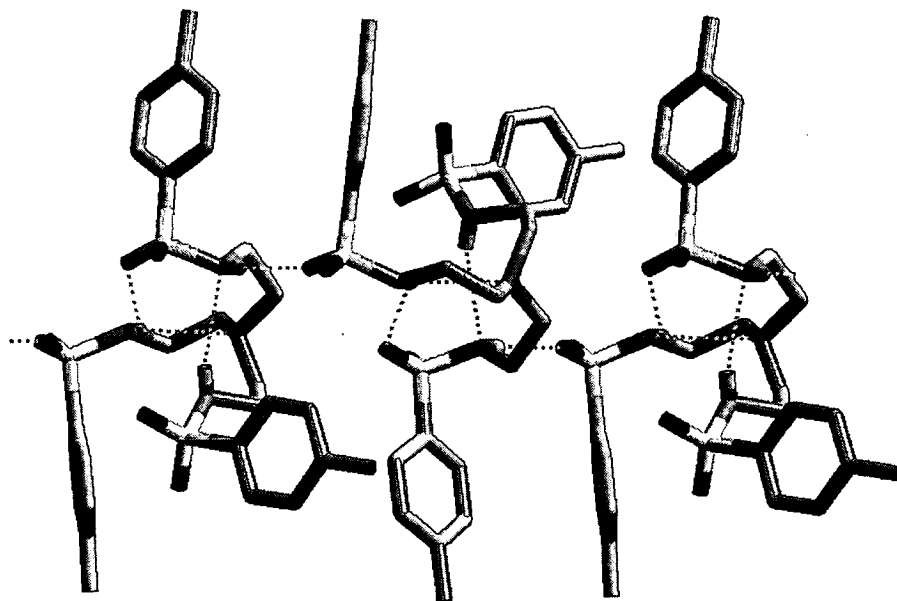
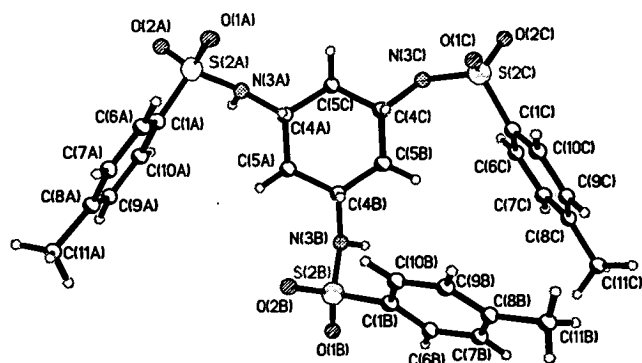


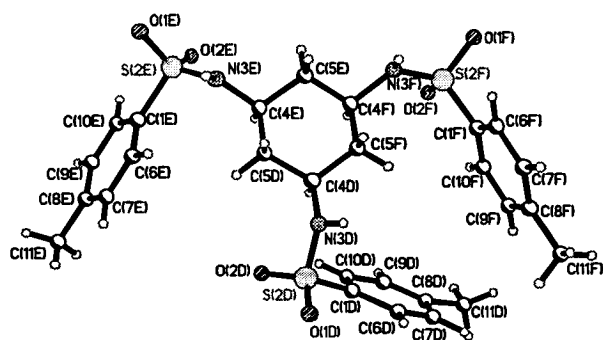
Figure 5.20: Hydrogen-bonded chain of type 1 molecules of **60** along the  $a$  axis.

#### 5.3.3.2 *Cis-cis*-1,3,5,tris-(4-methylbenzenesulfonamido)-cyclohexane (**61**)

There are two crystallographically independent molecules of **61** in the asymmetric unit (Figure 5.21).



1



2

**Figure 5.21:** The X-ray structures of the two crystallographically independent molecules, type 1 and type 2, of *Cis-cis*-1,3,5-tris(4-methylbenzenesulfonylamino)-cyclohexane (**61**).

There are no *intra*-molecular hydrogen-bonding interactions, however there are extensive *inter*-molecular interactions. Type 1 molecules (containing arms A, B and C) and type 2 molecules (containing arms D, E and F) form separate parallel-stacked chains along the *b* axis. Molecules are linked by three hydrogen-bonding interactions to form stacks, pairs of adjacent stacks are linked by further hydrogen-bonding. Stacks of type 1 molecules are linked by a hydrogen-bond from a sulfonamido oxygen of arm C to the sulfonamido hydrogen atom of arm B [N(3B)-H---O(1C), 2.977(4) Å; N-H-O, 175(3)°] and by hydrogen-bonds, *via* an ethanol molecule, between a sulfonamido oxygen of arm A and the sulfonamido hydrogen of arm A of the second molecule [O(1S1)-H---O(1A), 2.67(5) Å; O-H-O, 162°, N(3A)-



### 5.3.3.3 N,N',N''-tris-(4-methylbenzenesulfonyl)-2-aminomethyl-2-methylpropane-1, 3-diamine (**62**)

The asymmetric unit of **62** is shown in Figure 5.24. There is only one *intra*-molecular hydrogen-bond between the sulfonamido nitrogen atom of arm B and the sulfonamido hydrogen atom of arm A [N(3A)-H---N(3B), 2.90 Å; N-H-N, 108°].

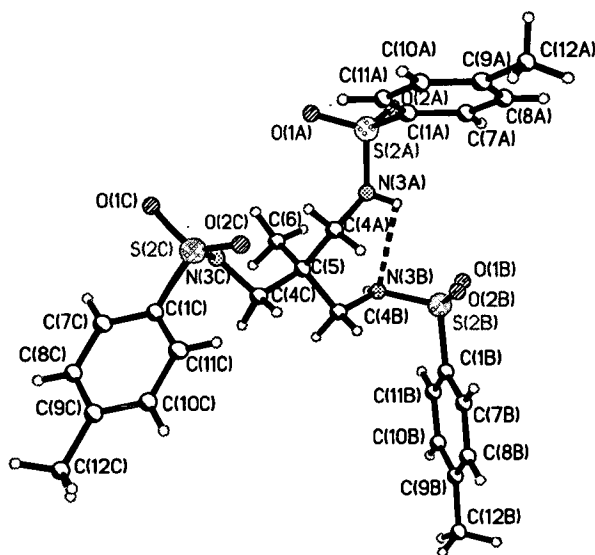


**Figure 5.24:** The asymmetric unit of N,N',N''-tris-(4-methylbenzenesulfonyl)-2-aminomethyl-2-methylpropane-1, 3-diamine (**62**).

Molecules of **62** are linked by pairs of hydrogen-bonds formed across inversion centres by the sulfonamido groups of arms B and C along the *c* axis to form a chain [N(3C)-H---O(1B), 2.924(4) Å; N-H-O; 172(3)°, N(3B)-H---O(1C), 2.913(4) Å; N-H-O, 159(4)°] (Figure 5.25).

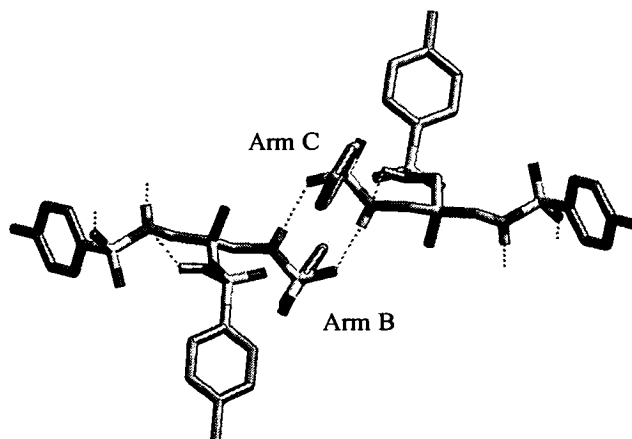


**Figure 5.25:** Hydrogen-bonding of the sulfonamido groups of arms B and C of **62** across inversion centres to form a chain along the *c* axis.

### 5.3.4 Hydrogen-bonding in tris-sulfonamidotriamine ligands

The *intra*- and *inter*-molecular hydrogen-bonding interactions in the tris-sulfonamido ligands are summarised in Tables 5.3 and 5.4.

**Table 5.3:** The *intra*-molecular hydrogen-bond lengths (Å) and angles (°) of tris-sulfonamido ligands **60**, **61** and **62**.

Ligand	Interaction type	Hydrogen-bond length / Å	Hydrogen-bond angle / °	
<b>60<sup>a</sup></b>	Molecule 1	N( <i>S</i> )-H---O( <i>S</i> )	3.187(4)	129(4)
		N( <i>S</i> )-H---N( <i>S</i> )	3.31(5)	155(5)
		N( <i>S</i> )-H---N( <i>A</i> )	2.849(4)	110(4)
	Molecule 2	N( <i>S</i> )-H---O( <i>S</i> )	2.956(4)	163(5)
		N( <i>S</i> )-H---O( <i>S</i> )	3.306(5)	170(5)
		N( <i>S</i> )-H---N( <i>A</i> )	2.91	102
		N( <i>S</i> )-H---N( <i>A</i> )	2.90	100
<b>62</b>	N( <i>S</i> )-H---N( <i>S</i> )	2.985(4)	108(3)	

<sup>a</sup> Ligand **60** has two crystallographically independent molecules in the asymmetric unit. Atoms labelled *S* are contained in a sulfonamido group. Atoms labelled *A* are tertiary amino nitrogen atoms.



**Table 5.4:** The *inter*-molecular hydrogen-bond lengths (Å) and angles (°) of tris-sulfonamido ligands **60**, **61** and **62**.

Ligand		Interaction type	Number of interactions	Hydrogen-bond length / Å	Hydrogen-bond angle / °
<b>60<sup>a</sup></b>	Molecule 1	N( <i>S</i> )-H---O( <i>S</i> )	2	2.793(4)	154(5)
	Molecule 2	N( <i>S</i> )-H---O( <i>S</i> )	2	2.900(5)	165(5)
<b>61<sup>a</sup></b>	Molecule 1	N( <i>S</i> )-H---O( <i>S</i> )	2	2.894(4)	160(4)
		N( <i>S</i> )-H---O( <i>S</i> )	1	2.977(4)	175(3)
		O( <i>E</i> )-H---O( <i>S</i> )	1	2.67(5)	162
	Molecule 2	N( <i>S</i> )-H---O( <i>E</i> )	1	2.813(5)	170(5)
		N( <i>S</i> )-H---O( <i>S</i> )	2	2.898(4)	165(3)
		N( <i>S</i> )-H---O( <i>S</i> )	1	2.899(4)	177(4)
		O( <i>E</i> )-H---O( <i>S</i> )	1	2.867(5)	162
		N( <i>S</i> )-H---O( <i>E</i> )	1	2.813(5)	170(5)
		N( <i>S</i> )-H---O( <i>S</i> )	1	2.924(4)	172(3)
<b>62</b>		N( <i>S</i> )-H---O( <i>S</i> )	1	2.924(4)	172(3)
		N( <i>S</i> )-H---O( <i>S</i> )	1	2.913(4)	159(4)

<sup>a</sup> Ligands **60** and **61** have two crystallographically independent molecules in the unit cell. Atoms labelled *S* are part of a sulfonamido group. Atoms labelled *E* are contained in an ethanol molecule.

In the tris-sulfonamidotriamine ligand **60** *inter*-molecular hydrogen-bonds (mean length and angle, 2.85 Å, 159°) appear to be stronger than *intra*-molecular interactions (mean length and angle, 3.06 Å, 133°). In molecule **62** *intra*- and *inter*-molecular interactions have similar mean lengths of 2.90 and 2.92 Å respectively. However the bond angles of the *inter*-molecular interactions (mean = 166°) are closer to linearity than the *intra*-molecular interactions (mean = 108°). The *inter*-molecular interactions of **61** have very similar values to those in molecules **60** and **62**. As a result of the rigidity of the backbone of ligand **61** no *intra*-molecular hydrogen-bonds are observed.

### 5.3.5 Coordination chemistry of tris-sulfonamidotriamine ligands

#### 5.3.5.1 Attempted formation of transition metal complexes of tris-sulfonamidotriamine ligands

Formation of metal complexes of the trifurcated tris-sulfonamido ligands proved more difficult than expected. Zinc, copper, cobalt and nickel(II) acetates or tetrafluoroborates were added to methanolic or acetonitrile solutions of ligands **60**,

**61** or **62** and sodium methoxide or potassium hydroxide was added in a 3:1 base to ligand ratio in an attempt to deprotonate each sulfonamido nitrogen atom. In most cases colour changes were observed however a solid material was not always isolated. Good analyses were obtained only for copper (**70**) and nickel (**71**) complexes of tris-[2-(4-methylbenzenesulfonamido)ethyl]amine (**60**). Characterisation of products of complexation reactions of *Cis-cis*-1,3,5-tris-(4-methylbenzenesulfonamido)cyclohexane (**61**) and N,N',N''-tris-(4-methylbenzene sulfonyl)-2-aminomethyl-2-methyl propane-1, 3-diamine (**62**) did not prove possible.

Attempts to form ternary complexes of the tripodal ligands in a one to one ratio with a triamine of an identical hydrocarbon backbone in methanol proved unsuccessful, using acetate and tetrafluoroborate transition metal(II) salts and sodium methoxide or potassium hydroxide as a base. Colour changes were consistent with formation of triamino complexes with copper, cobalt and nickel acetates and no evidence for a ternary sulfonamido-amino complex was observed.

#### 5.3.5.2 N,N',N'',N''''[Tris-(2-(4-methylbenzenesulfonylamino)ethyl)amino]copper(II) potassium(I) (**70**)

The asymmetric unit of N,N',N'',N''''[tris-(2-(4-methylbenzenesulfonylamino)ethyl)amine]copper(II) potassium(I) (**70**) comprises of one complex and one molecule of tetrahydrofuran (Figure 5.26). The copper has trigonal bipyramidal geometry and is coordinated to all four nitrogen atoms of ligand **60** and a water molecule. All three sulfonamido nitrogen atoms are deprotonated and a potassium cation balances the charge on the monoanionic complex. Lengths of bonds from the copper to the sulfonamidato nitrogen atoms are 2.052(3), 2.057(2) and 2.114(2) Å, the lengths of bonds to the central nitrogen atom and to the coordinated water molecule are 2.041(2) Å and 2.000(2) Å respectively. The potassium ion forms close contact interactions with three sulfonamido oxygen atoms, in the range of 2.65-2.84 Å.

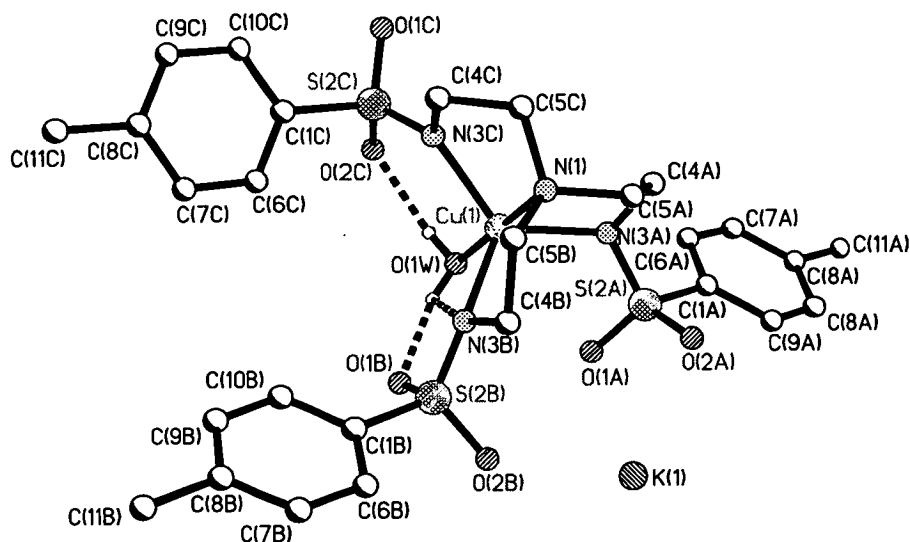


**Figure 5.26:** X-ray structure of  $N,N',N'',N'''$ [tris-(2-(4-methylbenzenesulfonylamino)ethyl)amine] copper(II) potassium(I) (**70**).

There is no extensive *inter-complex* hydrogen-bonding between sulfonamido units. However, there are three *intra-complex* hydrogen-bonds. There is a bifurcated hydrogen-bond involving a hydrogen atom of the water molecule and the nitrogen atom (N(3B)) and an oxygen atom (O(1B)) of arm B of the ligand [O(1W)-H---N(3B), 3.03 Å; O-H-N, 108°; O(1W)-H---O(1B), 2.665(3) Å; O-H-O, 167(4)°] and one interaction between the other hydrogen atom of the water molecule and an oxygen atom of arm C of the ligand [O(1W)H---O(2C), 2.694(3) Å; O-H-O 154(2)°]. These hydrogen-bonds are illustrated in Figure 5.26.

### 5.3.6 Attempted methylation of tris-[2-(4-methylbenzenesulfonylamino)ethyl]amine (**60**)

The X-ray structure of complex **70** showed that all four nitrogen atoms of ligand **60** can coordinate to the metal centre to form a monoanionic complex. This results in the encapsulation of the metal centre by the ligand rather than *fac*-coordination of the three sulfonamido nitrogen atoms which is required for the formation of a *pseudo-*

cage complex using a second tridentate hydrogen-bonding amine ligand (Figure 5.1). Methylation of the capping tertiary nitrogen atom to give ligand **I** (Figure 5.27) would dramatically change the ligating properties of this ligand type.

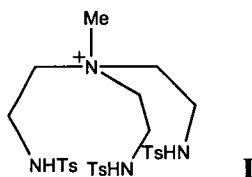


**Figure 5.27:** Methylated tris-[2-(4-methylbenzenesulfonylamino) ethyl]amine.

There is no longer a lone pair on the capping nitrogen atom to interact with metal centres. The incorporation of the methyl unit will result in an *exo*-configuration with the methyl located away from the sulfonamido-metal bonds. This would promote the desired *fac*-octahedral arrangement of the three deprotonated sulfonamido groups. Another potentially useful feature of **I** in its deprotonated form is that it would form neutral complexes with divalent metal ions, the quaternary ammonium centre providing the equivalent of the potassium ion in **70**. There are many literature examples of the methylation of similar tertiary amines.<sup>10,11</sup> However, only one example of the methylation of a tertiary nitrogen attached to three ethylamine groups was found in the literature and this was a cryptand.<sup>12</sup> Three different methylating agents were tried, methyl iodide, dimethyl sulfate and trimethyloxonium tetrafluoroborate. The first two reagents failed to give any product and the latter reagent resulted only in the protonation of the nitrogen atom. It is thought that the difficulty in methylating this species may be due to the hydrogen-bonding interactions of the lone pair of central nitrogen (see Figure 5.19).

### 5.3.7 Nitrogen geometry of bis- and tris-sulfonamide ligands

The planarity of the sulfonamido nitrogen atom of bis- and tris-sulfonamido ligands and complex **70** were investigated in a similar manner to that described for the monosulfonamido ligands (chapter 2, section 2.4.4.2) by the measurement of  $\theta$  (the sum of the angles S-N-H/M, H/M-N-C and C-N-S) and  $\alpha$  (the angle of the S-N bond from the plane defined by the nitrogen, carbon and hydrogen or metal atoms). The distance of the nitrogen atom from the plane defined by the carbon, sulfur and

hydrogen or metal atoms to which it is bonded. The results are given in Tables 5.5, 5.6 and 5.7.

**Table 5.4:** Values of the parameters  $\theta$ ,  $\alpha$  and the distance of the nitrogen atom from the HCS plane to define the planarity of the sulfonamide nitrogen atom in bis-sulfonamidodiamine ligands **57**, **58** and **59**.

Ligand	Distance of N from HCS plane / Å	Sum of 3 angles, $\theta$ , around N / °	Angle of S, $\alpha$ , from NCH plane / °
<b>57<sup>a</sup></b>	0.274	343.4	40.3
	0.274	343.4	40.4
<b>58<sup>a</sup></b>	0.224	349.6	31.9
	0.224	349.6	31.9
<b>59</b>	0.221	348.6	32.1
	0.202	351.1	28.0

<sup>a</sup> Ligands **57** and **58** are centrosymmetric.

**Table 5.6:** Values of the parameters  $\theta$ ,  $\alpha$  and the distance of the nitrogen atom from the HCS plane to define the planarity of the sulfonamide nitrogen atom in tris-sulfonamidodiamine ligands **60**, **61** and **62**.

Ligand	Distance of N from HCS plane / Å	Sum of 3 angles, $\theta$ , around N / °	Angle of S, $\alpha$ , from NCH plane / °	
<b>60<sup>a</sup></b> Molecule 1	0.273	345.2	37.1	
	0.311	340.4	42.5	
	0.285	343.8	41.0	
	Molecule 2	0.311	341.6	41.2
		0.298	343.2	40.3
<b>61<sup>a</sup></b> Molecule 1	0.198	352.3	27.9	
	0.228	350.9	29.1	
	0.313	340.1	42.8	
	0.239	347.1	33.8	
	Molecule 2	0.255	346.5	35.2
		0.142	356.3	19.0
0.244		346.7	34.4	
<b>62</b>	0.181	353.7	25.2	
	0.255	347.6	33.8	
	0.167	354.5	23.7	

<sup>a</sup> Ligands **60** and **61** have two independent molecules in the asymmetric unit.

**Table 5.7:** Values of the parameters  $\theta$ ,  $\alpha$  and the distance of the nitrogen atom from the MCS plane to define the planarity of the sulfonamide nitrogen atom in complex **70**.

Complex	Distance of N from MCS plane / Å	Sum of 3 angles, $\theta$ , around N / °	Angle of S, $\alpha$ , from NCM plane / °
<b>70</b>	0.394	343.5	36.9
	0.231	354.3	21.4
	0.081	359.3	7.6

In most cases in chapter 2 the sulfonamido nitrogen becomes more planar following the complexation of the ligand, this is also observed here on the complexation of ligand **60**. As discussed in chapters 2 and 3, if the planarity of the amide is associated with a delocalisation of electron density in the N-S=O unit then we might expect there to be a connection between the planarity of the nitrogen and the lengths of the sulfur to oxygen and sulfur to nitrogen bonds. S=O and S-N bond lengths are recorded in Tables 5.8 and 5.9. The correlation coefficients between bondlengths and parameters defining the planarity of the sulfonamido nitrogen atom (see also section 2.4.4.2) are recorded in Tables 5.10 and 5.11.

**Table 5.8:** S=O and S-N lengths of bis-sulfonamidodiamine ligands. *a* Ligands **57** and **58** are centrosymmetric.

Ligand	S=O(1) / Å	S=O(2) / Å	Average S=O Length / Å	S-N bond / Å
<b>57<sup>a</sup></b>	1.435	1.427	1.431	1.622
	1.435	1.427	1.431	1.622
<b>58<sup>a</sup></b>	1.428	1.434	1.431	1.611
	1.428	1.434	1.431	1.611
<b>59</b>	1.426	1.433	1.430	1.621
	1.425	1.440	1.433	1.625

**Table 5.9:** S=O and S-N lengths of tris-sulfonamidotriamine ligands. *a* Ligands **60** and **61** have two crystallographically independent molecules in the unit cell.

Complex	S=O(1) / Å	S=O(2) / Å	Average S=O Length / Å	S-N bond / Å	
<b>60<sup>a</sup></b>	Molecule 1	1.424	1.434	1.429	1.617
		1.431	1.426	1.429	1.616
		1.426	1.424	1.425	1.630
	Molecule 2	1.433	1.434	1.434	1.626
		1.436	1.427	1.432	1.623
		1.427	1.436	1.432	1.625
<b>61<sup>a</sup></b>	Molecule 1	1.432	1.438	1.435	1.598
		1.433	1.425	1.429	1.619
		1.432	1.442	1.437	1.603
	Molecule 2	1.429	1.431	1.430	1.619
		1.431	1.431	1.431	1.593
		1.438	1.433	1.436	1.611
<b>62</b>	1.433	1.430	1.432	1.609	
	1.438	1.424	1.431	1.612	
	1.452	1.427	1.440	1.607	

**Table 5.10:** The correlation coefficients of the parameters of nitrogen planarity in bis-sulfonamido ligands **57**, **58** and **59** with their S=O and S-N bond lengths.

X	Y	Correlation coefficient
S-N length / Å	Average S=O length / Å	0.35
Distance of N from HCS plane / Å	Average S=O length / Å	-0.36
Distance of N from HCS plane / Å	S-N bond length / Å	0.36
Sum of 3 angles around N, $\theta$	Average S=O length / Å	-0.41
Sum of 3 angles around N, $\theta$ .	S-N length / Å	0.20
Angle of S from NCH plane, $\alpha$	Average S=O length / Å	-0.33
Angle of S from NCH plane, $\alpha$	S-N bond length / Å	0.21

**Table 5.11:** The correlation coefficients of the parameters of nitrogen planarity in tris-sulfonamido ligands **60**, **61** and **62** with S=O and S-N bond lengths.

X	Y	Correlation coefficient
S-N length / Å	Average S=O length / Å	-0.49
Distance of N from MCS plane / Å	Average S=O length / Å	-0.44
Distance of N from MCS plane / Å	S-N bond length / Å	0.43
Sum of 3 angles around N, $\theta$	Average S=O length / Å	-0.46
Sum of 3 angles around N, $\theta$	S-N length / Å	0.66
Angle of S from NCM plane, $\alpha$	Average S=O length / Å	-0.64
Angle of S from NCM plane, $\alpha$	S-N bond length / Å	0.70

In the bis-sulfonamidodiamine ligands there is no correlation between the S-N and S=O lengths to suggest that nitrogen geometry is linked to a resonance effect, whereas in tris-sulfonamidotriamine ligands the expected negative correlation is observed (-0.49). Bis- and tris-sulfonamido ligands show correlations of the same sign in each of the six remaining cases, however the correlation is always stronger for tris-sulfonamido ligands. For  $\alpha$  and the distance of N from the HCS plane the expected correlations with S-N and S=O are observed, however  $\theta$  values show opposite correlations to those expected.

## 5.4 Conclusion

Bidentate and tridentate sulfonamido ligands have been successfully synthesised. However, in the limited studies of the formation of complexes with divalent transition metal ions carried out to date their application in the development of ternary complexes using ligands capable of forming *pseudo*-macrocycle or cage structures did not prove successful. This may be a result of the more favourable

formation of a simple amino complex  $[M(L^2)_2]^{2+}$  over the ternary  $[M(L^1-2H)L^2]$  or  $[M(L^1-3H)L^2]$  complexes. In the case of the bulky tridentate ligands it is also possible that steric crowding would discourage the formation of the ternary complexes.

## 5.5 Experimental

### 5.5.1 Instrumentation

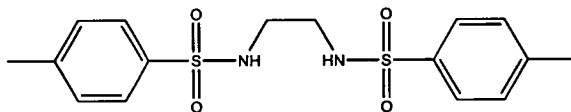
Melting points were determined with a Gallenkamp apparatus and are uncorrected. Elemental analysis was performed on a Perkin Elmer 2400 or a Carlo Erba 1108 elemental analyser. IR spectra for solid materials were obtained as potassium bromide discs and for liquid materials as neat samples using sodium chloride plates on a Perkin Elmer Paragon 1000 FT-IR spectrometer.  $^1\text{H}$  and  $^{13}\text{C}$  NMR spectra were run on Bruker WP200, AC250 and AVANCE DPX360 spectrometers. Chemical shifts ( $\delta$ ) are reported in parts per million (ppm) relative to residual solvent protons as internal standards. Electron impact (EI) mass spectra were obtained either on a Finnigan MAT4600 quadrupole spectrometer or on a Kratos MS50TC spectrometer. Fast atom bombardment (FAB) mass spectra were obtained on a Kratos MS50TC spectrometer in acetonitrile/3-nitrobenzyl alcohol/thioglycerol matrices. Electrospray ionisation (ESI) mass spectra were obtained on a Thermoquest LCQ spectrometer.

### 5.5.2 Solvent and reagent pretreatment

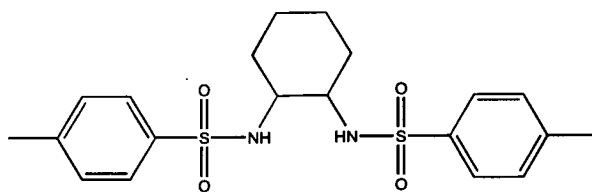
All reagents and solvents were commercially available (Acros or Aldrich) and were used as received. Solvents used for analytical purposes (NMR, MS) were of spectroscopic grade.



## 5.5.3 Synthesis of bis-sulfonamidodiamine ligands

**1, 2-Di(4-methylbenzenesulfonamido)ethane (57)**

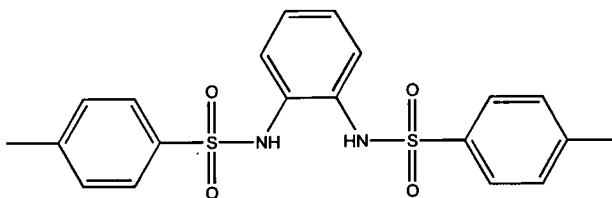
A solution of 1,2-diaminoethane (20 g, 0.33 mol) in toluene (100 cm<sup>3</sup>) was added dropwise over one hour to a solution of 4-methylbenzenesulfonyl chloride (126.89 g, 0.67 mol) in toluene (500 cm<sup>3</sup>). A white precipitate was formed which was isolated by filtration and washed with methanol (3 x 50 cm<sup>3</sup>). The powder was then recrystallised from ethanol (250 cm<sup>3</sup>) to give a white crystalline solid (27.77 g, 23%), mp 160-162°C (Found: C, 52.27; H, 5.50; N 7.64. Calc. for C<sub>16</sub>H<sub>20</sub>N<sub>2</sub>O<sub>4</sub>S<sub>2</sub>: C, 52.15; H, 5.47; N, 7.60%).  $\delta_{\text{H}}$  (DMSO-*d*<sub>6</sub>, 200 MHz): 2.38 (s, 6 H, CH<sub>3</sub>), 2.70 (m, 4 H, CH<sub>2</sub>), 7.38 (d, 4 H, J 8.5, Ar CH), 7.61 (d, 4 H, J 8.1, Ar CH);  $\delta_{\text{C}}$  (DMSO-*d*<sub>6</sub>, 50 MHz): 21 (2 C, CH<sub>3</sub>), 42 (2 C, CH<sub>2</sub>), 127 (4 C, Ar CH), 130 (4 C, Ar CH), 137 (2 C, Ar C), 143 (2 C, Ar C). IR data (KBr disc)/cm<sup>-1</sup>: 1156s, 1334s, 1496m, 1506w, 1559w, 1597m, 2886w, 2940w, 3288s. FAB MS, *m/z* 369 (MH<sup>+</sup>, 11.9%).

***Trans*-1, 2-di(4-methylbenzenesulfonamido)cyclohexane (58)**

A solution of 4-methylbenzenesulfonyl chloride (15.25 g, 0.08 mol) in pyridine (50 cm<sup>3</sup>) was added dropwise over 8 hours to a solution of 1,2-diaminocyclohexane (4.57 g, 0.04 mol) in pyridine (50 cm<sup>3</sup>). The solvent was removed *in vacuo* to give a yellow oil which was triturated with water (3 x 200 cm<sup>3</sup>) for 24 hours to produce a white solid which was isolated by filtration. The product was dried *in vacuo* and recrystallised from ethanol (50 cm<sup>3</sup>) to give a white crystalline solid (6.6 g, 39%), mp 179-180°C (Found: C, 56.73; H, 6.23; N, 6.53. Calc. for C<sub>20</sub>H<sub>26</sub>N<sub>2</sub>O<sub>4</sub>S<sub>2</sub>: C, 56.85; H,

6.20; N, 6.53%).  $\delta_{\text{H}}$  (DMSO- $d_6$ , 250 MHz) 1.05 (m, 4 H,  $\text{CH}_2$ ), 1.44 (m, 4 H,  $\text{CH}_2$ ), 2.37 (s, 6 H,  $\text{CH}_3$ ), 2.87 (s, 2 H,  $\text{NH}$ ), 7.34 (d, 4 H, J 7.3, Ar  $\text{CH}$ ), 7.65 (d, 4 H, J 7.7, Ar  $\text{CH}$ ).  $\delta_{\text{C}}$  (DMSO- $d_6$ , 63 MHz) 21 (2 C,  $\text{CH}_3$ ), 22 (2 C, CH), 29 (2 C,  $\text{CH}_2$ ), 54 (2 C,  $\text{CH}_2$ ), 127 (4 C, Ar CH), 130 (4 C, Ar CH), 139 (2 C, Ar C), 143 (2 C, Ar C). IR data (KBr disc)/ $\text{cm}^{-1}$ : 1170m, 1333m, 2859m, 2928m, 3064w, 3268s. FAB MS,  $m/z$  423 ( $\text{M}^+$ , 7.5%).

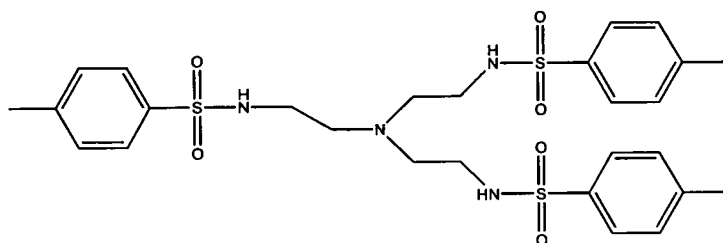
### 1, 2-Di(4-methylbenzenesulfonamido)benzene (59)



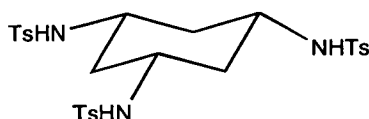
N-2-(4-methylbenzenesulfonylamino-cyclohexyl)-4-methylbenzenesulfonamide was prepared by the method of Cheng *et al.*<sup>1</sup> A solution of benzene-1,2-diamine (10 g, 92 mmol) in pyridine (125  $\text{cm}^3$ ) was added dropwise overnight to a solution of 4-methylbenzenesulfonyl chloride (52.89 g, 0.28 mol) in pyridine (125  $\text{cm}^3$ ). The solution was then neutralised using 15%  $\text{HCl}_{(\text{aq})}$  (350  $\text{cm}^3$ ) giving a cream precipitate which was isolated by filtration which was washed with water (250  $\text{cm}^3$ ) and diethyl ether (2 x 20  $\text{cm}^3$ ) and dried *in vacuo*. The powder was then recrystallised from ethanol (150  $\text{cm}^3$ ) to yield a white crystalline solid (39.30 g, 39%), mp 184-186 °C (Found: C, 57.44; H, 4.67; N, 6.49. Calc. for  $\text{C}_{20}\text{H}_{20}\text{N}_2\text{O}_4\text{S}_2$ : C, 57.67; H, 4.83; N, 6.74%).  $\delta_{\text{H}}$  (DMSO- $d_6$ , 250 MHz): 2.38 (s, 6 H,  $\text{CH}_3$ ), 6.98 (m, 4 H, Ar  $\text{CH}$ ), 7.20 (d, 4 H, J 8.0, Ar  $\text{CH}$ ), 7.56 (d, 4 H, J 8.3, Ar  $\text{CH}$ ).  $\delta_{\text{C}}$  (DMSO- $d_6$ , 50 MHz): 22 (2 C,  $\text{CH}_3$ ), 124 (2 C, Ar CH), 127 (2 C, Ar CH), 128 (4 C, Ar CH), 131 (2 C, Ar C), 131 (4 C, Ar CH), 137 (2 C, Ar C), 145 (2 C, Ar C). IR data (KBr disc)/ $\text{cm}^{-1}$ : 1147s, 1164s, 1326s, 1498m, 1596w, 2923w, 3318m, 3374. FAB MS,  $m/z$  417 ( $\text{MH}^+$ , 83.7%).

## 5.5.4 Synthesis of tris-sulfonamidotriamine ligands

## Tris-[2-(toluene-4-sulfonamido)ethyl]amine (60)



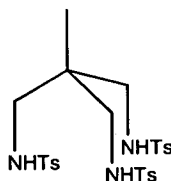
Tris-[2-(toluene-4-sulfonamido)ethyl]amine was prepared by the method of Chen et al.<sup>3</sup> 4-Methylbenzenesulfonyl chloride (100 g, 0.52 mol) in diethylether (300 cm<sup>3</sup>) was added dropwise to tris(2-aminoethyl)amine (25.2 g, 0.17 mol) dissolved in water (350 cm<sup>3</sup>) containing sodium hydroxide (29.1 g, 0.52 mol) with vigorous stirring at room temperature. Stirring was continued for two hours after the addition and the reaction mixture was then allowed to stand for twelve hours. The product which separated out was collected by filtration, washed with water and recrystallised from methanol (100 cm<sup>3</sup>) to yield a white crystalline solid (81.76 g, 79%), mp 116-118 °C (Found: C, 53.31; H, 5.98; N, 9.16. Calc. for C<sub>27</sub>H<sub>36</sub>N<sub>4</sub>O<sub>6</sub>S<sub>3</sub>: C, 53.27; H, 5.96; N, 9.20%).  $\delta_{\text{H}}$  (CDCl<sub>3</sub>, 200 MHz): 2.38 (s, 9H, CH<sub>3</sub>), 2.42 (m, 6 H, CH<sub>2</sub>), 2.86 (m, 6 H, CH<sub>2</sub>), 7.25 (d, 6 H, J 7.9, Ar CH), 7.76 (d, 6 H, J 8.3, Ar CH).  $\delta_{\text{C}}$  (CDCl<sub>3</sub>, 90 MHz): 22 (3C, CH<sub>3</sub>), 41 (3 C, CH<sub>2</sub>), 55 (3 C, CH<sub>2</sub>), 128 (6 C, Ar CH), 130 (6 C, Ar CH), 137 (3 C, Ar C), 144 (3 C, Ar C). IR data (KBr disc)/cm<sup>-1</sup>: 670m, 839m, 963m, 1179s, 1191m, 1359m, 1600w, 2924w, 2964w, 3457w. FAB MS,  $m/z$  583 (MH<sup>+</sup>, 100.0%).

*Cis-cis*-1, 3, 5, tris-(4-methylbenzenesulfonylamino)-cyclohexane (61)

*Cis-cis*-1,3,5, tris-(4-methylbenzenesulfonylamino)-cyclohexane was prepared by the method of Stetter *et al.*<sup>5</sup> 4-Methylbenzenesulfonyl chloride (16.96 g, 8.9 x 10<sup>-2</sup> mol) in diethylether (100 cm<sup>3</sup>) was added dropwise to *cis-cis*-cyclohexane-1,3,5-triamino-trihydrobromide (11.03 g, 30 mmol) dissolved in water (150 cm<sup>3</sup>) containing sodium

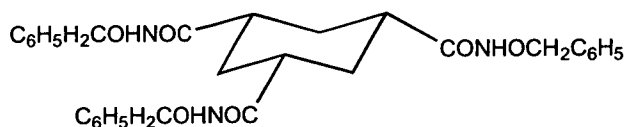
hydroxide (5 g, 89 mmol) with vigorous stirring at room temperature. Stirring was continued for two hours after the addition and the reaction mixture was then allowed to stand for twelve hours. A white solid was collected by filtration and dissolved in dichloromethane (100 cm<sup>3</sup>), the organic phase was then washed with 10% NaHCO<sub>3</sub> aqueous solution (100 cm<sup>3</sup>) and water (2 x 100 cm<sup>3</sup>). The organic phase was dried over anhydrous magnesium sulfate and the dichloromethane was removed *in vacuo* to yield a white material. This was recrystallised from ethanol (300 cm<sup>3</sup>) to yield a white crystalline solid (4.4g, 23%), mp 210-212 °C (Found: C, 54.88; H, 5.63; N, 6.97. Calc. for C<sub>27</sub>H<sub>33</sub>N<sub>3</sub>O<sub>6</sub>S<sub>3</sub>: C, 54.80; H, 5.62; N, 7.10%).  $\delta_{\text{H}}$  (DMSO-*d*<sub>6</sub>, 360 MHz): 0.88 (m, 3 H, CH<sub>2</sub>), 1.50 (m, 3 H, CH<sub>2</sub>), 2.42 (9 H, s, CH<sub>3</sub>), 2.97 (m, 3 H, CH), 7.35 (d, 6 H, J 8.1, Ar CH), 7.58 (d, 6 H, J 8.1, Ar CH).  $\delta_{\text{C}}$  (DMSO-*d*<sub>6</sub>, 90 MHz): 22 (3 C, CH<sub>3</sub>), 41 (3 C, CH<sub>2</sub>), 49 (3 C, CH), 127 (6 C, Ar CH), 130 (6 C, Ar CH), 140 (3 C, Ar C), 143 (3 C, Ar C). IR data (KBr disc)/cm<sup>-1</sup>: 1091m, 1159s, 1316m, 1438m, 3258m. FAB MS, *m/z* 592 (MH<sup>+</sup>, 26.6%).

**N,N',N''-tri(4-methylbenzenesulfonyl)-2-aminomethyl-2-methylpropane-1,3-diamine (62)**



N,N',N''-tri(4-methylbenzenesulfonyl)-2-aminomethyl-2-methylpropane-1,3-diamine was prepared by the method of Crank and Eastwood.<sup>9</sup> 4-Methylbenzenesulfonyl chloride (15.76 g, 83 mmol) in diethylether (300 cm<sup>3</sup>) was added dropwise to a solution of 2-aminomethyl-2-methylpropane-1,3-diamine (3.23 g, 28 mmol) in water (150 cm<sup>3</sup>) with vigorous stirring. The mixture was allowed to stir for one and a half hours and then left to stand overnight. The diethylether was then removed *in vacuo* and the water was decanted to leave a thick white oil. This was triturated with a hexane and diethylether mixture to yield a white solid. Recrystallisation from ethanol (350 cm<sup>3</sup>) yielded a white crystalline material (5.44 g, 34%), mp 220-222°C (Found: C, 53.92; H, 5.37; N, 6.99. Calc. for C<sub>26</sub>H<sub>33</sub>N<sub>3</sub>O<sub>6</sub>S<sub>3</sub>: C, 53.86; H, 5.74; N, 7.25%).  $\delta_{\text{H}}$  (CDCl<sub>3</sub>, 360 MHz): 0.77 (s, 3 H, CH<sub>3</sub>), 2.40 (s, 9 H, CH<sub>3</sub>), 2.58 (s, 6 H, CH<sub>2</sub>), 7.41 (d, 6 H, J 8.1, Ar CH), 7.66 (d, 6 H, J 8.3, Ar CH).  $\delta_{\text{C}}$  (CDCl<sub>3</sub>, 90 MHz): 19 (CH<sub>3</sub>), 22 (3 C, CH<sub>3</sub>), 48 (3 C, CH<sub>2</sub>), 127 (6 C, Ar CH), 131 (6 C, Ar CH), 138 (3 C, Ar C), 144 (3 C, Ar C). IR data (KBr disc)/cm<sup>-1</sup>: 664s, 819m, 1093m, 1156s, 1318, 1434m, 2923w, 3285m. FAB MS, *m/z* 580 (MH<sup>+</sup>, 19.4%).

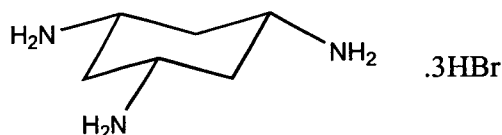
**Cis-cis-cyclohexane-1,3,5-tricarboxylic acid tris-(benzoxyamide) (63)**



Cis-cis-cyclohexane-1,3,5-tricarboxylic acid tris-(benzoxyamide) was prepared by the method of Bowen *et al.*<sup>4</sup> Cis-cis-1,3,5-cyclohexanetricarboxylic acid (8.97 g, 41 mmol) was washed into a one litre round bottom flask with benzene (300 cm<sup>3</sup>) and triethylamine (17.5 cm<sup>3</sup>, 0.12 mol) was added followed by diphenylphosphorylazide (34.65 g, 0.13 mol). The mixture was stirred for one hour and 30 minutes to allow

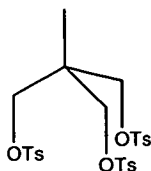
all the solid to dissolve before being held at reflux for 30 minutes before benzyl alcohol (14.92 g, 0.14 mol) was added. The mixture was then refluxed for a further 18 hours after which time it was cooled to room temperature and the white powder product isolated by vacuum filtration and washed with cold benzene ( $3 \times 10 \text{ cm}^3$ ) and dried *in vacuo* (12.2 g, 56%), mp 218-220 °C.  $\delta_{\text{H}}$  ( $\text{CDCl}_3$ , 200 MHz): 1.08 (m, 3 H,  $\text{CH}_2$ ), 1.90 (m, 3 H,  $\text{CH}_2$ ), 3.41 (m, 3 H,  $\text{CH}$ ), 5.02 (s, 6 H,  $\text{CH}_2$ ), 7.37 (m, 15 H, Ar  $\text{CH}$ ).  $\delta_{\text{C}}$  ( $\text{CDCl}_3$ , 63 MHz): 43 (3 C,  $\text{CH}_2$ ), 48 (3 C,  $\text{CH}$ ), 66 (3 C,  $\text{CH}_2$ ), 128 (6 C, Ar  $\text{CH}$ ), 129 (6 C, Ar  $\text{CH}$ ), 138 (3 C, Ar  $\text{CH}$ ), 156 (3 C, Ar C). IR data (KBr disc)/ $\text{cm}^{-1}$ : 1124s, 1227s, 1285s, 1542s, 1686s, 2949w, 3033w, 3313s. ESI MS,  $m/z$  532 ( $\text{MH}^+$ , 100.0%).

***Cis-cis-cyclohexane-1, 3, 5-triamino-trihydrobromide (64)***



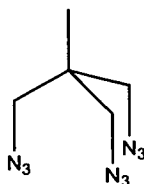
Cyclohexane-1,3,5-triamino-trihydrobromide was prepared by the method of Bowen *et al.*<sup>4</sup> 30% v/w hydrogen bromide in acetic acid ( $100 \text{ cm}^3$ ) was added to cyclohexane-1,3,5-tricarboxylic acid tris-(benzoxyamide) (**63**) (8.3 g,  $1.56 \times 10^{-2}$  mol) and the mixture was stirred for three hours during which time effervescence of carbon dioxide was observed. Ethanol ( $100 \text{ cm}^3$ ) was then added and the mixture was stirred for a further 30 minutes. A white solid was then isolated by filtration, (3.5 g, 60%).  $\delta_{\text{H}}$  ( $\text{D}_2\text{O}$ , 200 MHz): 1.62 (q, 3 H, J 12.2, axial  $\text{CH}$ ), 2.44 (d, 3 H, J 11.2, equatorial  $\text{CH}$ ), 3.49 (tt, 3 H, J 12.2, J 3.6,  $\text{CH-NH}_2$ ).  $\delta_{\text{C}}$  ( $\text{DMSO}-d_6$ , 90 MHz): 34 (3 C,  $\text{CH}_2$ ), 46 (3 C,  $\text{CH}$ ). IR data (KBr disc)/ $\text{cm}^{-1}$ : 1210m, 1406m, 1476s, 1588m, 2995s. FAB MS,  $m/z$  131 ( $\text{C}_6\text{N}_3\text{H}_{16}^+$ , 100.0%).

**2-methyl-1,3-bis-(toluene-4-sulfonyloxy)-2-(toluene-4-sulfonyloxymethyl)propane (65)**



2-methyl-1,3-bis-(toluene-4-sulfonyloxy)-2-(toluene-4-sulfonyloxymethyl)propane was prepared by the method of Stetter and Böckmann.<sup>7</sup> 4-Methylbenzenesulfonyl chloride (65.5 g, 0.83 mol) in pyridine (100 cm<sup>3</sup>) was added dropwise to a solution of 1,1,1, tris(hydroxymethyl) ethane (33.2 g, 0.28 mol) in pyridine (120 cm<sup>3</sup>) at 0°C. The temperature was maintained at 0°C for one hour and then stirred at ambient temperature for 24 hours. The solvent was removed *in vacuo* and the residue was dissolved in chloroform (200 cm<sup>3</sup>). This organic solution was washed with water (3 x 200 cm<sup>3</sup>), 6M sulfuric acid (200 cm<sup>3</sup>) and water (3 x 200 cm<sup>3</sup>). The chloroform layer was then dried over anhydrous magnesium sulfate, filtered and the solvent removed *in vacuo*. The resulting yellow oil was added to diethylether to obtain a white solid (117.9 g, 73%), mp 104-106°C (Found: C, 54.15; H, 5.20. Calc. for C<sub>26</sub>H<sub>30</sub>O<sub>9</sub>S<sub>3</sub>: C, 53.59; H, 5.15%).  $\delta_{\text{H}}$  (CDCl<sub>3</sub>, 200 MHz): 0.88 (s, CH<sub>3</sub>), 2.45 (s, 9 H, CH<sub>3</sub>), 3.74 (s, 6 H, CH<sub>2</sub>), 7.35 (d, 6 H, J 8.0, Ar CH), 7.70 (d, 6 H, J 8.3, Ar CH).  $\delta_{\text{C}}$  (CDCl<sub>3</sub>, 63 MHz): 16 (CH<sub>3</sub>), 22 (3 C, CH<sub>3</sub>), 39 (C), 70 (3 C, CH<sub>2</sub>), 128 (6 C, Ar CH), 130 (6 C, Ar CH), 132 (3 C, Ar C), 145 (3 C, Ar C). IR data (KBr disc)/cm<sup>-1</sup>: 670m, 839m, 963m, 1179s, 1191m, 1359m, 1600w, 2924w, 2964w, 3457w. FAB MS, *m/z* 583 (MH<sup>+</sup>, 100.0%).

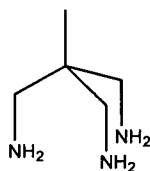
**1,1,1-Tris (azidomethyl) ethane (66)**



1,1,1-Tris (azidomethyl) ethane was prepared by the method of Fleischer *et al.*<sup>6</sup> A mixture of **65** (50 g, 88 mmol) and NaN<sub>3</sub> (30 g, 0.47 mol) in diethylene glycol (200 cm<sup>3</sup>) was stirred under nitrogen and maintained at 135°C for 16 hours. After cooling,

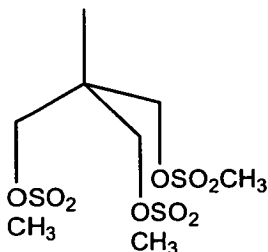
the mixture was poured into water (400 cm<sup>3</sup>) and extracted into diethylether (3 x 150 cm<sup>3</sup>). The diethylether was subsequently washed with water (3 x 150 cm<sup>3</sup>). The ethereal solution was dried over MgSO<sub>4</sub> then treated with activated charcoal and upon evaporation gave an almost colourless oil (12.89 g, 75%).  $\delta_{\text{H}}$  (CDCl<sub>3</sub>, 360 MHz) 1.02 (s, CH<sub>3</sub>), 3.30 (s, 6H, CH<sub>2</sub>).  $\delta_{\text{C}}$  (CDCl<sub>3</sub>, 90 MHz):  $\delta$  19 (CH<sub>3</sub>) 41 (C), 56 (3C, CH<sub>2</sub>). IR data (neat, NaCl plate)/cm<sup>-1</sup>: 2102(s).

### 2-Aminomethyl-2-methyl-propane-1,3-diamine (67)



2-Aminomethyl-2-methyl-propane-1,3-diamine was prepared by the method of Zompa and Anselme.<sup>8</sup> 1,1,1-Tris(azidomethyl) ethane (11.54 g, 59 mmol) in ethanol (200 cm<sup>3</sup>) and PdC (1 g) were placed in a Pyrex hydrogenating chamber. The mixture was hydrogenated at 3.4 atmospheres for 6 hours. The atmosphere was purged and recharged with hydrogen twice during this period. The mixture was then filtered through glass fibre filter paper, and the ethanol was then removed *in vacuo* to yield a yellow oil (5.4 g, 78%). The triamine was used with no further purification.  $\delta_{\text{H}}$  (CDCl<sub>3</sub>, 200 MHz): 0.76 (s, 3 H, CH<sub>3</sub>), 2.54 (s, 6 H, CH<sub>2</sub>).  $\delta_{\text{C}}$  (CDCl<sub>3</sub>, 90 MHz): 19 (CH<sub>3</sub>), 40 (C), 47 (3 C, CH<sub>2</sub>). IR data (neat, NaCl plate)/cm<sup>-1</sup>: 2867m, 2917m, 2966m. FAB MS, *m/z* 118 (MH<sup>+</sup>, 100.0%).

### 2-Methyl-1,3-bis(methylsulfoxy)-2-(methylsulfonyloxymethyl)propane (68)

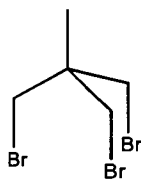


2-Methyl-1,3-bis(methylsulfoxy)-2-(methylsulfonyloxymethyl)-propane was prepared by the method of Latour *et al.*<sup>13</sup> Methanesulfonyl chloride (11.86 g, 100



mmol) in dry pyridine (25 cm<sup>3</sup>) was added dropwise at 0°C under nitrogen to a stirred solution of 1,1,1-tris(hydroxymethyl)ethane (3.84 g, 32 mmol) in a pyridine and chloroform mixture (50:50, 50cm<sup>3</sup>). The mixture was maintained at 0°C for 14 hours then the solvent was then removed *in vacuo*. Dichloromethane (100 cm<sup>3</sup>) was then added and the solution was washed with water (3 x 100 cm<sup>3</sup>). The organic layer was then separated and dried over anhydrous magnesium sulfate and the solvent removed *in vacuo* to give a white solid. Recrystallisation from ethanol (50 cm<sup>3</sup>) yielded a white crystalline solid (11.34 g, 62%), mp 79-80°C (Found: C, 27.12; H, 4.82. Calc. for C<sub>8</sub>H<sub>18</sub>O<sub>9</sub>S<sub>3</sub>: C, 27.11; H, 5.12%).  $\delta_{\text{H}}$  (DMSO-*d*<sub>6</sub>, 360 MHz): 1.07 (s, 3 H, CH<sub>3</sub>), 3.26 (s, 9 H, CH<sub>3</sub>), 4.17 (s, 6 H, CH<sub>2</sub>).  $\delta_{\text{C}}$  (DMSO-*d*<sub>6</sub>, 63 MHz): 4 (CH<sub>3</sub>), 25 (3 C, CH<sub>3</sub>), 28 (C), 59 (3 C, CH<sub>2</sub>). IR data (KBr disc)/cm<sup>-1</sup>: 855s, 981s, 1002s, 1173s, 1341s, 1466m, 2944w, 3015m, 3028m, 3449w. FAB MS, *m/z* 355 (MH<sup>+</sup>, 100.0%).

### 1,3-Dibromo-2-bromomethyl-2-methyl-propane (69)



1,3-Dibromo-2-bromomethyl-2-methyl-propane was prepared by the method of Kasowski and Bailer.<sup>14</sup> Sodium bromide was added to a solution of 2-methyl-1,3-bis-(toluene-4-sulfonyloxy)-2-(toluene-4-sulfonyloxy-methyl)-propane in diethylene glycol (250 cm<sup>3</sup>). The mixture was heated at 140°C for 12 hours under nitrogen. The resulting mixture was allowed to cool to 90°C before ice was added to cool the mixture to room temperature. The mixture was extracted with dichloromethane (3 x 150 cm<sup>3</sup>). The organic layer was separated and washed with water (3 x 300 cm<sup>3</sup>), dried over anhydrous magnesium sulfate, filtered and the dichloromethane was then removed *in vacuo* to yield a brown liquid. This was distilled at 73°C under 0.53 mm Hg to yield a colourless liquid (30.5 g, 49%), (Found: C, 19.47; H, 3.03. Calc. for C<sub>5</sub>H<sub>9</sub>Br<sub>3</sub>: C, 19.44; H, 2.94%).  $\delta_{\text{H}}$  (CDCl<sub>3</sub>, 250 MHz): 1.23 (s, 3 H, CH<sub>3</sub>), 3.44 (s, 6 H, CH<sub>2</sub>).  $\delta_{\text{C}}$  (CDCl<sub>3</sub>, 63 MHz): 2.07 (CH<sub>3</sub>), 38.8 (3 C, CH<sub>2</sub>), 39.4 (C). IR data (KBr

disc)/cm<sup>-1</sup>: 664m, 851m, 1246m, 1269s, 1377m, 1459s, 2833w, 2934m, 2971s, 3584w. FAB MS, *m/z* 307 (MH<sup>+</sup>, 23.3%).

### 5.5.5 Complexes of tris-sulfonamidotriamine ligands

#### **N,N',N'',N'''[Tris-(2-(4-methylbenzenesulfonylaminato)-ethyl)-amine]copper(II) potassium(I) (70)**

A solution of **60** (0.15 g, 0.25 mmol) and sodium hydroxide (0.75 mmol) in hot methanol (10 cm<sup>3</sup>) was added to a solution of copper(II) acetate monohydrate (83 mg, 0.25 mmol) also in methanol (10 cm<sup>3</sup>). The solution was left in a sealed vessel until the product separated as a green solid after 3 days which was collected by filtration, washed with methanol (3 x 5 cm<sup>3</sup>) and dried *in vacuo* (9 mg, 45%). Crystals suitable for X-ray crystallography were grown from a concentrated solution of **70** in tetrahydrofuran layered with *isopropylether* (Found: C, 46.39; H, 5.25; N, 7.13. Calc. for C<sub>31</sub>H<sub>43</sub>N<sub>4</sub>Cu K O<sub>8</sub>S<sub>3</sub>: C, 46.63; H, 5.43; N, 7.02%). IR data (KBr disc)/cm<sup>-1</sup>: 814s, 1128m, 1242m, 2919w, 3447m. FAB MS, *m/z* 707 ([Cu(L-3H)]K<sup>+</sup>, 100.0%).

#### **[Tris-(2-(4-methylbenzenesulfonylaminato)-ethyl)-amine]nickel(II) potassium(I) (71)**

The procedure described for **70** using nickel(II) acetate tetrahydrate yielded a green crystalline solid (57 mg, 30%), (Found: C, 45.01; H, 4.71; N, 7.29. Calc. for C<sub>27</sub>H<sub>35</sub>N<sub>4</sub>NiO<sub>7</sub>S<sub>3</sub>: C, 44.63; H, 5.22; N, 7.43%). IR data (KBr disc)/cm<sup>-1</sup>: 1078m, 1132s, 1249s, 2862w, 3503m. FAB MS, *m/z* 706 ([Ni(L-3H)]K<sup>+</sup>, 5.5%).

### 5.5.6 X-ray crystallography

Structures **57**, **58** and **60** were determined by Dr. Simon Parsons and structures **59**, **61**, **62** and **70** were determined by Andrew Parkin at the University of Edinburgh. In all cases data were collected at 220 K on a SMART or Stoe Stadi-4 diffractometer

equipped with an Oxford Cryosystems low temperature device, using Cu-K $\alpha$  radiation for **59** and **60**, and Mo-K $\alpha$  radiation for **57**, **58**, **61**, **62** and **70**. Reflections were scanned in  $\omega$ - $\theta$  mode. Structures **58-62** were solved by direct methods (SHELXTL or SIR92<sup>15,16</sup>) and **57** by Patterson methods (DIRDIF<sup>17</sup>). All were completed by iterative cycles of least squares refinement against  $F^2$  and difference Fourier synthesis (SHELXTL). H-atoms were idealised, being placed using geometric or difference maps and treated by riding or refall methods. All sulfonamido hydrogen atoms were placed using difference maps. In all cases non-H atoms were modelled with final anisotropic displacement parameters and final refinement statistics are presented in Tables 5.12 (**57-59**), 5.13 (**60-62**) and 5.14 (**70**).

**Table 5.12** : Crystallographic data for structures **57**, **58** and **59**.

Structure	<b>57</b>	<b>58</b>	<b>59</b>
Formula	C <sub>16</sub> H <sub>20</sub> N <sub>2</sub> O <sub>4</sub> S <sub>2</sub>	C <sub>20</sub> H <sub>26</sub> N <sub>2</sub> O <sub>4</sub> S <sub>2</sub>	C <sub>20</sub> H <sub>20</sub> N <sub>2</sub> O <sub>4</sub> S <sub>2</sub>
M	368.46	422.55	416.50
Crystal system	Monoclinic	Orthorhombic	Monoclinic
Space group	<i>P21/c</i>	<i>Pcca</i>	<i>Pccn</i>
a/Å	5.7761(14)	19.580(5)	36.994(7)
b/Å	8.0862(13)	8.5379(15)	8.371(2)
c/Å	18.328(3)	12.765(2)	12.9947(18)
$\alpha$ /°	90	90	90
$\beta$ /°	97.97	90	90
$\gamma$ /°	90	90	90
U/Å <sup>3</sup>	847.8(3)	2134.0(7)	4024.2(13)
Crystal size/mm	0.08 x 0.12 x 0.62	0.49 x 0.27 x 0.27	0.62 x 0.38 x 0.32
D <sub>c</sub> /g cm <sup>-3</sup>	1.443	1.315	1.375
Z	2	4	8
$\mu$ /mm <sup>-1</sup>	0.337	0.277	2.647
Scan type	omega-2theta	omega - theta	omega - theta
$\theta$ Limits/°	2.76-25.02	3.05-25.09	4.78-59.93
No. of unique data	1480	1900	2941
No. data with [F>4 $\sigma$ (F)]	1032	1321	2302
No. parameters	114	132	322
R1	0.0559	0.0424	0.0536
wR2	0.1230	0.1046	0.1390
$\Delta\rho_{\max}, \Delta\rho_{\min}/e \text{ \AA}^{-3}$	0.236, -0.318	0.274, -0.365	0.417, -0.458

Table 5.13: Crystallographic data for structures 60, 61 and 62.

Structure	60	61	62
Formula	C <sub>27</sub> H <sub>36</sub> N <sub>4</sub> O <sub>6</sub> S <sub>3</sub>	C <sub>29</sub> H <sub>39</sub> N <sub>3</sub> O <sub>7</sub> S <sub>3</sub>	C <sub>26</sub> H <sub>33</sub> N <sub>3</sub> O <sub>6</sub> S <sub>3</sub>
M	608.78	637.81	579.73
Crystal system	Orthorhombic	Monoclinic	Orthorhombic
Space group	<i>P</i> 212121	<i>P</i> 2 (1) / <i>n</i>	<i>Pna</i> 2 (1)
<i>a</i> /Å	13.0269(11)	28.6768(18)	15.5276(11)
<i>b</i> /Å	13.1314(13)	6.3737(4)	11.7498(8)
<i>c</i> /Å	35.332(6)	35.806(2)	15.7691(11)
$\alpha$ /°	90	90	90
$\beta$ /°	90	102.8730(10)	90
$\gamma$ /°	90	90	90
<i>U</i> /Å <sup>3</sup>	6043.9(13)	6380.1(7)	2877.0(3)
Crystal size/mm	0.62 x 0.42 x 0.21	0.36 x 0.24 x 0.05	0.40 x 0.17 x 0.13
<i>D<sub>c</sub></i> /g cm <sup>-3</sup>	1.338	1.328	1.338
<i>Z</i>	8	8	4
$\mu$ /mm <sup>-1</sup>	2.631	0.281	0.302
Scan type	omega - theta	phi + omega	phi + omega
$\theta$ Limits/°	3.59-70.19	0.83-26.40	2.16-26.38
No. of unique data	6035	12996	2947
No. data with [ <i>F</i> >4 $\sigma$ ( <i>F</i> )]	5482	10825	2781
No. parameters	746	791	359
<i>R</i> 1	0.0381	0.0813	0.0359
<i>wR</i> 2	0.0972	0.1915	0.0888
$\Delta\rho_{\max}, \Delta\rho_{\min}$ /e Å <sup>-3</sup>	0.243, -0.432	0.866, -0.496	0.359, -0.225

Table 5.14: Crystallographic data for structure 70.

<b>Structure</b>	<b>70</b>
<b>Formula</b>	$C_{31}H_{43}CuKN_4O_8S_3$
<b>M</b>	798.51
<b>Crystal system</b>	Monoclinic
<b>Space group</b>	$P2(1)$
<b>a/Å</b>	12.7387
<b>b/Å</b>	9.8238
<b>c/Å</b>	14.4844
<b><math>\alpha^\circ</math></b>	90
<b><math>\beta^\circ</math></b>	101.3780
<b><math>\gamma^\circ</math></b>	90
<b>U/Å<sup>3</sup></b>	1776.99(8)
<b>Crystal size/mm</b>	0.37 x 0.1 x 0.1
<b>D/g cm<sup>-1</sup></b>	1.492
<b>Z</b>	2
<b><math>\mu</math>/mm<sup>-1</sup></b>	0.962
<b>Scan type</b>	phi + omega
<b><math>\theta</math> Limits/<math>^\circ</math></b>	4.13-26.36
<b>No. of unique data</b>	6437
<b>No. data with [F&gt;4<math>\sigma</math>(F)]</b>	5899
<b>No. parameters</b>	441
<b>R1</b>	0.031
<b>wR2</b>	0.0703
<b><math>\Delta\rho_{max}</math> <math>\Delta\rho_{min}/e \text{ \AA}^{-3}</math></b>	0.571, -0.437

## 5.6 References

- <sup>1</sup> H.-Y. Cheng, C. -F. Lee and S. M. Peng, *Inorganica Chimica Acta*, 1991, **181**, 145-147.
- <sup>2</sup> D. H. Williams and I. Fleming, in *Spectroscopic methods in organic chemistry*, McGraw-Hill Book Company, London, 5<sup>th</sup> edn., 1995, ch. 3, pp 118.
- <sup>3</sup> D. Chen, R. J. Motekaitis, I. Murase and A. E. Martell, *Tetrahedron*, 1995, **51**, 77.
- <sup>4</sup> T. Bowen, R. P. Planalp and M. W. Brechbiel, *Bioorganic and Medicinal Chemistry Letters*, 1996, **6**, 807.
- <sup>5</sup> H. Stetter, D. Theisen and G. J. Steffens, *Chem. Ber.*, 1970, **103**, 200.
- <sup>6</sup> E. B. Fleischer, A. E. Gebala, A. Levey, and P. A. Tasker, *J. Org. Chem.*, 1971, **36**, 3042.
- <sup>7</sup> H. Stetter and W. Böckmann, *Chem. Ber.* 1951, **84**, 834.
- <sup>8</sup> L. J. Zompa and J. -P. Anselme, *Organic Preparations and Procedures int.* 1974, **6**, 103.
- <sup>9</sup> G. Crank and F. W. Eastwood, *Aust. J. Chem.*, 1965, **18**, 1967.
- <sup>10</sup> R. H. Lowack and R. Weiss, *J. Am. Chem. Soc.*, 1990, **112**, 333.
- <sup>11</sup> I. Tabushi, Y. Kimura and K. Yamamura, *J. Am. Chem. Soc.* 1981, **103**, 6486.
- <sup>12</sup> P. G. Potvin and M. H. Wong, *Can. J. Chem.* 1988, **66**, 2914.
- <sup>13</sup> S. Latour and J. D. Wuest, *Synthesis*, 1987, **8**, 742.
- <sup>14</sup> W. J. Kasowski and J. C. Bailor, *J. Amer. Chem. Soc.*, 1969, **91**, 3212.
- <sup>15</sup> G.M. Sheldrick, SHELXTL version 5, Siemens Analytical X-ray Instrument, Madison, Wisc., USA, 1995.
- <sup>16</sup> A. Altomare, G. Cascarano, C. Giacovazzi and A. Guagliardi, *J. Appl. Cryst.*, 1994, **27**, 1045-1050.
- <sup>17</sup> P.T. Beurskens, G. Beurskens, W.P. Bosman, R. de Gelder, S. García-Granda, R.O. Gould, R. Israël and J.M.M. Smits, DIRDIF, Crystallography Laboratory, University of Nijmegen, The Netherlands.

## **Chapter 6:**

# **Dinucleating sulfonamido oxime ligands**

<b>Contents</b>	<b>Page</b>
6.1 Introduction .....	289
6.2 Synthesis of dinucleating sulfonamido oxime ligands .....	289
6.3 Characterisation of dinucleating sulfonamido oxime ligands .....	291
6.3.1 NMR spectroscopy .....	291
6.3.2 IR spectroscopy and mass spectrometry .....	293
6.4 Complexation study of ligands <b>72</b> and <b>73</b> .....	294
6.4.1 Complexation of <b>72</b> .....	294
6.4.2 Complexation of <b>73</b> .....	294
6.5 Solid state structures of dinucleating sulfonamido oxime ligands .....	295
6.5.1 6-Hydroxy-3-methyl-5{2, 6-diaza-2-benzyl-6[N-(4-methylbenzene..... sulfonyl)]hex-1-yl} benzaldehyde ( <b>76</b> ) .....	295
6.5.2 Bis(6-hydroxy-3-methyl-5{2, 6-diaza-2-benzyl-6[N-(4-methylbenzene sulfonyl)]hex-1-yl} benzaldehyde oximato)copper(II) ( <b>78</b> ) .....	296
6.6 Conclusion .....	298
6.7 Experimental .....	299
6.7.1 Instrumentation .....	299
6.7.2 Solvent and reagent pretreatment .....	299
6.7.3 Ligand syntheses .....	300
6.7.4 Metal complexes .....	305
6.7.5 X-Ray Crystallography .....	306
6.8 References .....	308



## 6.1 Introduction

In Chapters 2 and 3 ligand systems following a similar design to P50 type phenolic oxime ligands (see Chapter 1) were explored. The promising results of these studies led to some preliminary work on the development of dinucleating sulfonamido oxime ligands. The aim of this work was to progress from  $ML_2$  systems to  $M_2L_2$  systems (Figure 6.1) with the same emphasis on hydrogen-bonded *pseudo*-macrocycle formation. Such ligands would encapsulate two metal centres, thus increasing the power of L as a metal extractant by 100%.

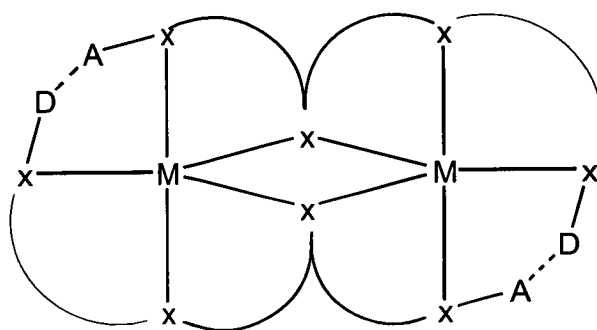


**Figure 6.1:**  $M_2L_2$  dinuclear systems where X are the donor atoms, A are the hydrogen-bond acceptor sites and D are the hydrogen-bond donor sites.

Figure 6.1 shows two five coordinate metal centres with trigonal pyramidal geometry coordinated by two penta-dentate ligands. The attempted synthesis of such structures is discussed in this chapter.

## 6.2 Synthesis of dinucleating sulfonamido oxime ligands

Such ligands required five coordinating atoms, one hydrogen-bond donor atom and one acceptor site. Ligand design had to allow some flexibility to successfully encapsulate two metal centres however care had to be taken that chelate ring sizes would not be too large. The target ligand system is shown in Figure 6.2 and incorporates aspects of the sulfonamidodiamine and sulfonamido oxime ligands discussed in Chapters 2 and 3.

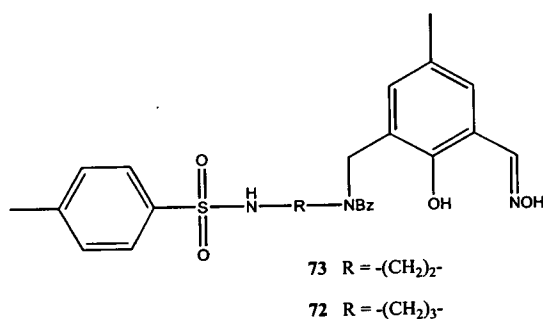


**Figure 6.2:** Target ligands **72** and **73**.

It was envisaged that the phenolic oxygen atom and the sulfonamido nitrogen atom would deprotonate on complexation resulting in a dianionic ligand and thus coordination of two ligands to two divalent metal ions would result in a neutral species.

The phenolic head group was chosen as dinuclear zinc(II), nickel(II) and copper(II) complexes with similar  $\text{N}_2\text{O}^-$  donor sets are known.<sup>1,2,3</sup> Fenton *et al* have developed a variety of dinucleating ligands, which form complexes with ligand to metal ratios of 1:1 or 1:2 depending on the substituents on the two nitrogen atoms, to model the active sites of some bimetallic biosites.<sup>4</sup>

The synthesis of **72** and **73** requires four steps (Figure 6.3). The triol precursor is commercially available, this was converted to **75** by the method of Lambert *et al*<sup>5</sup> via selective oxidation to give **74**, followed by the chlorination of the aliphatic alcohol. The reaction of **75** with either N-(N-benzyl-3-aminopropyl)-4-methylbenzenesulfonamide (**7**) or N-(N-benzyl-2-aminoethyl)-4-methylbenzenesulfonamide (**3**) yielded **76** and **77** respectively. Finally **76** and **77** were oximated to produce ligands **72** and **73**. Potassium hydrogen carbonate was necessary in step (iii) to avoid the formation of the hydrochloride salt of starting material **3** or **7** and in step (iv) to improve the yield.

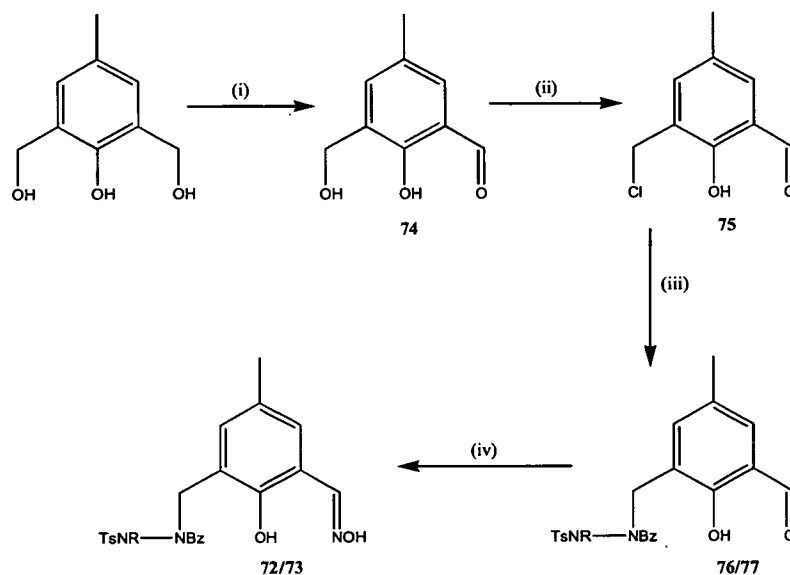


**Figure 6.3:** Synthesis of dinucleating sulfonamido oxime ligands 6-hydroxy-3-methyl-5{2, 6-diaza-2-benzyl-6[N-(4-methylbenzenesulfonyl)]hex-1-yl}benzaldehyde oxime (72) and 6-hydroxy-3-methyl-5{2,5-diaza-2-benzyl-5[N-(4-methylbenzenesulfonyl)]pent-1-yl}benzaldehyde oxime (73). (i)  $\text{MnO}_2$ , toluene. (ii)  $\text{SOCl}_2$ ,  $\text{CH}_2\text{Cl}_2$ . (iii)  $\text{BzHN-R-NHTs}$  { $\text{R} = -(\text{CH}_2)_3-$  (7),  $= -(\text{CH}_2)_2-$  (3)},  $\text{K}_2\text{CO}_3$ , dimethylformamide. (iv)  $\text{NH}_2\text{OH}\cdot\text{HCl}$ ,  $\text{K}_2\text{CO}_3$ ,  $\text{EtOH}$ .

## 6.3 Characterisation of dinucleating sulfonamido oxime ligands

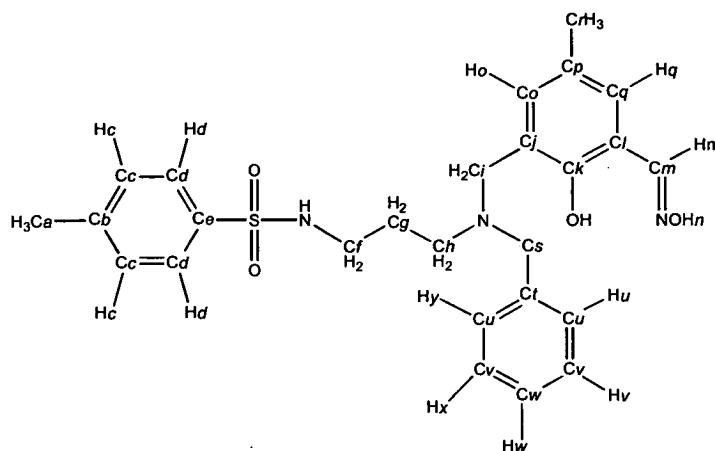
### 6.3.1 NMR spectroscopy

The  $^1\text{H}$  and the  $^{13}\text{C}$  nmr spectra of ligands 72 and 73 may be easily interpreted. In each case the two doublets at roughly 7.3 and 7.7 ppm identify the *p*-methylbenzenesulfonamido moiety of these ligands. The peaks of the two methyl groups at approximately 2.3 and 2.4 ppm with intensities in the ratio of 1:1 indicate that the correct product has been formed. A more detailed discussion of the spectra of 72 (Figure 6.4) follows.

The two doublets arising from the two chemically equivalent pairs of protons *c* and *d* are at 7.25 and 7.70 ppm respectively. The signal for the *d* protons is shifted to lower field due to the electron withdrawing nature of the sulfonyl group. The two peaks for the methyl groups are assigned as 2.25 (*a*) and 2.14 (*r*), following a

comparison of the spectrum with that of the starting precursor (7). The methylene protons *f*, *g* and *h* are at 2.88, 1.64 and 2.43 ppm. The central unit (*g*) is shielded from the electron withdrawing amino and sulfonamido groups and may therefore be assigned to the signal found at the lowest ppm value. The sulfonamido group is more electron withdrawing than the amino group and therefore the protons of methylene group *f* are found at lower field to those of group *h*. The remaining methylene groups *i* and *s* are singlets at 3.59 and 3.41 ppm, these values were assigned as the aromatic ring attached to methylene unit *i* has two electron withdrawing groups attached, therefore the signal for *i* was expected at lower field. Finally, the two aromatic protons *o* and *q* were identified and assigned as 6.95 and 7.01 ppm. The aromatic protons *u*, *v* and *w* of the benzyl group form a multiplet at 7.20 ppm. Signals for the oximic proton, the sulfonamido proton and the alcoholic proton were not observed.

The  $^{13}\text{C}$  nmr spectrum may be used to support the previous characterization. The two signals for the methyl groups are easily identified at high field (21 and 22 ppm). The signals for methylene units, aromatic CH, quaternary carbons and the signal for the oximic carbon are all present in the correct numbers. The signals were assigned using the same rationale used for the  $^1\text{H}$  spectrum and DEPT techniques.<sup>6</sup> Assignments are listed in Figure 6.4.



Signal	<sup>1</sup> H nmr	<sup>13</sup> C nmr	Signal	<sup>1</sup> H nmr	<sup>13</sup> C nmr
<i>a</i>	2.25	21	<i>l</i>	—	143
<i>b</i>	—	118	<i>m</i>	—	151
<i>c</i>	7.25	130	<i>o</i>	6.95	129
<i>d</i>	7.70	130	<i>p</i>	—	125
<i>e</i>	—	129	<i>q</i>	7.01	33
<i>f</i>	2.88	53	<i>r</i>	2.41	22
<i>g</i>	1.64	26	<i>s</i>	3.41	56
<i>h</i>	2.43	43	<i>t</i>	—	138
<i>i</i>	3.59	59	<i>u</i>	7.20	129
<i>j</i>	—	139	<i>v</i>	7.20	127
<i>k</i>	—	154	<i>w</i>	7.20	128

Figure 6.4: <sup>1</sup>H and <sup>13</sup>C nmr assignments for ligand 72.

### 6.3.2 IR spectroscopy and mass spectrometry

IR and mass spectrometry have been routinely used for characterisation. IR spectroscopy was used to confirm the presence of the sulfonamide group by one strong band in the 1370-1330 cm<sup>-1</sup> region and another in the 1180-1160 cm<sup>-1</sup> region for the -SO<sub>2</sub>-N group. A weak peak was expected for the C=N bond of the oxime group between 1690 and 1640 cm<sup>-1</sup>. Of the mass spectrometry techniques available (EI, FAB and ESI) fast atom bombardment has been used primarily for analysis purposes.

## 6.4 Complexation study of ligands 72 and 73

Complexation of ligands 72 and 73 were attempted in methanol solution in 1:2 and 2:2 ligand to metal(II) acetate ratios with the required amount of sodium hydroxide added as a base.

### 6.4.1 Complexation of 72

A 1:2 mixture of copper(II) acetate and 72 gave green crystals which upon analysis by X-ray diffraction proved this material to be a 1:2 complex. A bright green powder (79) from the reaction of nickel(II) acetate with 72 again in a 1:2 ratio. Reaction with both zinc and cobalt salts proved unsuccessful.

### 6.4.2 Complexation of 73

Two visually different products were isolated from the reaction with copper. A brown/yellow precipitate (80) was isolated from the 1:2 mixture and a pale green precipitate (81) from the 2:2 mixture. Microanalysis proved 80 to be a 1:2 complex however the only evidence for 81 as a 2:2 ligand:metal complex was from ESI MS where a peak for  $[\text{Cu}_2(\text{73-H})_2]^+$  at 1059 of intensity 39.2% was observed, however a peak for a 1:2 complex at 996 of intensity 52.7% was also observed. The reaction of nickel(II) acetate with 73 in the two different ratios produced a bright green solid (82) from the 1:2 mixture and a pale green solid from the 2:2 mixture. It did not prove possible to characterise the latter product however good evidence for a complex with a metal to ligand ratio of 1:2 was obtained for 82 from ESI MS,  $[\text{Ni}(\text{73-H})_2]^+$  m/z 991 100.0%.

No products were isolated from the 1:2 mixtures of cobalt or zinc to 73. However a 2:2 mixture with cobalt yielded a dark brown solid (83), peaks in the ESI spectrum were present for both complex type,  $[\text{Co}_2(\text{73-H})_2]^+$  m/z 1047, 23.2% and  $[\text{Co}(\text{73-H})_2]^+$  m/z 525, 33.4%. A yellow precipitate was isolated from a 2:2 mixture with zinc and 73 (84) and evidence for a 2:2 complex was also found from analysis by ESI MS,  $[\text{Zn}_2(\text{73-H})_2]^+$  m/z 1093, 58.7%.

Good microanalysis was only obtained for complexes **78** and **79**. This may have been a result of the unreliability of the apparatus at the time or a result of a mixture of products being formed. Due to time limitations the materials were not purified further.

## 6.5 Solid state structures of dinucleating sulfonamido oxime ligands

### 6.5.1: 6-Hydroxy-3-methyl-5{2, 6-diaza-2-benzyl-6[N-(4-methylbenzene sulfonyl)]hex-1-yl} benzaldehyde (**76**)

The X-ray structure of the intermediate sulfonamido molecule **76** is shown in Figure 6.5.

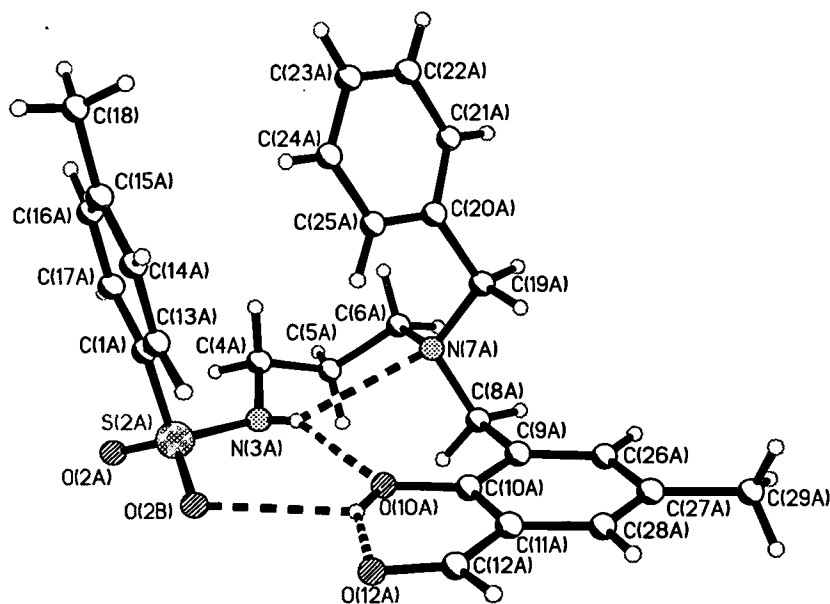


**Figure 6.5:** The X-ray structure of **76**.

The value of  $\theta$  (the sum of the three angles around the nitrogen atom) is  $348.7^\circ$ , and the value of  $\alpha$  (the angle of the S-N bond from the plane defined by the sulfonamido nitrogen and hydrogen atoms and the adjacent carbon atom) is  $0.229\text{\AA}$ . There is no *inter*-molecular hydrogen-bonding in **76** however, there are four *intra*-molecular

bonds. The phenolic hydrogen atom (H(10A)) is bifurcated and forms interactions with the carbonyl oxygen atom (O(12A)) and sulfonamido oxygen atom (O(2B)) [O(10A)-H---O(12A), 2.6407(17) Å; O-H-O, 141.6(18)°; O(10A)-H---O(2B), 2.9913(18) Å; O-H-O, 110°]. The sulfonamido hydrogen atom H(3A) is also bifurcated and forms interactions with the tertiary nitrogen atom N(7A) and the phenolic oxygen atom O(10A) [N(3A)-H---N(7A), 3.13 Å; N-H-N, 124°, N(3A)-H--O(10A), 2.8748(18) Å; O-H-N, 151.6(16)°].

### 6.5.2 Bis(6-hydroxy-3-methyl-5{2, 6-diaza-2-benzyl-6[N-(4-methylbenzene sulfonyl)]hex-1-yl}benzaldehyde oximato)copper(II) (78)

Complexation of **72** with copper(II) acetate in a 2:1 ratio yields complex **78** (Figure 6.6). The ligand is monodeprotonated and binds to one metal centre with a ligand to metal ratio of 2:1. The asymmetric unit consists of half of the complex. The copper atom has a planar geometry with bond lengths to the deprotonated phenolic oxygen atom and the oximic nitrogen atom of 1.8936(11) and 1.9499(13) Å respectively and a N-Cu-N chelate angle of 92.3°. The values of  $\theta$  and  $\alpha$  for the sulfonamido group of **72** are 350.4° and 0.21 Å respectively. The sulfonamido nitrogen is not involved in binding to the metal centre and its geometry is very similar to the sulfonamido nitrogen in molecule **76**.



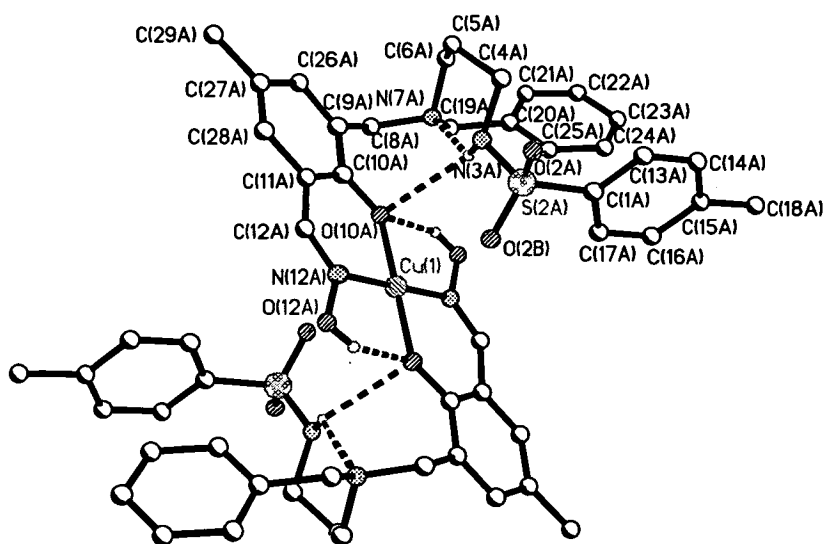


**Figure 6.6:** X-ray structure of 6-Hydroxy-3-methyl-5{2, 6-diaza-2-benzyl-6[N-(4-methylbenzene sulfonyl)]hex-1-yl}benzaldehyde oximate copper(II) (**78**).

The inner great ring of the *pseudo*-macrocyclic which is formed around the copper centre is very similar to that of P50 (see Chapter 1) and is formed *via* hydrogen-bonding interactions between the oximic hydrogen atoms and the deprotonated phenolic oxygen atoms [O(12A)-H---O(10A), 2.615 Å; O-H-O, 141°]. There are four other hydrogen-bonds per complex, each sulfonamido hydrogen atom is bifurcated and forms interactions with the deprotonated phenolic oxygen atom and the tertiary amino nitrogen atom [N(3A)-H---O(10A), 3.08 Å; N-H-O, 137°, N(3A)-H---N(7A), 3.06 Å; N-H-N, 129°].

Two of the three types of hydrogen bond in complex **78**, are similar to those observed in molecule **76**. The interaction between the sulfonamido proton H(3A) and the deprotonated oximic oxygen atom O(10A) is longer and less linear in complex **78** than in molecule **76** however the interaction between the bifurcated sulfonamido proton H(3A) and the amino nitrogen N(7A) is similar in both length and linearity. These changes are a result of a change in conformation of the ligand upon complexation. The sulfonamidodiamine arm of the ligand does not change its shape significantly, however it has been pushed further from the central coordinating

oxygen atom resulting in the elongation of the O(10A)---H-N(3A) bond. The hydrogen-bonds involved in the formation of the *pseudo*-macrocyclic ring are both shorter and more linear than the other two interactions, the optimisation of these interactions may have been achieved as a result of the planar nature of the N<sub>4</sub><sup>2-</sup> donor set.

## 6.6 Conclusion

Two potentially dinucleating ligands have been successfully synthesised and preliminary complexation studies undertaken. The simple coordination mode of **78** to one copper centre to give a *pseudo*-macrocyclic structure shows how favourable this arrangement is. No crystals of X-ray quality were grown of materials believed to contain 2:2, ligand:metal complexes however encouraging information was achieved by ESI MS analysis.

## 6.7 Experimental

### 6.7.1 Instrumentation

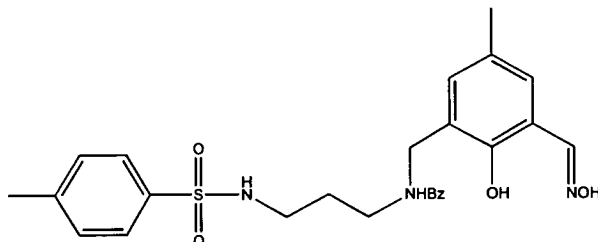
Melting points were determined with a Gallenkamp apparatus and are uncorrected. Elemental analysis was performed on a Perkin Elmer 2400 elemental analyser and a Carlo Erba 1108 Elemental analyser. IR spectra were obtained on a Perkin Elmer Paragon 1000 FT-IR spectrometer as potassium bromide discs.  $^1\text{H}$  and  $^{13}\text{C}$  NMR spectra were run on Bruker WP200, AC250 and AVANCE DPX360 spectrometers. Chemical shifts ( $\delta$ ) are reported in parts per million (ppm) relative to residual solvent protons as internal standards. Electron impact (EI) mass spectra were obtained either on a Finnigan MAT4600 quadrupole spectrometer or on a Kratos MS50TC spectrometer. Fast atom bombardment (FAB) mass spectra were obtained on a Kratos MS50TC spectrometer in acetonitrile/3-nitrobenzyl alcohol/thioglycerol matrices. Electrospray ionisation (ESI) mass spectra were obtained on a Thermoquest LCQ spectrometer.

### 6.7.2 Solvent and reagent pretreatment

All reagents and solvents were commercially available (Acros or Aldrich) and were used as received. Solvents used for analytical purposes (NMR, MS) were of spectroscopic grade.

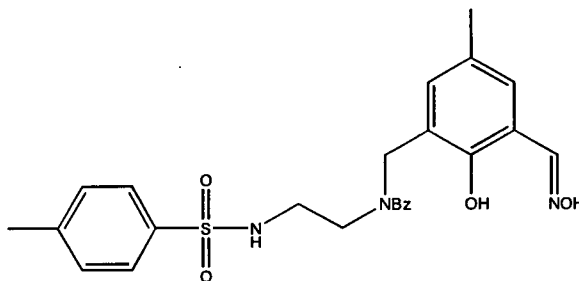
## 6.7.3 Ligand syntheses

## 6-Hydroxy-3-methyl-5{2, 6-diaza-2-benzyl-6[N-(4-methylbenzenesulfonyl)]hex-1-yl}benzaldehyde oxime (72)



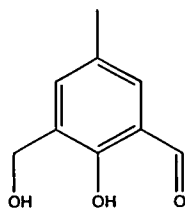
Ethanol (50 cm<sup>3</sup>) was added to 6-hydroxy-3-methyl-5{2, 6-diaza-2-benzyl-6[N-(4-methylbenzenesulfonyl)]hex-1-yl}benzaldehyde (76) (0.44 g, 0.97 mmol), hydroxylamine hydrochloride (0.20 g, 2.9 mmol) and potassium carbonate (0.4 g, 2.9 mol). The mixture was heated at reflux for one hour. The solution was cooled and subsequently filtered and the ethanol was then removed *in vacuo* to yield a yellow oil. The oil was dissolved in dichloromethane (50 cm<sup>3</sup>) and the solution was washed with water (3 x 50 cm<sup>3</sup>) and dried over anhydrous magnesium sulfate. The solution was then filtered before the dichloromethane was removed *in vacuo* to yield a second yellow oil. This was triturated with hexane to yield a yellow powder (0.71g, 86%), mp 116-118°C.  $\delta_{\text{H}}$  (CDCl<sub>3</sub>, 200 MHz): 1.64 (t, 2 H, J 5.3, CH<sub>2</sub>), 2.25 (s, 3 H, CH<sub>3</sub>), 2.41 (s, 3 H, CH<sub>3</sub>), 2.43 (t, 2 H, J 6.1, CH<sub>2</sub>), 2.88 (t, 2 H, J 5.7, CH<sub>2</sub>), 3.41 (s, 2 H, CH<sub>2</sub>), 3.59 (s, 2 H, CH<sub>2</sub>), 6.95 (s, 1 H, Ar CH), 7.01 (s, 1 H, Ar CH), 7.20 (m, 5 H, Ar CH), 7.25 (d, 2 H, J 7.9, Ar CH), 7.70 (2 H, d, J 8.3, Ar CH), 8.24 (s, 1 H, Ar CH).  $\delta_{\text{C}}$  (CDCl<sub>3</sub>, 90 MHz): 21 (CH<sub>3</sub>), 22 (CH<sub>3</sub>), 26 (CH<sub>2</sub>), 43 (CH<sub>2</sub>), 53 (CH<sub>2</sub>), 56 (CH<sub>2</sub>), 59 (CH<sub>2</sub>), 118 (Ar C), 125 (Ar C), 127 (2 C, Ar CH), 128 (Ar CH), 129 (2 C, Ar CH), 129 (Ar C), 130 (2 C Ar CH), 130 (2 C, Ar CH), 133 (Ar CH), 138 (Ar C), 139 (Ar C), 143 (Ar C), 151 (C=N-OH), 154 (Ar C). IR data (KBr disc)/cm<sup>-1</sup>: 668m, 1093m, 1153s, 1319s, 1459s, 1599w, 1655w, 2950m, 3360s. FAB MS, *m/z* 482 (MH<sup>+</sup>, 92.8%). HRMS *m/z* calc. for MH<sup>+</sup> 482.6239, found 482.2156.

**6-Hydroxy-3-methyl-5{2,5-diaza-2-benzyl-5[N-(4-methylbenzenesulfonyl)]pent-1-yl}benzaldehyde oxime (73)**



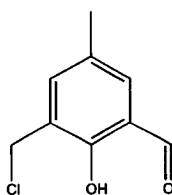
6-Hydroxy-3-methyl-5{2,5-diaza-2-benzyl-5[N-(4-methylbenzenesulfonyl)]pent-1-yl}benzaldehyde (77) (0.56 g, 1.2 mmol), hydroxylamine hydrochloride (0.26 g, 3.7 mmol) and potassium carbonate (0.51 g, 3.7 mmol) were added to ethanol (50 cm<sup>3</sup>). The mixture was heated at reflux for one hour. The solution was cooled and then filtered. The ethanol was then removed *in vacuo* to yield a yellow oil. Dichloromethane (50 cm<sup>3</sup>) was added and the solution was washed with water (3 x 50 cm<sup>3</sup>) and dried over anhydrous magnesium sulfate. The solution was then filtered before the dichloromethane was removed *in vacuo* to yield a second yellow oil. This was triturated with hexane to yield a yellow powder (0.52 g, 89%), mp 129-131.  $\delta_{\text{H}}$  (CDCl<sub>3</sub>, 200 MHz): 2.28 (s, 3 H, CH<sub>3</sub>), 2.38 (s, 3 H, CH<sub>3</sub>), 2.59 (t, 2 H, J 5.6, CH<sub>2</sub>), 2.95 (t, 2 H, J 5.5, CH<sub>2</sub>), 3.51 (s, 2 H, CH<sub>2</sub>), 3.58 (s, 2 H, CH<sub>2</sub>), 6.94 (d, 2 H, J 9.3, Ar CH), 7.18 (m, 7 H, Ar CH), 7.67 (d, 2 H, J 8.3, Ar CH).  $\delta_{\text{C}}$  (CDCl<sub>3</sub>, 90 MHz): 20 (CH<sub>3</sub>), 22 (CH<sub>3</sub>), 41 (CH<sub>2</sub>), 52 (CH<sub>2</sub>), 55 (CH<sub>2</sub>), 55 (CH<sub>2</sub>), 58 (CH<sub>2</sub>), 118 (Ar C), 125 (Ar C), 128 (2 C, Ar CH), 129 (2 C, Ar CH), 130 (2 C, Ar CH), 130 (2 C, Ar CH), 130 (Ar CH), 133 (Ar CH), 140 (Ar C), 138 (Ar C), 144 (Ar C), 152 (Ar CH), 154 (Ar C). IR data (KBr disc)/cm<sup>-1</sup>: 1160s, 1326m, 1654m, 2924m, 3432s. FAB MS, *m/z* 468 (MH<sup>+</sup>, 24.5%). HRMS *m/z* calc. for (MH<sup>+</sup>) 468.597, found 468.195.

**2-(Hydroxymethyl)-6-carbaldehyde-4-methylphenol (74)**



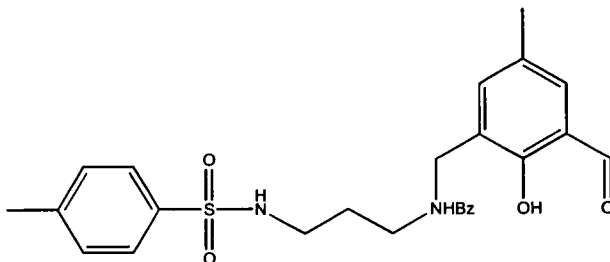
2-(Hydroxymethyl)-6-carbaldehyde-4-methylphenol was prepared by the method of Lambert *et al.*<sup>5</sup> 2,6-Bis(hydroxymethyl)-4-methylphenol (15 g, 89 mmol) and manganese dioxide (19.3 g, 0.22 mol) were stirred in toluene (3 dm<sup>3</sup>) at room temperature for 4 days. The MnO<sub>2</sub> was filtered off, and evaporation of toluene gave a brown powder. Recrystallisation from toluene (50 cm<sup>3</sup>) afforded a white powder (7.5 g, 51%), mp 71-73 °C (Found: C, 65.15; H, 5.82. Calc. for C<sub>9</sub>H<sub>10</sub>O<sub>3</sub>: C, 65.05; H, 6.07%).  $\delta_{\text{H}}$  (CDCl<sub>3</sub>, 360 MHz) 2.37 (s, 3 H, CH<sub>3</sub>), 2.55 (s, -OH), 4.76 (s, 2 H, CH<sub>2</sub>), 7.32 (s, 1 H, Ar CH), 7.43 (s, 1 H, Ar CH), 9.88 (s, 1 H, -CHO), 11.20 (s, 1 H, Ar-OH).  $\delta_{\text{C}}$  (CDCl<sub>3</sub>, 90 MHz) 21 (CH<sub>3</sub>), 129 (Ar C), 130 (Ar C), 133 (Ar CH), 137 (Ar CH), 158 (Ar C), 197 (C=O). IR data (KBr disc)/cm<sup>-1</sup>: 1435m, 1648s, 2925m, 3379m. EI MS, *m/z* 166 (MH<sup>+</sup>, 56,3%).

### 2-(Chloromethyl)-6-carbaldehyde-4-methylphenol (75)



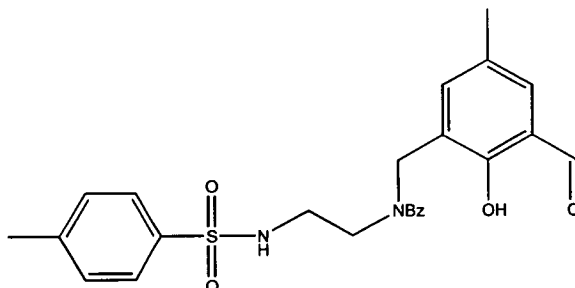
2-(Chloromethyl)-6-carbaldehyde-4-methylphenol was prepared by the method of Lambert *et al.*<sup>5</sup> Thionyl chloride (4 cm<sup>3</sup>, 55 mmol) in dichloromethane (6 cm<sup>3</sup>) was added dropwise a solution of 2-(hydroxymethyl)-6-carbaldehyde-4-methylphenol (74) (3.05 g, 18 mmol) suspended in dichloromethane (6 cm<sup>3</sup>) to yield a clear bright yellow solution. The mixture was stirred for 1 hour and the solvent and SOCl<sub>2</sub> were removed *in vacuo*. The residue was recrystallised from hexane/dichloromethane to yield a white crystalline solid (2.17 g, 64%), mp 92-94 °C.  $\delta_{\text{H}}$  (CDCl<sub>3</sub>, 360 MHz): 2.39 (s, 3 H, CH<sub>3</sub>), 4.70 (s, 2 H, CH<sub>2</sub>), 7.38 (s, 1 H, Ar CH), 7.50 (s, 1 H, Ar CH), 9.90 (s, 1 H, -COH), 11.29 (s, 1 H, -OH).  $\delta_{\text{C}}$  (CDCl<sub>3</sub>, 90 MHz): 21 (CH<sub>3</sub>), 40 (CH<sub>2</sub>), 121 (Ar C), 126 (Ar C), 130 (Ar C), 134 (Ar CH), 139 (Ar CH), 158 (Ar C), 197 (>C=O). IR data (KBr disc)/cm<sup>-1</sup>: 3186m, 2853m, 1644s, 1601m, 1472m, 1303m, 1257m, 1208m, 704m. EI MS, *m/z* 184 (M<sup>+</sup>, 36.5%). HRMS *m/z* calc. for (M<sup>+</sup>) 184.6196, found 184.0291.

**6-Hydroxy-3-methyl-5{2, 6-diaza-2-benzyl-6[N-(4-methylbenzenesulfonyl)]hex-1-yl}benzaldehyde (76)**



4-Methyl-N-(2-benzylamino-propyl)-benzenesulfonamide (1.72 g, 5.4 mmol) in dimethylformamide (25 cm<sup>3</sup>) was added dropwise to a mixture of K<sub>2</sub>CO<sub>3</sub> and 2-(chloromethyl)-6-carbaldehyde-4-methylphenol (1 g, 5.4 mmol) in dimethylformamide (25 cm<sup>3</sup>). The mixture was stirred for 48 hours before H<sub>2</sub>O (50 cm<sup>3</sup>) was added. The product was extracted into dichloromethane (3 x 70 cm<sup>3</sup>) and the extracts were combined and then washed with water (5 x 200 cm<sup>3</sup>), dried over MgSO<sub>4</sub> and filtered. The solvent was removed *in vacuo* to yield a yellow oily solid which was triturated with a mixture of *iso*-propyl ether and *iso*-propyl alcohol to produce a yellow solid. This was recrystallised from ethanol (50 cm<sup>3</sup>) to give a yellow crystalline material (0.66 g, 26%), mp 105-107°C (Found: C, 67.08; H, 6.59; N, 6.13. Calc. for C<sub>26</sub>H<sub>30</sub>N<sub>2</sub>O<sub>4</sub>S: C, 67.13; H, 6.51; N, 6.19%). δ<sub>H</sub> (CDCl<sub>3</sub>, 360 MHz): 1.72 (m, 2 H, CH<sub>2</sub>), 2.35 (s, 3 H, CH<sub>3</sub>), 2.44 (s, 3 H, CH<sub>3</sub>), 2.53 (t, 2 H, J 6.3, CH<sub>2</sub>), 2.97 (t, 2 H, J 6.2, CH<sub>2</sub>), 3.55 (s, 2 H, CH<sub>2</sub>), 3.66 (s, 2 H, CH<sub>2</sub>), 7.31 (m, 9 H, Ar CH), 7.70 (d, 2 H, J 8.1, Ar CH), 10.06 (s, 1 H, H-C=O). δ<sub>C</sub> (CDCl<sub>3</sub>, 90 MHz): 21 (CH<sub>3</sub>), 22 (CH<sub>3</sub>), 26 (CH<sub>2</sub>), 43 (CH<sub>2</sub>), 52 (CH<sub>2</sub>), 54 (CH<sub>2</sub>), 59 (CH<sub>2</sub>), 122 (Ar C), 126 (Ar C), 127 (2 C, Ar CH), 128 (Ar CH), 129 (Ar C), 129 (2 C, Ar CH), 130 (2 C, Ar CH), 130 (2 C, Ar CH), 132 (Ar CH), 138 (Ar C), 138 (Ar C), 143 (Ar C), 159 (Ar C), 195 (>C=O). IR data (KBr disc)/cm<sup>-1</sup>: 3450w, 3252s, 2948m, 2925m, 2837m, 2815m, 1653s, 1325m, 1266m, 1158s, 1091m, 735m. FAB MS, *m/z* 667 (MH<sup>+</sup>, 67.2%).

**6-Hydroxy-3-methyl-5{2, 5-diaza-2-benzyl-5[N-(4-methylbenzenesulfonyl)]pent-1-yl}benzaldehyde (77)**



4-Methyl-N-(2-benzylamino-ethyl)-benzenesulfonamide (1.16 g, 5.4 mmol) in dimethylformamide (25 cm<sup>3</sup>) was added dropwise to a mixture of K<sub>2</sub>CO<sub>3</sub> (0.75 g, 5.4 mmol) and 2-(chloromethyl)-6-carbaldehyde-4-methylphenol (1 g, 5.4 mmol) in dimethylformamide (25 cm<sup>3</sup>). The mixture was stirred for 48 hours before it was added to 50 cm<sup>3</sup> H<sub>2</sub>O. The product was extracted into dichloromethane (3 x 70 cm<sup>3</sup>). The dichloromethane extracts were then combined and washed with water (5 x 100 cm<sup>3</sup>), dried over MgSO<sub>4</sub> and filtered. The solvent was removed *in vacuo* to yield a yellow oil which was triturated with a mixture of hexane and diethylether to yield a pale yellow solid (0.56 g, 23%), mp 102-104 °C.  $\delta_{\text{H}}$  (CDCl<sub>3</sub>, 360 MHz): 2.37 (s, 3 H, CH<sub>3</sub>), 2.42 (s, 3 H, CH<sub>3</sub>), 2.59 (m, 2 H, CH<sub>2</sub>), 3.01 (m, 2 H, CH<sub>2</sub>), 3.53 (s, 2 H, CH<sub>2</sub>), 3.58 (s, 2 H, CH<sub>2</sub>), 5.29 (s, 1 H, NH), 7.27 (m, 9 H, Ar CH), 7.66 (d, 2 H, J 8.1, Ar CH), 9.95 (s, 1 H, H-C=O), 11.27 (s, 1 H, -OH).  $\delta_{\text{C}}$  (CDCl<sub>3</sub>, 90 MHz): 21 (CH<sub>3</sub>), 23 (CH<sub>3</sub>), 41 (CH<sub>2</sub>), 53 (CH<sub>2</sub>), 53 (CH<sub>2</sub>), 59 (CH<sub>2</sub>), 121 (Ar C), 127 (Ar C), 128 (2 C, Ar CH), 128 (Ar CH), 129 (2 C, Ar CH), 129 (2 C, Ar CH), 130 (2 C, Ar CH), 133 (Ar CH), 137 (Ar C), 139 (Ar C), 139 (Ar CH), 144 (Ar C), 158 (q, Ar CH), 196 (C=O). IR data (KBr disc)/cm<sup>-1</sup>: 1159s, 1326s, 1647s, 2828w, 2916w, 3028w, 3248s. FAB MS, *m/z* 453 (MH<sup>+</sup>, 100.0%). HRMS *m/z* calc. for (MH<sup>+</sup>) 452.5744, found 453.18621.



### 6.7.4 Metal complexes

#### **Bis(6-Hydroxy-3-methyl-5{2, 6-diaza-2-benzyl-6[N-(4-methylbenzenesulfonyl)]hex-1-yl}benzaldehyde oximato)copper(II) (78)**

A solution of **72** (0.07 g, 0.15 mmol) in hot methanol (10 cm<sup>3</sup>) was added to copper(II) acetate monohydrate (14.5 mg, 0.08 mmol) in methanol (10 cm<sup>3</sup>) and the mixture was stirred for 30 minutes. The solution was left sealed until the product separated as a green crystalline solid after 3 days which was collected by filtration, washed with methanol (3 x 5 cm<sup>3</sup>) and dried *in vacuo* (45 mg, 55%), (Found: C, 61.01; H, 6.45; N, 8.44. Calc. for C<sub>52</sub>H<sub>60</sub>N<sub>6</sub>CuO<sub>8</sub>S<sub>2</sub>: C, 60.95; H, 5.90; N, 8.20%). IR data (KBr disc)/cm<sup>-1</sup>: 1139m, 1262m, 1412w, 2929m, 3191m. FAB MS, *m/z* 1023 ([Cu(L-H)<sub>2</sub>]<sup>+</sup>, 38.8%).

#### **Bis(6-Hydroxy-3-methyl-5{2,6-diaza-2-benzyl-6[N-(4-methylbenzenesulfonyl)]hex-1-yl}benzaldehyde oximato)nickel(II) (79)**

Using nickel(II) acetate tetrahydrate in the procedure described for **78** yielded a green solid which was dried *in vacuo* (20 mg, 26%), (Found: C, 61.45; H, 5.92; N, 8.23. Calc. for C<sub>52</sub>H<sub>60</sub>N<sub>6</sub>CuO<sub>8</sub>S<sub>2</sub>: C, 61.18; H, 5.63; N, 8.20%). IR data (KBr disc)/cm<sup>-1</sup>: 1136s, 1279m, 2929m, 3447m. ESI MS, *m/z* 1019 ([Ni(L-H)<sub>2</sub>]<sup>+</sup>, 10.1%).

#### **Cu(II)(73-H)<sub>2</sub> (80)**

A solution of **73** (0.07 g, 0.15 mmol) in hot methanol (10 cm<sup>3</sup>) was added to copper(II) acetate monohydrate (15 mg, 0.08 mmol) in methanol (10 cm<sup>3</sup>) and the mixture was stirred for 30 minutes. The solution was left sealed until the product separated as a brown/yellow solid after 3 days which was collected by filtration, washed with methanol (3 x 5 cm<sup>3</sup>) and dried *in vacuo* (20 mg, 27%) (Found: C, 60.25; H, 5.66; N, 8.43. Calc. for C<sub>50</sub>H<sub>56</sub>N<sub>6</sub>CuO<sub>8</sub>S<sub>2</sub>: C, 59.64; H, 5.66; N, 8.43%). IR data (KBr disc)/cm<sup>-1</sup>: 1159s, 1324m, 2907m, 3518m. ESI MS, *m/z* 996 ([Cu(L-H)<sub>2</sub>]<sup>+</sup>, 100.0%).

#### **Cu<sub>2</sub>(II)(73-2H)<sub>2</sub> (81)**

A solution of **73** (0.07 g, 0.15 mmol) in hot methanol (10 cm<sup>3</sup>) was added to copper(II) acetate monohydrate (30 mg, 0.15 mmol) in methanol (10 cm<sup>3</sup>) and the mixture was

stirred for 30. The solution was left sealed until the product separated as a pale green solid after 3 days which was collected by filtration, washed with methanol (3 x 5 cm<sup>3</sup>) and dried *in vacuo* (15 mg, 19%). ESI MS, *m/z* 996 [Cu(L-H)<sub>2</sub>]<sup>+</sup>, 52.3%, *m/z* 1059 [Cu<sub>2</sub>(L-2H)<sub>2</sub>]<sup>+</sup>, 39.2%.

**Bis(6-Hydroxy-3-methyl-5{2,5-diaza-2-benzyl-5[N-(4-methylbenzenesulfonyl)]pent-1-yl}benzaldehyde oximato)nickel(II) (82)**

Using nickel(II) acetate tetrahydrate in the procedure described for **80** yielded a bright green solid which was dried *in vacuo* (8 mg, 11%). ESI MS, *m/z* 991 ([Ni(L-H)<sub>2</sub>]<sup>+</sup>, 100.0%).

**Co<sub>2</sub>(II)(73-2H)<sub>2</sub> (83)**

Using cobalt(II) acetate tetrahydrate in the procedure described for **81** yielded a dark brown solid which was dried *in vacuo* (8 mg, 11%). ESI MS, *m/z* 525 [Co(L-H)<sub>2</sub>]<sup>+</sup>, 33.4%, *m/z* 1047 [Co<sub>2</sub>(L-2H)<sub>2</sub>]<sup>+</sup>, 23.2%.

**Zn<sub>2</sub>(II)(73-2H)<sub>2</sub> (84)**

Using zinc(II) acetate dihydrate in the procedure described for **81** yielded a yellow solid which was dried *in vacuo* (8 mg, 11%). ESI MS *m/z* 1093 [Zn<sub>2</sub>(L-2H)<sub>2</sub>]<sup>+</sup>Na<sup>+</sup>, 58.7%.

### 6.7.5 X-Ray Crystallography

Structures were determined by Andrew Parkin at the University of Edinburgh. In all cases data were collected at 220 K on a SMART diffractometer equipped with an Oxford Cryosystems low temperature device, using Mo-K $\alpha$  radiation. Reflections were scanned in  $\omega$ - $\theta$  mode. Structures **76** and **78** were solved by direct methods SHELXS-97 and SIR92 respectively. All were completed by iterative cycles of least squares refinement against  $F^2$  and difference Fourier synthesis (SHELXTL). H-atoms were idealised, being placed using difference maps and treated by riding or

refinement methods. In all cases non-H atoms were modelled with final anisotropic displacement parameters and final refinement statistics are presented in Table 6.1.

**Table 6.1:** Crystallographic data for structures **76** and **78**.

Structure	76	78
Formula	C <sub>26</sub> H <sub>30</sub> N <sub>2</sub> O <sub>4</sub> S	C <sub>52</sub> H <sub>60</sub> CuN <sub>6</sub> O <sub>8</sub> S <sub>2</sub>
M	466.58	1024.72
Crystal system	Monoclinic	Triclinic
Space group	<i>P2 (1) / c</i>	<i>P-1</i>
a/Å	9.5809(9)	7.5641(10)
b/Å	15.7180(14)	12.7392(16)
c/Å	16.0848(14)	13.3729(17)
α/°	90	79.513(2)
β/°	104.249(2)	85.618(2)
γ/°	90	78.047(2)
U/Å <sup>3</sup>	2347.7(4)	1238.6(3)
Crystal size/mm	0.38 x 0.28 x 0.10	0.30 x 0.27 x 0.08
D <sub>c</sub> /mg m <sup>-3</sup>	1.320	1.374
Z	4	1
μ/mm <sup>-1</sup>	0.174	0.586
Scan type	phi + omega	phi + omega
θ Limits/°	1.84-26.40	1.55-26.40
No. of unique data	4775	4974
No. data with [F > 4σ(F)]	3506	4185
No. parameters	418	433
R1	0.0354	0.0314
wR2	0.0826	0.0837
Δρ <sub>max</sub> , Δρ <sub>min</sub> /e Å <sup>-3</sup>	0.215, -0.385	0.390, -0.337

## 6.8 References

- <sup>1</sup> H. Adams, D. Bradshaw and D. E. Fenton, *Eur. J. Inorg. Chem.*, 2001, **3**, 859.
- <sup>2</sup> H. Adams, D. E. Fenton, S. R. Haque, S. L. Heath, M. Ohba, H. Okawa and S. E. Spey, *J. Chem. Soc., Dalton Trans.*, 2000, **12**, 1849.
- <sup>3</sup> S. Uozumi, M. Ohba, H. Okawa and D. E. Fenton, *Chem. Lett.*, 1997, **7**, 673.
- <sup>4</sup> D. E. Fenton and H. Okawa, in *Perspectives on Bioinorganic Chemistry*, ed. R. W. Hay, J. R. Dilworth and K. B. Nolan, JAI Press, London, 1993, vol. 2, p. 81.
- <sup>5</sup> E. Lambert, B. Chabut, S. Chardon-Noblat, A. Deronzier, G. Chottard, A. Bousseksou, J. -P. Tuchagues, J. Laugier, M. Bardet, and J. -M. Latour, *J. Am. Chem. Soc.* **1997**, **119**, 9424.
- <sup>6</sup> D. H. Williams and I. Fleming, in *Spectroscopic Methods in Organic Chemistry*, McGraw-Hill Book Company, London, 5<sup>th</sup> edn., 1995, ch. 3, pp 118.

**Chapter 7:**  
**Conclusions**

The class of sulfonamido ligands used to mimic the hydrogen-bonding effects shown by the commercial phenolic oxime extractants for copper have proved to have very rich coordination chemistry. Several solid state structures of free ligands and their complexes were obtained which in addition to solution studies of the ligands lead us to believe that self-association *via* hydrogen-bonding occurs in certain solvents. Investigation of “the role of hydrogen-bonding of sulfonamido ligands on their ability to act as metal extractants” led us to carry out research in two further areas, the use of ternary sulfonamido systems as metal extractants and the development of binucleating ligands to increase the metal:ligand ratio to 2:2.

Monosulfonamidodiamine ligands proved to be relatively simple to make and are versatile complexing agents. Two to one ligand:metal complexes were formed exclusively and X-ray crystal structures of two complexes displayed hydrogen-bonded *pseudo*-macrocyclic ligand arrangements around the nickel and copper centres analogous to copper complexes of phenolic oximes. Extraction experiments proved that the ligands show high selectivity for copper. However the ligands are much weaker copper extractants than the commercial phenolic oximes.

Synthesis of sulfonamido oxime ligands, which are closer in design to phenolic oximes, proved to be straight forward. However, preparation of pure ligands with high solubility in solvents of low polarity such as toluene proved more difficult. These sulfonamide oxime ligands were found to have very rich coordination chemistry as a result of the additional potential donor atoms which can coordinate to the metal centres. Two to one ligand:metal complexes analogous to those of phenolic oximes were isolated. It is also possible to isolate polynuclear complexes. In each of these clusters methanol or methoxide were coordinated. If such ligands were to be used as solvent extractants the working medium would not be methanol but a hydrocarbon solvent. Under these conditions it is likely that only 2:1 ligand:metal complexes would be observed.

Solution studies of both monosulfonamidodiamine and sulfonamido oxime ligands indicate that aggregation in solution is occurring, but it has not been possible to assign structures to these aggregates. It was therefore difficult to assess the importance of preorganisation in enhancing the “strength” of extractants. Although the difference in number of the hydrogen-bond donor and acceptor sites in both ligand types is not large (monosulfonamidodiamine ligands have one additional acceptor site and sulfonamido oxime ligands have one extra donor site) a much larger variety of secondary structures dependant on hydrogen bonding is observed for the former. The prediction of the hydrogen-bonded secondary structure of monosulfonamidodiamine ligands proved extremely difficult. Secondary structures of sulfonamido oximes proved to be much more predictable and dependent on the *E/Z* stereochemistry of the oxime function. Individual dimer units were formed which may be a result of their more rigid backbone.

The strategy of forming ternary complexes by assembly of a bis- or tris-hydrogen-bond donor ligand with a bis- or tris-hydrogen-bond acceptor ligand around a metal cation did not prove successful. This approach is likely to be less successful for the development of selective metal-recovery reagents because the formation of binary complexes may arise.

Whilst it proved possible (Chapter 6) to synthesise potentially dinucleating ligands which could undergo head-to-tail hydrogen-bonding *via* sulfonamido and oxime units, it was not possible to characterise solid state samples of 2:2 copper complexes in the complexation studies to date. A 2:1 complex with copper was shown to have the same 14-membered inner great ring as in the commercial phenolic oxime complexes, providing further evidence for how readily this structural motif is found. This approach to enhancing the copper-transfer efficiency by using pseudo-macrocyclic assemblies which incorporate bridging donor atoms has great potential, but the intrinsically low solubility of the sulfonamido group means that larger solubilising functional groups will have to be introduced into the ligand, reducing the benefit of the lower ligand-to-metal mass ratios used in transport.

The structural analyses undertaken have shown that sulfonamide ligands are significantly different from amides of carboxylic acids and solid state structures contain a wide range of hydrogen-bonded motifs. The formation of inter-molecular hydrogen-bonds appears to contribute to their generally low solubilities which will limit their usefulness as reagents to recover metals by solvent extraction. Their relatively low pKa's are potentially useful for the development of reagents with anionic nitrogen donors which could operate a "pH swing" process. On the basis of the equilibria studies in this thesis sulfonamido ligands derived from aliphatic amines are unlikely to be "strong" enough to allow recovery from acidic pregnant leach solutions. Derivatives of aromatic amines are likely to be stronger reagents but these have lower solubility in solvents which are used in commercial operations.

It is difficult to know how to try to determine the effect which self-assembly or ligand pre-organisation actually has on the "strength" of a metal extractant. If this work were continued it would be a good idea to choose a ligand system with only the required number of hydrogen-bond donor and acceptor groups per molecule to limit the number of possible hydrogen-bonding interactions and also to improve the solubility characteristics of the ligand. A greater ligand solubility should mean that solution equilibria could be determined using the nmr techniques used in chapter 4. Ideally two very similar ligand systems with different known solution equilibria would be studied. Such nmr experiments in addition to extraction experiments should achieve more insight into this area of work.

Concerning the sulfonamido systems discussed in this thesis, those included in chapter 6 have been studied the least. Further complexation studies of these molecules may yield 2:2 metal:ligand complexes. It would also be interesting to try and design other ligand systems to accommodate metals of other geometries or even to look at binding two different metal ions in the same complex.



## **Appendix I**

### Vapour pressure osmometry data

Data for sulfonamidodiamine ligands **1**, **4**, **5**, **8** and **10** are recorded in Table I (ligands **1**, **5** and **10**), Tables II-VI (Ligand **4**), Tables VII-XI (Ligand **8**) and sulfonamido oxime ligands **28** and **33** are recorded in Table XII.

**Table I:** The aggregation number (n), [where n is the average mass determined in solution divided by the relative molecular mass of the molecule] determined by vapour pressure osmometry for N-(2-amino-ethyl)-4-methyl benzenesulfonamide (**1**), N-(3-amino-propyl)-4-methyl benzenesulfonamide (**5**) and N-(2-amino-phenyl)-4 methylbenzene-sulfonamide (**10**).

Ligand	Calculated osmolality (mmolal)	Average mass in solution	Aggregation number (n)	Standard deviation of the average mass	Standard deviation of n
<b>1</b>	20.54	232.18	1.08	9.07	0.027
	41.39	268.88	1.25	6.86	0.032
	81.47	299.61	1.40	5.79	0.042
<b>5</b>	20.71	252.97	1.11	7.47	0.031
	38.51	268.82	1.17	4.40	0.019
	51.54	300.96	1.32	7.07	0.033
<b>10</b>	20.37	279.15	1.06	14.11	0.027
	38.28	284.91	1.09	6.42	0.024
	83.89	316.70	1.21	7.16	0.054

**Table II:** VPO results for N-(N-2-ethylhexyl-2-aminoethyl)-4-methylbenzenesulfonamide (**4**) in toluene.

Calculated osmolality (mmolal)	Average mass in solution	Aggregation number (n)	Standard deviation of the average mass	Standard deviation of n
5.01	335.21	1.03	19.59	0.060
15.03	484.63	1.48	5.33	0.016
25.05	473.00	1.45	10.08	0.031
35.07	428.16	1.31	6.41	0.020
45.10	440.66	1.35	5.93	0.018
55.12	454.69	1.39	2.9	0.009
65.14	485.06	1.49	7.14	0.022
75.16	486.32	1.49	4.83	0.015
85.18	477.64	1.46	2.77	0.008
95.20	442.55	1.36	2.8	0.009

**Table III:** VPO results for N-(N-2-ethylhexyl-2-aminoethyl)-4-methylbenzenesulfonamide (4) in cyclohexane.

Calculated osmolality (mmolal)	Average mass in solution	Aggregation number (n)	Standard deviation of the average mass	Standard deviation of n
5.01	604.61	1.85	50.76	0.155
15.02	513.86	1.57	58.51	0.179
25.03	516.06	1.58	18.13	0.056
35.04	478.27	1.46	17.17	0.053
45.05	511.65	1.57	11.87	0.036
55.06	531.59	1.63	19.45	0.060
65.07	335.43	1.66	19.76	0.061
75.08	541.93	1.66	15.36	0.047
85.09	569.72	1.74	9.08	0.028
95.10	580.35	1.78	11.7	0.036

**Table IV:** VPO results for N-(N-2-ethylhexyl-2-aminoethyl)-4-methylbenzenesulfonamide (4) in chloroform.

Calculated osmolality (mmolal)	Average mass in solution	Aggregation number (n)	Standard deviation of the average mass	Standard deviation of n
5	1151.76	3.53	277.69	0.761
15	347.96	1.07	23.38	0.064
25	320.62	0.98	26.08	0.071
35	352.13	1.08	14.71	0.040
45	352.14	1.08	20.51	0.056
55	356.90	1.09	19.66	0.054
65	393.75	1.20	6.69	0.018
75	374.09	1.15	7.39	0.020
85	384.82	1.18	9.85	0.027
95	403.39	1.24	12.07	0.033

**Table V:** VPO results for N-(N-2-ethylhexyl-2-aminoethyl)-4-methylbenzenesulfonamide (4) in acetonitrile.

Calculated osmolality (mmolal)	Average mass in solution	Aggregation number (n)	Standard deviation of the average mass	Standard deviation of n
4.99	263.26	0.81	29.91	0.092
14.97	411.86	1.26	39.96	0.122
24.95	483.23	1.48	16.29	0.050
34.93	427.04	1.31	18.34	0.056
44.91	379.43	1.16	11.38	0.035
54.89	388.6	1.19	8.9	0.027
64.87	363.12	1.11	8.53	0.026

74.85	351.10	1.08	6.25	0.019
84.83	341.34	1.05	8.2	0.025
94.81	336.75	1.03	4.83	0.015

**Table VI:** VPO results for N-(N-2-ethylhexyl-2-aminoethyl)-4-methylbenzenesulfonamide (**4**) in acetone.

Calculated osmolality (mmolal)	Average mass in solution	Aggregation number (n)	Standard deviation of the average mass	Standard deviation of n
4.98	826.97	2.53	74.84	0.229
14.95	634.11	1.94	43.19	0.132
24.92	477.08	1.46	29.38	0.090
34.89	392.92	1.20	27.02	0.083
44.85	407.28	1.25	13.49	0.041
54.82	402.56	1.23	25.47	0.078
64.79	391.56	1.20	9.93	0.030
74.76	383.23	1.17	7.83	0.024
84.72	360.26	1.10	12.71	0.039
94.69	386.69	1.18	22.83	0.070

**Table VII:** VPO results for N-(N-2-ethylhexyl-3-aminopropyl)-4-methylbenzene sulfonamide (**8**) in toluene.

Calculated osmolality (mmolal)	Average mass in solution	Aggregation number (n)	Standard deviation of the average mass	Standard deviation of n
5.02	335.57	0.99	22.08	0.065
15.07	442.89	1.30	22.14	0.065
25.12	416.73	1.22	7.66	0.022
35.17	395.01	1.16	4.23	0.012
45.22	408.24	1.20	2.23	0.007
55.27	410	1.20	2.64	0.008
65.32	408.05	1.20	3.36	0.010
75.37	417.21	1.23	2.39	0.007
85.42	419.68	1.23	2.33	0.007
95.47	420.89	1.24	2.54	0.007

**Table VIII:** VPO results for N-(N-2-ethylhexyl-3-aminopropyl)-4-methylbenzenesulfonamide (**8**) in cyclohexane.

Calculated osmolality (mmolal)	Average mass in solution	Aggregation number (n)	Standard deviation of the average mass	Standard deviation of n
5.02	434.07	1.27	14.45	0.042
15.07	517.34	1.52	22.26	0.065

25.11	501.95	1.47	10.87	0.032
35.15	547.9	1.61	16.19	0.048
45.20	540.77	1.59	22.03	0.065
55.24	539.55	1.58	14.03	0.041
65.29	573.81	1.69	17.37	0.051
75.33	596.1	1.75	14.63	0.043
85.37	640.1	1.88	15.72	0.046
95.42	643.68	1.89	14.28	0.042

**Table IX:** VPO results for N-(N-2-ethylhexyl-3-aminopropyl)-4-methylbenzenesulfonamide (**8**) in chloroform.

Calculated osmolality (mmolal)	Average mass in solution	Aggregation number (n)	Standard deviation	Standard deviation of n
5.00	479.55	1.41	16.7	0.049
15.00	354.31	1.04	10.71	0.031
25.00	336.69	0.99	9.51	0.028
4.99	333.28	0.98	10.26	0.030
44.99	334.85	0.98	6.28	0.018
54.99	321.72	0.94	4.8	0.014
65.99	324.39	0.95	8.49	0.025
74.99	313.31	0.92	8.02	0.024
84.98	328.57	0.96	5.98	0.017
94.98	310.1	0.91	10.46	0.031

**Table X:** VPO results for N-(N-2-ethylhexyl-3-aminopropyl)-4-methylbenzenesulfonamide (**8**) in acetonitrile.

Calculated osmolality (mmolal)	Average mass in solution	Aggregation number (n)	Standard deviation of the average mass	Standard deviation of n
5.05	213.10	0.63	6.96	0.020
15.15	387.09	1.14	34.49	0.101
25.25	397.34	1.17	20.77	0.061
35.35	383.55	1.13	6.23	0.018
45.45	365.50	1.07	17.81	0.052
55.55	346.66	1.02	3.2	0.009
65.66	355.80	1.04	3.93	0.011
75.76	361.19	1.06	7.41	0.022
85.86	343.13	1.01	2.92	0.009
95.96	358.16	1.05	4.02	0.012

**Table XI:** VPO results for N-(N-2-ethylhexyl-3-aminopropyl)-4-methylbenzenesulfonamide (**8**) in acetone.

Calculated osmolality (mmolal)	Average mass in solution	Aggregation number (n)	Standard deviation of the average mass	Standard deviation of n
5.31	418.27	1.23	33.63	0.099
15.94	497.72	1.46	31.29	0.092
26.56	463.6	1.36	32.88	0.097
37.19	460.47	1.35	21.14	0.062
47.81	495.91	1.46	13.17	0.039
58.44	488.17	1.43	9.56	0.028
69.07	505.13	1.48	11.35	0.033
79.69	479.14	1.41	10.33	0.030
90.32	491.13	1.44	19.08	0.056
100.94	491.56	1.44	16.85	0.049

**Table XII:** The aggregation number (n), determined by vapour pressure osmometry for 1-{2-[N-(4-methylbenzenesulfonamido)] phenyl}ethan-1-one oxime (**28**) and 2-[N-(4-methylbenzenesulfonamido)](phenyl)methanone oxime (**33**).

Ligand	Calculated osmolality (mmolal)	Average mass in solution	Aggregation number (n)	Standard deviation of the average mass	Standard deviation of n
28	21.34	315.21	1.04	7.56	0.025
	41.77	378.87	1.25	14.60	0.048
	71.60	406.47	1.34	6.38	0.021
33	20.79	428.96	1.41	9.82	0.032
	41.13	471.79	1.56	16.23	0.054
	77.15	492.25	1.62	8.80	0.029

## Appendix II

### Proton nmr data

Data for sulfonamido oxime ligands **28**, **31** and **33** are recorded in Table I (ligands **28** and **33**), Table II-V (Ligand **28**), Tables VI-VIII (Ligand **31**).

**Table I:** The change in chemical shift of the oximic protons of 1-{2-[N-(4-methylbenzenesulfonamido)] phenyl}ethan-1-one oxime (**28**) and 2-[N-(4-methylbenzenesulfonamido)](phenyl)methanone oxime (**33**) with concentration at 297K in chloroform.

Concentration (mmol)	Chemical shift of the oximic proton of <b>28</b> (ppm)	Chemical shift of the oximic proton of <b>33</b> (ppm)
20	10.60	10.57
40	10.66	10.60
80	10.74	10.64

**Table II:** The change in chemical shift of the oximic and the sulfonamido protons of a 70 mmolar deuterated chloroform solution of 1-{2-[N-(4-methylbenzenesulfonamido)] phenyl}ethan-1-one oxime (**28**) with temperature.

Temperature / K	Chemical shift of the oximic proton (ppm)	Chemical shift of the sulfonamido proton (ppm) <sup>a</sup>
298	10.7484	7.9362
301	10.7236	7.8997
304	10.6980	7.8637
307	10.6746	7.8302
310	10.6505	7.7972
313	10.6269	7.7664
316	10.6047	7.7365
319	10.5818	7.7062
322	10.5584	
325	10.5373	
328	10.5143	

<sup>a</sup> The peak of the sulfonamido proton was sometimes hidden by peaks in the aromatic region of the spectrum.

**Table III:** The change in chemical shift of the oximic and the sulfonamido protons of 1-{2-[N-(4-methylbenzenesulfonamido)] phenyl}ethan-1-one oxime (**28**) with concentration at 297K in chloroform.

Concentration (mmol)	Chemical shift of the oximic proton (ppm)	Chemical shift of the sulfonamido proton (ppm) <sup>a</sup>
129.099	10.8025	8.2697
118.255	10.8012	8.2624
107.539	10.7853	8.2127
96.8242	10.7774	8.186
85.9799	10.7586	8.1241
75.2647	10.7455	8.083
64.5495	10.7278	8.0279
53.8342	10.7069	7.9602
42.9899	10.6849	7.8947



32.2747	10.6658	7.832
21.4304	10.6249	7.718
10.7152	10.5792	
8.52053	10.5661	
6.45495	10.5562	7.5739
4.26026	10.5372	7.4742
2.19468	10.5415	

<sup>a</sup> The peak of the sulfonamido proton was sometimes hidden by peaks in the aromatic region of the spectrum.

**Table IV:** The change in chemical shift of the oximic and the sulfonamido protons of 1-{2-[N-(4-methylbenzenesulfonamido)] phenyl}ethan-1-one oxime (**28**) with concentration at 307K in chloroform.

Concentration (mmol)	Chemical shift of the oximic proton (ppm)	Chemical shift of the sulfonamido proton <sup>a</sup> (ppm)
129.066	10.734	8.1562
118.224	10.7362	8.1568
107.512	10.7752	8.1626
96.7995	10.7085	8.0697
85.9579	10.6943	8.0254
75.2454	10.6795	7.9808
64.533	10.66	7.9237
53.8205	10.644	7.8775
42.979	10.6723	7.9092
32.2665	10.5849	7.7058
21.4249	10.5528	
10.7125	10.5048	7.4852
8.51835	10.4985	7.4645
6.4533	10.4789	7.4223
4.25918	10.4751	7.401
2.19412	10.5034	7.4587

<sup>a</sup> The peak of the sulfonamido proton was sometimes hidden by peaks in the aromatic region of the spectrum.

**Table V:** The change in chemical shift of the oximic and the sulfonamido protons of 1-{2-[N-(4-methylbenzenesulfonamido)] phenyl}ethan-1-one oxime (**28**) with concentration at 317K in chloroform.

Concentration (mmol)	Chemical shift of the oximic proton (ppm)	Chemical shift of the sulfonamido proton <sup>a</sup> (ppm)
129.066	10.656	8.0434
118.224	10.6574	8.0407
107.512	10.7207	8.1086
96.7995	10.6303	7.957
85.9579	10.6151	7.9136
75.2454	10.602	7.872
64.533	10.5829	7.8169
53.8205	10.5677	7.7743
42.979	10.5881	7.7905
32.2665	10.5117	
21.4249	10.4843	
10.7125	10.4533	7.4362
8.51835	10.435	7.4047

6.4533	10.4188	7.3708
4.25918	10.4148	7.3525
2.19412	10.4376	7.397

<sup>a</sup> The peak of the sulfonamido proton was sometimes hidden by peaks in the aromatic region of the spectrum.

**Table VI:** The change in chemical shift of the oximic and the sulfonamido protons of 1-{2-[N-(4-pentylbenzenesulfonamido)]phenyl}ethan-1-one oxime (**31**) with concentration in chloroform.

Concentration (mmol)	Chemical shifts at 297K		Chemical shifts at 307K		Chemical shifts at 317K	
	C=N-OH	NH <sup>a</sup>	C=N-OH	NH <sup>a</sup>	C=N-OH	NH <sup>a</sup>
120.47	10.8325	8.3834	10.7556	8.2538	10.6813	8.1371
110.43	10.8246	8.3637	10.7526	8.2453	10.6799	8.1293
100.39	10.8122	8.3203	10.7397	8.2031	10.667	8.0901
90.35	10.7983	8.2734	10.7246	8.1534	10.653	8.0433
80.31	10.7804	8.2171	10.7054	8.0973	10.6349	7.9915
70.27	10.7756	8.2146	10.7013	8.0948	10.6286	7.9841
60.24	10.7496	8.1184	10.6789	8.0099	10.6099	7.9075
50.20	10.7243	8.0388	10.65	7.9255	10.5796	7.8234
40.16	10.7042	7.9756	10.6325	7.8708	10.5646	7.7769
30.12	10.678	7.9061	10.6105	7.8125	10.5483	7.73
20.08	10.6502	7.8154	10.579		10.5147	
10.04	10.6055		10.543		10.4875	7.5517
8.03	10.598		10.5366		10.4844	7.5352
6.02	10.5744		10.5173	7.5419	10.4559	7.4743
4.02	10.5778		10.5126	7.5244	10.4593	7.4729
2.01	10.5633		10.4983	7.4922	10.445	7.4413

<sup>a</sup> The peak of the sulfonamido proton was sometimes hidden by peaks in the aromatic region of the spectrum.

**Table VII:** The change in chemical shift of the oximic and the sulfonamido protons of 1-{2-[N-(4-pentylbenzenesulfonamido)]phenyl}ethan-1-one oxime (**31**) with concentration in toluene.

Concentration (mmol)	Chemical shifts at 297K		Chemical shifts at 307K		Chemical shifts at 317K	
	C=N-OH	NH <sup>a</sup>	C=N-OH	NH <sup>a</sup>	C=N-OH	NH <sup>a</sup>
119.70	11.2816	8.2361	11.1777	8.051	11.0773	
109.72	11.2641	8.1608	11.1539	7.96	11.0548	7.792
99.75	11.256	8.1189	11.148		11.048	7.757
89.77	11.2341	8.0206	11.1277	7.837	11.0267	
79.80	11.2169		11.1039	7.746	11.0038	7.5848
69.82	11.1933	7.8498	11.0844		10.9965	7.5151
59.85	11.1755	7.7805	11.0621	7.579	10.9628	7.4243
49.87	11.1395		11.0303	7.447	10.9324	7.3003
39.90	11.1022	7.49	10.9952	7.3182	10.8999	7.182
29.92	11.0584	7.3218	10.9527	7.1593	10.8594	
19.95	11.0151	7.1527	10.9127		10.8227	
9.97	10.9346		10.8357		10.7499	
7.98	10.916		10.8196		10.7411	
5.98	10.8971		10.805		10.7334	

3.99	10.8704	10.7771	10.7922	6.5256
1.99	10.8496	10.7625	10.6909	6.3911

<sup>a</sup>The peak of the sulfonamido proton was sometimes hidden by peaks in the aromatic region of the spectrum.

**Table VIII:** The change in chemical shift of the oximic proton of 1-{2-[N-(4-pentylbenzenesulfonamido)]phenyl}ethan-1-one oxime (31) with concentration in acetonitrile.

Concentration (mmol)	Chemical shifts at 297K	Chemical shifts at 307K	Chemical shifts at 317K
124.13	10.9389	10.8952	10.8573
113.79	10.9371	10.8939	10.8559
103.44	10.9346	10.8924	10.8539
93.10	10.9335	10.8905	10.853
82.75	10.9315	10.889	10.8508
72.41	10.9297	10.8865	10.8489
62.06	10.9279	10.886	10.8484
51.72	10.9263	10.884	10.8449
41.38	10.9243	10.8832	10.8459
31.03	10.9226	10.8816	10.8444
20.69	10.9209	10.8797	10.8413
10.34	10.9193	10.8771	10.8398
8.28	10.9185	10.8774	10.8391
6.21	10.9182	10.878	10.8398
4.14	10.9179	10.8765	10.8393
2.07	10.9146	10.8735	10.8372